

Structure and function of bacterial viruses and viral communities

Dissertation
for the award of the degree
“Doctor rerum naturalium” (Dr. rer. nat.)
of the Georg-August University Göttingen

within the doctoral program “Microbiology and Biochemistry”
of the Göttingen Graduate School for Neurosciences, Biophysics, and Molecular Biosciences
(GGNB)

submitted by

Ines Friedrich

from Wolfsburg

Göttingen, 2022

Thesis Committee:

Prof. Dr. Rolf Daniel, Department of Genomic and Applied Microbiology, Institute of Microbiology and Genetics, Georg-August University Göttingen

PD Dr. Michael Hoppert, Department of General Microbiology, Institute of Microbiology and Genetics, Georg-August University Göttingen

Prof. Dr. Stefanie Pöggeler, Department of Genetics of Eukaryotic Microorganisms, Institute of Microbiology and Genetics, Georg-August University Göttingen

Member of the examination board:

First Referee: Prof. Dr. Rolf Daniel, Department of Genomic and Applied Microbiology, Institute of Microbiology and Genetics, Georg-August University Göttingen

Second Referee: PD Dr. Michael Hoppert, Department of General Microbiology, Institute of Microbiology and Genetics, Georg-August University Göttingen

Further members of the examination board:

Prof. Dr. Stefanie Pöggeler, Department of Genetics of Eukaryotic Microorganisms, Institute of Microbiology and Genetics, Georg-August University Göttingen

Prof. Dr. Kai Heimel, Department of Microbial Cell Biology, Institute of Microbiology and Genetic, Georg-August-University Göttingen

Prof. Dr. Gerhard Braus, Department of Molecular Microbiology and Genetics, Institute of Microbiology and Genetics, Georg-August University Göttingen

Prof. Dr. Jan de Vries, Department of Applied Bioinformatics, Institute of Microbiology and Genetics, Georg-August University Göttingen

Date of oral examination: 17.11.2022

*This thesis is dedicated to my parents.
For their endless love, support, and encouragement.
And to my little adventurers.
For bringing joy and happiness into my life. I am proud of you!*

Table of contents

Chapter ONE – Summary.....	1
Chapter TWO – General Introduction.....	3
1. Bacteriophages	3
2. A short history of bacteriophages	3
3. Life cycle of bacteriophages	4
4. Classification of bacteriophages	5
5. Host systems of bacteriophages	6
5.1. The bacterial family <i>Caulobacteraceae</i>	7
5.2. The genus <i>Serratia</i>	9
5.3. The genus <i>Janthinobacterium</i>	11
5.4. The genus <i>Luteibacter</i>	12
5.5. The genus <i>Stenotrophomonas</i>	13
5.6. The genus <i>Kinneretia</i>	13
6. Research goals.....	13
Chapter THREE – Results and publications	16
1. Living in a puddle of mud: Isolation and characterization of two novel <i>Caulobacteraceae</i> strains <i>Brevundimonas pondensis</i> sp. nov. and <i>Brevundimonas goettingensis</i> sp. nov.	17
2. Down in the pond: Isolation and characterization of a new <i>Serratia marcescens</i> strain (LVF3) from the surface water near frog's lettuce (<i>Groenlandia densa</i>)	40
3. First complete genome sequences of <i>Janthinobacterium lividum</i> EIF1 and EIF2 and their comparative genome analysis	59
4. Complete genome sequence of <i>Stenotrophomonas indicatrix</i> DAIF1	67
5. Complete genome sequence of <i>Kinneretia</i> sp. strain DAIF2, isolated from a freshwater pond.....	71
6. Isolation of a host-confined phage metagenome allows the detection of phages both capable of plaque formation	75
7. <i>Brevundimonas</i> and <i>Serratia</i> as host systems for assessing associated environmental viromes and phage diversity by complementary approaches	86

Supplement:	118
8. Isolation and characterization of a <i>Janthinobacterium lividum</i>-associated bacteriophage and analysis of its prophage.....	120
Supplement:	137
9. <i>Luteibacter flocculans</i> sp. nov., isolated from a eutrophic pond and introduction of <i>Luteibacter</i> phage vB_LflM-Pluto	138
Supplement:	157
Chapter FOUR – General Discussion.....	159
1. Isolation of bacterial host systems and their characterization	159
2. Ways to analyze phage-host interaction	165
General References	171
Appendix.....	179
1. Supplement	179
2. Publications.....	180
3. Posters at conferences.....	181
Acknowledgements.....	182

CHAPTER ONE

Summary

Bacterial viruses, known as bacteriophages or phages, are the most abundant biological entities on the planet and the least studied in terms of abundance and diversity. Searching the sequence databases of viral genomes, one becomes the impression that most of the viral sphere consists of dsDNA bacteriophages. First objective of the studies was to verify whether this is true or a methodical artefact of our usual approach of assessing the viral world. Second, bacterial host strains were needed for the investigation of bacteriophages. Third, besides the classic overlay plaque assay for isolation, the dsDNA, ssDNA, dsRNA, and ssRNA was also isolated from phage plaques as well.

To accomplish this endeavor, a local bacterial host system associated with various RNA and DNA viruses was required. Such hosts were not available at the beginning of this work and making it necessary to isolate a suitable prokaryotic system. To this end, environmental samples were successfully screened for new hosts, resulting in 37 new candidate bacterial strains, eight of which were sequenced and genomically analyzed (*Brevundimonas pondensis*, *B. goettingensis*, *Serratia marcescens* LVF3, *Luteibacter flocculans*, *Stenotrophomonas indicatrix* DAIF1, *Kinneretia* sp. DAIF2, and *Janthinobacterium lividum* EIF1 and EIF2). These were evaluated for their suitability as host systems (chapter 3.1 to 3.5, 3.8 and 3.9). A total of four new species were discovered and described. Using genomic analyses three of these were fully characterized (*Brevundimonas pondensis*, *Brevundimonas goettingensis*, and *Luteibacter flocculans*).

Brevundimonas pondensis LVF1 and *Serratia marcescens* LVF3 proved to be particularly promising candidates to achieve the main objectives of this thesis (chapter 3.7). They were used for classical phage isolation, resulting in 25 new dsDNA phages: 14 were associated with *Brevundimonas* and 11 with *Serratia*. TEM analysis revealed that six are myoviruses, 18 siphoviruses and one podovirus, while the *Brevundimonas*-associated phages are all

siphoviruses. The classical approach was complemented by Next Generation Sequencing (NGS)-based methods that provided dsDNA, ssDNA, dsRNA, and ssRNA host-associated virome data. Furthermore, the complementary NGS approach enabled the identification of vB_SmaP-Kaonashi and vB_SmaM-Otaku. The latter is a virus that infects both host systems. In addition, the ssDNA virome associated with *Brevundimonas pondensis* revealed promising results as two contigs associated with ssDNA phages could be detected. These belong to the family *Microviridae* and *Inoviridae*. Further, the ssRNA virome of *Brevundimonas goettingensis* contained a contig associated with the *Caulobacter*-associated RNA phage phiCb5 which belong to the family *Leviviridae*.

In addition, bacteriophage isolates associated with the bacterial host strains *Janthinobacterium* (chapter 3.8) and *Luteibacter* (chapter 3.9) were found. Here, using the classical phage isolation approach, one phage was discovered for each bacterial host system. *Janthinobacterium lividum* produces the medically relevant antivacterial substance violacein. We were able to identify, that the induction of violacein is phage-dependent in this organism. Both phage isolates (*Luteibacter* phage vB_lflM-Pluto and *Janthinobacterium* phage vB_JliS-Donnerlittchen) are the first sequenced phages associated with the respective host systems.

In conclusion, the results of this work demonstrate that dsDNA phages are the most prominent. Furthermore, the classical approach to phage isolation, which is still practical but biased, has successfully been demonstrated. Its limitations can be overcome by NGS-based methods to access viral diversity as efficiently as possible.

General Introduction

1. Bacteriophages

The “predators” of bacteria are bacteriophages. A bacteriophage is a virus that infects and replicates within bacterial cells. The term was derived from “bacteria” and the Greek φαγεῖν (*phagein*), literally “to devour”. Viruses belong to the most diverse entities on the planet (Casas and Rohwer, 2007; Dion et al., 2020). Bacteriophages are ubiquitous viruses and found wherever bacteria are present. With an estimated number of 10^{31} virions in the world’s biosphere, phages exceed the number of bacterial cells in various environments by about tenfold (Dion et al., 2020). The highest phage densities have been observed in wastewater treatment plants (WWTPs), and are 10–1000 times higher than in any other aqueous habitat (Wu and Liu, 2009).

2. A short history of bacteriophages

Bacteriophages were first discovered by the English bacteriologist William Twort in 1915 who described viruses as deadly enzymes secreted by bacteria. At that time, smallpox vaccines had to be produced in the skin of calves and were almost always contaminated with the bacterial genus *Staphylococcus*. After streaking the smallpox vaccine on an agar plate, he discovered tiny glassy areas that did not grow in the subcultures. Twort quickly realized that these glassy areas were the result of bacterial cell destruction. He was able to extract some of these areas and transfer them from one *Staphylococcus* colony to another. In 1915, he published these results in *The Lancet* and called the contamination the “bacteriolytic agent”.

Independent of Twort’s research, Felix d’Hérelle, a French-Canadian microbiologist recognized that bacteriophages had the potential to kill bacteria. He conducted research on intestinal bacteria of dysentery patients at the Pasteur Institute in Paris, France. In 1917, he

published a short paper in the *Comptes rendus de l'Académie des Sciences* (D'Hérelle, 1917). He described the lysis of bacteria over several propagations. He named this "invisible microbe antagonistic to the dysentery bacillus" bacteriophage (bacterial eater). D'Hérelle concluded his paper by stating that a bacteriophage is a "microbe of immunity," which is specific. He also recognized the potential of phages as treatment for bacterial infections, namely phage therapy (D'Hérelle, 1917). After experiencing a heyday before the antibiotic era, they were then essentially disregarded as important therapeutic agents in the West, largely due to the easier application of antibiotics. However, research and therapeutic use of bacteriophages continued in some countries of the former USSR such as Georgia, Russia, and Poland due to the lack of western antibiotics. They are still routinely isolated and used to treat numerous diseases in these countries (Reardon, 2014).

3. Life cycle of bacteriophages

As intracellular parasites, phages rely on the metabolic processes of their bacterial hosts for replication. The host range is phage-strain-specific and might comprise a single host strain or multiple bacterial strains (Garmaeva et al., 2019). Phages either reduce the population through direct replication (lytic route) (Carding et al., 2017) or enter a long-term relationship with their host by integrating into the host genome as a prophage (lysogenic route) (Principi et al., 2019). An overview of both cycles is depicted in Figure 1. As prophage, they provide additional genetic information and extra properties to the host. When a bacterium containing prophages is exposed to stressors such as UV light, nutrient-depleted conditions, or chemicals such as mitomycin C, the prophages may spontaneously detach from the host genome and enter the lytic cycle; this process is known as induction.

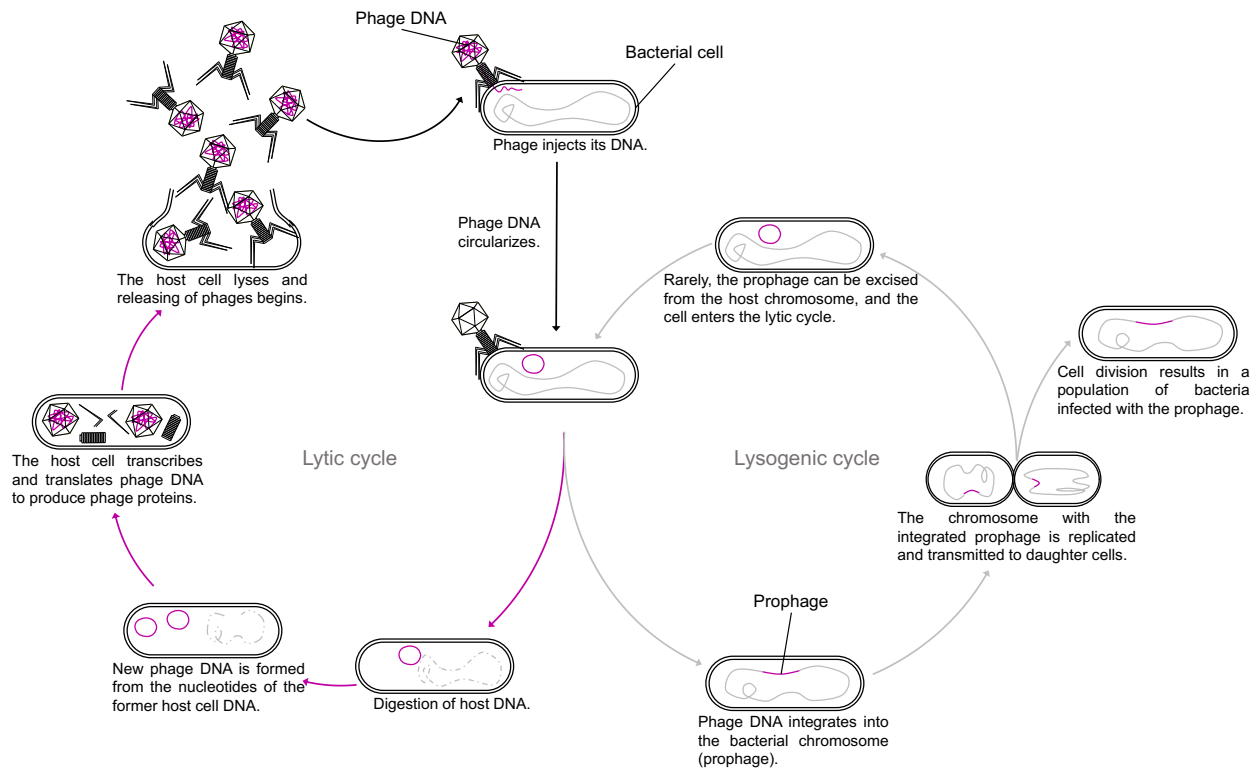


Figure 1. Overview of the lytic and lysogenic cycles of bacteriophages. Infection with viral DNA leads to replication of the virus and lysis of the bacterial host cell. In the lysogenic cycle, an inactive prophage is replicated as part of the host chromosome and, in some rare cases, can lyse out again following induction.

4. Classification of bacteriophages

Today bacteriophages are classified based on their genomic sequence and its organization (Dion et al., 2020). The resulting groups usually correlate with viral morphology. An overview of all morphology types of bacteriophages is provided in Figure 2. Some have a head-tail morphology (*Caudovirales*), others are filamentous (*Inoviridae*), pleomorphic (*Plasmaviridae*) or polyhedral (*Microviridae*, *Corticoviridae*, *Tectiviridae*, *Cystoviridae* and *Leviviridae*) viral capsids. In addition to the viral capsid, internal or external lipid membranes may also exist. Unlike other phages, pleomorphic phages do not have capsids but rather a proteinaceous lipid vesicle. Another distinguishing phage feature is the type of its genomic material, which is RNA or DNA and varies from single- to double-stranded and linear or circular (Dion et al., 2020). Most of the characterized phages isolated to date are tailed and use dsDNA as genomic material (Dion et al., 2020; Zrelavs et al., 2020). The tailed dsDNA phages (*Caudovirales*) and non-tailed phage *Tectiviridae* have a linear genome. In contrast, non-tailed dsDNA phages *Corticoviridae* and *Plasmaviridae* have a circular genome. Both, *Microviridae* and *Inoviridae*, have a circular

ssDNA genome. dsRNA phage *Cystoviridae* and ssRNA phage *Leviviridae* have a linear genome.

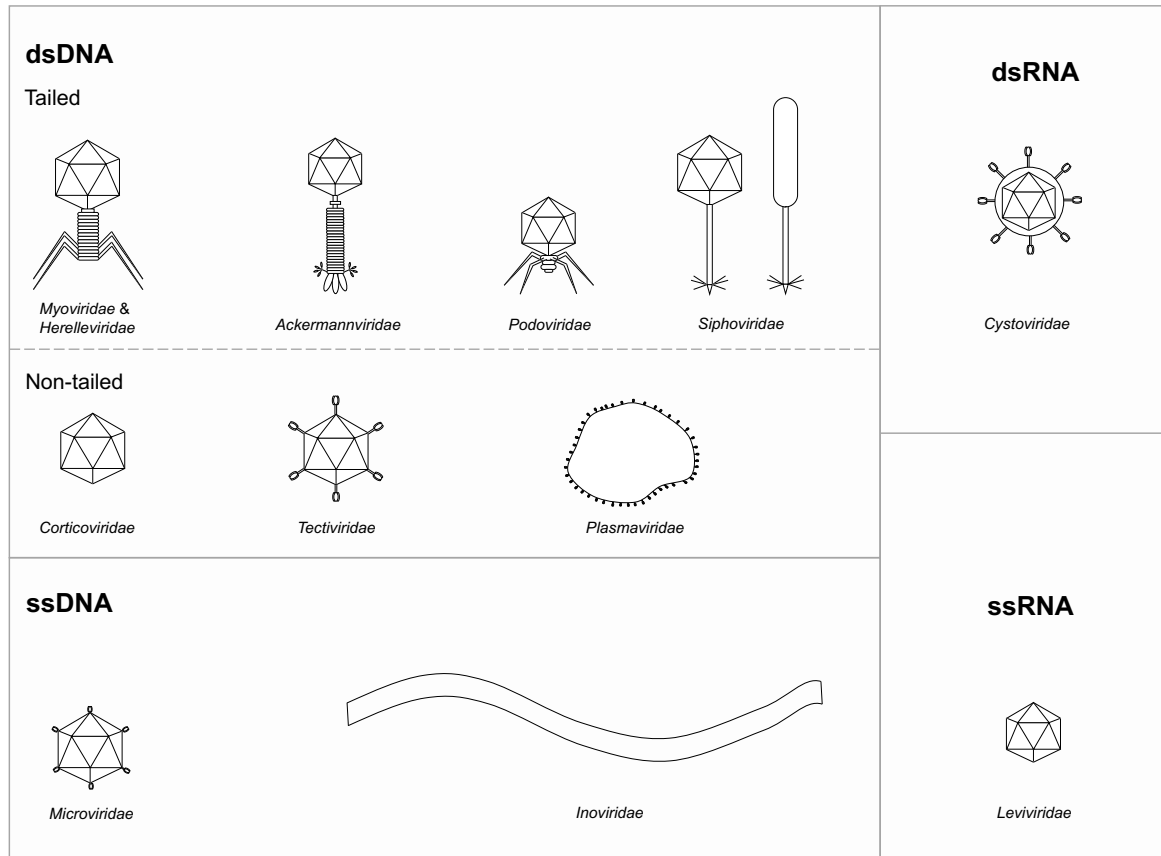


Figure 2. A schematic representation for each bacteriophage morphology. The dsDNA phages are either tailed (*Myoviridae*, *Herelleviridae*, *Ackermannviridae*, *Podoviridae*, *Siphoviridae*) or non-tailed (*Corticoviridae*, *Tectiviridae*, *Plasmaviridae*). The ssDNA phages are *Microviridae* and *Inoviridae*. For the dsRNA and ssRNA phages only one phage family is known each known: *Cystoviridae* and *Leviviridae*, respectively.

5. Host systems of bacteriophages

Phages are highly host-specific, infecting and killing only one species or even subspecies of bacteria. Most of the characterized phages isolated to date are tailed and use dsDNA as genomic material (Dion et al., 2020; Zrelavs et al., 2020). Furthermore, some groups are particularly dominant regarding the virus type and genome (Zrelavs et al., 2020).

To explore virus types and their genome sizes, bacterial host systems are needed. In general, well-characterized host strains, which are safe with respect to human health, are necessary to extract new phages from the environment. The host should ideally be non-

pathogenic and contain no or few prophages to avoid prophage-induced resistance, which would result in a strain that cannot be infected by some phage types.

For instance, members of the bacterial family *Caulobacteraceae* and genera *Serratia*, *Janthinobacterium*, *Luteibacter*, *Stenotrophomas*, and *Kinneretia* are bacterial host systems fulfilling these criteria.

5.1. The bacterial family *Caulobacteraceae*

The bacterial family *Caulobacteraceae* is the only family belonging to the order Caulobacterales (Henrici and Johnson, 1935), which is grouped into the α -subclass of Proteobacteria. It comprises the genera *Asticcacaulis*, *Brevundimonas*, *Caulobacter* and *Phenylobacterium* (Abraham et al., 1999). *Caulobacteraceae* thrive in several environments, including freshwater, saltwater, soil, plants, and humans (Abraham et al., 2014). Each member is Gram-negative, aerobic, or facultatively anaerobic, and rod-shaped or vibrioid. They divide asymmetrically, with one cell possessing prosthecae (Staley, 1968) and the other possessing a motile polar flagellum (Jin et al., 2014). Daughter swarmer cells roam freely in the environment until they form a stalk and adhere to substrates (Stove and Stanier, 1962). The stalked cell is capable of asymmetric division. The unique cell cycle of *Caulobacter* has been investigated. Representatives of the genus *Caulobacter* are frequently found in “rosettes”, which are clusters of stalk cells that attach to one another (Poindexter, 1964). Henrici and Johnson (Henrici and Johnson, 1935) first characterized the unicellular organism in 1935. His description is based on microscopic observations of microbes clinging to glass slides that had been incubated in a freshwater lake.

Caulobacter inhabits a variety of habitats, including freshwater, marine, and terrestrial ecosystems (Wilhelm, 2018). Their closest relatives are members of the genus *Brevundimonas* (Segers et al., 1994). Based on the reclassifications of two *Pseudomonas* species as *Brevundimonas diminuta* and *Brevundimonas vesicularis* (Segers et al., 1994), the genus *Brevundimonas* was established. *Brevundimonas* is present in a variety of environments, including soils, deep subseafloor sediments, activated sludge, black sand, blood and aquatic environments (Choi et al., 2010; Estrela and Abraham, 2010; Ryu et al., 2007; Tsubouchi et al., 2014; Vu et al., 2010; Wang et al., 2012; Yoon et al., 2006). With the exception of a few sessile species (Abraham et al., 2010; Ryu et al., 2007; Tóth et al., 2017; Tsubouchi et al., 2014), they are mostly non-prosthecate, motile bacteria with polar flagella (Figure 3). Abraham et al. indicate that species

in the genus *Brevundimonas* may have lost the ability to produce prosthecae during evolution or have permanently relocated the motile phase of their developmental cycle (Abraham et al., 1999).

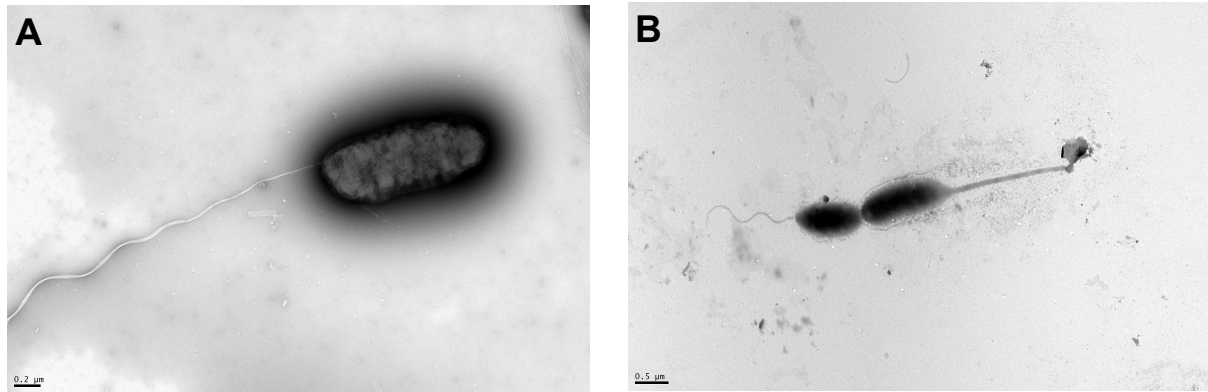


Figure 3. Transmission electron microscopy image of (A) *B. pondensis* and (B) *B. goettingensis*. Both were grown in liquid diluted peptone-yeast extract medium for (A) 24 h and (B) 48 h at 30 °C.

Brevundimonas and *Caulobacter* have similar lifestyles. Both species utilize the K-strategy and live in oligotrophic environments (Gorbatyuk and Marczynski, 2005). There are no distinguishing nutritional properties between the two genera. *Caulobacter subvibrioides*, *Caulobacter bacteroides* and *Caulobacter vesicularis* were therefore reclassified as *Brevundimonas subvibrioides*, *Brevundimonas bacteroides*, and *Brevundimonas vesicularis*, respectively (Abraham et al., 1999). Currently, 38 *Brevundimonas* and 16 *Caulobacter* species are recognized (LPSN (Parte et al., 2020), retrieved on 24 July 2022).

Three phages that infect the Caulobacterales member *Asticcacaulis biprosthecium* (Abraham et al., 2014) and seven phages linked with *Brevundimonas vesicularis* have been identified and genetically characterized (Beilstein and Dreiseikelmann, 2006). Only three *Brevundimonas*-associated bacteriophage genomes are available in the NCBI Virus database. In addition, *Caulobacteraceae* are known to be infected by RNA phages, namely ϕ Cb5, a small polyhedral RNA phage belonging to the *Leviviridae* family. This phage has extensively been utilized as model for research in molecular biology research (Kazaks et al., 2011; Schmidt and

Stainer, 1965). The confirmed relationship of *Caulobacter* with many phage types suggests that this genus is suitable for analyzing viral presence and diversity in different ecosystems.

5.2. The genus *Serratia*

The genus *Serratia* is a member of the order Enterobacterales, a vast and diverse group of facultatively anaerobic, non-spore-forming, Gram-negative, rod-shaped bacteria. This group is part of the Gammaproteobacteria. *Yersiniaceae*, *Morganellaceae*, *Pectobacteriaceae*, *Erwiniaceae*, *Hafniaceae*, *Budviciaceae*, and *Enterobacteriaceae* are related families (Adeolu et al., 2016). The family *Yersiniaceae*, includes also the eight genera *Chania*, *Chimaeribacter*, *Ewingella*, *Rahnella*, *Rouxiella*, *Samsonia*, *Serratia* and *Yersinia* (Adeolu et al., 2016). Members of the *Yersiniaceae* are described as motile, catalase-positive, and incapable of producing hydrogen disulfide (Adeolu et al., 2016). Currently, 23 species are grouped into the genus *Serratia* (LPSN (Parte et al., 2020) retrieved on 24 July 2022), which originate from a variety of environments including soil, plants, animals, insects, and water (Grimont and Grimont, 1978; Mahlen, 2011).

The genus *Serratia* was initially described in 1819 by Bartolomeo Bizio in Padua, Italy, and is named after the Italian scientist Serafino Serrati. However, *Serratia*'s history dates to the Middle Ages when it was involved in miraculous eucharistic events. Prodigiosin is a red, non-diffusible pigment that is produced by some *Serratia* strains. Since they can grow on bread, these *Serratia* may have been employed at the time to simulate blood on church bread (Bennett and Bentley, 2000). Except for the potentially spore-forming *Serratia marcescens* subsp. *sakuensis* (Ajithkumar et al., 2003), *Serratia* cells are Gram-negative and rod-shaped with rounded ends (Grimont and Grimont, 1978) (Figure 4).

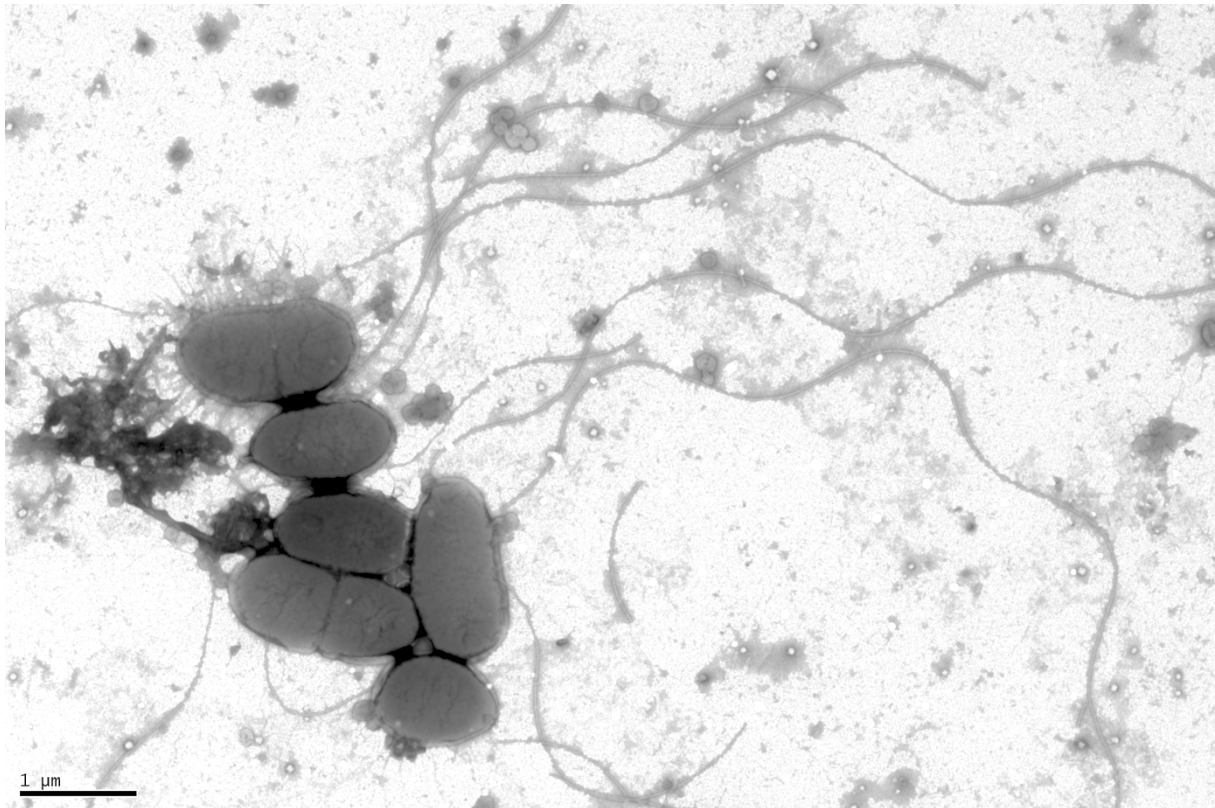


Figure 4. Transmission electron microscopy image of *Serratia marcescens* LVF3. LVF3 was grown in liquid tryptic soy broth medium for 24 h at 30 °C.

Serratia is often associated with both animals and plants. It may be isolated from healthy people (Grimont and Grimont, 1978) and has been linked to conjunctivitis in horses, septicemia in foals, pigs and goats, and mastitis in cows (Carter and Chengappa, 1990; Wijewanta and Fernando, 1970). Some strains are opportunistic pathogens that cause pneumonia, septicemia or skin lesions (Manfredi et al., 2000; Ray et al., 2015). *Serratia marcescens* causes 1–2% of nosocomial infections in humans, primarily in the respiratory and urinary tracts, surgical wounds, and soft tissues (Abreo and Altier, 2019; Khanna et al., 2013; Maki et al., 1973). *Serratia marcescens* strains can cause cucurbit yellow vine disease (CYVD) in watermelons, pumpkins, and yellow squash, as well as soft-rot disease in bell peppers (Gillis et al., 2013; Rascoe et al., 2003; Sikora et al., 2012). Nonetheless, some *S. marcescens* strains can also promote plant growth (Devi et al., 2016; Khan et al., 2017).

Serratia bacteriophages are commonly detected in rivers and sewage (Bhetwal et al., 2017; Frederick and Lloyd, 1995; Matsushita et al., 2009). *Serratia* phages can often infect related genera (Evans et al., 2010; Prinsloo, 1966; Prinsloo and Coetzee, 1964). Lysogeny is widely

mentioned in the genus *Serratia* (Grimont and Grimont, 1978). To date, the complete genomic sequences of 14 *Serratia*-associated phages are accessible in the NCBI Virus database (Brister et al., 2015) (accessed on 24 July 2022).

5.3. The genus *Janthinobacterium*

The genus *Janthinobacterium* belongs to the family *Oxalobacteraceae*, which is part of the β -subclass of the Proteobacteria and includes 13 genera (Baldani et al., 2014). *Janthinobacterium* contains the species *J. agaricidamnorum* (Lincoln et al., 1999), *J. aquaticum* (Lu et al., 2020), *J. lividum* (De Ley et al., 1978), *J. psychrotolerans* (Gong et al., 2017), *J. rivuli* (Lu et al., 2020), *J. svalbardensis* (Ambrožič Avguštin et al., 2013), *J. tructae* (Jung et al., 2021), and *J. violaceinigrum* (Lu et al., 2020).

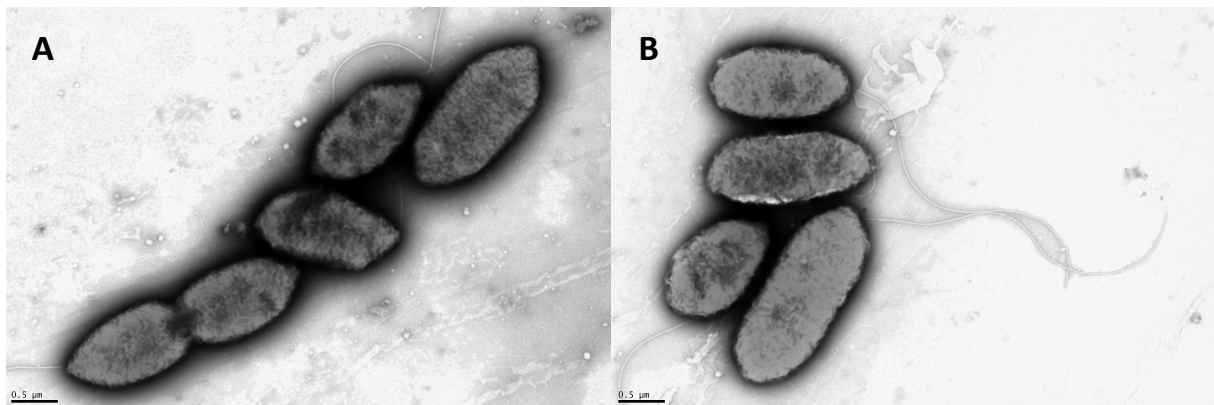


Figure 5. Transmission electron microscopy image of EIF1 and EIF2. Micrographs show the general morphology of negatively stained cells of both strains which were grown at 30 °C in liquid tryptic soy broth medium for 24 h.

Members of the genus *Janthinobacterium* are motile, rod-shaped (Figure 5), and Gram-negative. They are strictly aerobic, chemoorganotrophic, and thrive between 25 and 30 °C (Baldani et al., 2014). Members of this genus are present in soils, lakes, rainwater cisterns, and water sediments (Asencio et al., 2014; Haack et al., 2016; McTaggart et al., 2015; Shoemaker et al., 2015; Wu et al., 2017). Due to the pigment violacein, the capacity to generate a violet-purple color is a distinguishing characteristic of this species. Violacein is a secondary metabolite with antibacterial, antiviral, and anticancer effects (Andrighetti-Fröhner et al., 2003; Asencio et al., 2014; Bromberg et al., 2010). Consequently, these bacteria are of biotechnological interest (Li et al., 2016). Members of the *Janthinobacterium* can nonetheless cause significant agricultural losses in the form of soft rot in farmed button mushrooms, necessitating the hunt for *Janthinobacterium*-associated bacteriophages. To date, one lytic *Janthinobacterium*-associated

bacteriophage (MYSP06) from the *Siphoviridae* family that infects the purple pigment-producing strain *Janthinobacterium* sp. MYB06 has been identified, however, the genome has not yet been sequenced (Li et al., 2016).

5.4. The genus *Luteibacter*

Luteibacter is a member of the *Xanthomonadaceae* family, which belongs to the γ -subclass of Proteobacteria. Johansen et al. established the genus based on the species *Luteibacter rhizovicinus* DSM 16549^T (Johansen et al., 2005). Currently, the genus *Luteibacter* consists of five species, three of which are validly published: *L. rhizovicinus* DSM 16549^T (Johansen et al., 2005), *L. yejuensis* DSM 17673^T (Kämpfer et al., 2009; Kim et al., 2006), *L. anthropi* CCUG 25036^T (Kämpfer et al., 2009), *L. jiangsuensis* (Wang et al., 2011), and *L. pinisoli* (Akter and Huq, 2018). The genus *Luteibacter* is comprised of Gram-negative, aerobic, yellow-colored rods (Figure 6). To date, neither *Luteibacter*- nor *Rhodanobacterceae*-associated phages have been identified.

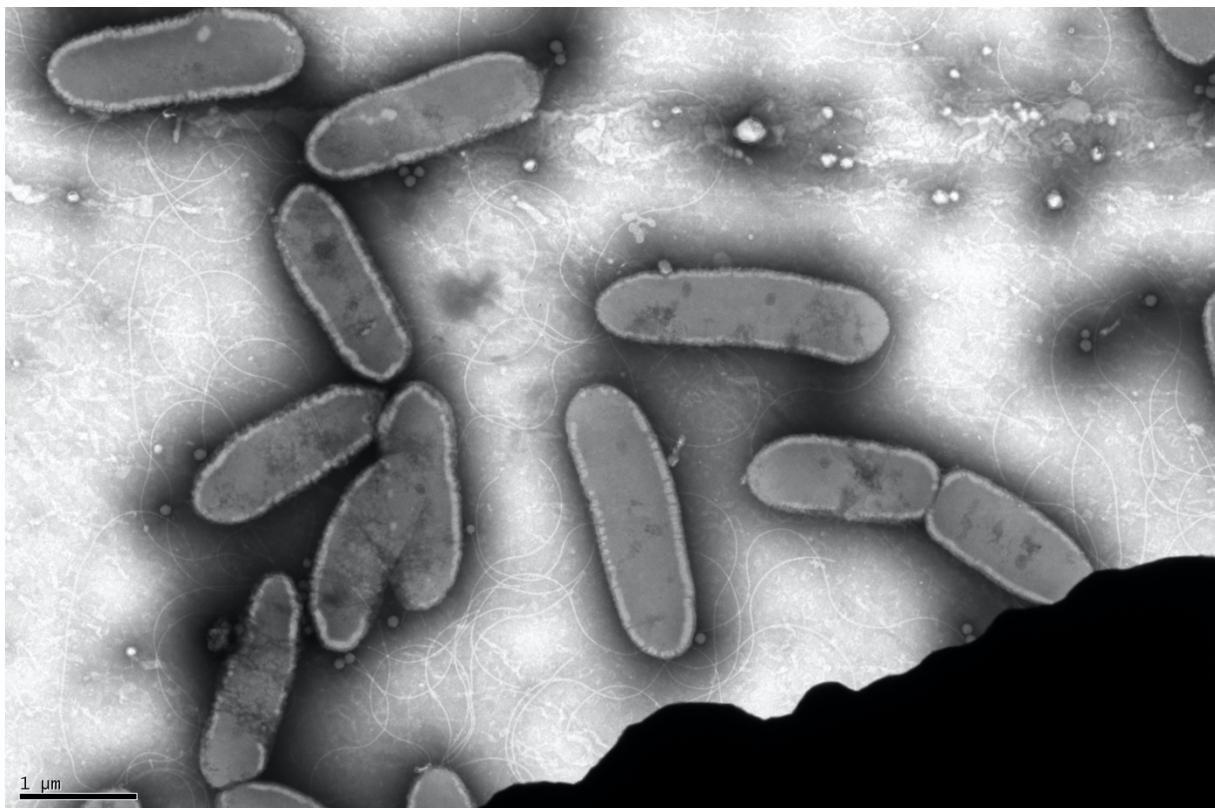


Figure 6. Transmission electron microscopy image of *Luteibacter flocculans* EIF3. Micrograph shows the new morphotype of the isolate. Negative staining and TEM analysis after 24 h of cell growth at 30 °C in LB medium.

5.5. The genus *Stenotrophomonas*

The genus *Stenotrophomonas* belongs to the family *Lysobacteraceae*, which is part of γ -subclass Proteobacteria which includes 16 genera (Parte et al., 2020). The genus *Stenotrophomonas* consists of 16 species of which *Stenotrophomonas maltophilia* is the most prominent. *S. maltophilia* is the only species of *Stenotrophomonas* known to be an opportunistic pathogen with multidrug resistance (Brooke, 2012). In immunocompromised patients, it causes nosocomial and community-acquired infections. Currently, 81 phage genomes (either consisting of dsDNA or ssDNA) are available in the NCBI Virus database (Brister et al., 2015).

5.6. The genus *Kinneretia*

The genus *Kinneretia* is a member of the *Comamonadaceae* family, which is part of the β -subclass of the Proteobacteria and includes 53 genera (Parte et al., 2020). The genus *Kinneretia* consists only of the species *Kinneretia asaccharophila* which is not able to grow on glucose and was therefore named “not sugar loving” (Gomila et al., 2010). To date, no *Kinneretia*-associated phages have been identified but 16 *Comamonadaceae*-associated phages have been described (Brister et al., 2015).

6. Research goals

Based on the examination of sequence data from public databases, the majority of bacteriophage genomes appear to consist of double-stranded DNA (dsDNA). According to Dion et al., over 85% of all phages in public genome databases belong to the *Caudovirales*. The authors state that, with the discovery of new phages, the disproportionate representation of tailed dsDNA phages will likely decrease soon (Dion et al., 2020). This raises the question of whether the phage diversity we currently know is affected by methodology? Will a more complex composition reveal itself when new techniques are applied? Are we missing phages by relying solely on plaque overlay assays for isolation and standard dsDNA sequencing techniques? Our hypothesis is, that the diversity of phages is greater than currently known, as metagenomic data indicate an immense viral diversity (Dion et al., 2020). As not all bacteria can be isolated in pure cultures, neither can their associated phages. This indicates a great hidden phage diversity.

This study aimed to identify novel bacteriophages and verify whether the viral diversity in our environment is more pronounced than we can recover using standard methods. Our host systems were selected based on the proximity to the strains *Escherichia* and *Caulobacter* which are associated with DNA and diverse RNA viruses. Here, the dsDNA giant phage ϕ Cp34, associated with *Caulobacter crescentus* (Fukuda et al., 1976) was successfully isolated. Further, RNA phages were isolated by the group during the same time (Miyakawa et al., 1976). The genus *Escherichia* is associated with the ssDNA phage ϕ X174 (Sanger et al., 1977), the dsDNA phage T7 (Demerec and Fano, 1945), and the ssRNA phage MS2 (Davis et al., 1961). Thus, they may be infected by as many genomically distinct phage types as possible. Therefore, the initial step in this thesis, was the isolation of strains which belong to the same family or order as *Caulobacter*, and *Enterobacter*. The bacterial community of twelve different sampling sites (oligotrophic and eutrophic ponds) was investigated and a total of 37 unique strains were isolated. Six of these strains were studied in detail, namely: *B. pondensis*, *B. goettingensis*, *S. marcescens* LVF3, *J. lividum* EIF1 and EIF2, *L. flocculans*, *S. indicatrix* DAIF1 and *Kinneretia* sp. DAIF2.

Brevundimonas pondensis LVF1 (Friedrich et al., 2021c) and *Serratia marcescens* LVF3 (Friedrich et al., 2021a) were investigated as host systems. Both showed the closest proximity to *Caulobacter* and *Escherichia*, which are associated with diverse DNA and RNA viruses. *B. pondensis* is an oligotrophic bacterium and a member of the *Caulobacteraceae* family, the same family *Caulobacter* belongs to. The strain is Gram negative, aerobic, has a single flagellum, and grows best at 30 °C. *Serratia marcescens* belongs to the *Yersiniaceae* family and the order Enterobacterales, which also includes *Escherichia*. It is Gram-negative and flagellated, but copiotrophic. Optimal growth temperature is also at 30 °C. Both host systems are ideal for studying viral diversity, as preliminary plaque assays on both, yielded a high number of distinct plaques. Subsequently, we addressed not only dsDNA but also ssDNA, dsRNA and ssRNA viromes. Sewage, which is the most phage-rich environment, was used as source material. Samples were taken in two different seasons (winter and summer). To investigate the undiscovered potential of phages, isolates were characterized by morphology, genome sequence, and alignment to metagenomic data (Figure 7).

Further, viral diversity was investigated with the sister strain of *B. pondensis* – *B. goettingensis* from the winter season. In addition, phage isolates of *Janthinobacterium lividum* EIF1 and *Luteibacter flocculans* were isolated and analyzed further.

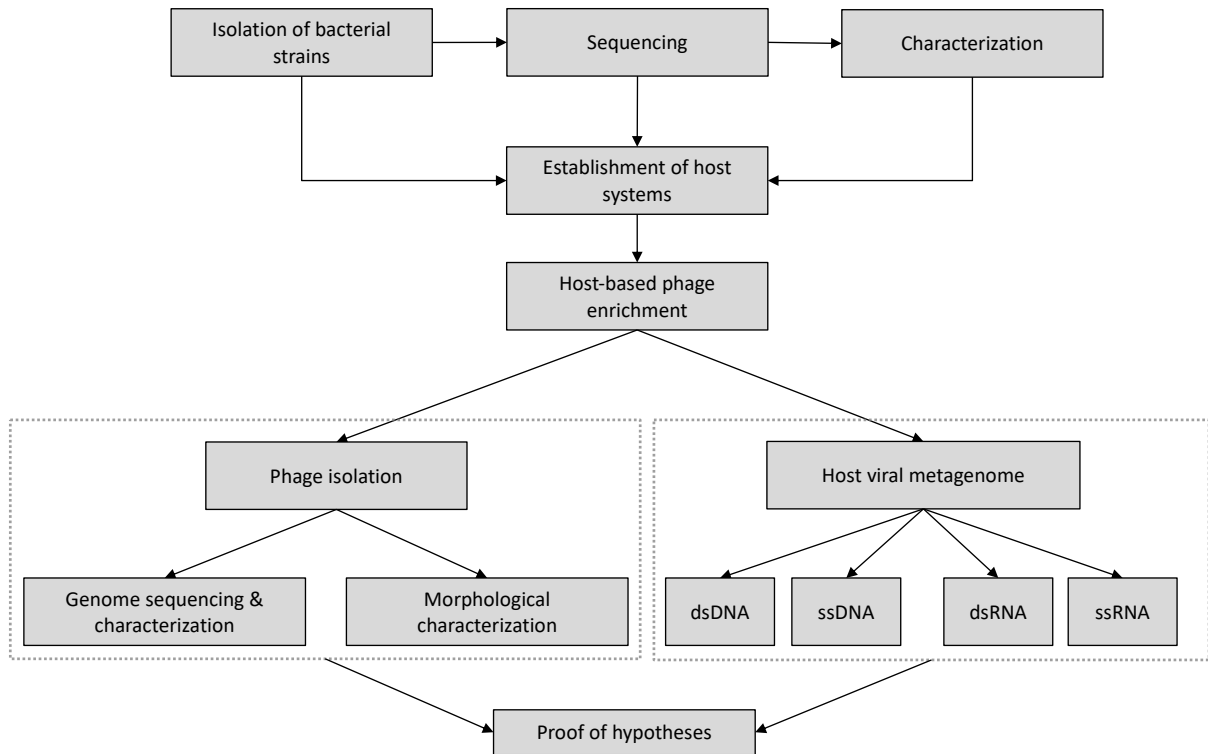


Figure 7. Experimental overview.

Results and publications

1. Living in a puddle of mud: Isolation and characterization of two novel *Caulobacteraceae* strains *Brevundimonas pondensis* sp. nov. and *Brevundimonas goettingensis* sp. nov.

Ines Friedrich¹, Anna Klassen¹, Hannes Neubauer¹, Dominik Schneider¹, Robert Hertel² and Rolf Daniel¹

Applied Microbiology (13 May 2021), 1, 1: 38–59
<https://doi.org/10.3390/applmicrobiol1010005>

Affiliations

¹Genomic and Applied Microbiology & Göttingen Genomics Laboratory, Institute of Microbiology and Genetics, Georg-August-University of Göttingen, Grisebachstraße 8, 37077 Göttingen, Germany

²FG Synthetic Microbiology, Institute of Biotechnology, BTU Cottbus-Senftenberg, Senftenberg, Germany

Author contributions:

Conceptualization: **IF**, RH, RD

Experiments: **IF**, AK, NH

Data analysis: **IF**, DS, RH

Writing: **IF**, RH

Interpretation of results: **IF**, AK, NH, DS, RH, RD

Writing – review & editing: **IF**, AK, NH, DS, RH, RD



Article

Living in a Puddle of Mud: Isolation and Characterization of Two Novel *Caulobacteraceae* Strains *Brevundimonas pondensis* sp. nov. and *Brevundimonas goettingensis* sp. nov.

Ines Friedrich ¹, Anna Klassen ¹, Hannes Neubauer ¹, Dominik Schneider ¹, Robert Hertel ² and Rolf Daniel ^{1,*}

- ¹ Genomic and Applied Microbiology and Göttingen Genomics Laboratory, Institute of Microbiology and Genetics, Georg-August-University of Göttingen, 37077 Göttingen, Germany; ines.friedrich@uni-goettingen.de (I.F.); ge35ruh@mytum.de (A.K.); hannes.neubauer@stud.uni-goettingen.de (H.N.); dschnei1@gwdg.de (D.S.)
- ² FG Synthetic Microbiology, Institute of Biotechnology, BTU Cottbus-Senftenberg, 01968 Senftenberg, Germany; hertel@b-tu.de
- * Correspondence: rdaniel@gwdg.de

Abstract: *Brevundimonas* is a genus of freshwater bacteria belonging to the family *Caulobacteraceae*. The present study describes two novel species of the genus *Brevundimonas* (LVF1^T and LVF2^T). Both were genomically, morphologically, and physiologically characterized. Average nucleotide identity analysis revealed both are unique among known *Brevundimonas* strains. In silico and additional ProphageSeq analyses resulted in two prophages in the LVF1^T genome and a remnant prophage in the LVF2^T genome. Bacterial LVF1^T cells form an elliptical morphotype, in average 1 µm in length and 0.46 µm in width, with a single flagellum. LVF2^T revealed motile cells approximately 1.6 µm in length and 0.6 µm in width with a single flagellum, and sessile cell types 1.3 µm in length and 0.6 µm in width. Both are Gram-negative, aerobic, have optimal growth at 30 °C (up to 0.5 to 1% NaCl). Both are resistant towards erythromycin, meropenem, streptomycin, tetracycline and vancomycin. Anaerobic growth was observed after 14 days for LVF1^T only. For LVF1^T the name *Brevundimonas pondensis* sp. nov. and for LVF2^T the name *Brevundimonas goettingensis* sp. nov. are proposed. Type strains are LVF1^T (=DSM 112304^T = CCUG 74982^T = LMG 32096^T) and LVF2^T (=DSM 112305^T = CCUG 74983^T = LMG 32097^T).



Citation: Friedrich, I.; Klassen, A.; Neubauer, H.; Schneider, D.; Hertel, R.; Daniel, R. Living in a Puddle of Mud: Isolation and Characterization of Two Novel *Caulobacteraceae* Strains *Brevundimonas pondensis* sp. nov. and *Brevundimonas goettingensis* sp. nov.. *Appl. Microbiol.* **2021**, *1*, 38–59. <https://doi.org/10.3390/applmicrobiol1010005>

Academic Editor:
Zuzanna Drulis-Kawa

Received: 6 April 2021
Accepted: 11 May 2021
Published: 13 May 2021

Publisher's Note: MDPI stays neutral with regard to jurisdictional claims in published maps and institutional affiliations.



Copyright: © 2021 by the authors. Licensee MDPI, Basel, Switzerland. This article is an open access article distributed under the terms and conditions of the Creative Commons Attribution (CC BY) license (<https://creativecommons.org/licenses/by/4.0/>).

Keywords: *Brevundimonas*; phage host system; prophages; *Caulobacteraceae*

1. Introduction

The bacterial family *Caulobacteraceae* belongs to the α -subclass of Proteobacteria and is the only member within the order *Caulobacterales* [1]. It includes the genera *Asticcacaulis*, *Brevundimonas*, *Caulobacter* and *Phenylobacterium* [2]. The members of *Caulobacteraceae* thrive in diverse habitats such as freshwater, seawater, soil, plants and humans [3]. All members are Gram-negative, aerobic or facultative anaerobic, and rod-shaped or vibrioid. They divide asymmetrically while one cell is sessile with prosthecae [4], and the other cell is motile with a polar flagellum [5]. The swarmer daughter cells move freely in the environment until they form a stalk and attach to substrates [6]. The stalked cell has the ability to divide asymmetrically. This unusual cell cycle was intensively studied in *Caulobacter*. Representatives of the genus *Caulobacter* often occur in “rosettes”, which can be interpreted as clusters of stalk cells attached to each other in groups [7]. The single-celled organism was originally described in 1935 by Henrici and Johnson based on microscopic findings with respect to microorganisms attached to microscopic slides that had been hatched in a freshwater lake (Henrici and Johnson, 1935).

Caulobacter has a broad habitat range and occurs in freshwater, seawater and terrestrial environments [8]. Their closest relatives are organisms that are classified as members of the

genus *Brevundimonas* [9]. The genus *Brevundimonas* was introduced based on the reclassification of two *Pseudomonas* species as *Brevundimonas diminuta* and *Brevundimonas vesicularis* [9]. *Brevundimonas* appears in various habitats such as soils, deep seafloor sediments, activated sludge, black sand, blood, and aquatic habitats [10–16]. They are usually non-prosthecate motile bacteria with polar flagella with only a few sessile species [11,16–18]. Abraham et al., suggest that species from the genus *Brevundimonas* may have lost the ability to form prosthecate during evolution or permanently migrated in the motile stage of the developmental cycle [2].

Moreover, *Brevundimonas* and *Caulobacter* are similar regarding their lifestyles. Both species are K-strategists and can survive under oligotrophic conditions [19]. There are no nutritional characteristics that distinguish both genera clearly. Therefore, *Caulobacter* strains such as *Caulobacter subvibrioides*, *Caulobacter bacteroides* and *Caulobacter vesicularis* were reclassified to *Brevundimonas subvibrioides*, *Brevundimonas bacteroides* and *Brevundimonas vesicularis*, respectively [2]. Nowadays, 32 *Brevundimonas* species and 12 *Caulobacter* species (LPSN [20] accessed on 1 November 2020) are known.

Three phages infecting *Asticcacaulis biprotheticum* are known [3] and seven *Brevundimonas vesicularis*-associated phages have been isolated and genetically characterized [21]. *Caulobacter*-associated phages like *Caulobacter vibrioides* CB13B1a bacteriophage ϕ Cd1 is an icosahedral DNA phage with a short non-contractile tail. It infects both prosthecate and swarmer cells [22]. Besides common dsDNA phages [23], RNA phages are known to infect *Caulobacteraceae*, i.e., ϕ Cb5, a small polyhedral RNA phage belonging to the *Leviviridae* family. The phage has been broadly used as model for molecular biology studies [24,25]. The verified association of *Caulobacter* with diverse phage types indicates that this genus is suitable for analysis of exceptionally diverse viral communities. This contributes also to how a virome associated with a particular host is composed concerning the ssDNA, dsDNA, dsRNA and ssRNA genomes of its phages. The aim of the present investigation was to isolate and characterize a bacterial strain of the *Caulobacteraceae* family suitable to serve in further studies as a host system to access the viral diversity of *Caulobacteraceae*-related phages present in the environment.

2. Materials and Methods

2.1. Isolation of the Bacteria and DNA Extraction

Environmental samples of twelve different sampling sites were collected. Six samples were taken from an oligotrophic pond located in the northern part of Weende, Göttingen, Germany. These environmental samples derived from frog's lettuce (*Groenlandia densa*) (PM), pond water (PW), surface water near pond algae (WSA), surface water near frog's lettuce (WSP), surface water of reed (WSR) and surface water close from Weende River entrance (WSW). Additionally, three samples were collected from the Weende River nearby the oligotrophic pond. Those samples are river water (RW) and (mixed = different sizes) river stones (RS and MRS). Further, two samples were gathered from a eutrophic pond at the North Campus of the Georg-August University Göttingen, which are surface water (POW) and surface water of stale eutrophic pond (PSW). In addition, samples from a puddle close by the eutrophic pond were collected as well (PUW). The specific coordinates of the sites and dates of the sampling are depicted in Table 1.

Table 1. Coordinates of sampling sites and dates sampling.

Samples	Coordinates	Date
MRS	51°33'58'' N 9°56'18'' E 230 m	6 September 2018
PW	51°33'57'' N 9°57'20'' E 230 m	6 September 2018
RS	51°33'58'' N 9°56'18'' E 230 m	6 September 2018
RW	51°33'58'' N 9°56'18'' E 230 m	6 September 2018
WSP	51°33'59'' N 9°56'22'' E 230 m	11 September 2018
WSW	51°33'59'' N 9°56'23'' E 230 m	11 September 2018
WSA	51°33'58'' N 9°56'22'' E 230 m	11 September 2018
WSR	51°33'58'' N 9°56'22'' E 230 m	11 September 2018
PM	51°33'58'' N 9°56'22'' E 230 m	11 September 2018
POW	51°33'29'' N 9°56'41'' E 173 m	24 September 2018
PSW	51°33'29'' N 9°56'41'' E 173 m	24 September 2018
PUW	51°33'27'' N 9°56'40'' E 173 m	24 September 2018

Enrichment cultures were performed as described by Friedrich et al., (2020, 2021) and Hollensteiner et al., (2021) using environmental water samples and river stones as inoculum for peptone medium containing 0.001% (*w/v*) peptone (Carl Roth GmbH + Co. KG, Karlsruhe, Germany) [26–28]. Cultures were incubated undisturbed for three weeks at 25 °C [29]. Additionally, MRS, PW, RS, and RW were enriched with 5% (*v/v*) MeOH and 0.001% (*w/v*) peptone. Biofilm and water surface material were sampled and streaked on 0.05% peptone-containing agar medium supplemented with 1% vitamin solution No. 6 [4] and 1.5% agar. After colony formation, they were transferred onto a diluted peptone agar plate supplemented with CaCl₂ (PCa) [29] and incubated for four days at 25 °C. For the singularization, colonies were re-streaked at least four consecutive times.

Singularized colonies were cultured in liquid PCa medium. Bacterial genomic DNA was extracted with MasterPure™ complete DNA and RNA purification kit as recommended by the manufacturer (Epicentre, Madison, WI, USA). Bacterial cells were suspended in 500 µL Tissue and Cell Lysis Solution and transferred into Lysing Matrix B tubes (MP Biomedicals, Eschwege, Germany) and mechanically disrupted for 10 s at 6.5 m/s using FastPrep®-24 (MP Biomedicals, Eschwege, Germany). After centrifugation for 10 min at 11,000 × *g*, the supernatant was transferred into a 2.0 mL tube and 1 µL of Proteinase K (20 mg/mL; Epicenter) was added. The procedure was performed as recommended by the manufacturer with the modification of increasing MPC Protein Precipitation Reagent to 300 µL.

2.2. Amplicon Based 16S rRNA Gene Sequencing of Enrichment Cultures

The bacterial composition of each sample was determined via amplicon-based analysis of the V3-V4 region of the 16S rRNA gene using the bacterial primers S-D-Bact-0341-b-S-17 and S-D-Bact-0785-a-A-21 [30] containing adapters for Illumina MiSeq sequencing (Illumina, San Diego, CA, USA). The PCR reaction solution (50 µL) contained 1-fold Phusion GC buffer, 200 µM dNTPs, 5% DMSO, 0.2 µM of each primer, 200 µM MgCl₂, 1 U Phusion polymerase (Thermo Fisher Scientific, Waltham, MA, USA) and 25 ng extracted DNA. Initial denaturation was performed at 98 °C for 1 min, followed by 25 cycles of denaturation at 98 °C for 45 s, annealing at 55 °C for 45 s and elongation at 72 °C for 45 s. The final elongation was for 5 min at 72 °C. PCR Reactions were performed in triplicate for each sample. The resulting PCR products were pooled in equal amounts and purified through MagSi-NGS^{PREP} Plus as recommended by the manufacturer (MagnaMedics, Aachen, Germany). Quantification of the PCR products was performed using the Quant-iT dsDNA HS assay kit and a Qubit fluorometer (Invitrogen, Carlsbad, CA, USA). Illumina paired-end sequencing libraries were constructed using the Nextera XT DNA sample preparation kit (Illumina, Inc., San Diego, CA, USA). Sequencing was performed with an Illumina MiSeq instrument using the dual index paired-end approach (2 × 300 bp) and V3 chemistry as recommended by the manufacturer (Illumina). The sequencing was performed in-house by the Göttingen Genomics Laboratory.

The 16S rRNA genes of specific isolates were amplified with the primer pair 27F (5'-AGAGTTTGATCMTGGCTCAG-3') and 1492R (5'-TACGGYTACCTTGTTACGACTT-3') [31]. PCR reaction mixture (50 µL) contained 10 µL 5-fold Phusion HF buffer, 200 µM of each dNTP, 3% DMSO, 0.2 µM of each primer, and 1 U Phusion polymerase (Thermo Fisher Scientific, Waltham, MA, USA) and 100 ng DNA. The previously mentioned cycling scheme was modified to an annealing temperature of 50 °C and 30 cycles. Sanger sequencing of the PCR products was done by Microsynth Seqlab (Göttingen, Germany).

2.3. Amplicon Sequence Analysis

Raw paired-end reads from the Illumina MiSeq were quality-filtered with fastp v0.20.0 [32]. Default settings were used with the addition of an increased per base phred score of 20, 5'- and 3'-end read-trimming with a sliding window of 4, a mean quality of 20, minimal sequence length of 50 bp and removal of paired-end read adapters. The paired-end reads were merged using PEAR v0.9.11 [33]. Potential remaining primer sequences were clipped with cutadapt v2.5 [34]. VSEARCH v2.14.1 [35] was used to sort and size-filter the merged reads using a minimum sequence length of 300 bp. Then, reads were dereplicated and denoised with UNOISE3 [36] using default settings. Finally, chimeras were removed de novo and afterwards reference-based against the SILVA SSU database v138.1 [37] resulting in the final set of amplicon sequence variants (ASVs). Quality-filtered and merged reads were mapped against the ASVs to create an abundance table with VSEARCH using default settings. The taxonomy was assigned using BLAST 2.9.0+ [38] against the SILVA SSU 138.1 NR database [37] with an identity of at least 90% to the query sequence. To improve classification results, the best hits were only accepted if “% sequence identity + % alignment coverage)/2 ≥ 93” (see SILVAngs_User_Guide_2019_08_29.pdf). Additionally, all extrinsic taxa (Chloroplast, Eukaryota, Mitochondria, Archaea) were removed from the dataset resulting in a total of 1029 amplicon sequence variants (ASVs). The dataset was analyzed in R (v4.0.2) [39] and RStudio (v1.3.1056) [40]. Bar charts were generated with ggplot2 (v3.3.2) [41] using standard R packages.

2.4. Genome Sequencing, Assembly and Annotation

Illumina paired-end sequencing libraries were prepared using Nextera XT DNA Sample Preparation kit and sequenced using the MiSeq-system and reagent kit version 3 (2 × 300 bp) as recommended by the manufacturer (Illumina, San Diego, CA, USA). To perform Nanopore sequencing, 1.5 µg DNA were utilized for library preparation using Ligation Sequencing kit (SQK-LSK109) and Native Barcode Expansion kit EXP-NBD103 (Barcodes 4 and 5; Oxford Nanopore Technologies, Oxford, UK). Sequencing was performed for 72 h by using MiniON device, a SpotON Flow Cell and MinKNOW software v19.05.00 as recommended by the manufacturer (Oxford Nanopore Technologies). For demultiplexing, Guppy version v3.0.3 was employed. Raw Illumina MiSeq sequences were adapter—and quality—trimmed employing Trimmomatic v0.39 [42] and paired reads joined with FLASH v1.2.11 [43]. Nanopore reads were adapter- and quality-trimmed with fastp v0.20.0 [32] and only reads >10 kb were included in further analysis. The obtained quality-filtered Nanopore reads served as input for a hybrid assembly employing the Unicycler pipeline v0.4.9b in normal mode [44], which included SPAdes v3.14.1 [45], Racon vv.1.4.15 [46], makeblastdb v2.10.0+ and tblastn v.2.10.0+ [47], bowtie2-build v2.4.1, bowtie2 v.2.4.1 [48], SAMtools v.1.10 [49], java v.1.8.0_152 [50], and Pilon v.1.23 [51]. Illumina short-read coverage information was obtained through read-mapping with bowtie2 to the final genome. Mapping and sorting was done with SAMtools and analysis with Qualimap v.2.2.2 [52]. Nanopore long-read coverage information was obtained through QualiMap v.2.2.2. Mapping, sorting and analysis were performed as described for the short reads. Genome orientation of both genomes was performed based on the gene encoding the chromosomal replication initiation protein DnaA. Assembled genomes were checked with Bandage v0.8.1 [53]. CRISPR regions were identified with CRISPRFinder [54]. Quality of assembled genomes was assessed with CheckM v1.1.2 [55] (Supplementary Table S1).

Genome annotation was performed using the Prokaryotic Genome Annotation Pipeline v4.13 (PGAP) [56].

2.5. Preparation and Sequencing of Prophages and Visualization Using TraV

An overnight culture of *Brevundimonas* sp. nov. LVF1^T and LVF2^T was set up in a 100 mL Erlenmeyer flask using 25 mL PYE medium (0.2% peptone, 0.1% yeast extract, 0.02% MgSO₄ × 7 H₂O) and inoculated with an OD₆₀₀ of 0.1. The cultures were incubated over a 3-day period on a shaker (180 rpm, Infors HT (Orbitron, Einsbach, Germany)) at 30 °C without using Mitomycin C for prophage induction [57]. After the incubation period, the cultures were transferred into a 50 mL centrifuge tube and centrifuged at 10,020 × g and 4 °C for 15 min. The supernatant was sterile-filtered (0.2 µm pore size of filter) and supplemented with PEG-8000 (10% (w/v) final concentration), MgSO₄ (1 mM final concentration) and 5 µL salt-active nuclease (SERVA Electrophoresis GmbH, Heidelberg, Germany). The suspension was precipitated for 24 h at 4 °C and centrifuged at 10,020 × g and 4 °C for 1 h. The supernatant was discarded, and the pellet suspended in 300 µL TMK buffer (10 mM Tris, 5 mM MgCl₂, 300 mM KCl, pH 7.5).

Prophage DNA was extracted with MasterPure™ complete DNA and RNA purification kit and was sequenced using the above-mentioned protocol for Illumina genome sequencing.

Illumina MiSeq raw paired-end reads were merged and adapter and quality-trimmed employing Trimmomatic v0.39 [42]. Sequences were then mapped against the host genome through bowtie2 v2.4.1 [48]. SAM table was converted to TDS format (flat file data format), which is the input for TraV (Transcriptome Viewer). The program TraV was designed to map transcriptome data on a genome [58]. In this study, it was employed to display the read coverages from the sequencing runs for the prophages of LVF1^T and LVF2^T mapped onto their host genomes [59]. Integration sites of the prophages (*attL* and *attR* sites) were identified through the comparison of experimentally indicated *att* regions (1 kb to each side from the indicated coordinate), against the remaining genome sequence.

2.6. Phylogenetic Classification of *Brevundimonas* sp. nov. LVF1^T and LVF2^T

To provide an initial taxonomic classification of the *Brevundimonas* sp. nov. isolates, Genome Taxonomy Database Toolkit (GTDB-Tk) v1.0.2 [60] was employed. In addition, a phylogenetic analysis was performed with ANIm method of pyani v0.2.10 [61]. The typical percentage threshold for species boundary (95% ANI) was used [62]. Based on the list of Deutsche Sammlung von Mikroorganismen und Zellkulturen (DSMZ, Braunschweig, Germany), available type strain genomes were downloaded from the National Centre for Biotechnological Information (NCBI, accessed 30 September 2020) including *B. alba* DSM 4736^T (PRJNA583246), *B. aurantiaca* DSM 4731^T (PRJNA583252), *B. aveniformis* DSM 17977^T (PRJNA185350), *B. bacteroides* DSM 4726^T (PRJNA221004), *B. basaltis* DSM 25335^T (PRJNA632231), *B. bullata* HAMBI_262^T (PRJNA224116), *B. diminuta* NCTC 8545^T (PRJEB6403), *B. halotolerans* DSM 24448^T (PRJNA546766), *B. halotolerans* MCS24^T (PRJNA484836) *B. lenta* DSM 23960^T (PRJNA583271), *B. mediterranea* DSM 14878^T (PRJNA583270), *B. naejangsensis* DSM 23858^T (PRJNA188849), *B. nasdae* JCM 11415^T (PRJNA269640), *B. subvibrioides* ATCC 15264^T (PRJNA36643), *B. terrae* DSM 17329^T (PRJNA546765), *B. vancouverensis* NCTC 9239^T (PRJEB6403), *B. variabilis* DSM 4737^T (PRJNA583272), *B. vesicularis* NBRC 12165^T (PRJDB1343) and *B. viscosa* CGMCC 1.10683^T (PRJEB17543). The type strain genome of the species *B. halotolerans* was sequenced twice (DSM 14878^T and MCS24^T). Both were included in the analysis due to their differences in coverage and annotation.

2.7. Comparative Genomics

Metabolic analysis of LVF1^T and LVF2^T was investigated using BlastKOALA v2.2 [63] (Supplementary Figure S1). Putative secondary metabolite biosynthetic gene clusters were identified with antiSMASH v5.2.0 [64,65]. Putative phage regions were identified with

PHASTER [66]. Antibiotic resistance annotation was investigated employing Resfams v1.2.2 [67].

2.8. Cell Morphology and Gram Staining Procedure

Colony morphology was studied on R2A agar medium (Fluka, Munich, Germany) by microscopy (Primo Star, Zeiss, Carl Zeiss Microscopy, Jena, Germany) of single colonies of each isolate (4× magnification). Subsequently, colonies were observed after 24 and 48 h using image processing software ZEISS Labscope (Carl Zeiss Microscopy, Jena, Germany). A Gram-staining analysis was performed according to Claus [68] using reagents Hucker's crystal violet, an iodine and safranin solution and 1-propanol to determine the Gram classification of each isolate. Each preparation was evaluated using Labscope software.

2.9. Transmission Electron Microscopy

Colony morphology of the isolates was observed by transmission electron microscopy (TEM). Data were imaged onto the screen using the software program digital Micrograph (Gatan GmbH, Munich, Germany). Both isolates were grown in liquid PYE medium [29] overnight at 30 °C. Afterwards, a negative staining technique was performed. 5 µL cell suspension were mixed with the same amount of diluted 0.1% phosphotungstic acid (3% stock, pH 7) and were transferred to a vaporized carbon mica for 1 min. Subsequently, the mica was briefly washed in demineralized water and transferred to a thin copper-coated grid (PLANO GmbH, Marburg, Germany). The coated grids were dried at room temperature and were examined by Jeol 1011 TEM (Georgia Electron Microscopy, Freising, Germany).

2.10. Determination of Temperature Optimum and Salt Tolerance

To quantify the temperature optimum, both isolates were grown in 4 mL PYE medium at 10, 20, 30, 35 and 40 °C at 180 rpm in a Infors HT shaker (Orbitron, Einsbach, Germany). The optical density of the cell suspensions was measured using the Ultraspec 3300 pro photometer (Amersham Pharmacia Biotec Europe GmbH, Munich, Germany) at a wavelength of 600 nm (OD₆₀₀). The starting OD₆₀₀ of the cell cultures was 0.1.

For the determination of the salt tolerance, LVF1^T and LVF2^T were also inoculated in 4 mL PYE medium amended with 0, 5, 10, 20, 30 and 40 gL⁻¹ NaCl. OD₆₀₀ of the cell suspensions was set to 0.3 at the beginning of the experiment [2]. LVF1^T was incubated at 30 °C and 180 rpm in a Infors HT shaker (Orbitron, Einsbach, Germany). After the incubation period, the optical density of the isolates was measured at 600 nm. The differences between these two measurements were used for the determination of the salt tolerance [2]. All measurements were performed in biological replicates for each isolate. The collected data were illustrated with R studio version 4.0.2 [40] using the ggplot2 package [41].

2.11. Determination of Growth Kinetics

The growth kinetics in liquid cultures were measured with the cell growth quantifier (CGQuant 8.1) (Aquila Biolabs GmbH, Baesweiler, Germany) at 30 °C for 47 h. Pre-cultures were resuspended to a final OD₆₀₀ of 0.1 in 25 mL PYE medium and were filled into 250 mL shake flasks. Afterwards, all flasks were mounted onto the CGQ sensor plate and were shaken for 47 h. The CGQ enables a dynamic approach of backscattered light measurement, implementing to follow the growth of the liquid cultures in real time [69]. All measurements were performed in biological replicates. All collected data were illustrated with R studio version 4.0.2 [40] using ggplot2 package [41].

2.12. Anaerobic Growth

First, cultures from aerobic growth were used to inoculate 5 mL pre-reduced PYE medium in Hungate tubes [70] with a final OD₆₀₀ of 0.1. The cell suspensions were incubated at 30 °C. After five days, the pre-cultures were transferred to new Hungate tubes (final OD₆₀₀ of 0.1) and were incubated at 30 °C. Potential growth was observed

in a time frame of 14 days. The determination of anaerobic growth was performed in biological replicates.

2.13. Metabolic Activity and Antibiotic Resistances

Metabolic activities were identified using API ZYM and API 20 NE tests. Both tests were performed by following the instructions given by the manufacturer (BioMérieux, Nuertingen, Germany). Catalase activity was determined using 3% H₂O₂ [71].

For the determination of antibiotic resistances, the following discs and strips (Oxoid, Wesel, Germany) were used: ampicillin (25 µg), chloramphenicol (30 µg), doxycycline (30 µg), kanamycin (30 µg/mL), oxytetracycline (30 µg), rifampicin (2 µg), streptomycin (10 µg), vancomycin (30 µg), erythromycin (0.015–256 µg), meropenem (0.002–32 µg), tetracycline (0.015–256 µg). To determine the response of both strains to the antibiotic a soft-agar (0.4% (*w/v*) agarose in PYE medium) overlay technique was used. 2.5 mL soft agar were used to inoculate the isolates with a final OD₆₀₀ of 0.1. Afterwards, discs or strips were attached to the soft agar. All plates were incubated overnight at 30 °C.

3. Results

3.1. Enrichment of *Caulobacteraceae* from the Environment

To isolate organisms belonging to the family *Caulobacteraceae*, environmental samples were taken from plant material (frog's lettuce) from an oligotrophic pond (PM), surface water near pond algae (WSA), surface water near frog's lettuce (*Groenlandia densa*) (WSP), surface water of reed (WSR), surface water of Weende River entrance (WSW), mixed river stones (MRS), river stones (RS), pond water (PW), Weende River water (RW), eutrophic pond water (POW), surface water of stale eutrophic pond (PSW), and puddle water (PUW). These samples were used as inoculum for a 0.001% (*w/v*) peptone-based enrichment with and without methanol. Bacterial community compositions of the resulting cultures were analyzed based on the 16S rRNA gene amplicon analysis (Figure 1). Depending on the sample origin, we observed specific structures of the established bacterial community at order level. Cultures inoculated with oligotrophic samples always resulted in a similar composition of the microbial community regardless of the sampling site. There was also no significant difference between enrichment medium supplied with or without methanol at order level. Eutrophic water samples led to more diverse bacterial communities at order level with 105 different orders on average while oligotrophic water samples showed on average 10 different orders (Figure 1a). Detailed investigation of the alphaproteobacterial fraction revealed PW and PUW as the most promising samples for *Brevundimonas* isolation (Figure 1b). At genus level, a medium-dependent effect could be observed during the enrichments. Cultures enriched with methanol revealed *Brevundimonas* as the most dominant genus. The pond water (PW) sample showed the highest relative abundance of *Brevundimonas*. Cultures without methanol also contained genera of *Caulobacteraceae*, but those were not predominant and were surpassed by families such as *Rhodospiriliaceae* and *Rhizobiaceae*. Cultures of eutrophic enrichment showed a more diverse composition (105 different orders on average) and a relatively homogeneous distribution within the Alphaproteobacteria with an average of 8 bacterial genera. Only the puddle water (PUW) sample exhibited higher abundance of *Brevundimonas* and *Caulobacter* and was therefore used for further bacterial isolations together with the PW enrichment.

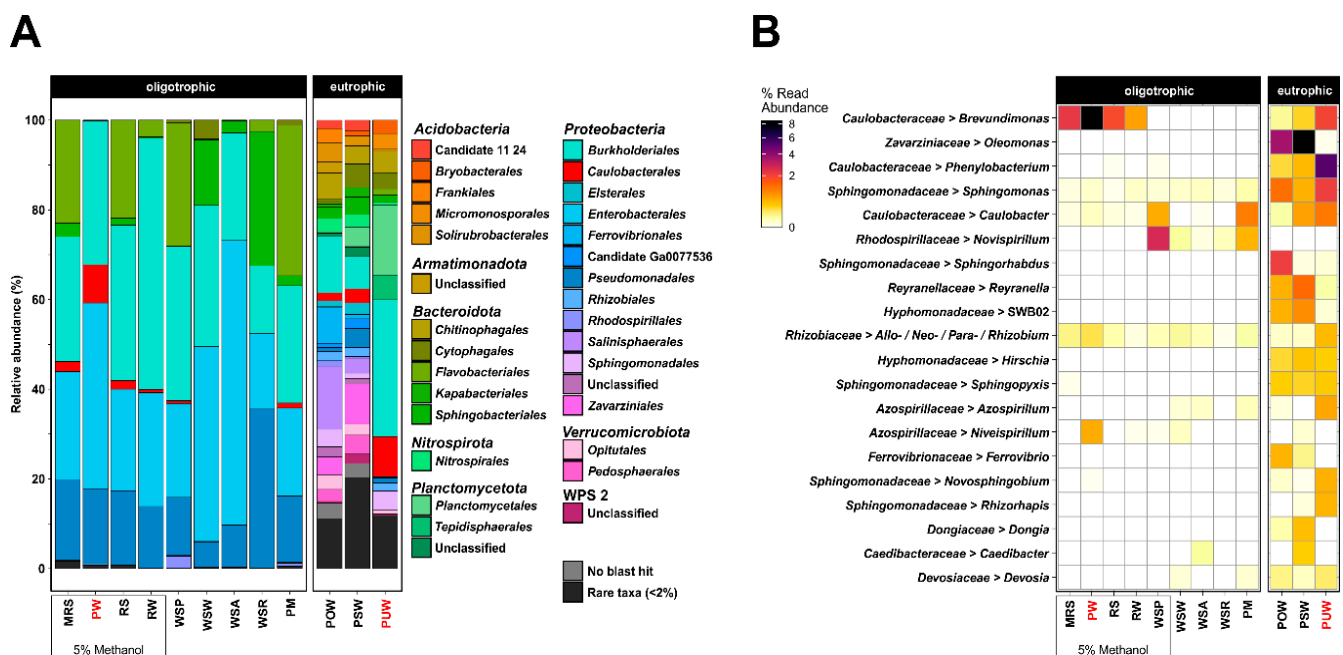


Figure 1. Amplicon-based analysis of the *Caulobacteraceae* enrichment from the different sampling sites. Relative abundance of bacterial family based on 16S rRNA gene analysis in cultures after enrichment with 0.001% (w/v) peptone and 0.001% (w/v) peptone with 5% (v/v) methanol. MRS, PW, RS and RW comprise the samples which were enriched with peptone and methanol. Red letters indicated enrichments of *Caulobacteraceae* used for isolation. (A) Each bacterial phylum depicted here comprises more than 2% relative abundance in at least one sample. (B) Relative read abundance of the top 20 enriched bacterial genera (including family) belonging to Alphaproteobacteria. Genera without cultured representatives and unclassified genera have been removed.

3.2. *Caulobacteraceae* Isolation from Enriched Environmental Samples

The different isolation attempts led to 37 individual isolates, which were all investigated by 16S rRNA gene sequencing (Supplementary Tables S2–S4). Three 16S rRNA gene sequences (LVF1, DAIF19 and LVF2) matched with those of known *Brevundimonas* strains (99.1 to 100% identity). Strains LVF1^T and DAIF19 derived from PW were identical, which was confirmed through Illumina sequencing (data not shown). Therefore, only the data from LVF1^T and LVF2^T were considered further. The remaining isolates did not belong to the *Caulobacteraceae* and were not further investigated. Examination of the remaining enrichment cultures resulted in 34 additional isolates. None of these could be assigned to the *Caulobacteraceae* family (Supplementary Table S5). Thus, we were able to isolate only members of *Brevundimonas* from the originally identified genera *Brevundimonas*, *Phenylobacterium* and *Caulobacter* of the family *Caulobacteraceae* (Figure 1b).

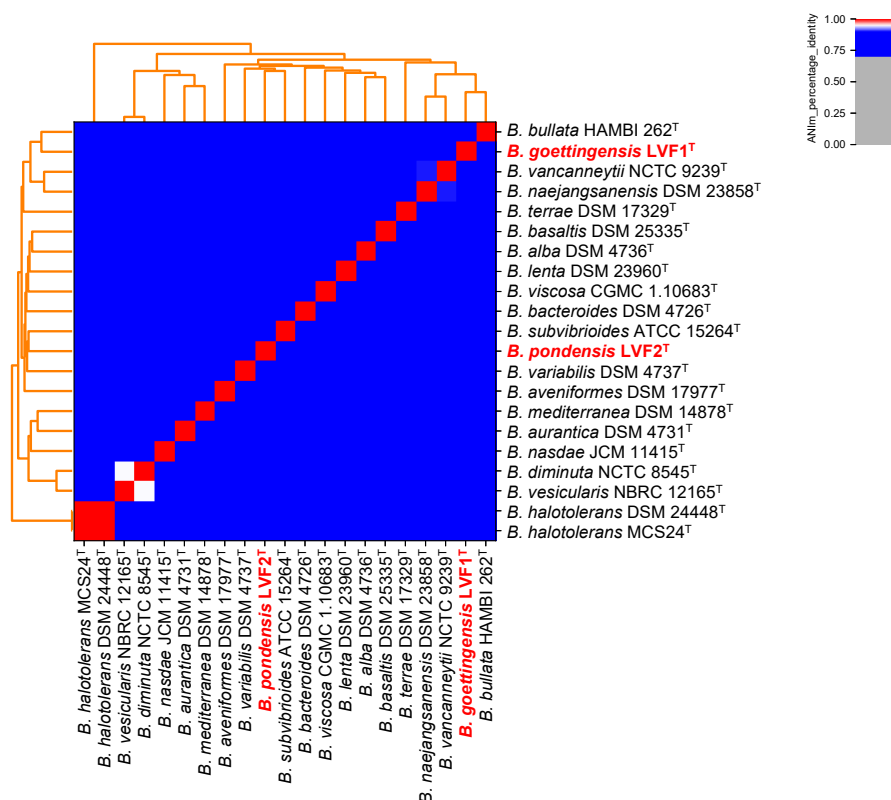
3.3. Phylogeny of LVF1^T and LVF2^T Based on Their Full Genome Sequence

In order to further classify the unique isolates LVF1^T and LVF2^T genome sequences were obtained. Both isolates were sequenced by Illumina and Oxford Nanopore technology. We were able to obtain high-quality closed genomes for both strains. The de novo hybrid genome assembly of LVF1^T, with an overall coverage (short- and long-reads) of 252.9-fold, resulted in one circular chromosome with a size of 3,550,773 bp and a GC-content of 67.04%. It encodes 3445 putative proteins, 58 rRNAs and 48 tRNAs. Assembly of strain LVF2^T exhibiting an overall sequence coverage of 245.4-fold resulted in a genome size of 3,984,955 bp with a GC-content of 67.79%. The chromosome encodes 3857 putative proteins, 57 rRNAs, 48 tRNAs. No plasmids and CRISPR regions were detected in both genomes. Genomic characteristics are listed in Table 2.

Table 2. Genome statistics of *Brevundimonas pondensis* sp. nov. LVF1^T and *Brevundimonas goettingensis* sp. nov. LVF2^T.

Features	<i>Brevundimonas pondensis</i> Sp. Nov. LVF1 ^T	<i>Brevundimonas goettingensis</i> Sp. Nov. LVF2 ^T
Genome size (bp)	3,550,773	3,984,955
GC content (%)	67.04	67.79
Coverage	252.9-fold	245.4-fold
CDS	3445	3857
rRNA genes	58	57
tRNA genes	48	48
ncRNA	4	3
CRISPR	0	0
Prophage(s)	2	1

Genome-based taxonomic assignment was performed with GTDB-Tk [60] and revealed an average nucleotide identity (ANI) for each strain of approximately 90% to the closest related species (ANI values 90.63-LVF1^T and 90.85-LVF2^T) (Supplementary Table S6). Additionally, the two isolates were confirmed as new species by employing the Type Strain Genome Server (TYGS) [72]. ANI-analysis with known type strains of the genus *Brevundimonas* is shown in Figure 2 (data in Supplementary Table S7). No cluster formation with any other characterized *Brevundimonas* strain was observed. Close nucleotide sequence identity shares LVF1^T with *B. diminuta* NCTC 8545^T with 85.06% and *B. naejangsanensis* DSM 23858^T with 86.44%, and LVF2^T with *B. lenta* DSM 23960^T with 85.35% and *B. subvibrioides* ATCC 15264^T with 85.06% respectively. The genomes of strains LVF1^T and LVF2^T share a sequence identity of 84.55%.

**Figure 2.** Phylogenetic analysis of *Brevundimonas pondensis* sp. nov. LVF1^T and *Brevundimonas goettingensis* sp. nov. LVF2^T. All available type strains (T) and representative strains (R) from the genus *Brevundimonas* were examined. Calculations were performed with pyani [61,73] using the ANIm method with standard parameters. Isolated strains LVF1^T and LVF2^T are depicted in bold red.

Thus, both strains are regarded as novel type strains of *Brevundimonas*, which we designated *Brevundimonas pondensis* sp. nov. LVF1^T and *Brevundimonas goettingensis* sp. nov. LVF2^T.

3.4. Identification of Prophage Regions

Prophage regions were initially analyzed with PHASTER [66], which revealed two putative prophage regions for *Brevundimonas pondensis* sp. nov. LVF1^T (region 1: 233,337–275,001; region 2: 330,414–348,898). The regions comprised 41.6 and 18.4 kb and were classified as incomplete (Supplementary Table S8). *Brevundimonas goettingensis* sp. nov. LVF2^T revealed one putative prophage region (245,339–261,838), comprising 16.5 kb. This was classified as intact despite its small size (Supplementary Table S9).

ProphageSeq [59] was applied for both strains and data of phage particle-packed dsDNA was mapped on the bacterial genomes and visualized (Figure 3). For LVF1^T, prophage reads accumulation associated with the PHASTER-predicted prophage regions, thereby indicating prophage activity. However, the coverage profile exhibits an uneven distribution of reads with a substantial coverage increase from base 254,001, followed by a constant decrease over 170 kbp following the replication direction of the genome (Figure 3). Thus, the mapping alone did not allow robust conclusions about the precise size of prophage 1 or prophage 2. Reads derived from assembled particle-packed dsDNA resulted in two contigs of 90,274 bp and 38,784 bp. The 38.8 kb contig was indicated as circular by the assembler. Sequence alignment with the host chromosome revealed that it represents the genome of prophage 2, including its *att* sites. Those were 73 bp long with one base deviation at position 15(TCAATCAAC-TAAGTa/gATTGAAAAGAATGGTGGACGCGACAGGGATTGAACCTGTGACCCCTACGATGCAACG). The integration locus of this prophage is a valine tRNA.

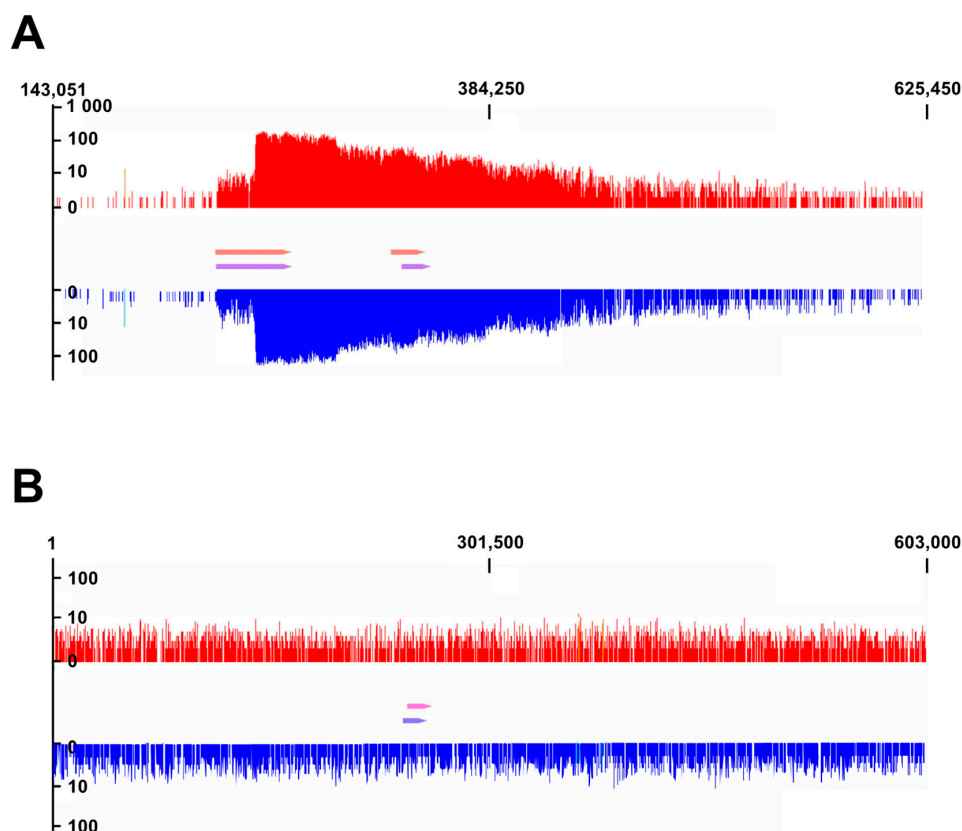


Figure 3. Read coverage profile of sequenced (A) LVF1^T and (B) LVF2^T prophages, mapped onto the corresponding host genome. The pinkish arrows depict the prophage regions, which were predicted with PHASTER [66]. In purple and blue are the experimentally verified prophage regions. Image A displays the read coverage of the LVF1^T genome between base 143,051 to 625,450 (482,399 kb). Image B displays the coverage of the LVF2^T genome between base 1 to 603,000 (629,999 kb).

The 90 kb contig represents mainly the sequence accumulation over the two prophage regions. The alignment with the host chromosome revealed the absence of prophage 2 in this genome fragment. Such an assembly result is only feasible if sequence reads are present crossing the prophage 2 region, which in turn is only possible if prophage 2 is excised from the host genome. Thus, this result indicates that prophage 2 is functional and capable to excise its viral genome from the host chromosome, circularize it, and package it in the procapsid.

Since it was not possible to obtain information on prophage 1, neither through sequence mapping nor read assembly, we aimed to narrow down its size by identifying its *att* sites. Due to the sequence accumulation of the particle-packaged DNA on its upstream boundary we suspected its *attL* site at position 233,401. Sequence analysis around this position and comparison against the entire genome of LVF1^T revealed an exact 58 bp long sequence at position 275,001 to 275,058 (TGGTGCGGGTGGGCCGGGCTCGAACCGGGCACTCTCTCGGAACAGGATTTGAATCCAG), representing the *attL/R* site of prophage 1. A leucine tRNA was identified as integration locus of prophage 1. The genome size of prophage 1 is 41,600 bp.

ProphageSeq of LVF2^T revealed no read accumulation neither at the predicted prophage location nor elsewhere on the bacterial chromosome. All phage particle-derived sequence reads mapped equally distributed over the entire host chromosome. Investigation of the surrounding gene annotations associated with the prophage prediction did not uncover any phage integration sites. However, the annotation enabled to adapt the boundaries of the predicted prophage region to 242,355 to 258,254, resulting in a final region size of 15,899 bp. Deduced proteins present in this region frequently encoded phage-related protein domains.

In conclusion, two prophage regions in the genome LVF1^T were identified and experimentally confirmed as particle-forming and capable of packing their genome. The prophage identified in the genome of LVF2^T is probably defective due to the random packing of the host chromosome.

3.5. Morphological Analysis of LVF1^T and LVF2^T

To get insights into strain-specific morphological characteristics, both colony morphology and cell morphology were analyzed. Colonies of LVF1^T, grown on PYE and R2A solid media, were colored grey-white, while colonies of strain LVF2^T were yellow. If grown overnight, the colony form of LVF1^T was elliptically shaped, convex and smooth and exhibited an average diameter of 0.8 mm. The same applies for LVF2^T colonies, which had an average diameter of approximately 1 mm (Supplementary Figure S2).

A Gram-staining of both isolates indicated a Gram-negative type (Supplementary Figure S3).

For transmission electron microscopy (TEM), liquid cultures (Supplementary Figure S4) of the isolates were used, which were grown in PYE medium and prepared with a negative staining technique. Single cells of LVF1^T were homogeneous in structure and size (Figure 4a,b). They were all motile, and stalks were not observed. The rod-shaped cells were approximately 1.0 µm in length and 0.46 µm in width with one flagellum. Cells of LVF2^T showed evidence for asymmetrical cell division. A sessile mother cell with 1.7 µm long prostheca (stalk) and a daughter cell with a polar flagellum (Figure 4c,d) was observed. The cell bodies of the sessile cells were vibrio-shaped with a length of approximately 1.3 and 0.7 µm width while the cell body of the swarmer cell was elliptical and 1.6 µm in length and 0.6 µm in width. Furthermore, cells attached to each other with the terminal ends of their stalks were detected (Figure 4c). This documents the ability of LVF2^T cells to adhere to surfaces or form rosettes, which were frequently reported for three genera of *Caulobacteraceae* [3]. Thus, both isolates are motile, and LVF2^T is able to differentiate into two cell types.

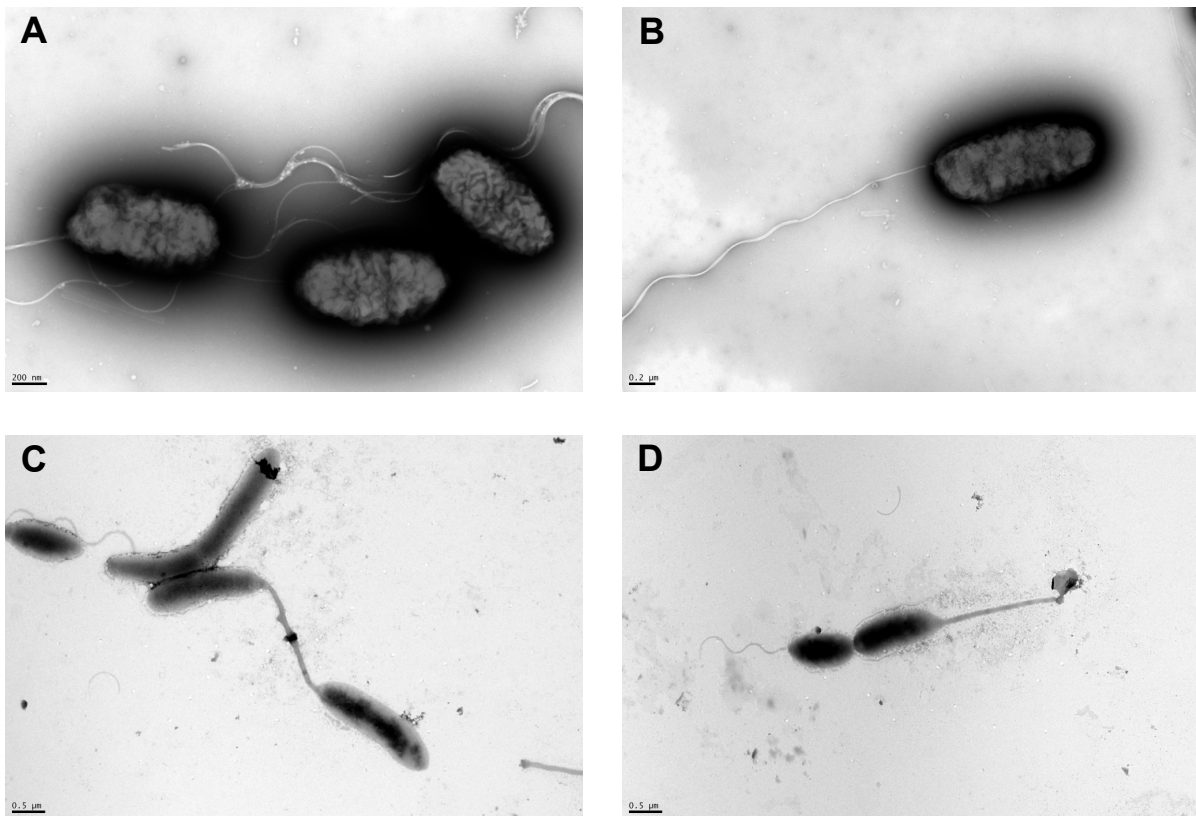


Figure 4. Transmission electron microscopy image of LVF1^T and LVF2^T. Micrographs show the general morphology of negatively stained cells of strains LVF1^T (A,B), and LVF2^T (C,D). LVF1^T at 30 °C was grown in liquid PYE medium for 24 h and LVF2^T in the same medium for 48 h.

3.6. Physiological Characterization

The physiological properties and the metabolic potential of the new proposed type strains were characterized by growth and metabolic experiments. Additionally, an antibiogram was generated to reveal the antibiotic resistance potential of both strains. LVF1^T was able to grow at a temperature range between 10 and 40 °C and LVF2^T between 10 and 35 °C. Both strains are mesophiles as their growth optimum was at 30 °C. LVF1^T reached higher cell densities at 30 °C than LVF2^T (OD₆₀₀ of 1.533 and 0.887, respectively; Figure 5a).

Both strains were able to grow in the presence of up to 4% (*w/v*) NaCl in PYE medium. The salt optimum of LVF1^T was between 0–1% (*w/v*) NaCl and that of LVF2^T between 0–0.5% (*w/v*) (Figure 5b).

Growth kinetics of both strains were determined under optimal salt and temperature conditions (Figure 5c). Under the experimental conditions, the lag phase of LVF1^T lasted for approximately three hours and that of LVF2^T for approximately eight hours. The duration of the exponential growth phase was 7.5 h for LVF1^T and 8 h for LVF2^T and thus almost identical between both strains. LVF1^T has a doubling time of 146 min and LVF2^T of 165 min. The growth rate μ of LVF1^T is 0.28 h⁻¹ and 0.25 h⁻¹ for LVF2^T. However, the transient phase of LVF2^T was extended in comparison to LVF1^T and resulted in a higher final cell density of LVF2^T. In addition, the ability for anaerobic growth was also investigated. Therefore, aerobic pre-cultures were gassed with nitrogen and used as inoculum for cultures in Hungate tubes filled with anaerobic PYE medium. Anaerobic cultures were inoculated with OD₆₀₀ of 0.1 and incubated at optimal temperature without addition of sodium chloride for 14 days. Cell growth of LVF1^T increased almost eightfold, resulting in a final OD₆₀₀ of 0.765. LVF2^T showed no growth under these conditions.

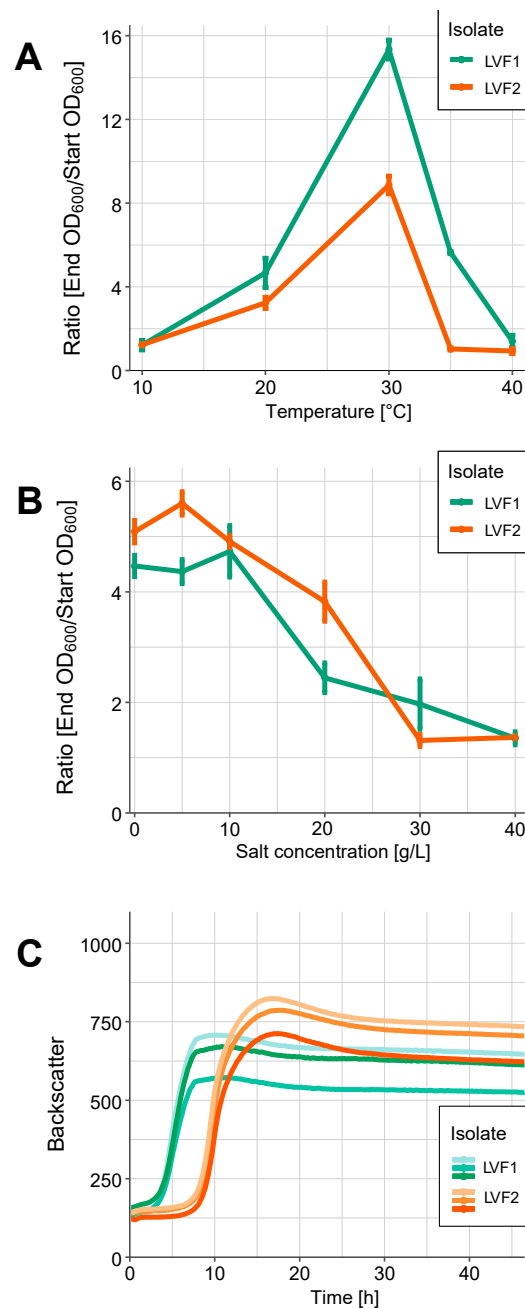


Figure 5. Growth analysis of LVF1^T and LVF2^T. (A) Growth of LVF1^T (green) and LVF2^T (orange) in 4 mL test tubes at different temperatures inoculated in PYE medium and incubated for 24 h (LVF2^T) and 16 h (LVF1^T) at 180 rpm in a Infors HT shaker (Orbitron, Einsbach, Germany). (B) Samples were inoculated in PYE medium and incubated for 30 h (LVF2^T, orange) and 24 h (LVF1^T, green) at 180 rpm. (C) Growth analysis of LVF1^T (green) and LVF2^T (orange) at optimum temperature (30 °C) in 25 mL PYE medium. Measurements were performed in triplicate and for (A,B) the standard deviation is shown as error bars, for (C) in different shades of green or orange.

The metabolic potential of both isolates was analyzed by using the API ZYM and the API 20 NE tests. In this way, forty different enzyme activities were determined for both isolates. Both showed no enzymatic activities in 27 cases. Ten were present in both strains, which included alkaline phosphatase, esterase, lipase, leucine arylamidase, trypsin, acid phosphatase, Naphthol- and AS-BI-phosphohydrolase, as well as the ability to utilize esculin, D-maltose and capric acid. Three enzyme activities were strain specific. Valine arylamidase or α -chymotrypsin were detected in LVF2^T whereas the activity of

β -glucosidase was observed for LVF1^T. In addition, both strains were catalase positive. Oxidase reagent from API ZYM test showed oxidase activity for both isolates. A general overview of all enzyme activities is listed in Table 3.

Table 3. Differential phenotypic characteristics of strains LVF1^T and LVF2^T and phylogenetically related species *B. diminuta* NCTC 9239^T, *B. lenta* DSM 23960^T, *B. naejangsensis* DSM 23858^T, and *B. subvibrioides* ATCC 15264^T. Taxa: 1, strain LVF1^T; 2, strain LVF2^T; 3, *B. diminuta* NCTC 9239^T (data from [9] BacDive [74] accessed on 12 January 2021); 4, *B. lenta* DSM 23960^T (data from [10]); 5, *B. naejangsensis* DSM 23858^T (data from BacDive [74] accessed on 12 January 2021); 6, *B. subvibrioides* ATCC 15264^T (data from [7]). +, Positive; −, negative; v, some strains showed activity; n/a, not available.

Characteristics	<i>B. pondensis</i> LVF1 ^T	<i>B.</i> <i>goettingensis</i> LVF2 ^T	<i>B. diminuta</i> NCTC 9239 ^T	<i>B. lenta</i> DSM 23960 ^T	<i>B.</i> <i>naejangsensis</i> DSM 23858 ^T	<i>B.</i> <i>subvibrioides</i> ATCC 15264 ^T
Source of isolation	Oligotrophic pond water	Puddle water	Water	Soil	Soil	Pond water
Colony pigmentation	Gray-white (PYE/R2A)	Yellow (PYE/R2A)	None (NA)	Grayish-yellow (NA)	Grayish-yellow (TSA)	Dark orange (PYE)
Stalk formation	−	+	n/a	n/a	−	+
Anaerobic growth	+	−	−	−	+	−
Temperature (°C)						
Range	10–40	10–40	n/a	4–34	4–50	n/a
Optimum	30	30	28	25	30	30
NaCl (g/L)						
Range	0–40	0–40	n/a	0–10	0–40	0–20
Optimum	0–10	0–5	n/a	0	5	20
Enzymatic activity						
Alkaline phosphatase	+	+	+	+	+	n/a
Esterase	+	+	+	+	+	n/a
Esterase lipase	+	+	+	+	+	n/a
Lipase	−	−	−	−	−	n/a
Leucine arylamidase	+	+	+	+	+	v
Valine arylamidase	+	−	−	−	−	−
Cysteine arylamidase	−	−	−	−	−	n/a
Trypsin	+	+	+	+	+	n/a
α -Chymotrypsin	+	−	+	−	+	n/a
Acid phosphatase	+	+	+	+	+	n/a
Naphthol-AS-BI-phosphohydrolase	+	+	+	+	+	n/a
α -Galactosidase	−	−	−	−	−	n/a
β -Galactosidase	−	−	−	−	−	n/a
β -Glucuronidase	−	−	−	−	−	n/a
α -Glucosidase	−	−	−	n/a	−	n/a
β -Glucosidase	−	+	−	n/a	−	n/a
N-Acetyl- β -glucosaminidase	−	−	−	−	−	n/a
α -Mannosidase	−	−	−	−	−	n/a
α -Fucosidase	−	−	−	−	−	n/a
Utilization of						
Potassium nitrate	−	−	−	n/a	−	−
L-Tryptophane	−	−	−	n/a	−	n/a
D-Glucose (fermentation)	−	−	−	n/a	−	n/a
L-Arginine	−	−	−	n/a	−	−
Urea	−	−	−	n/a	−	n/a

Table 3. Cont.

Characteristics	<i>B. pondensis</i> LVF1 ^T	<i>B.</i> <i>goettingensis</i> LVF2 ^T	<i>B. diminuta</i> NCTC 9239 ^T	<i>B. lenta</i> DSM 23960 ^T	<i>B.</i> <i>naejangsanensis</i> DSM 23858 ^T	<i>B.</i> <i>subvibrioides</i> ATCC 15264 ^T
Esculin/ferric citrate	+	+	–	n/a	–	n/a
Gelatin	–	–	–	n/a	–	n/a
4-Nitrophenyl-β-D-galactopyranoside	–	–	–	n/a	–	n/a
D-Glucose (assimilation)	–	–	–	–	–	+
L-Arabinose	–	–	–	–	–	v
D-Mannose	–	–	–	–	–	–
D-Mannitol	–	–	–	–	–	n/a
N-Acetyl-D-glucosamine	–	–	–	–	–	n/a
D-Maltose	+	+	–	–	–	+
Potassium gluconate	–	–	–	–	–	n/a
Capric acid	+	+	–	n/a	–	n/a
Adipic acid	–	–	–	n/a	–	n/a
Malic acid	–	–	–	n/a	+	n/a
Trisodium citrate	–	–	–	n/a	–	n/a
Phenylacetic acid	–	–	–	n/a	–	n/a
Oxidase	+	+	+	n/a	+	+
Catalase	+	+	+	n/a	+	+
Resistance to						
Ampicillin	–	–	+	+	+	n/a
Chloramphenicol	–	–	–	–	–	n/a
Doxycycline	–	–	–	n/a	n/a	n/a
Erythromycin	+	+	–	n/a	n/a	n/a
Kanamycin	–	–	–	–	–	n/a
Meropenem	+	+	n/a	n/a	n/a	n/a
Oxytetracycline	–	–	n/a	n/a	n/a	n/a
Rifampicin	–	–	n/a	n/a	n/a	n/a
Streptomycin	+	+	n/a	n/a	–	–
Tetracycline	+	+	–	–	–	n/a
Vancomycin	+	+	–	n/a	n/a	n/a
G + C %	67.04	67.79	67	68.7	67	67

In bold: Sorted by categories.

The antibiogram (Supplementary Figure S5) revealed that both isolates are resistant to erythromycin (LVF1^T 2 µg/disc and LVF2^T 4 µg/disc), meropenem (up to 2 µg/disc), streptomycin (10 µg/disc), tetracycline (up to 1 µg/disc), and vancomycin (30 µg/disc). Resfams in silico analysis [67] indicated genes present coding for an ABC transporter using erythromycin as substrate, β-lactamases for meropenem inactivation, tetracycline inactivation enzyme (*tetX*), and RND antibiotic efflux systems. The latter could be responsible for the aminoglycoside tolerance (Supplementary Tables S10 and S11).

B. pondensis sp. nov. LVF1^T and *B. goettingensis* sp. nov. LVF2^T show a different antibiogram compared to their phylogenetically closest relatives. Both are not resistant against ampicillin and comparing them with *B. diminuta* NCTC 9239^T, *B. lenta* DSM 23960^T and *B. naejangsanensis* DSM 23858^T but both possess a streptomycin and tetracycline resistance (Table 3).

4. Discussion

The aim of this study was to isolate new host strains of the *Caulobacteraceae* family to access the associated phage diversity present in the corresponding environments. This was realized successfully from environmental enrichment cultures with suitable amounts of *Caulobacterales* members. However, WSW (water surface of Weende River entrance), WSA (water surface of algae), and WSR (water surface of reed) revealed no or almost no members of this order. This was not expected as these were plant-associated samples, and members of the order *Caulobacterales* are known to be associated with plant material [8]. Some plants

such as reed (*Phragmites australis*) are able to increase microbial degradation due to oxygen availability but also the presence of certain microorganisms depends on the compounds released by reed [75]. WSW is the entrance of the river Weende. Here, the flow rate of the water is fast and would require strong adhesion of the stalked cells [3]. This might explain the lack of isolates from *Caulobacterales*. Enrichments from PW (oligotrophic pond water) or PUW (puddle water) revealed significant presence of *Caulobacterales*. These promising samples differed from the samples lacking *Caulobacterales* mainly in their standing waters, which are also at risk of drying out. Thus, the ability of *Caulobacterales* to withstand such seasonal fluctuations might be the crucial factor. Fazi et al. (2008) reported that the *Caulobacterales* are among the first to colonize a habitat after rehydration, which is often the case in Italian river sediments after heavy rain [76]. The authors of this study hypothesized that this characteristic is due to the ability of many members to form rigid biofilms [76].

The promising PW and PUW samples finally led to the isolation of the strains described here, which are associated with *Brevundimonas* based on their 16S rRNA gene sequence. Comparison of the whole genome with the representative type strains of this genus revealed LVF1^T and LVF2^T to represent new species (Figure 2). Apart from the genome, *Brevundimonas pondensis* sp. nov. LVF1^T and *Brevundimonas goettingensis* sp. nov. LVF2^T also show phenotypic differences. The colonies of LVF1^T are grayish-white, while that of LVF2^T are yellow. The origin of the coloration may be due to the production of carotenoids, which some *Brevundimonas* species are capable to synthesize [3]. In the genome of LVF1^T (white colony) we could not identify any putative genes for carotenoid biosynthesis, but we could in the genome of LVF2^T (yellowish colony) (Supplementary Tables S12 and S13).

Both strains exhibited distinct cell morphologies. LVF2^T showed prosthecate and non-prosthecate vibrio shape cell types, whereas LVF1^T showed only motile cells with polar flagella. The ability to divide asymmetrically, resulting in the distinct cell types, is rarely observed in *Brevundimonas*, i.e., in *B. subvibrioides* ATCC 15264^T [7]. It is more frequently observed in *Caulobacter* [4,5]. Since LVF2^T exhibits characteristics of both genera, its scientific importance goes beyond its service as a phage host strain.

Physiological analyses revealed that both strains grow optimally at 30 °C, which is in agreement with the literature, as freshwater and terrestrial members of *Caulobacteraceae* grow optimally at 30 °C [7,9,77]. Initial growth experiments showed that LVF1^T achieves higher cell densities than LVF2^T. However, this apparent advantage could be due to the conditions used. These experiments were conducted in test tubes with 4 mL medium under vigorous shaking. The still suboptimal aeration affected LVF2^T more than LVF1^T, since LVF2^T unlike LVF1^T is only capable of aerobic growth. Growth in conical flasks with optimal aeration resulted in an opposite behavior as LVF2^T reached higher densities than LVF1^T under these conditions (Figure 5c). LVF2^T also presented its competitive advantage at extreme temperatures such as 4 °C. It showed detectable growth after nine days, whereas LVF1^T required 16 days (data not shown). The data regarding growth in different NaCl concentrations correlate well with those known from literature for this genus [2,78] and are in good agreement with parameters frequently observed in environments from which both strains originated [78].

Both strains showed only minor differences with respect to the tested metabolic activities. Enzyme activity of valine arylamidase and α -chymotrypsin is missing in LVF2^T, whereas β -glucosidase activity is present. These experimental data were confirmed by genetic analysis using the KEGG pathway database (Supplementary Tables S14 and S15). The β -glucosidase activity of LVF2^T is significant, and to our knowledge, it has only been observed previously in *B. staley* [17]. Both isolates were oxidase- and catalase-positive, which is expected for the *Caulobacteraceae* family [7,9,77].

Antibiograms and the in silico investigations of both strains revealed a resistance potential with respect to medically relevant antibiotics. These results might be an indication of how far antibiotic contamination of our environment has progressed [79], especially as both isolates were isolated from protected habitats. However, this could also indicate that presence of antibiotic resistance genes are a natural phenomenon, as the presented

isolates originate from a complex environment where they likely face natural producers of antibiotics, e.g., *Streptomyces* [80]. In the future, analysis of the sample material with respect to content of different antibiotics should be considered to obtain clarity on this point.

The prophage potential of both strains was of particular interest as both isolates represent potential host systems for studying phage diversity in the environment. Our data confirmed that bioinformatical prediction using PHASTER [66] was imprecise. Since the prediction is mainly based on protein similarity to known phage proteins, the results indicate that phage diversity associated with Caulobacterales is not yet well understood. ProphageSeq of LVF1^T showed that read mappings are distributed far downstream of the identified prophages. This is likely related to the packaging mechanisms of the prophage. One of them may frequently recruit the packaging sites (*pac*) located in the prophage instance and translocate the chromosome constantly and unidirectionally into the prophage heads. The fadeout of reads reflects the likelihood of the phage translocase holding on to the initially grabbed dsDNA strand. We assume that both prophages of LVF1^T are able of forming phage particles. Prophage 2 due to the assembly of its genome and Prophage 1 as we could observe particle-packed sequence reads upstream the chromosomal *pac* site. In LVF2^T, we detected that the prophage randomly packs the host chromosome into its particles. This prophage is damaged or already domesticated by the host to perform a function required by the host. Similar cases are known for the PBSX prophages of *Bacillus pumilus* (Jin et al., 2014) and the gene transfer agents of *Rhodobacteraceae* [81].

In conclusion, although we did not manage to isolate a strain of the genus *Caulobacter*, we recovered two interesting isolates. LVF2 shows significant morphological similarity to the *Caulobacter* genus, although assigned as *Brevundimonas*. As a host strain, it might unite the viromes of both genera and be of particular value for the investigation of the environmental phage diversity. The presence of only a few prophages in the genome makes them even more attractive for this purpose. It is known that prophages can protect their host from infections of related and unrelated viruses [82–84]. The good manageability of the strains with respect to culture conditions make them promising candidates for future model organisms. For these reasons, we share the isolated strains with the scientific community and make them available with the help of the German Collection of Microorganisms and Cell Cultures GmbH (DSMZ), the Culture Collection University of Gothenburg (CCUG), and the Belgian Coordinated Collections of Microorganisms (BCCM/LMG).

4.1. Description of *Brevundimonas Pondensis* sp. nov.

Brevundimonas pondensis (pon. den' sis. N.L. fem. adj. *pondensis* pertaining to pond (51°33'57'' N 9°57'20'' E, collected on 6 September 2018), the source from which the type strain was isolated.

Cells are Gram-negative and rod-shaped (1.0 × 0.46 μm). Motile by means of a single polar flagellum. Colonies on PYE and R2A are round, slightly convex smooth and grayish-white with 0.8 mm diameter after 24 h of incubation at 30 °C. Growth occurs between 10 and 40 °C. Growth occurs in the presence of 0–4% (*w/v*) NaCl, with an optimum in the presence of 0–1% (*w/v*) NaCl. Growth occurs under anaerobic conditions. Susceptible to ampicillin, chloramphenicol, doxycycline, kanamycin, oxytetracycline, rifampicin, but not to erythromycin, meropenem, streptomycin, tetracycline, and vancomycin. In assays with the API 20 NE system, it showed the utilization of esculin, D-maltose, and capric acid. In assays with the API ZYM system, alkaline phosphatase, esterase, esterase lipase, leucine arylamidase, valine arylamidase, trypsin, α-Chymotrypsin, acid phosphatase, and naphthol-AS-BI-phosphohydrolase are present. Other phenotypic characteristics are given in Table 3.

The type strain, LVF1^T (=DSM 112304^T = CCUG 74982^T = LMG 32096^T), was isolated from an oligotrophic pond located in Göttingen, Germany. The DNA G + C content of the type strain is 67.04 mol% (determined by PGAP).

4.2. Description of *Brevundimonas Goettingensis* sp. nov.

Brevundimonas goettingensis (goet.tin.gen'sis N.L. fem. adj. *goettingensis* pertaining to Göttingen city (51°33'27'' N 9°56'40'' E, collected on 24 September 2018) where the type strain was isolated).

Stalked cells are Gram-negative and vibrio-shaped ($1.3 \times 0.7 \mu\text{m}$), the swarmer cells are elliptical ($1.0 \times 0.6 \mu\text{m}$). Motile by means of a single polar flagellum. Colonies on PYE and R2A are elliptical, slightly convex, smooth and yellow with 1.0 mm diameter after 48 h of incubation at 30 °C. Growth occurs between 10 and 40 °C. Growth occurs in the presence of 0–4% (*w/v*) NaCl, with an optimum in the presence of 0–0.05% (*w/v*) NaCl. Susceptible to ampicillin, chloramphenicol, doxycycline, kanamycin, oxytetracycline, rifampicin, but not to erythromycin, meropenem, streptomycin, tetracycline, and vancomycin. In assays with the API 20 NE system, it showed the utilization of esculin, D-maltose, and capric acid. In assays with the API ZYM system, alkaline phosphatase, esterase, esterase lipase, leucine arylamidase, trypsin, acid phosphatase, naphthol-AS-BI-phosphohydrolase, and β -Glucosidase are detected. Other phenotypic characteristics are given in Table 3.

The type strain LVF2^T (=DSM 112305^T = CCUG 74983^T = LMG 32097^T), was isolated from an oligotrophic pond located in Göttingen, Germany. The DNA G + C content of the type strain is 67.79 mol% (determined by PGAP).

Supplementary Materials: The figures and tables are available online at <https://www.mdpi.com/article/10.3390/applmicrobiol1010005/s1>, Figure S1: Visualization of BLASTKoala output for both isolates, Figure S2: Phenotype of both isolates, Figure S3: Colony morphology of both isolates, Figure S4: Gram staining of both isolates, Figure S5: Analysis of antibiotic resistances of both isolates, Table S1: CheckM evaluation of both isolates, Table S2: Metadata of sampling sites, Table S3: ASV counts and taxonomic assignments, Table S4: Assigned ASV sequences after bioinformatic processing, Table S5: Identification results of bacterial isolates from enriched environmental sampling sites, Table S6: GTDB-Tk result of both isolates, Table S7: Phylogenetic analysis of both isolates, Table S8: PHASTER analysis of *Brevundimonas pondensis* LVF1^T, Table S9: PHASTER analysis of *Brevundimonas goettingensis* LVF2^T, Table S10: Resfams prediction of *Brevundimonas pondensis* LVF1^T, Table S11: Resfams prediction of *Brevundimonas goettingensis* LVF2^T, Table S12: List of putative biosynthetic gene clusters in *Brevundimonas pondensis* LVF1^T, Table S13: List of putative biosynthetic gene clusters in *Brevundimonas goettingensis* LVF2^T, Table S14: KEGG Mapper Reconstruction Result of *Brevundimonas pondensis* LVF1^T, Table S15: KEGG Mapper Reconstruction Result of *Brevundimonas goettingensis* LVF2^T.

Author Contributions: Conceptualization, I.F., R.H. and R.D.; experiments, I.F., A.K. and H.N.; data analysis, I.F., D.S. and R.H.; writing, I.F. and R.H. All authors interpreted the results, edited and reviewed the manuscript, and approved submission of the manuscript. All authors have read and agreed to the published version of the manuscript.

Funding: This research received no external funding.

Institutional Review Board Statement: Not applicable.

Informed Consent Statement: Not applicable.

Data Availability Statement: The 16S rRNA gene amplicon raw reads were deposited to the National Center for Biotechnology Information Sequence Read Archive (SRA) under the accession numbers SRR13285071 (eutrophic pond), SRR13285072 (frog's lettuce (*Groenlandia densa*)), SRR13285073 (surface water of reed), SRR13285074 (surface water near pond algae), SRR13285075 (surface water close from Weende River entrance), SRR13285076 (surface water near frog's lettuce), SRR13285077 (river water), SRR13285078 (river stones), SRR13285079 (puddle water), SRR13285080 (surface water of stale eutrophic pond), SRR13285081 (pond water), and SRR13285082 (mixed river stones). As well with the BioProject number PRJNA686076. The whole-genome shotgun project of *Brevundimonas pondensis* sp. nov. LVF1^T and *Brevundimonas goettingensis* sp. nov. LVF2^T has been deposited at GenBank under the accession numbers CP062006 and CP062222, respectively and the BioProject accession number PRJNA664909 and PRJNA664918. BioSample accession numbers are SAMN16237053 and SAMN16237121. The raw reads have been deposited in the NCBI SRA database with the accession

numbers SRR12931068 and SRR12951179 (Oxford Nanopore) and SRR12931069 and SRR12951180 (Illumina MiSeq).

Acknowledgments: We thank Anja Poehlein for sequencing, Melanie Heinemann and Mechthild Bömeke for technical assistance and Michael Hoppert for the support of TEM-imaging of both isolates. We acknowledge the support by the Open Access Publication Funds of the University of Göttingen.

Conflicts of Interest: The authors declare no conflict of interest.

References

- Henrici, A.T.; Johnson, D.E. Studies of Freshwater Bacteria: II. Stalked Bacteria, a New Order of Schizomycetes. *J. Bacteriol.* **1935**, *30*, 61–93. [[CrossRef](#)]
- Abraham, W.-R.; Strompl, C.; Meyer, H.; Lindholst, S.; Moore, E.R.B.; Christ, R.; Vancanneyt, M.; Tindall, B.J.; Bennasar, A.; Smit, J.; et al. Phylogeny and Polyphasic Taxonomy of *Caulobacter* Species. Proposal of *Maricaulis* gen. nov. with *Maricaulis maris* (Poindexter) comb. nov. as the Type Species, and Emended Description of the Genera *Brevundimonas* and *Caulobacter*. *Int. J. Syst. Bacteriol.* **1999**, *49*, 1053–1073. [[CrossRef](#)] [[PubMed](#)]
- Abraham, W.-R.; Rohde, M.; Bennasar, A. The family *Caulobacteraceae*. In *The Prokaryotes*; Rosenberg, E., DeLong, E.F., Lory, S., Stackebrandt, E., Thompson, F., Eds.; Springer: Berlin/Heidelberg, Germany, 2014; pp. 179–205. ISBN 978-3-642-30197-1.
- Staley, J.T. Prosthecomicrobium and Ancalomicrobium: New Prosthecate Freshwater Bacteria. *J. Bacteriol.* **1968**, *95*, 1921–1942. [[CrossRef](#)]
- Jin, L.; Lee, H.-G.; Kim, H.-S.; Ahn, C.-Y.; Oh, H.-M. *Caulobacter daechungensis* sp. nov., a Stalked Bacterium Isolated from a Eutrophic Reservoir. *Int. J. Syst. Evol. Microbiol.* **2014**, *63*, 2559–2564. [[CrossRef](#)]
- Stove, J.L.; Stanier, R.Y. Cellular Differentiation in Stalked Bacteria. *Nature* **1962**, *196*, 1189–1192. [[CrossRef](#)]
- Poindexter, J.S. Biological Properties and Classification of the *Caulobacter* Group. *Bacteriol. Rev.* **1964**, *28*, 231–295. [[CrossRef](#)]
- Wilhelm, R.C. Following the Terrestrial Tracks of *Caulobacter*—Redefining the Ecology of a Reputed Aquatic Oligotroph. *ISME J.* **2018**, *12*, 3025–3037. [[CrossRef](#)]
- Segers, P.; Vancanneyt, M.; Pot, B.; Torck, U.; Hoste, B.; Dewettinck, D.; Falsen, E.; Kersters, K.; De Vos, P. Classification of *Pseudomonas diminuta* Leifson and Hugh 1954 and *Pseudomonas vesicularis* Büsing, Döll, and Freytag 1953 in *Brevundimonas* gen. nov. as *Brevundimonas diminuta* comb. nov. and *Brevundimonas vesicularis* comb. nov., Respectively. *Int. J. Syst. Evol. Microbiol.* **1994**, *44*, 499–510. [[CrossRef](#)]
- Yoon, J.H.; Kang, S.J.; Oh, H.W.; Lee, J.S.; Oh, T.K. *Brevundimonas kwangchunensis* sp. nov., Isolated from an Alkaline Soil in Korea. *Int. J. Syst. Evol. Microbiol.* **2006**, *56*, 613–617. [[CrossRef](#)]
- Ryu, S.H.; Park, M.; Lee, J.R.; Yun, P.-Y.; Jeon, C.O. *Brevundimonas aveniformis* sp. nov., a Stalked Species Isolated from Activated Sludge. *Int. J. Syst. Evol. Microbiol.* **2007**, *57*, 1561–1565. [[CrossRef](#)] [[PubMed](#)]
- Estrela, A.B.; Abraham, W.R. *Brevundimonas vancanneytii* sp. nov., Isolated from Blood of a Patient with Endocarditis. *Int. J. Syst. Evol. Microbiol.* **2010**, *60*, 2129–2134. [[CrossRef](#)] [[PubMed](#)]
- Choi, J.H.; Kim, M.S.; Roh, S.W.; Bae, J.W. *Brevundimonas basaltis* sp. nov., Isolated from Black Sand. *Int. J. Syst. Evol. Microbiol.* **2010**, *60*, 1488–1492. [[CrossRef](#)] [[PubMed](#)]
- Vu, H.T.T.; Manangkil, O.E.; Mori, N.; Yoshida, S.; Nakamura, C. Post-Germination Seedling Vigor under Submergence and Submergence-Induced SUB1A Gene Expression in Indica and Japonica Rice (*Oryza sativa* L.). *Aust. J. Crop Sci.* **2010**, *4*, 264–272. [[CrossRef](#)]
- Wang, J.; Zhang, J.; Ding, K.; Xin, Y.; Pang, H. *Brevundimonas viscosa* sp. nov., Isolated from Saline Soil. *Int. J. Syst. Evol. Microbiol.* **2012**, *62*, 2475–2479. [[CrossRef](#)] [[PubMed](#)]
- Tsubouchi, T.; Koyama, S.; Mori, K.; Shimane, Y.; Usui, K.; Tokuda, M.; Tame, A.; Uematsu, K.; Maruyama, T.; Hatada, Y. *Brevundimonas denitrificans* sp. nov., a Denitrifying Bacterium Isolated from Deep Subseafloor Sediment. *Int. J. Syst. Evol. Microbiol.* **2014**, *64*, 3709–3716. [[CrossRef](#)] [[PubMed](#)]
- Abraham, W.-R.; Estrela, A.B.; Nikitin, D.I.; Smit, J.; Vancanneyt, M. *Brevundimonas halotolerans* sp. nov., *Brevundimonas poindexteriae* sp. nov. and *Brevundimonas staleyii* sp. nov., Prosthecate Bacteria from Aquatic Habitats. *Int. J. Syst. Evol. Microbiol.* **2010**, *60*, 1837–1843. [[CrossRef](#)]
- Tóth, E.; Szuróczi, S.; Kéki, Z.; Kosztik, J.; Makk, J.; Bóka, K.; Spröer, C.; Márialigeti, K.; Schumann, P. *Brevundimonas balnearis* sp. nov., Isolated from the Well Water of a Thermal Bath. *Int. J. Syst. Evol. Microbiol.* **2017**, *67*, 1033–1038. [[CrossRef](#)]
- Gorbatyuk, B.; Marczyński, G.T. Regulated Degradation of Chromosome Replication Proteins DnaA and CtrA in *Caulobacter crescentus*. *Mol. Microbiol.* **2005**, *55*, 1233–1245. [[CrossRef](#)]
- Parte, A.C.; Carbasse, J.S.; Meier-Kolthoff, J.P.; Reimer, L.C.; Göker, M. List of Prokaryotic Names with Standing in Nomenclature (LPSN) Moves to the DSMZ. *Int. J. Syst. Evol. Microbiol.* **2020**, *70*, 5607–5612. [[CrossRef](#)]
- Beilstein, F.; Dreiseikelmann, B. Bacteriophages of Freshwater *Brevundimonas vesicularis* Isolates. *Res. Microbiol.* **2006**, *157*, 213–219. [[CrossRef](#)]
- West, D.; Lagenaur, C.; Agabian, N. Isolation and Characterization of *Caulobacter crescentus* Bacteriophage Phi Cd1. *J. Virol.* **1976**, *17*, 568–575. [[CrossRef](#)]

23. Ackermann, H.-W. Bacteriophage electron microscopy. In *Advances in Virus Research*; Elsevier Inc.: Amsterdam, The Netherlands, 2012; Volume 82, pp. 1–32. ISBN 978-0-12-394621-8.
24. Schmidt, J.M.; Stainer, R.Y. Isolation and Characterization of Bacteriophages Active against Stalked Bacteria. *J. Gen. Microbiol.* **1965**, *39*, 95–107. [[CrossRef](#)]
25. Kazaks, A.; Voronkova, T.; Rumnieks, J.; Dishlers, A.; Tars, K. Genome Structure of *Caulobacter* Phage PhiCb5. *J. Virol.* **2011**, *85*, 4628–4631. [[CrossRef](#)]
26. Friedrich, I.; Hollensteiner, J.; Schneider, D.; Poehlein, A.; Hertel, R.; Daniel, R. First Complete Genome Sequences of *Janthinobacterium lividum* EIF1 and EIF2 and Their Comparative Genome Analysis. *Genome Biol. Evol.* **2020**, *12*, 1782–1788. [[CrossRef](#)] [[PubMed](#)]
27. Friedrich, I.; Hollensteiner, J.; Scherf, J.; Weyergraf, J.; Klassen, A.; Poehlein, A.; Hertel, R.; Daniel, R. Complete Genome Sequence of *Stenotrophomonas indicatrix* DAIF1. *Microbiol. Resour. Announc.* **2021**, *10*, 15–17. [[CrossRef](#)]
28. Hollensteiner, J.; Friedrich, I.; Hollstein, L.; Lamping, J.; Wolf, K.; Liesegang, H.; Poehlein, A.; Hertel, R.; Daniel, R. Complete Genome Sequence of *Kinneretia* sp. Strain DAIF2, Isolated from a Freshwater Pond. *Microbiol. Resour. Announc.* **2021**, *10*, 5–7. [[CrossRef](#)]
29. Poindexter, J.S. Dimorphic prosthecate bacteria: The genera *Caulobacter*, *Asticcacaulis*, *Hyphomicrobium*, *Pedomicrobium*, *Hyphomonas* and *Thiodendron*. In *The Prokaryotes*; Springer: New York, NY, USA, 2006; Volume 5, pp. 72–90. ISBN 978-0-387-30745-9.
30. Klindworth, A.; Pruesse, E.; Schweer, T.; Peplies, J.; Quast, C.; Horn, M.; Glöckner, F.O. Evaluation of General 16S Ribosomal RNA Gene PCR Primers for Classical and Next-Generation Sequencing-Based Diversity Studies. *Nucleic Acids Res.* **2013**, *41*, e1. [[CrossRef](#)]
31. Fredriksson, N.J.; Hermansson, M.; Wilén, B.-M. The Choice of PCR Primers Has Great Impact on Assessments of Bacterial Community Diversity and Dynamics in a Wastewater Treatment Plant. *PLoS ONE* **2013**, *8*, e76431. [[CrossRef](#)]
32. Chen, S.; Zhou, Y.; Chen, Y.; Gu, J. Fastp: An Ultra-Fast All-in-One FASTQ Preprocessor. *Bioinformatics* **2018**, *34*, i884–i890. [[CrossRef](#)]
33. Zhang, J.; Kobert, K.; Flouri, T.; Stamatakis, A. PEAR: A Fast and Accurate Illumina Paired-End ReAd MergeR. *Bioinformatics* **2014**, *30*, 614–620. [[CrossRef](#)]
34. Martin, M. Cutadapt Removes Adapter Sequences from High-Throughput Sequencing Reads. *EMBnet J.* **2011**, *17*, 10–12. [[CrossRef](#)]
35. Rognes, T.; Flouri, T.; Nichols, B.; Quince, C.; Mahé, F. VSEARCH: A Versatile Open Source Tool for Metagenomics. *PeerJ* **2016**, *4*, e2584. [[CrossRef](#)]
36. Nearing, J.T.; Douglas, G.M.; Comeau, A.M.; Langille, M.G.I. Denoising the Denoisers: An Independent Evaluation of Microbiome Sequence Error-Correction Approaches. *PeerJ* **2018**, *2018*, e5364. [[CrossRef](#)]
37. Quast, C.; Pruesse, E.; Yilmaz, P.; Gerken, J.; Schweer, T.; Yarza, P.; Peplies, J.; Glöckner, F.O. The SILVA Ribosomal RNA Gene Database Project: Improved Data Processing and Web-Based Tools. *Nucleic Acids Res.* **2012**, *41*, D590–D596. [[CrossRef](#)]
38. Altschul, S.F.; Gish, W.; Miller, W.; Myers, E.W.; Lipman, D.J. Basic Local Alignment Search Tool. *J. Mol. Biol.* **1990**, *215*, 403–410. [[CrossRef](#)]
39. R Core Team. *R: A Language and Environment for Statistical Computing*; R Foundation for Statistical Computing: Vienna, Austria, 2020.
40. RStudio Team. *RStudio: Integrated Development for R*; RStudio, PBC: Boston, MA, USA, 2020.
41. Wickham, H. *Ggplot2—Elegant Graphics for Data Analysis*; Springer: New York, NY, USA, 2009; Volume 77, p. 3. ISBN 978-0-387-98140-6.
42. Bolger, A.M.; Lohse, M.; Usadel, B. Trimmomatic: A Flexible Trimmer for Illumina Sequence Data. *Bioinformatics* **2014**, *30*, 2114–2120. [[CrossRef](#)]
43. Magoč, T.; Salzberg, S.L. FLASH: Fast Length Adjustment of Short Reads to Improve Genome Assemblies. *Bioinformatics* **2011**, *27*, 2957–2963. [[CrossRef](#)]
44. Wick, R.R.; Judd, L.M.; Gorrie, C.L.; Holt, K.E. Unicycler: Resolving Bacterial Genome Assemblies from Short and Long Sequencing Reads. *PLoS Comput. Biol.* **2017**, *13*, e1005595. [[CrossRef](#)]
45. Bankevich, A.; Nurk, S.; Antipov, D.; Gurevich, A.A.; Dvorkin, M.; Kulikov, A.S.; Lesin, V.M.; Nikolenko, S.I.; Pham, S.; Pribelski, A.D.; et al. SPAdes: A New Genome Assembly Algorithm and Its Applications to Single-Cell Sequencing. *J. Comput. Biol.* **2012**, *19*, 455–477. [[CrossRef](#)]
46. Vaser, R.; Sović, I.; Nagarajan, N.; Šikić, M. Fast and Accurate *de novo* Genome Assembly from Long Uncorrected Reads. *Genome Res.* **2017**, *27*, 737–746. [[CrossRef](#)]
47. BLAST Command Line Applications User Manual [Internet]. Available online: <https://www.ncbi.nlm.nih.gov/books/NBK279690/> (accessed on 20 November 2020).
48. Langmead, B.; Salzberg, S.L. Fast Gapped-Read Alignment with Bowtie 2. *Nat. Methods* **2012**, *9*, 357–359. [[CrossRef](#)] [[PubMed](#)]
49. Li, H.; Handsaker, B.; Wysoker, A.; Fennell, T.; Ruan, J.; Homer, N.; Marth, G.; Abecasis, G.; Durbin, R. The Sequence Alignment/Map Format and SAMtools. *Bioinformatics* **2009**, *25*, 2078–2079. [[CrossRef](#)] [[PubMed](#)]
50. Arnold, K.; Gosling, J.; Holmes, D. *The Java Programming Language*, 4th ed.; Addison-Wesley Professional: Lebanon, IN, USA, 2005; ISBN 978-0-321-34980-4.

51. Walker, B.J.; Abeel, T.; Shea, T.; Priest, M.; Abouelliel, A.; Sakthikumar, S.; Cuomo, C.A.; Zeng, Q.; Wortman, J.; Young, S.K.; et al. Pilon: An Integrated Tool for Comprehensive Microbial Variant Detection and Genome Assembly Improvement. *PLoS ONE* **2014**, *9*, e112963. [[CrossRef](#)]
52. Okonechnikov, K.; Conesa, A.; García-Alcalde, F. Qualimap 2: Advanced Multi-Sample Quality Control for High-Throughput Sequencing Data. *Bioinformatics* **2016**, *32*, 292–294. [[CrossRef](#)]
53. Wick, R.R.; Schultz, M.B.; Zobel, J.; Holt, K.E. Bandage: Interactive Visualization of *de novo* Genome Assemblies. *Bioinformatics* **2015**, *31*, 3350–3352. [[CrossRef](#)] [[PubMed](#)]
54. Grissa, I.; Vergnaud, G.; Pourcel, C. CRISPRfinder: A Web Tool to Identify Clustered Regularly Interspaced Short Palindromic Repeats. *Nucleic Acids Res.* **2007**, *35*, W52–W57. [[CrossRef](#)] [[PubMed](#)]
55. Parks, D.H.; Imelfort, M.; Skennerton, C.T.; Hugenholtz, P.; Tyson, G.W. CheckM: Assessing the Quality of Microbial Genomes Recovered from Isolates, Single Cells, and Metagenomes. *Genome Res.* **2015**, *25*, 1043–1055. [[CrossRef](#)] [[PubMed](#)]
56. Tatusova, T.; DiCuccio, M.; Badretdin, A.; Chetvernin, V.; Nawrocki, E.P.; Zaslavsky, L.; Lomsadze, A.; Pruitt, K.D.; Borodovsky, M.; Ostell, J. NCBI Prokaryotic Genome Annotation Pipeline. *Nucleic Acids Res.* **2016**, *44*, 6614–6624. [[CrossRef](#)] [[PubMed](#)]
57. Otsuji, N.; Sekiguchi, M.; Iijima, T.; Takagi, Y. Induction of Phage Formation in the Lysogenic *Escherichia coli* K-12 by Mitomycin C. *Nature* **1959**, *184*, 1079–1080. [[CrossRef](#)]
58. Dietrich, S.; Wiegand, S.; Liesegang, H. TraV: A Genome Context Sensitive Transcriptome Browser. *PLoS ONE* **2014**, *9*, e93677. [[CrossRef](#)]
59. Hertel, R.; Volland, S.; Liesegang, H. Conjugative Reporter System for the Use in *Bacillus licheniformis* and Closely Related Bacilli. *Letts. Appl. Microbiol.* **2015**, *60*, 162–167. [[CrossRef](#)]
60. Chaumeil, P.-A.; Mussig, A.J.; Hugenholtz, P.; Parks, D.H. GTDB-Tk: A Toolkit to Classify Genomes with the Genome Taxonomy Database. *Bioinformatics* **2019**, *36*, 1925–1927. [[CrossRef](#)]
61. Pritchard, L.; Glover, R.H.; Humphris, S.; Elphinstone, J.G.; Toth, I.K. Genomics and Taxonomy in Diagnostics for Food Security: Soft-Rotting Enterobacterial Plant Pathogens. *Anal. Methods* **2016**, *8*, 12–24. [[CrossRef](#)]
62. Parks, D.H.; Chuvochina, M.; Chaumeil, P.A.; Rinke, C.; Mussig, A.J.; Hugenholtz, P. Selection of Representative Genomes for 24,706 Bacterial and Archaeal Species Clusters Provide a Complete Genome-Based Taxonomy. *BioRxiv* **2019**, 771964. [[CrossRef](#)]
63. Kanehisa, M.; Sato, Y.; Morishima, K. BlastKOALA and GhostKOALA: KEGG Tools for Functional Characterization of Genome and Metagenome Sequences. *J. Mol. Biol.* **2016**, *428*, 726–731. [[CrossRef](#)] [[PubMed](#)]
64. Medema, M.H.; Blin, K.; Cimermancic, P.; de Jager, V.; Zakrzewski, P.; Fischbach, M.A.; Weber, T.; Takano, E.; Breitling, R. AntiSMASH: Rapid Identification, Annotation and Analysis of Secondary Metabolite Biosynthesis Gene Clusters in Bacterial and Fungal Genome Sequences. *Nucleic Acids Res.* **2011**, *39*, W339–W346. [[CrossRef](#)]
65. Blin, K.; Shaw, S.; Steinke, K.; Villebro, R.; Ziemert, N.; Lee, S.Y.; Medema, M.H.; Weber, T. AntiSMASH 5.0: Updates to the Secondary Metabolite Genome Mining Pipeline. *Nucleic Acids Res.* **2019**, *47*, W81–W87. [[CrossRef](#)]
66. Arndt, D.; Grant, J.R.; Marcu, A.; Sajed, T.; Pon, A.; Liang, Y.; Wishart, D.S. PHASTER: A Better, Faster Version of the PHAST Phage Search Tool. *Nucleic Acids Res.* **2016**, *44*, W16–W21. [[CrossRef](#)] [[PubMed](#)]
67. Gibson, M.K.; Forsberg, K.J.; Dantas, G. Improved Annotation of Antibiotic Resistance Determinants Reveals Microbial Resistomes Cluster by Ecology. *ISME J.* **2015**, *9*, 207–216. [[CrossRef](#)] [[PubMed](#)]
68. Claus, D. A Standardized Gram Staining Procedure. *World J. Microbiol. Biotechnol.* **1992**, *8*, 451–452. [[CrossRef](#)]
69. Bruder, S.; Reifenrath, M.; Thomik, T.; Boles, E.; Herzog, K. Parallelized Online Biomass Monitoring in Shake Flasks Enables Efficient Strain and Carbon Source Dependent Growth Characterisation of *Saccharomyces cerevisiae*. *Microb. Cell Fact.* **2016**, *15*, 127. [[CrossRef](#)]
70. Macy, J.M.; Snellen, J.E.; Hungate, R.E. Use of Syringe Methods for Anaerobiosis. *Am. J. Clin. Nutr.* **1972**, *25*, 1318–1323. [[CrossRef](#)]
71. Clarke, P.H.; Cowan, S.T. Biochemical Methods for Bacteriology. *J. Gen. Microbiol.* **1952**, *6*, 187–197. [[CrossRef](#)]
72. Meier-Kolthoff, J.P.; Göker, M. TYGS Is an Automated High-Throughput Platform for State-of-the-Art Genome-Based Taxonomy. *Nat. Commun.* **2019**, *10*, 2182. [[CrossRef](#)] [[PubMed](#)]
73. Richter, M.; Rosselló-Móra, R. Shifting the Genomic Gold Standard for the Prokaryotic Species Definition. *Proc. Natl. Acad. Sci. USA* **2009**, *106*, 19126–19131. [[CrossRef](#)]
74. Reimer, L.C.; Vetcinina, A.; Carbasse, J.S.; Söhngen, C.; Gleim, D.; Ebeling, C.; Overmann, J. BacDive in 2019: Bacterial Phenotypic Data for High-Throughput Biodiversity Analysis. *Nucleic Acids Res.* **2019**, *47*, D631–D636. [[CrossRef](#)]
75. Milke, J.; Gałczyńska, M.; Wróbel, J. The Importance of Biological and Ecological Properties of *Phragmites australis* (Cav.) Trin. Ex Steud., in Phytoremediation of Aquatic Ecosystems—The Review. *Water* **2020**, *12*, 1770. [[CrossRef](#)]
76. Fazi, S.; Amalfitano, S.; Piccini, C.; Zoppini, A.; Puddu, A.; Pernthaler, J. Colonization of Overlaying Water by Bacteria from Dry River Sediments. *Environ. Microbiol.* **2008**, *10*, 2760–2772. [[CrossRef](#)]
77. Eberspächer, J.; Lingens, F. The genus *Phenylobacterium*. In *The Prokaryotes*; Springer: New York, NY, USA, 2006; pp. 250–256. ISBN 978-0-387-30745-9.
78. Vancanneyt, M.; Segers, P.; Abraham, W.; Vos, P.D. *Brevundimonas*. In *Bergey's Manual of Systematics of Archaea and Bacteria*; Trujillo, M.E., Dedys, S., DeVos, P., Hedlund, B., Kämpfer, P., Rainey, F.A., Whitman, W.B., Eds.; John Wiley & Sons, Inc.: Hoboken, NJ, USA, 2015; pp. 1–14. ISBN 978-1-118-96060-8.

79. Willms, I.M.; Yuan, J.; Penone, C.; Goldmann, K.; Vogt, J.; Wubet, T.; Schöning, I.; Schrumpf, M.; Buscot, F.; Nacke, H. Distribution of Medically Relevant Antibiotic Resistance Genes and Mobile Genetic Elements in Soils of Temperate Forests and Grasslands Varying in Land Use. *Genes* **2020**, *11*, 150. [[CrossRef](#)] [[PubMed](#)]
80. Zhang, Z.; Du, C.; de Barse, F.; Liem, M.; Liakopoulos, A.; van Wezel, G.P.; Choi, Y.H.; Claessen, D.; Rozen, D.E. Antibiotic Production in *Streptomyces* Is Organized by a Division of Labor through Terminal Genomic Differentiation. *Sci. Adv.* **2020**, *6*, eaay5781. [[CrossRef](#)]
81. Tomasch, J.; Wang, H.; Hall, A.T.K.; Patzelt, D.; Preusse, M.; Petersen, J.; Brinkmann, H.; Bunk, B.; Bhujju, S.; Jarek, M.; et al. Packaging of *Dinoroseobacter shibae* DNA into Gene Transfer Agent Particles Is Not Random. *Genome Biol. Evol.* **2018**, *10*, 359–369. [[CrossRef](#)] [[PubMed](#)]
82. McLaughlin, J.R.; Wong, H.C.; Ting, Y.E.; Van Arsdell, J.N.; Chang, S. Control of Lysogeny and Immunity of *Bacillus subtilis* Temperate Bacteriophage SP Beta by Its *d* Gene. *J. Bacteriol.* **1986**, *167*, 952–959. [[CrossRef](#)] [[PubMed](#)]
83. Rettenmier, C.W.; Gingell, B.; Hemphill, H.E. The Role of Temperate Bacteriophage SP Beta in Prophage-Mediated Interference in *Bacillus subtilis*. *Can. J. Microbiol.* **1979**, *25*, 1345–1351. [[CrossRef](#)] [[PubMed](#)]
84. Yamamoto, T.; Obana, N.; Yee, L.M.; Asai, K.; Nomura, N.; Nakamura, K. SP10 Infectivity Is Aborted after Bacteriophage SP10 Infection Induces NonA Transcription on the Prophage SP β Region of the *Bacillus subtilis* Genome. *J. Bacteriol.* **2014**, *196*, 693–706. [[CrossRef](#)]

2. Down in the pond: Isolation and characterization of a new *Serratia marcescens* strain (LVF3) from the surface water near frog's lettuce (*Groenlandia densa*)

Ines Friedrich¹, Bernhard Bodenberger¹, Hannes Neubauer¹, Robert Hertel² and Rolf Daniel¹

PLoS ONE (8 November 2021), **16**, 11: e0259673
<https://doi.org/10.1371/journal.pone.0259673>

Affiliations

¹Genomic and Applied Microbiology & Göttingen Genomics Laboratory, Institute of Microbiology and Genetics, Georg-August-University of Göttingen, Grisebachstraße 8, 37077 Göttingen, Germany

²FG Synthetic Microbiology, Institute of Biotechnology, BTU Cottbus-Senftenberg, Senftenberg, Germany

Author contributions:

Conceptualization: **IF**, RH, RD

Data curation: **IF**, RH

Formal analysis: **IF**, RH, RD

Funding acquisition: RD

Investigation: **IF**, BB, HN

Project administration: RD

Supervision: RD

Validation: **IF**, RH, RD

Visualization: **IF**, BB, HN

Writing – original draft: **IF**, RH

Writing – review & editing: **IF**, BB, HN, RD

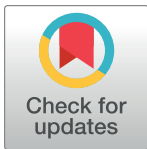
RESEARCH ARTICLE

Down in the pond: Isolation and characterization of a new *Serratia marcescens* strain (LVF3) from the surface water near frog's lettuce (*Groenlandia densa*)

Ines Friedrich¹, Bernhard Bodenberger¹, Hannes Neubauer¹, Robert Hertel^{1,2}, Rolf Daniel^{1*}

1 Genomic and Applied Microbiology & Göttingen Genomics Laboratory, Institute of Microbiology and Genetics, Georg-August-University of Göttingen, Göttingen, Germany, **2** FG Synthetic Microbiology, Institute of Biotechnology, BTU Cottbus-Senftenberg, Senftenberg, Germany

* rdaniel@gwdg.de



OPEN ACCESS

Citation: Friedrich I, Bodenberger B, Neubauer H, Hertel R, Daniel R (2021) Down in the pond: Isolation and characterization of a new *Serratia marcescens* strain (LVF3) from the surface water near frog's lettuce (*Groenlandia densa*). PLoS ONE 16(11): e0259673. <https://doi.org/10.1371/journal.pone.0259673>

Editor: Chih-Horng Kuo, Academia Sinica, TAIWAN

Received: July 26, 2021

Accepted: October 22, 2021

Published: November 8, 2021

Copyright: © 2021 Friedrich et al. This is an open access article distributed under the terms of the [Creative Commons Attribution License](https://creativecommons.org/licenses/by/4.0/), which permits unrestricted use, distribution, and reproduction in any medium, provided the original author and source are credited.

Data Availability Statement: The whole-genome shotgun project of *Serratia marcescens* LVF3R has been deposited at GenBank under the accession numbers CP063229 (chromosome) and CP063230 (plasmid) and BioProject accession number PRJNA669584. BioSample accession number is SAMN16456043. The raw reads have been deposited in the NCBI SRA database under the accession numbers SRR12951277 (Oxford Nanopore) and SRR12951278 (Illumina MiSeq) and BioProject PRJNA669584. The strain has been

Abstract

Serratia marcescens is a species that belongs to the family of *Yersiniaceae*. This family comprises taxa representing opportunistic human- and phytopathogens but also plant growth-promoting rhizobacteria (PGPR). This study describes a novel Gram-negative strain (LVF3^R) of the species *Serratia marcescens*. The strain was characterized genomically, morphologically, and physiologically. In addition, the potential of the isolate to act as a host strain to assess the diversity of *Serratia* associated phages in environmental samples was explored. Average nucleotide identity analysis revealed that LVF3^R belongs to the species *Serratia marcescens*. *In silico* analysis and ProphageSeq data resulted in the identification of one prophage, which is capable of viral particle formation. Electron microscopy showed cells of a rod-shaped, flagellated morphotype. The cells revealed a length and width of 1–1.6 µm and 0.8 µm, respectively. LVF3^R showed optimal growth at 30 C and in the presence of up to 2% (w/v) NaCl. It exhibited resistances to ampicillin, erythromycin, oxacillin, oxytetracycline, rifampicin, tetracycline, and vancomycin. Genome data indicate that strain *S. marcescens* LVF3^R is a potential PGPR strain. It harbors genes coding for indole acetic acid (IAA) biosynthesis, siderophore production, plant polymer degradation enzymes, acetoin synthesis, flagellar proteins, type IV secretion system, chemotaxis, phosphorous solubilization, and biofilm formation.

Introduction

The genus *Serratia* belongs to the order Enterobacterales, which is part of the Gammaproteobacteria, a large and diverse group of facultatively anaerobic, non-spore-forming, Gram-negative, rod-shaped bacteria. Related families are *Budviciaceae*, *Enterobacteriaceae*, *Erwiniaceae*, *Hafniaceae*, *Morganellaceae*, *Pectobacteriaceae* and *Yersiniaceae* [1]. The genus *Serratia* is part of the family *Yersiniaceae*, consisting of the eight genera *Chania*, *Chimaeribacter*, *Ewingella*,

deposited at the DSMZ under collection number DSM 112280.

Funding: The authors received no specific funding for this work.

Competing interests: The authors have declared that no competing interests exist.

Rahnella, *Rouxiella*, *Samsonia*, *Serratia* and *Yersinia* [1]. *Yersiniaceae* members are described as motile, catalase-positive and unable to produce hydrogen disulfide [1]. To date, the genus *Serratia* consists of 24 species (LPSN [2] accessed on 28 January 2021), which can be isolated from diverse environments such as soil, plants, animals, insects, and water [3,4].

The genus *Serratia* is named after the Italian physicist Serafino Serrati and was first discovered in 1819 by Bartolomeo Bizio in Padua, Italy. However, the history of *Serratia* reaches back to the Middle Ages when it played a role in eucharist miracles. Some *Serratia* strains produce a red and non-diffusible pigment designated prodigiosin. As they are able to grow on bread, these *Serratia* may have been used to mimic blood on church bread at the time [5]. *Serratia* cells are Gram-negative and rod-shaped with rounded ends, and do not form endospores [3], except the potential spore-forming *Serratia marcescens* subsp. *Sakuensis* [6]. However, the International Committee on Systematics of Prokaryotes has not yet been able to confirm this [4].

Serratia is frequently associated with animals and plants. It can be isolated from healthy individuals [3] and is associated with conjunctivitis in horses, septicemia in foals, pigs and goats, and mastitis in cows [7,8]. Some strains are opportunistic pathogens causing pneumonia, septicemia, or cutaneous lesions [9,10]. *Serratia marcescens* account for 1–2% of nosocomial infections in humans, mostly occurring in the respiratory or urinary tract, surgical wounds, and soft tissues [11–13]. On plants, *Serratia marcescens* strains can cause the cucurbit yellow vine disease (CYVD) in watermelons, pumpkins, and yellow squash, as well as soft-rot disease in the bell pepper [14–16]. Nevertheless, reports of plant-promoting *S. marcescens* strains also exist [17,18].

Serratia strains can produce industrially relevant extracellular enzymes such as highly active DNA/RNA endonucleases, lipases, proteinases and chitinases [3,19]. The pigment prodigiosin has antibacterial and antitumor properties and is produced by *S. marcescens*, *S. plymuthica* and *S. rubidaea* [3,20,21]. As *Serratia* species exhibit multiple antibiotic resistances, there is now a revival of interest in phages as therapeutic agents [22].

Phages or bacteriophages are viruses of bacteria. Lytic phages reproduce directly after infection, while temperate phages can integrate into the bacterial genome. There they inactivate, and replicate together with their host, resulting in a prophage and a lysogenic bacterium. A prophage can impart new properties to its host through the addition of its genetic material, thereby protecting it from infection with related and unrelated viruses [23].

Active *Serratia* bacteriophages can frequently be found in rivers and sewage [24–26]. *Serratia* phages are often able to infect related genera [27–29]. Lysogeny can frequently be observed within the genus *Serratia* [3]. To date, the complete genomic sequences of 14 *Serratia*-associated phages are available (accessed on 28 January 2021) in the NCBI Viral RefSeq database [30]. In order to isolate novel phages from the environment, safe and well-characterized host strains are required. Ideally, these should be non-pathogenic and have no or only few prophages to avoid prophage-induced resistance, which would lead to a strain which cannot be infected by phages.

In a previous study, we succeeded to isolate an environmental *Serratia marcescens* strain which originated from an oligotrophic pond in Göttingen, Germany (51° 33' 59" N 9° 56' 22" E 230 m, collected on 18 September 2018). The *Serratia* strain was isolated as potential model strain to study the local viral diversity associated with it. While 16S rRNA gene analysis confirmed its species assignment, no further characterization has been done previously [31].

In this study, an environmental *Serratia marcescens* isolate is characterized morphologically, physiologically and genomically. In addition, its potential as a host strain to access the environmental diversity of *Serratia* associated phages is explored.

Material and methods

Isolation of *Serratia marcescens* LVF3 strain, DNA extraction, and 16S rRNA gene sequencing

Serratia marcescens LVF3^R was isolated from the surface water near frog's lettuce (*Groenlandia densa*) from an oligotrophic pond located in the northern part of Weende, Göttingen, Germany [31]. In this study, no specific permissions were required for the location, which is a public pond in Göttingen outside of any protected area. As culture medium, 25 mL TSB-10 (1.7% peptone from casein, 0.3% peptone from soybean, 0.25% K₂HPO₄, 1% NaCl, 0.25% glucose monohydrate) were used. DNA was extracted as described by Friedrich et al., 2021 [31].

Genome and prophage sequencing, assembly, and annotation

The genome and prophages were sequenced, assembled and annotated as described in Friedrich et al. 2021. In brief, Illumina paired-end sequencing libraries were prepared using the Nextera XT DNA Sample Preparation kit and sequenced using the MiSeq System and Reagent Kit version 3 (2 x 300 bp) according to the manufacturer's recommendations (Illumina, San Diego, CA, USA) [31]. For Nanopore sequencing, the Ligation Sequencing Kit (SQK-LSK109) and the Native Barcode Expansion Kit EXP-NBD114 (Barcode 14; Oxford Nanopore Technologies, Oxford, UK) were used [31].

Potential CRISPR regions were identified with CRISPRFinder [32]. Assembled genomes were quality-checked with CheckM v1.1.2 [33]. Genome annotation was performed by the NCBI (National Centre for Biotechnological Information) using the Prokaryotic Genome Annotation Pipeline v4.13 (PGAP) [34].

The whole-genome sequence of *Serratia marcescens* LVF3^R has been deposited at GenBank under the accession numbers CP063229 (chromosome) and CP063230 (plasmid). The BioProject with the accession number PRJNA669584 contains the BioSample SAMN16456043. The raw reads have been deposited in the NCBI SRA database under the accession numbers SRR12951277 (Oxford Nanopore) and SRR12951278 (Illumina MiSeq) and BioProject PRJNA669584. The strain has been deposited at the DSMZ (Deutsche Sammlung von Mikroorganismen und Zellkulturen, Braunschweig, Germany) under collection number DSM 112280.

Phylogenetic classification of *Serratia marcescens* LVF3^R

To provide an initial taxonomic classification of the *Serratia marcescens* isolate, the Genome Taxonomy Database Toolkit (GTDB-Tk) v1.0.2 [35] was used as well a whole-genome-based phylogeny with Type (Strain) Genome Server (TYGS [36], accessed on 31 January 2021). In-depth phylogenetic analysis was done with the ANIm method included in pyani v0.2.10 [37]. A species boundary of 95% ANI was used [35]. The isolate was compared to all available type strain and reference genomes based on the lists of the DSMZ and the NCBI (accessed on 28 April 2021): *Enterobacter asburiae* ATCC 35953^T (PRJNA285282), *Kluyvera cryocrescens* NBRC 102467^T (PRJDB285), *Raoultella planticola* ATCC 33531^T (PRJNA65511), *Raoultella planticola* DSM 2688^R (PRJNA500331), *Serratia ficaria* NBRC 102596^T (PRJDB1514), *S. inhibens* S40^T (PRJNA491277), *S. liquefaciens* ATCC 27592^T (PRJNA208332), *S. marcescens* ATCC 13880^T (PRJNA59561), *S. marcescens* subsp. *sakuensis* KCTC 42172^T (PRJNA484649), *S. nematodiphila* DSM 21420^T (PRJNA257492), *S. plymuthica* NBRC 102599^T (PRJDB268), *S. proteamaculans* CCUG 14510^T (PRJNA563568), *S. quinivorans* NCTC 11544^T (PRJEB6403), *S. rubidae* NBRC 103169^T (PRJDB269), *Serratia* sp. S119^R (PRJNA342012) and *Skermanella stiibiirensis* SB22^T (PRJNA214805).

Comparative genomics

Metabolic capabilities of LVF3^R were investigated using BlastKOALA v2.2 [38] (S2 Fig). Putative secondary metabolite biosynthetic gene clusters were identified with antiSMASH v6.0.0b [39,40]. Putative phage regions were identified with PHASTER [41]. Antibiotic resistance annotation was investigated through Resfams v1.2.2 [42].

Cell morphology and Gram staining procedure

Colony morphology was studied by microscopy (Primo Star, Zeiss, Carl Zeiss Microscopy, Jena, Germany) of single colonies (4X magnification) after growth on TSA-10 solid medium (Fluka, Munich, Germany) for 24 h. A Gram staining analysis was performed using Hucker's crystal violet, an iodine and safranin solution and 1-propanol [43]. Microscopy images and staining were processed and evaluated with the software ZEISS Labscope (Carl Zeiss).

Transmission electron microscopy

Cell morphology of LVF3^R was assessed by transmission electron microscopy (TEM). Data were imaged onto the screen using the digital Micrograph software (Gatan GmbH, Munich, Germany). The isolate was grown in liquid TSB-10 medium overnight at 30°C. Afterwards, a negative staining technique was performed. For this purpose, 5 µL cell suspension were mixed with the same amount of diluted 0.5% phosphotungstic acid (3% stock, pH 7) and were transferred to a vaporized carbon mica for 1 min. The mica was washed briefly with demineralized water and transferred to a thin copper-coated grid (PLANO GmbH, Marburg, Germany). The coated grids were dried at room temperature and examined through a Jeol 1011 TEM (Georgia Electron Microscopy, Freising, Germany).

Determination of salt tolerance and temperature optimum

For the determination of the salt tolerance, LVF3^R was inoculated in 4 mL TSB medium amended with 0, 5 and 10 to 100 g/L NaCl in increments of 10 g. The optical density of the cell suspensions was measured using the Ultraspec 3300 pro photometer (Amersham Pharmacia Biotec Europe GmbH, Munich, Germany) at a wavelength of 600 nm (OD₆₀₀). OD₆₀₀ of the cell suspensions were set to 0.3 at the beginning of the experiment [44], followed by an incubation period of 3 h at 30°C and 180 rpm in a Infors HT shaker (Orbitron, Einsbach, Germany). After 3 h incubation, the OD₆₀₀ was measured and the initial OD subtracted to assess growth [44]. All measurements were performed in biological replicates.

To quantify the temperature optimum, the isolate was grown in 4 mL TSB-10 medium at 10°C, 20°C, 30°C, 37°C, 40°C and 50°C at 180 rpm. The starting OD₆₀₀ of the cell cultures was set to 0.1. The optical cell density of LVF3^R was measured after 3 h. The collected data was illustrated with R studio version 4.0.0 [45] using ggplot2 package [46].

Determination of growth kinetics

The growth kinetics in liquid cultures were measured with the cell growth quantifier (CGQuant 8.1) (Aquila Biolabs GmbH, Baesweiler, Germany) at 30°C for 47 h. 25 mL of LVF3^R with a final OD₆₀₀ of 0.1 in TSB-10 medium were filled into 250 mL shake flasks. All flasks were mounted onto the CGQuant sensor plate and were shaken for 47 h. The CGQuant enables a dynamic approach of backscattered light measurement, monitoring the growth of the liquid cultures in real-time [47]. All measurements were performed as biological replicates. All collected data were illustrated with R studio version 4.0.0 [45] using ggplot2 package [48].

Metabolic activity and antibiotic resistances

Metabolic activities were identified using API ZYM and API 20 E tests (BioMérieux, Nuertingen, Germany). Both tests were performed according to the instructions of the manufacturer. Catalase activity was determined using 3% H₂O₂ [49]. For determination of antibiotic resistances, a soft-agar (0.4% (w/v) agarose in TSA-10 medium) overlay technique was used with discs, and strips (Oxoid, Thermo Fisher Scientific) containing ampicillin (25 µg), chloramphenicol (30 µg), doxycycline (30 µg), erythromycin (10 µg), kanamycin (30 µg), oxytetracycline (30 µg), rifampicin (2 µg), streptomycin (10 µg), vancomycin (30 µg), meropenem (0.002–32 µg), and oxacillin (0.015–256 µg). Soft agar (2.5 mL) was used to inoculate the isolates with a final OD₆₀₀ of 0.1. Afterwards, discs or strips were placed on the soft agar. All plates were incubated overnight at 30°C.

Plaque assay with sewage water

For phage enrichment, the same procedure was conducted as described by Willms & Hertel, 2016 [50] and Willms et al., 2017 [51]. After incubation, different plaque morphologies such as clear or turbid, the size of plaques, and the presence or absence of a halo were differentiated. Generally, the performance of a plaque assay requires the ability of the host to grow in bacterial lawns [52].

Results and discussion

Morphological characterization

Grown on TSA-10 medium agar LVF3^R revealed round cream-white colonies with an average diameter of 0.340 mm (S3 Fig). A Gram staining of LVF3^R resulted in pink stained cells (S4 Fig), indicating a Gram-negative type. The cells' size ranged from 1–1.6 µm, with epileptic and short cells or straight rods with rounded ends (Fig 1A). The isolate displays a typical morphological characteristic of the *Serratia* genus, such as motility by means of polar flagella, a cell size that ranges from 0.9–2.0 µm and rod-shaped cells with rounded ends [3]. Further, phage particles, presumably originating from activated prophages, could be observed in the bacterial culture (Fig 1B).

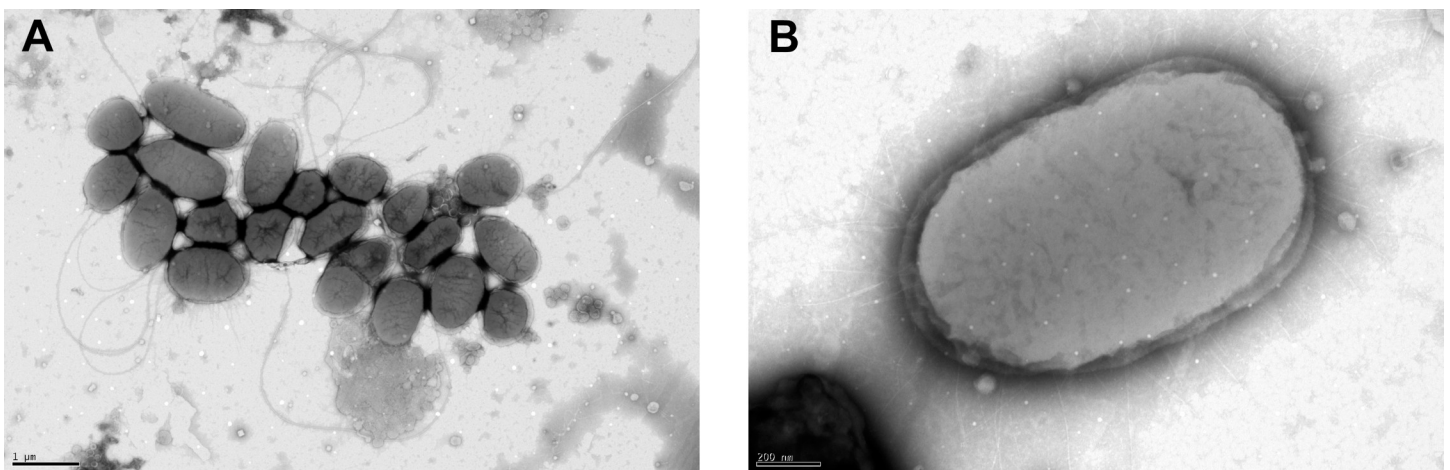


Fig 1. Transmission electron microscopy images of LVF3^R. The micrograph (A) shows the typically observed cell morphotypes of *S. marcescens* strain LVF3^R. Micrograph (B) shows *S. marcescens* LVF3^R surrounded by its active prophages. Cells were grown for 24 h at 30°C in TSB-10 medium, negatively stained and used for TEM analysis.

<https://doi.org/10.1371/journal.pone.0259673.g001>

Physiological characterization

LVF3^R showed growth up to 10% (w/v) NaCl in TSB medium with an optimum between 0–2% (w/v) NaCl (Fig 2A). The LVF3^R strain was able to grow at a temperature range between 20 and 40°C, which is indicative of a mesophilic organism. The highest cell densities were observed at 30°C with an OD₆₀₀ of 2.670 (which is a ratio of 8.9) (Fig 2B). This observation is in good agreement with data obtained from related strains [3].

The growth kinetics of LVF3^R were determined under optimal salt and temperature conditions (Fig 2C). The isolate enters the log phase after a lag phase of approximately three hours which continued for 12 hours until entering a transient phase with reduced growth. Maximum cell densities were observed after around 28 h of cultivation. After the culture reached its peak of maximum growth, cell densities decline, indicating cell-lysis. LVF3^R has a doubling time of 304 minutes and a growth rate μ of 0.14 h⁻¹.

The metabolic capabilities of LVF3^R were analyzed by using the API ZYM and the API 20 E tests. Twenty different enzyme activities were determined via API ZYM for the *S. marcescens* isolate. In 13 cases, no enzymatic activity could be determined. The remaining enzymes activities comprised alkaline phosphatase, esterase, esterase lipase, leucine arylamidase, acid phosphatase, naphthol-AS-BI-phosphohydrolase and β -galactosidase activity. Enzymes such as alkaline phosphatase and β -galactosidase were confirmed in the genome playing a role in signaling and cellular processes as well galactose metabolism were confirmed by genome analysis (S1 Table). The alkaline phosphatase is part of the periplasm, whereas the β -galactosidase is part of the outer membrane in *Serratia marcescens* [53]. Interestingly, strain LVF3^R is able to utilize urea, which has previously only been described in *Serratia ureilytica* [54]. LVF3^R was oxidase-negative and catalase-positive, which is characteristic for the *Yersiniaceae* family [1]. A general overview of all enzymatic activities of the strain and closely related strains from TYGS [36] is listed in Table 1. LVF3^R is capable of D-glucose fermentation/oxidation. The antibiogram (S5 Fig) showed that LVF3^R is resistant to ampicillin (25 μ g/disc), erythromycin (10 μ g/disc), oxytetracycline (30 μ g/disc), rifampicin (2 μ g/disc), tetracycline (30 μ g/disc), vancomycin (30 μ g/disc), oxacillin (256 μ g/disc) and meropenem (until 0.06 μ g/disc). Resfams in silico analysis [42] identified genes encoding an ABC transporter for erythromycin or vancomycin (PRJNAA669584|IM817_08890), an MFS transporter for tetracycline or oxytetracycline (IM817_13485), β -lactamases for meropenem (IM817_13270), oxacillin and ampicillin inactivation (IM817_09360), and an efflux pump system of the RND family putatively exporting rifampicin (IM817_09370; S2 Table). The antibiogram as well the congruent in silico investigation of strain LVF3^R, showed a resistance potential to medically relevant antibiotics. *Serratia marcescens* LVF3^R shows a different antibiogram compared to its phylogenetically closest relatives. It is not resistant to chloramphenicol, doxycycline, kanamycin, meropenem and streptomycin. Like *S. marcescens* DSM 17174^R and *S. nematodiphila* DSM 21420^T, LVF3^R is not resistant to chloramphenicol, kanamycin, and streptomycin. Ampicillin and oxacillin resistance seem to be unique to our isolate (Table 1).

Interestingly, non-pigmented strains of *S. marcescens* are usually more resistant to antibiotics than pigmented strains as they often harbor resistance plasmids [59]. No potential genes encoding antibiotic resistance were detected in the plasmid sequence of strain LVF3^R. Environmental *Serratia marcescens* strains are resistant to colistin, cephalothin, ampicillin, tetracycline, and nitrofurantoin [3]. Strain LVF3^R does not produce the red-pigmented antibiotic prodigiosin. This is in agreement with the genome analysis as genes of the *pig* cluster encoding the biosynthesis of prodigiosin [60]. were not detected. In a study by Haddix & Shanks (2018), pigmented cells were shown to have twice the biomass yield of non-pigmented *S. marcescens* strains [61]. Furthermore, LVF3^R appears to produce secondary metabolites such as the

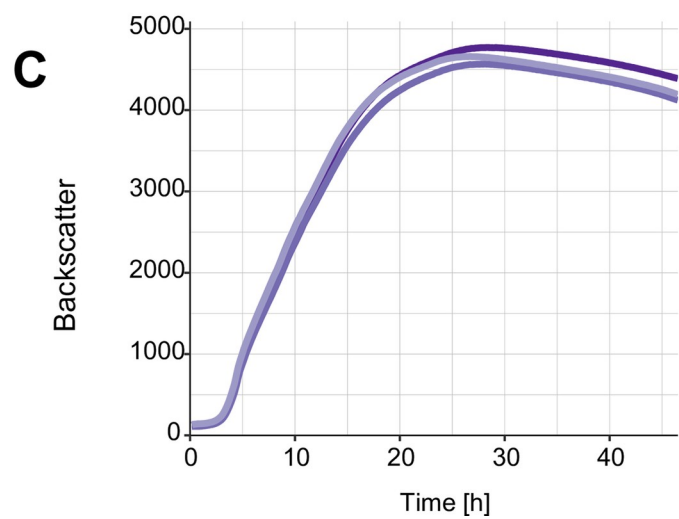
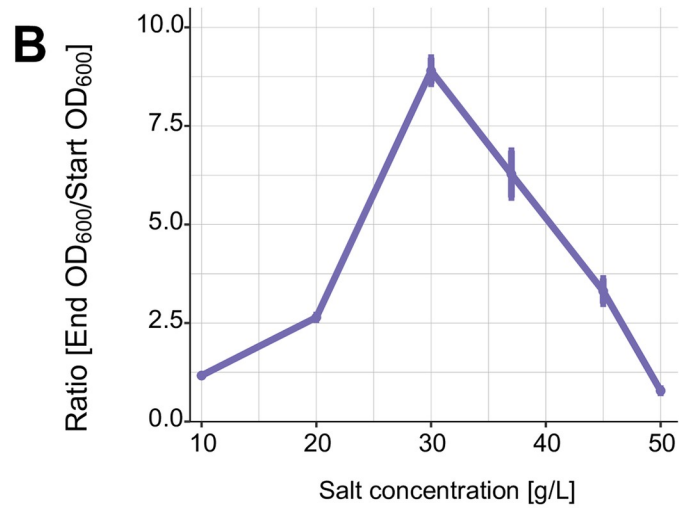
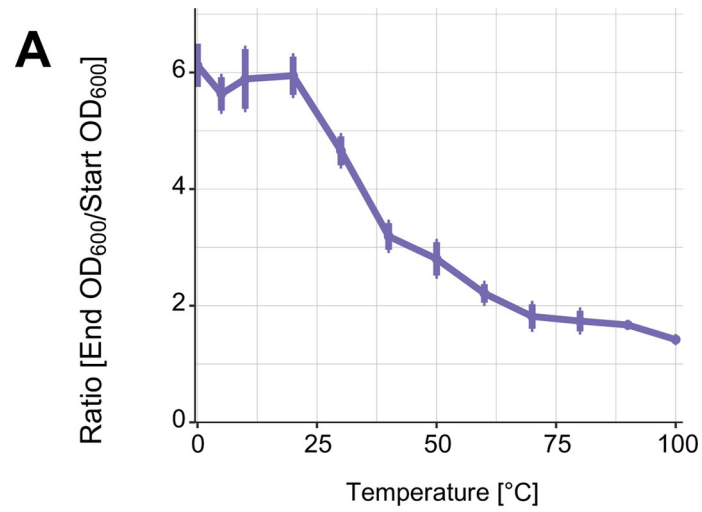


Fig 2. *S. marcescens* LVF3^R growth properties. (A) Growth of LVF3^R in 4 mL TSB medium with different salt concentrations after 3 h incubation at 180 rpm and 30°C. (B) LVF3^R growth in TSB-10 medium at different temperatures after 3 h incubation at 180 rpm. (C) Growth analysis of LVF3^R at the optimum temperature (30°C) in 25 mL TSB-10 medium. Measurements were performed in triplicate. The standard deviation in (A) and (B) is shown as error bars. In (C) different shades of purple indicate each replicate.

<https://doi.org/10.1371/journal.pone.0259673.g002>

Table 1. Phenotypic characteristics of strain LVF3^R and phylogenetically related species *Serratia* sp. S119^R, *S. marcescens* ATCC 13880^T, *S. marcescens* DSM 17174^R, *S. nematodiphila* DSM 21420^T.

Characteristics	<i>S. marcescens</i> LVF3 ^R	<i>Serratia</i> sp. S119 ^R	<i>S. marcescens</i> ATCC 13880 ^T	<i>S. marcescens</i> subsp. <i>sakuensis</i> KCTC 42172 ^T	<i>S. nematodiphila</i> DSM 21420 ^T
Source of isolation	Surface water	Peanut nodule	Pond water	Activated sludge	Intestine of nematode
Spore formation	–	–	–	+	–
Red colony pigmentation	–	–	+	+	+
Motility	+	+	+	+	+
Glucose oxidation	+	n/a	n/a	n/a	n/a
Glucose fermentation	+	n/a	n/a	+	n/a
Temperature (°C)					
Range	10–45	n/a	n/a	n/a	4–42
Optimum	30	28	30–37	28–37	33.5
NaCl (g/L)					
Range	0–60	n/a	n/a	0–70	20–70
Optimum	0–20	10	5	5	45
Utilization of					
2-nitrophenyl-βD-galactopyranoside	+	+	+	n/a	n/a
L-arginine	–	–	–	+	+
L-lysine	+	+	+	+	+
L-ornithine	+	+	+	+	+
Trisodium citrate	+	+	+	+	+
Sodium thiosulfate	–	–	–	–	–
Urea	+	–	–	–	–
L-tryptophane	–	–	–	+	+
L-tryptophane (indole production)	–	–	v	–	–
Sodium pyruvate (Voges Proskauer)	+	–	v	+	+
Gelatin	+	+	+	n/a	+
D-glucose	+	+	+	+	+
D-mannitol	+	+	+	n/a	+
Inositol	+	+	v	n/a	n/a
D-sorbitol	+	+	+	+	+
L-rhamnose	+	–	v	n/a	n/a
D-sucrose	+	+	+	+	+
D-melibiose	+	+	+	–	+
Amygdalin	+	+	+	n/a	n/a
L-arabinose	–	+	v	–	+
Catalase	+	n/a	n/a	+	+
Oxidase	–	–	–	–	–
Resistance to					
Ampicillin	+	n/a	–	–	–

(Continued)

Table 1. (Continued)

Characteristics	<i>S. marcescens</i> LVF3 ^R	<i>Serratia</i> sp. S119 ^R	<i>S. marcescens</i> ATCC 13880 ^T	<i>S. marcescens</i> subsp. <i>sakuensis</i> KCTC 42172 ^T	<i>S. nematodiphila</i> DSM 21420 ^T
Chloramphenicol	–	+	+	–	–
Doxycycline	–	n/a	+	n/a	n/a
Erythromycin	+	n/a	+	+	n/a
Kanamycin	–	n/a	+	–	–
Meropenem	–	n/a	n/a	n/a	–
Oxacillin	+	n/a	–	n/a	n/a
Oxytetracycline	+	n/a	n/a	n/a	n/a
Rifampicin	+	n/a	n/a	n/a	–
Tetracycline	+	n/a	+	+	–
Streptomycin	–	n/a	n/a	–	–
Vancomycin	+	n/a	–	n/a	+
G + C %	59.29	59.85	59.8	58	59.52

In bold: Sorted by categories.

Taxa: 1, strain *S. marcescens* LVF3^R; 2, *Serratia* sp. S119^R (data from [55]); 3, *S. marcescens* ATCC 13880^T (data from BacDive [56] on 24 February 2021); 4, *S. marcescens* subsp. *sakuensis* KCTC 42172^T (data from [6,57]; LPSN [58] accessed on 24 February 2021); 5, *S. nematodiphila* DSM 21420^T (data from [57]; BacDive [56] accessed on 24 February 2021); +, Positive; –, negative; v, some strains showed activity; n/a, not available.

<https://doi.org/10.1371/journal.pone.0259673.t001>

antibiotic andrimid, the cyclic lipopeptide orfamid and the O-antigen of lipopolysaccharides (S3 Table). Andrimid production was also detected in the plant-associated *Serratia plymuthica* A153 and *Serratia marcescens* MSU97 [62,63]. Orfamid as a bioactive compound may be released for plant protection [64]. The O-antigen of lipopolysaccharides is responsible for a normal growth rate in plants such as tomatoes [65].

Comparisons of the LVF3^R genome to the genomes of the phylogenetically most closely related strain *Serratia* sp. S119^R and the PGPR strain *Serratia marcescens* UENF-22GI showed that they share numerous plant-growth promoting genes (49 with S119^R and 11 with UENF-22GI). These genes code for components of indole acetic acid (IAA) biosynthesis, siderophore production, plant polymer degradation enzymes, acetoin synthesis, flagellar proteins, type IV secretion system, chemotaxis, phosphorous solubilization, and biofilm formation (S4 Table). All of these genes are known to provide important plant growth-promoting properties [55,66]. *Serratia* sp. S119^R, a known biofertilizer for peanut and maize, is closely related to LVF3^R with 96.08% average nucleotide identity (S5 Table). Based on these results, the environmental origin of isolation (surface water near frog's lettuce) and the detected physiological properties, it is indicated that *Serratia marcescens* strain LVF3 has the potential to promote plant growth.

Genomic characterization

Genome. Genome sequencing using Illumina and Oxford Nanopore technologies resulted in a high-quality closed genome (S6 Table). The genome of LVF3^R consists of one circular chromosome (5,440,698 bp) with a GC-content of 59.29% and one circular plasmid (87,710 bp) with a GC-content of 53.27%. The difference in GC content (6.02%) suggests that the plasmid was obtained recently. The chromosome has a 285.9-fold and the plasmid a 418.7-fold coverage, implying that the plasmid is present in two copies per cell. The chromosome encodes 5,159 protein-encoding genes, 129 rRNAs and 92 tRNAs. The plasmid encodes 94 protein-encoding genes. No CRISPR regions were detected. Genomic characteristics are listed in Table 2.

Table 2. Genome statistics of the LVF3^R chromosome and p87710 plasmid.

Features	Chromosome	Plasmid
Genome size (bp)	5,440,698	87,710
GC content (%)	59.29	53.27
Coverage	285.9-fold	418.7-fold
CDS	5,159	94
rRNA genes	129	0
tRNA genes	92	0
ncRNA	15	0
CRISPR	0	0
Prophage(s)	2	0

<https://doi.org/10.1371/journal.pone.0259673.t002>

Whole-genome phylogeny. Initial taxonomic assignment of strain LVF3^R was performed with GTDB-Tk pipeline [35]. It revealed an average nucleotide identity (ANI) of approximately 96% to the closest related species *Serratia marcescens* (ANI value of 96.3). This supports LVF3^R's assignment to the species *S. marcescens* (S6 Table). However, taxonomic assignment of LVF3^R employing the Type Strain Genome Server (TYGS) suggests that our strain is a potential new species, although the calculated digital DNA-DNA hybridization (dDDH) value is 73.3%, showing close relationship with the type strain *Serratia marcescens* ATCC 13880 (S1 Fig; S7 Table). The threshold for a new species is below 70% dDDH [67]. ANI-analysis using the 15 closest related type strain genomes derived from the TYGS database [36] as well as the genome of the reference strain (*Serratia* sp. S119) is shown in Fig 3 (data in S6 Table).

The genome of strain LVF3^R builds a cluster with the type strains *S. marcescens* ATCC 13880, *S. nematodiphila* DSM 21420 and *S. marcescens* subsp. *sakuensis* KCTC 42172, and the reference strain *Serratia* sp. S119. LVF3^R shares the closest average nucleotide identity with *Serratia* sp. S119^R (96.08%) and *S. marcescens* ATCC 13880^T (95.33%).

Based on the results of TYGS, GTDB-Tk and ANI analyses, we suggest that strain LVF3 belongs to the species *Serratia marcescens*.

Prophages. The prophage potential of LVF3^R was of particular interest as the strain represents a potential host system for studying phage diversity in the environment. Prophage region were initially analyzed using PHASTER [41], revealing two putative prophage regions (region 1: 2,088,804–2,147,829; region 2: 2,353,448–2,400,701). The regions comprised 59.0 and 47.2 kb and were classified as intact (S7 Table).

Sequence data of phage particle-packed dsDNA was mapped to the LVF3^R genome using ProphageSeq [69] (Fig 4). Prophage activity is indicated when prophage reads accumulate closely associated with the PHASTER-predicted prophage regions. The coverage profile exhibits an even distribution of reads with a substantial coverage increase from base 2,089,081 to 2,143,727 (Fig 4). As the PHASTER-predicted prophage region one was annotated with a preceding start site, the precise location of prophage one was investigated. Reads obtained from particle-packed dsDNA were used for genome assembly. This resulted in one circular contig with a size of 45,631 bp representing the phage genome of the identified prophage. Comparison of the phage genome with the chromosome of LVF3^R enabled us to precisely locate the corresponding prophage region. Thus, prophage one is located between 2,098,352 and 2,144,007 bp flanked by perfect direct repeats of 25 bp (5' AGGAATCGTATTCGGTCTTT TTTTG), which represented the *attL* and *attR* sites. For prophage two, neither a pronounced sequence accumulation was observed at the predicted prophage region, nor was it possible to assemble the respective phage genome.

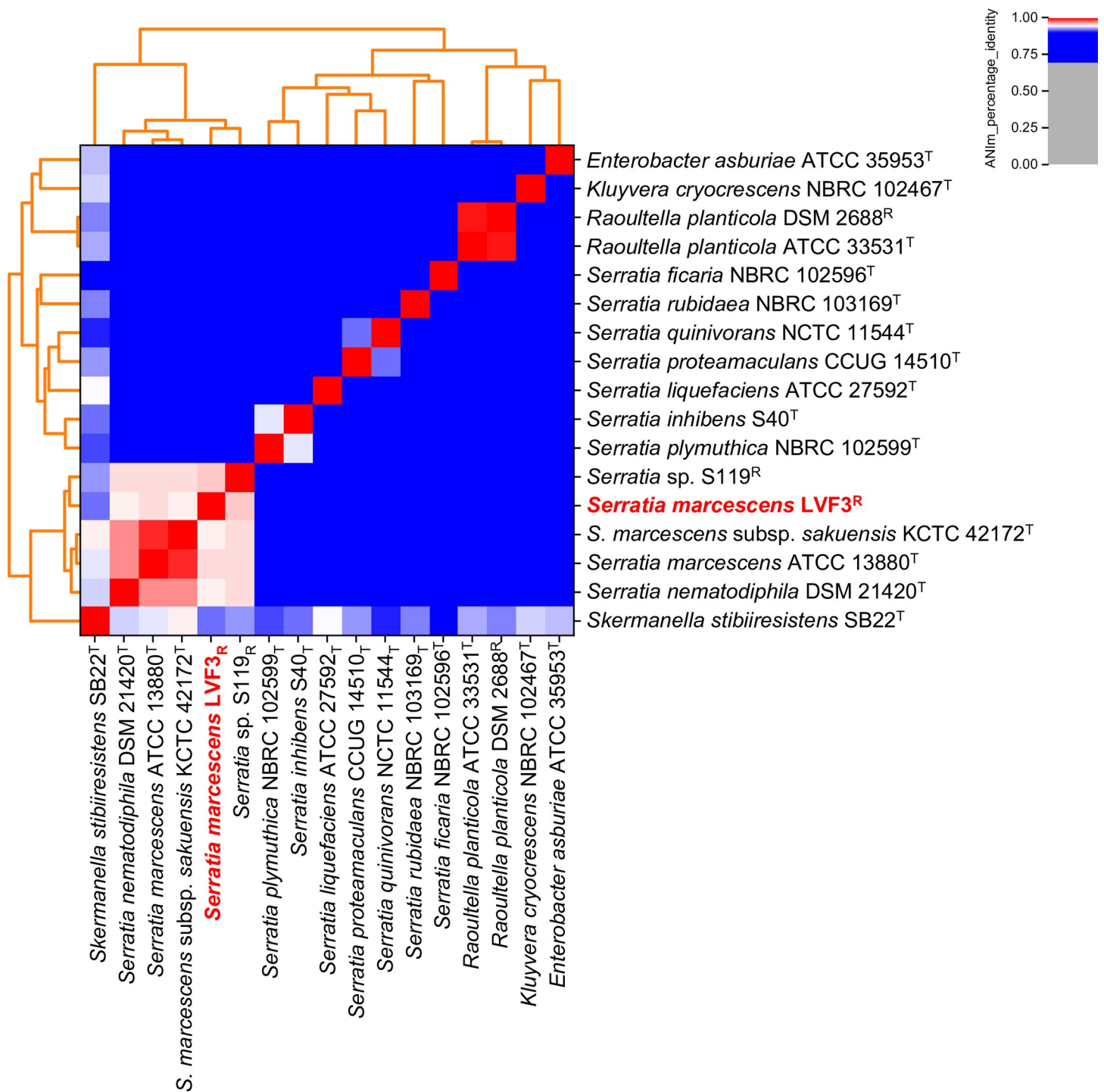


Fig 3. Genome-based phylogenetic analysis of *Serratia marcescens* LVF3^R. All genomes from available type strains (T) included in the TYGS database [36] and a representative strain (R) from the genus *Serratia* were examined. Calculations were done with pyani [37,68] using ANIm method with default parameters. LVF3^R is depicted in bold red.

<https://doi.org/10.1371/journal.pone.0259673.g003>

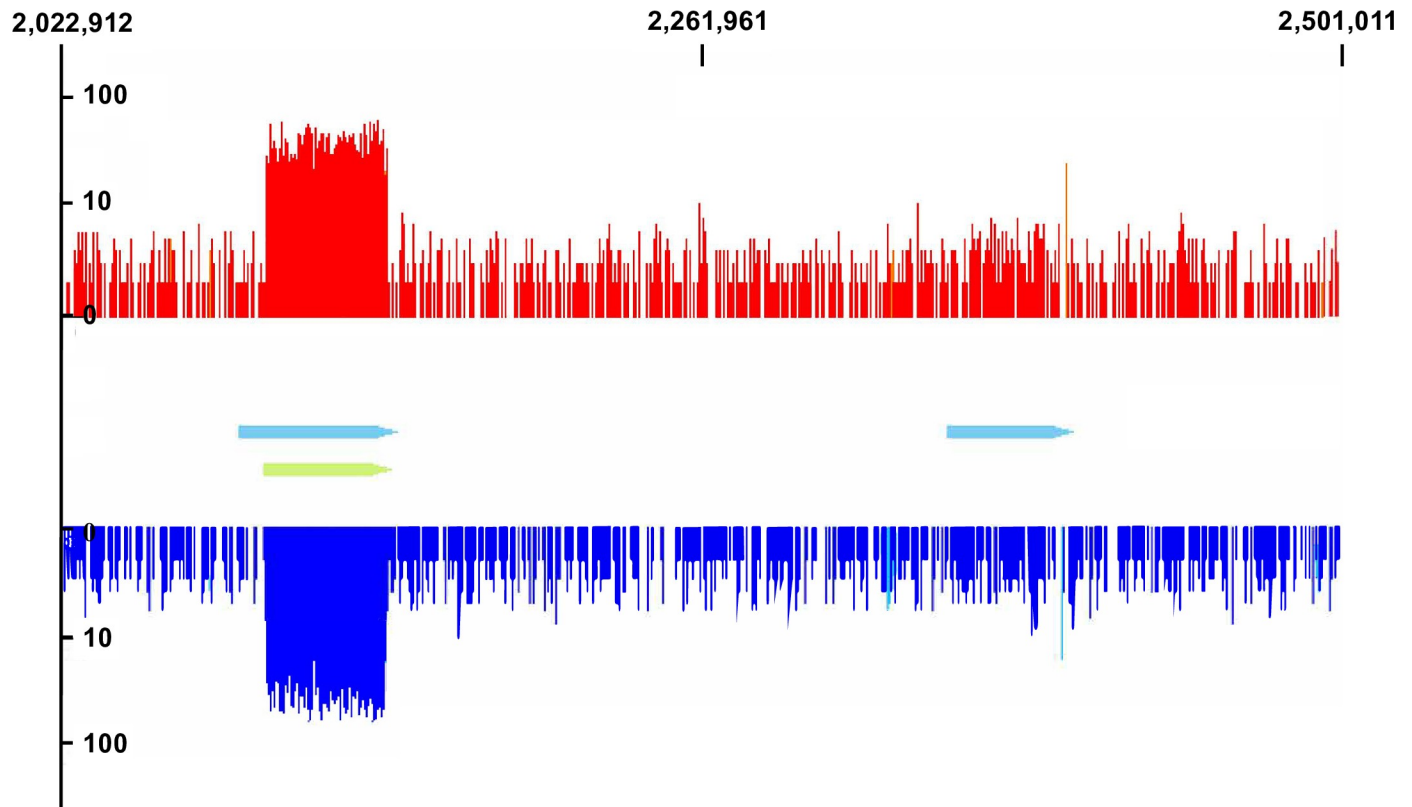


Fig 4. Read coverage profile of sequenced LVF3^R prophages, mapped onto its corresponding host genome. The blue arrows depict the prophage regions predicted by PHASTER [41]. Green arrows indicate the experimentally verified prophage region. The image displays the read coverage of the genome between base 2,022,912 to 2,501,011 (478,099 kb).

<https://doi.org/10.1371/journal.pone.0259673.g004>

In conclusion, one prophage region was experimentally confirmed as particle-forming and capable of packing its genome. The second predicted prophage was unable to form particles under the employed experimental conditions. As prophages can mediate resistance against related phages, a low number or absence of prophages in the genome is required for a potential host strain employed for phage isolation [23] and covering viral diversity in an isolation experiment.

Strain suitability for phage isolation. So far, *S. marcescens* strain LVF3^R has proven to be an easy-to-cultivate organism with simple growth requirements and few intrinsic antibiotic resistances. This provides a good basis for making it a potential working strain in molecular biology. In a next step, we aimed to assess its potential as host strain for environmental phage isolations. For this purpose, LVF3^R was infected with a viral suspension derived from raw sewage. An overlay plaque assay was employed to analyze the infected cells (Fig 5). Results revealed diverse plaque morphologies corresponding to different phages, thus confirming the suitability of *S. marcescens* LVF3^R as a host strain for phage isolation,

Conclusion

In the framework of this study, the novel *Serratia* strain LVF3R was characterized and determined to be a suitable host strain for environmental phage isolation as it only contains one active and one degenerated prophage in its genome. Further, we could confirm that our strain showed after infection with a viral pool, a high phage diversity. The viral diversity associated with this strain will be the subject of future studies.

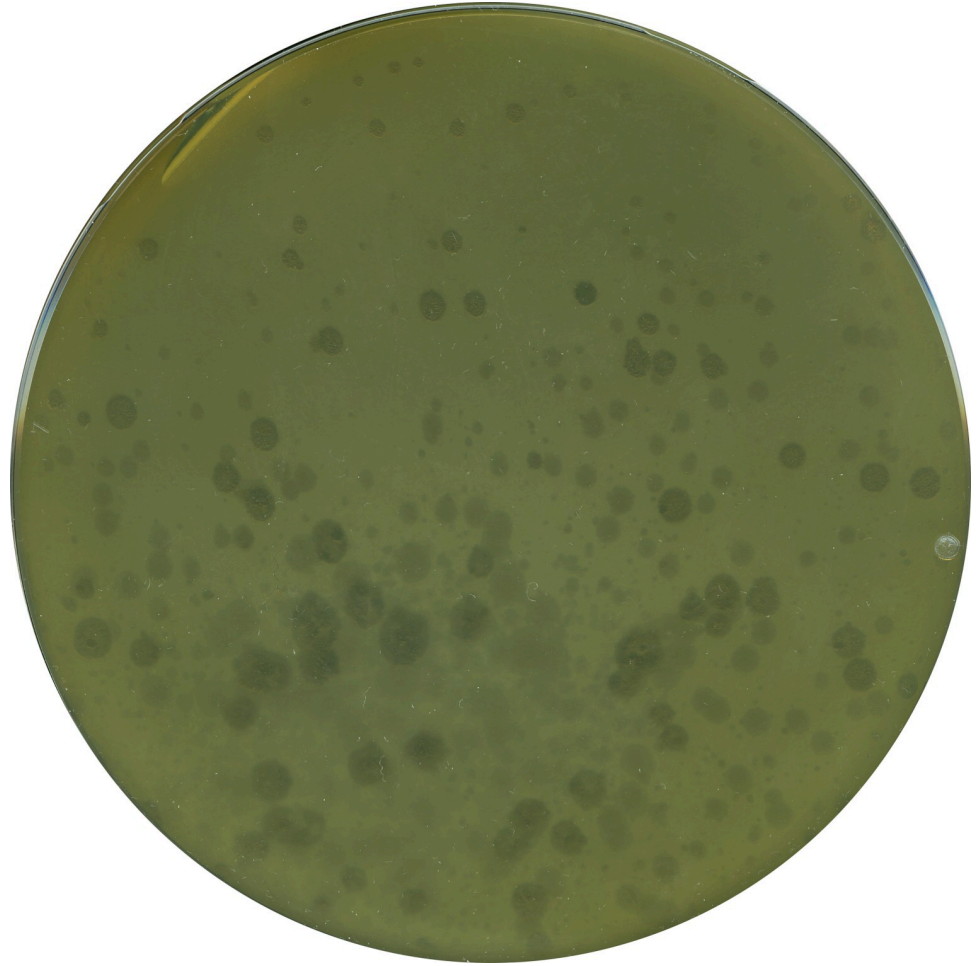


Fig 5. Host strain LVF3 challenged with metaviral sample. Different plaque morphologies can be observed.

<https://doi.org/10.1371/journal.pone.0259673.g005>

Supporting information

S1 Fig. Phylogenetic classification of *Serratia marcescens* strain LVF3.

(PDF)

S2 Fig. Visualization of functional categories through BlastKoala (Kanehisa et al., 2016) [38] for *Serratia marcescens* LVF3^R. Functional categories of (A) chromosome and (B) plasmid can be seen by the presented color code.

(PDF)

S3 Fig. Colony morphotype of *Serratia marcescens* LVF3^R. Growth experiments were performed using TSA-10 agar plates.

(PDF)

S4 Fig. Gram staining of *Serratia marcescens* LVF3^R.

(PDF)

S5 Fig. Analysis of antibiotic resistances through soft-agar assay with discs (A) and strips (B). Exemplarily, antibiotic resistance of isolate LVF3R is indicated by halo formation. Incubation took place overnight at 30°C. (A) Meropenem (0.002–32 µg), and (B) kanamycin (30 µg),

chloramphenicol (30 µg), streptomycin (10 µg) and rifampicin (2 µg) were used as antibiotics. (PDF)

S1 Table. KEGG Mapper Reconstruction Result of *Serratia marcescens* LVF3^R.
(XLSX)

S2 Table. Resfams prediction of *Serratia marcescens* LVF3^R.
(XLSX)

S3 Table. List of putative biosynthetic gene clusters in *Serratia marcescens* LVF3^R.
(XLSX)

S4 Table. Comparison of putative genes involved in important plant growth promoting traits of *Serratia marcescens* LVF3^R, *Serratia* sp. S119^R and *Serratia marcescens* UENF-22GI. Table was modified from Ludueña et al., 2017 and Matteoli et al., 2018. In purple: Potential plant growth promoting gene products encoded by the genome of LVF3^R. References: Ludueña LM, Anzuay MS, Angelini JG, McIntosh M, Becker A, Rupp O, et al. Strain *Serratia* sp. S119: A potential biofertilizer for peanut and maize and a model bacterium to study phosphate solubilization mechanisms. *Appl Soil Ecol.* 2017;126:107–12. Matteoli FP, Passarelli-Araujo H, Reis RJA, da Rocha LO, de Souza EM, Aravind L, et al. Genome sequencing and assessment of plant growth-promoting properties of a *Serratia marcescens* strain isolated from vermicompost. *BMC Genomics.* 2018;19:750.
(XLSX)

S5 Table. Phylogenetic analysis for *Serratia marcescens* LVF3^R.
(XLSX)

S6 Table. GTDB-Tk of *Serratia marcescens* LVF3^R isolate.
(XLSX)

S7 Table. Pairwise comparisons of LVF3 against type strain genomes from TYGS (Meier-Kolthoff and Göker, 2019). Reference: Meier-Kolthoff JP, Göker M. TYGS is an automated high-throughput platform for state-of-the-art genome-based taxonomy. *Nat Commun.* 2019;10:2182.
(XLSX)

S8 Table. PHASTER analysis of *Serratia marcescens* LVF3^R.
(XLSX)

Acknowledgments

We thank Dr. Anja Poehlein for sequencing, Sarah-Theresa Schüßler and Mechthild Bömeke for technical assistance, Dr. Dominik Schneider for his help with bioinformatics and Dr. Michael Hoppert for support with TEM-imaging. We thank Avril von Hoyningen-Huene for her diligent proofreading of this paper. We also acknowledge support by the Open Access Publication Funds of the University of Göttingen.

Author Contributions

Conceptualization: Ines Friedrich, Robert Hertel, Rolf Daniel.

Data curation: Ines Friedrich, Robert Hertel.

Formal analysis: Ines Friedrich, Robert Hertel, Rolf Daniel.

Funding acquisition: Rolf Daniel.

Investigation: Ines Friedrich, Bernhard Bodenberger, Hannes Neubauer.

Project administration: Rolf Daniel.

Supervision: Rolf Daniel.

Validation: Ines Friedrich, Robert Hertel, Rolf Daniel.

Visualization: Ines Friedrich, Bernhard Bodenberger, Hannes Neubauer.

Writing – original draft: Ines Friedrich, Robert Hertel.

Writing – review & editing: Ines Friedrich, Bernhard Bodenberger, Hannes Neubauer, Rolf Daniel.

References

1. Adeolu M, Alnajar S, Naushad S, S. Gupta R. Genome-based phylogeny and taxonomy of the 'Enterobacteriales': proposal for Enterobacterales ord. nov. divided into the families *Enterobacteriaceae*, *Erwiniaceae* fam. nov., *Pectobacteriaceae* fam. nov., *Yersiniaceae* fam. nov., *Hafniaceae* fam. nov., *Morganellaceae* fam. nov., and *Budviciaceae* fam. nov. *Int J Syst Evol Microbiol*. 2016; 66:5575–99. <https://doi.org/10.1099/ijsem.0.001485> PMID: 27620848
2. Parte AC, Carbasse JS, Meier-Kolthoff JP, Reimer LC, Göker M. List of prokaryotic names with standing in nomenclature (LPSN) moves to the DSMZ. *Int J Syst Evol Microbiol*. 2020; 70:5607–12. <https://doi.org/10.1099/ijsem.0.004332> PMID: 32701423
3. Grimont PAD, Grimont F. The genus *Serratia*. *Annu Rev Microbiol*. 1978; 32:221–48. <https://doi.org/10.1146/annurev.mi.32.100178.001253> PMID: 360966
4. Mahlen SD. *Serratia* infections: from military experiments to current practice. *Clin Microbiol Rev*. 2011; 24:755–91. <https://doi.org/10.1128/CMR.00017-11> PMID: 21976608
5. Bennett JW, Bentley R. Seeing red: the story of prodigiosin. *Adv Appl Microbiol*. 2000; 47:1–32. [https://doi.org/10.1016/s0065-2164\(00\)47000-0](https://doi.org/10.1016/s0065-2164(00)47000-0) PMID: 12876793
6. Ajithkumar B, Ajithkumar VP, Iriye R, Doi Y, Sakai T. Spore-forming *Serratia marcescens* subsp. *sakuensis* subsp. nov., isolated from a domestic wastewater treatment tank. *Int J Syst Evol Microbiol*. 2003; 53:253–8. <https://doi.org/10.1099/ijse.0.02158-0> PMID: 12656181
7. Carter ME, Chengappa MM. Enterobacteria. In: *Diagnostic Procedure in Veterinary Bacteriology and Mycology*. Elsevier; 1990. p. 107–28.
8. Wijewanta E, Fernando M. Infection in goats owing to *Serratia marcescens*. *Vet Rec*. 1970; 87:282–4. <https://doi.org/10.1136/vr.87.10.282> PMID: 4919387
9. Manfredi R, Nanetti A, Ferri M, Chiodo F. Clinical and microbiological survey of *Serratia marcescens* infection during HIV disease. *Eur J Clin Microbiol Infect Dis*. 2000; 19:248–53. <https://doi.org/10.1007/s100960050471> PMID: 10834812
10. Ray U, Dutta S, Chakravarty C, Sutradhar A. A case of multiple cutaneous lesions due to *Serratia marcescens* in an immunocompromised patient. *JMM Case Rep*. 2015; 2:1–4.
11. Khanna A, Khanna M, Aggarwal A. *Serratia marcescens*—a rare opportunistic nosocomial pathogen and measures to limit its spread in hospitalized patients. *J Clin Diagn Res*. 2013; 7:243–6. <https://doi.org/10.7860/JCDR/2013/5010.2737> PMID: 23543704
12. Abreo E, Altier N. Pangenome of *Serratia marcescens* strains from nosocomial and environmental origins reveals different populations and the links between them. *Sci Rep*. 2019; 9:1–8. <https://doi.org/10.1038/s41598-018-37186-2> PMID: 30626917
13. Maki DG, Hennekens CG, Phillips CW, Shaw WV, Bennett JV. Nosocomial urinary tract infection with *Serratia marcescens*: an epidemiologic study. *J Infect Dis*. 1973; 128:579–87. <https://doi.org/10.1093/infdis/128.5.579> PMID: 4588701
14. Rascoe J, Berg M, Melcher U, Mitchell FL, Bruton BD, Pair SD, et al. Identification, phylogenetic analysis, and biological characterization of *Serratia marcescens* strains causing cucurbit yellow vine disease. *Phytopathology*. 2003; 93:1233–9. <https://doi.org/10.1094/PHYTO.2003.93.10.1233> PMID: 18944322
15. Sikora EJ, Bruton BD, Wayadande AC, Fletcher J. First report of the cucurbit yellow vine disease caused by *Serratia marcescens* in watermelon and yellow squash in Alabama. *Plant Dis*. 2012; 96:761. <https://doi.org/10.1094/PDIS-09-11-0739-PDN> PMID: 30727534

16. Gillis A, Rodríguez M, Santana MA. *Serratia marcescens* associated with bell pepper (*Capsicum annuum* L.) soft-rot disease under greenhouse conditions. *Eur J Plant Pathol*. 2013; 138:1–8.
17. Khan AR, Park GS, Asaf S, Hong SJ, Jung BK, Shin JH. Complete genome analysis of *Serratia marcescens* RSC-14: a plant growth-promoting bacterium that alleviates cadmium stress in host plants. *PLOS ONE*. 2017; 12:1–17. <https://doi.org/10.1371/journal.pone.0171534> PMID: 28187139
18. Devi KA, Pandey P, Sharma GD. Plant growth-promoting endophyte *Serratia marcescens* AL2-16 enhances the growth of *Achyranthes aspera* L., a medicinal plant. *Hayati*. 2016; 23:173–80.
19. Monreal J, Reese ET. The chitinase of *Serratia marcescens*. *Can J Microbiol*. 1969; 15:689–96. <https://doi.org/10.1139/m69-122> PMID: 4894282
20. Ibrahim D, Nazari TF, Kassim J, Lim SH. Prodigiosin—an antibacterial red pigment produced by *Serratia marcescens* IBRL USM 84 associated with a marine sponge *Xestospongia testudinaria*. *J Appl Pharm Sci*. 2014; 4:1–6.
21. Hong B, Prabhu VV, Zhang S, van den Heuvel APJ, Dicker DT, Kopelovich L, et al. Prodigiosin rescues deficient p53 signaling and antitumor effects via upregulating p73 and disrupting its interaction with mutant p53. *Cancer Res*. 2014; 74:1153–65. <https://doi.org/10.1158/0008-5472.CAN-13-0955> PMID: 24247721
22. Parmar KM, Dafale NA, Tikariha H, Purohit HJ. Genomic characterization of key bacteriophages to formulate the potential biocontrol agent to combat enteric pathogenic bacteria. *Arch Microbiol*. 2018; 200:611–22. <https://doi.org/10.1007/s00203-017-1471-1> PMID: 29330592
23. Kohm K, Hertel R. The life cycle of SPβ and related phages. *Arch Virol*. 2021; 166:2119–30. <https://doi.org/10.1007/s00705-021-05116-9> PMID: 34100162
24. Bhetwal A, Maharjan A, Shakya S, Satyal D, Ghimire S, Khanal PR, et al. Isolation of potential phages against multidrug-resistant bacterial isolates: promising agents in the rivers of Kathmandu, Nepal. *Biomed Res Int*. 2017; 1–10. <https://doi.org/10.1155/2017/3723254> PMID: 29359149
25. Frederick GL, Lloyd BJ. Evaluation of bacteriophage as a tracer and a model for virus removal in waste stabilization ponds. *Water Sci Technol*. 1995; 31:291–302.
26. Matsushita K, Uchiyama J, Kato S, Ujihara T, Hoshiba H, Sugihara S, et al. Morphological and genetic analysis of three bacteriophages of *Serratia marcescens* isolated from environmental water. *FEMS Microbiol Lett*. 2009; 291:201–8. <https://doi.org/10.1111/j.1574-6968.2008.01455.x> PMID: 19087204
27. Prinsloo HE, Coetzee JN. Host-range of temperate *Serratia marcescens* bacteriophages. *Nature*. 1964; 203:211. <https://doi.org/10.1038/203211a0> PMID: 14207257
28. Prinsloo HE. Bacteriocins and phages produced by *Serratia marcescens*. *J Gen Microbiol*. 1966; 45:205–12. <https://doi.org/10.1099/00221287-45-2-205> PMID: 5339480
29. Evans TJ, Crow MA, Williamson NR, Orme W, Thomson NR, Komitopoulou E, et al. Characterization of a broad-host-range flagellum-dependent phage that mediates high-efficiency generalized transduction in, and between, *Serratia* and *Pantoea*. *Microbiology*. 2010; 156:240–7. <https://doi.org/10.1099/mic.0.032797-0> PMID: 19778959
30. Brister JR, Ako-Adjei D, Bao Y, Blinkova O. NCBI viral genomes resource. *Nucleic Acids Res*. 2015; 43:D571–7. <https://doi.org/10.1093/nar/gku1207> PMID: 25428358
31. Friedrich I, Klassen A, Neubauer H, Schneider D, Hertel R, Daniel R. Living in a puddle of mud: Isolation and characterization of two novel *Caulobacteraceae* strains *Brevundimonas pondensis* sp. nov. and *Brevundimonas goettingensis* sp. nov. *Appl Microbiol*. 2021; 1:38–59.
32. Grissa I, Vergnaud G, Pourcel C. CRISPRFinder: a web tool to identify clustered regularly interspaced short palindromic repeats. *Nucleic Acids Res*. 2007; 35:W52–7. <https://doi.org/10.1093/nar/gkm360> PMID: 17537822
33. Parks DH, Imelfort M, Skennerton CT, Hugenholtz P, Tyson GW. CheckM: assessing the quality of microbial genomes recovered from isolates, single cells, and metagenomes. *Genome Res*. 2015; 25:1043–55. <https://doi.org/10.1101/gr.186072.114> PMID: 25977477
34. Tatusova T, DiCuccio M, Badretdin A, Chetvernin V, Nawrocki EP, Zaslavsky L, et al. NCBI prokaryotic genome annotation pipeline. *Nucleic Acids Res*. 2016; 44:6614–24. <https://doi.org/10.1093/nar/gkw569> PMID: 27342282
35. Chaumeil P-A, Mussig AJ, Hugenholtz P, Parks DH. GTDB-Tk: a toolkit to classify genomes with the Genome Taxonomy Database. *Bioinformatics*. 2019; 36:1925–7. <https://doi.org/10.1093/bioinformatics/btz848> PMID: 31730192
36. Meier-Kolthoff JP, Göker M. TYGS is an automated high-throughput platform for state-of-the-art genome-based taxonomy. *Nat Commun*. 2019; 10:2182. <https://doi.org/10.1038/s41467-019-10210-3> PMID: 31097708
37. Pritchard L, Glover RH, Humphris S, Elphinstone JG, Toth IK. Genomics and taxonomy in diagnostics for food security: soft-rotting enterobacterial plant pathogens. *Anal Methods*. 2016; 8:12–24.

38. Kanehisa M, Sato Y, Morishima K. BlastKOALA and GhostKOALA: KEGG tools for functional characterization of genome and metagenome sequences. *J Mol Biol.* 2016; 428:726–31. <https://doi.org/10.1016/j.jmb.2015.11.006> PMID: 26585406
39. Medema MH, Blin K, Cimermancic P, de Jager V, Zakrzewski P, Fischbach MA, et al. antiSMASH: rapid identification, annotation and analysis of secondary metabolite biosynthesis gene clusters in bacterial and fungal genome sequences. *Nucleic Acids Res.* 2011; 39:W339–46. <https://doi.org/10.1093/nar/gkr466> PMID: 21672958
40. Blin K, Shaw S, Steinke K, Villebro R, Ziemert N, Lee SY, et al. antiSMASH 5.0: updates to the secondary metabolite genome mining pipeline. *Nucleic Acids Res.* 2019; 47:W81–7. <https://doi.org/10.1093/nar/gkz310> PMID: 31032519
41. Arndt D, Grant JR, Marcu A, Sajed T, Pon A, Liang Y, et al. PHASTER: a better, faster version of the PHAST phage search tool. *Nucleic Acids Res.* 2016; 44:W16–21. <https://doi.org/10.1093/nar/gkw387> PMID: 27141966
42. Gibson MK, Forsberg KJ, Dantas G. Improved annotation of antibiotic resistance determinants reveals microbial resistomes cluster by ecology. *ISME J.* 2015; 9:207–16. <https://doi.org/10.1038/ismej.2014.106> PMID: 25003965
43. Claus D. A standardized Gram staining procedure. *World J Microbiol Biotechnol.* 1992; 8:451–2. <https://doi.org/10.1007/BF01198764> PMID: 24425522
44. Abraham W-R, Strompl C, Meyer H, Lindholst S, Moore ERB, Christ R, et al. Phylogeny and polyphasic taxonomy of *Caulobacter* species. Proposal of *Maricaulis* gen. nov. with *Maricaulis maris* (Poindexter) comb. nov. as the type species, and emended description of the genera *Brevundimonas* and *Caulobacter*. *Int J Syst Bacteriol.* 1999; 49:1053–73. <https://doi.org/10.1099/00207713-49-3-1053> PMID: 10425763
45. R Core Team. R: a language and environment for statistical computing [Internet]. R Foundation for Statistical Computing, Vienna, Austria; 2020. Available from: <https://www.r-project.org/>
46. Wickham H. ggplot2—elegant graphics for data analysis. Vol. 77, *Journal of Statistical Software*. New York, NY: Springer New York; 2009.
47. Bruder S, Reifenrath M, Thomik T, Boles E, Herzog K. Parallelized online biomass monitoring in shake flasks enables efficient strain and carbon source dependent growth characterization of *Saccharomyces cerevisiae*. *Microb Cell Fact.* 2016; 15:127. <https://doi.org/10.1186/s12934-016-0526-3> PMID: 27455954
48. Wickham H. *Journal of Statistical Software*. 2017; 77:3–5.
49. Clarke PH, Cowan ST. Biochemical methods for bacteriology. *J Gen Microbiol.* 1952; 6:187–97. <https://doi.org/10.1099/00221287-6-1-2-187> PMID: 14927866
50. Willms IM, Hertel R. Phage vB_BsuP-Goe1: the smallest identified lytic phage of *Bacillus subtilis*. *FEMS Microbiol Lett.* 2016; 363:fnw208. <https://doi.org/10.1093/femsle/fnw208> PMID: 27609230
51. Willms I, Hoppert M, Hertel R. Characterization of *Bacillus subtilis* viruses vB_BsuM-Goe2 and vB_BsuM-Goe3. *Viruses.* 2017; 9:146. <https://doi.org/10.3390/v9060146> PMID: 28604650
52. Kropinski AM, Mazzocco A, Waddell TE, Lingohr E, Johnson RP. Enumeration of bacteriophages by double agar overlay plaque assay. *Methods Mol Biol.* 2009; 501:69–76. https://doi.org/10.1007/978-1-60327-164-6_7 PMID: 19066811
53. Bogomol'naya LM, Filimonova MN. Activity dynamics of potential marker enzymes of *Serratia marcescens* cytoplasm and periplasm. *Appl Biochem Microbiol.* 2010; 46:390–4.
54. Bhadra B, Roy P, Chakraborty R. *Serratia ureilytica* sp. nov., a novel urea-utilizing species. *Int J Syst Evol Microbiol.* 2005; 55:2155–8. <https://doi.org/10.1099/ijs.0.63674-0> PMID: 16166724
55. Ludueña LM, Anzuay MS, Angelini JG, McIntosh M, Becker A, Rupp O, et al. Strain *Serratia* sp. S119: A potential biofertilizer for peanut and maize and a model bacterium to study phosphate solubilization mechanisms. *Appl Soil Ecol.* 2017; 126:107–12.
56. Reimer LC, Vetcinova A, Carbasse JS, Söhnngen C, Gleim D, Ebeling C, et al. BacDive in 2019: bacterial phenotypic data for high-throughput biodiversity analysis. *Nucleic Acids Res.* 2019; 47:D631–6. <https://doi.org/10.1093/nar/gky879> PMID: 30256983
57. Zhang C-X, Yang S-Y, Xu M-X, Sun J, Liu H, Liu J-R, et al. *Serratia nematodiphila* sp. nov., associated symbiotically with the entomopathogenic nematode *Heterorhabditidoides chongmingensis* (Rhabditida: Rhabditidae). *Int J Syst Evol Microbiol.* 2009; 59:1603–8. <https://doi.org/10.1099/ijs.0.65718-0> PMID: 19578149
58. Parte AC. LPSN—List of prokaryotic names with standing in nomenclature (bacterio.net), 20 years on. *Int J Syst Evol Microbiol.* 2018; 68:1825–9. <https://doi.org/10.1099/ijs.0.002786> PMID: 29724269
59. Roy P, Ahmed, Nishat Hussain, Grover RK. Non-pigmented strain of *Serratia marcescens*: an unusual pathogen causing pulmonary infection in a patient with malignancy. *J clin diagn.* 2014; 8:DD05–6.

60. Harris AKP, Williamson NR, Slater H, Cox A, Abbasi S, Foulds I, et al. The *Serratia* gene cluster encoding biosynthesis of the red antibiotic, prodigiosin, shows species- and strain-dependent genome context variation. *Microbiology*. 2004; 150:3547–60. <https://doi.org/10.1099/mic.0.27222-0> PMID: 15528645
61. Haddix PL, Shanks RMQ. Prodigiosin pigment of *Serratia marcescens* is associated with increased biomass production. *Arch Microbiol*. 2018; 200:989–99. <https://doi.org/10.1007/s00203-018-1508-0> PMID: 29616306
62. Matilla MA, Nogellova V, Morel B, Krell T, Salmond GPC. Biosynthesis of the acetyl-coA carboxylase-inhibiting antibiotic, andrimid in *Serratia* is regulated by hfq and the LysR-type transcriptional regulator, admX. *Environ Microbiol*. 2016; 18:3635–50. <https://doi.org/10.1111/1462-2920.13241> PMID: 26914969
63. Matilla MA, Udaondo Z, Krell T, Salmond GPC. Genome sequence of *Serratia marcescens* MSU97, a plant-associated bacterium that makes multiple antibiotics. *Genome Announc*. 2017; 5:e01752–16. <https://doi.org/10.1128/genomeA.01752-16> PMID: 28254993
64. Ruiu L. Plant-growth-promoting bacteria (PGPB) against insects and other agricultural pests. *Agronomy*. 2020; 10:861.
65. Dekkers LC, van der Bij AJ, Mulders IHM, Phoelich CC, Wentwoord RAR, Glandorf DCM, et al. Role of the O-antigen of lipopolysaccharide, and possible roles of growth rate and of NADH:ubiquinone oxidoreductase (*nuo*) in competitive tomato root-tip colonization by *Pseudomonas fluorescens* WCS365. *Mol Plant Microbe Interact*. 1998; 11:763–71. <https://doi.org/10.1094/MPMI.1998.11.8.763> PMID: 9675892
66. Matteoli FP, Passarelli-Araujo H, Reis RJA, da Rocha LO, de Souza EM, Aravind L, et al. Genome sequencing and assessment of plant growth-promoting properties of a *Serratia marcescens* strain isolated from vermicompost. *BMC Genomics*. 2018; 19:750. <https://doi.org/10.1186/s12864-018-5130-y> PMID: 30326830
67. Chun J, Oren A, Ventosa A, Christensen H, Arahal DR, da Costa MS, et al. Proposed minimal standards for the use of genome data for the taxonomy of prokaryotes. *International Journal of Systematic and Evolutionary Microbiology*. 2018; 68:461–6. <https://doi.org/10.1099/ijsem.0.002516> PMID: 29292687
68. Richter M, Rosselló-Móra R. Shifting the genomic gold standard for the prokaryotic species definition. *PNAS*. 2009;10: 191:26–31. <https://doi.org/10.1073/pnas.0906412106> PMID: 19855009
69. Hertel R, Rodríguez DP, Hollensteiner J, Dietrich S, Leimbach A, Hoppert M, et al. Genome-based identification of active prophage regions by next generation sequencing in *Bacillus licheniformis* DSM13. *PLOS ONE*. 2015; 10:e0120759. <https://doi.org/10.1371/journal.pone.0120759> PMID: 25811873

3. First complete genome sequences of *Janthinobacterium lividum* EIF1 and EIF2 and their comparative genome analysis

Ines Friedrich¹, Jacqueline Hollensteiner¹, Dominik Schneider¹, Anja Poehlein¹, Robert Hertel² and Rolf Daniel¹

Genome Biology and Evolution (10 October 2020), **12**, 10: 1782–1788
<https://doi.org/10.1093/gbe/evaa148>

Affiliations

¹Genomic and Applied Microbiology & Göttingen Genomics Laboratory, Institute of Microbiology and Genetics, Georg-August-University of Göttingen, Grisebachstraße 8, 37077 Göttingen, Germany

²FG Synthetic Microbiology, Institute of Biotechnology, BTU Cottbus-Senftenberg, Senftenberg, Germany

Author contributions:



Conceptualization: **IF**, JH, RH, RD

Experiments: **IF**

Data analysis: **IF**, JH, DS, AP, RH

Writing: **IF**, JH, DS, AP, RH, RD

First Complete Genome Sequences of *Janthinobacterium lividum* EIF1 and EIF2 and Their Comparative Genome Analysis

Ines Friedrich ^{1,†}, Jacqueline Hollensteiner ^{1,* ,†}, Dominik Schneider¹, Anja Poehlein¹, Robert Hertel², and Rolf Daniel¹

¹Genomic and Applied Microbiology and Göttingen Genomics Laboratory, Institute of Microbiology and Genetics, Georg-August University of Göttingen, Germany

²FG Synthetic Microbiology, Institute of Biotechnology, BTU Cottbus–Senftenberg, Senftenberg, Germany

[†]These authors contributed equally to this work.

*Corresponding author: E-mail: jhollen@gwdg.de.

Accepted: 7 July 2020

Abstract

We present the first two complete genomes of the *Janthinobacterium lividum* species, namely strains EIF1 and EIF2, which both possess the ability to synthesize violacein. The violet pigment violacein is a secondary metabolite with antibacterial, antifungal, antiviral, and antitumoral properties. Both strains were isolated from environmental oligotrophic water ponds in Göttingen. The strains were phylogenetically classified by average nucleotide identity (ANI) analysis and showed a species assignment to *J. lividum* with 97.72% (EIF1) and 97.66% (EIF2) identity. These are the first complete genome sequences of strains belonging to the species *J. lividum*. The genome of strain EIF1 consists of one circular chromosome (6,373,589 bp) with a GC-content of 61.98%. The genome contains 5,551 coding sequences, 122 rRNAs, 93 tRNAs, and 1 tm-RNA. The genome of EIF2 comprises one circular chromosome (6,399,352 bp) with a GC-content of 61.63% and a circular plasmid p356839 (356,839 bp) with a GC-content of 57.21%. The chromosome encodes 5,691 coding sequences, 122 rRNAs, 93 tRNAs, and 1 tm-RNA and the plasmid harbors 245 coding sequences. In addition to the highly conserved chromosomally encoded violacein operon, the plasmid comprises a non-ribosomal peptide synthetase cluster with similarity to xenoamicin, which is a bioactive compound effective against protozoan parasites.

Key words: *Janthinobacterium lividum*, secondary metabolites, violacein operon, antimicrobial, antifungal, xenoamicin.

Introduction

Janthinobacterium lividum is a betaproteobacterium and belongs to the family of *Oxalobacteraceae*. This family comprises 13 genera including the genus *Janthinobacterium* (Baldani et al. 2014), which in turn contains the species

J. lividum (Kämpfer et al. 2008), *Janthinobacterium svalbardensis* (Ambrozic Avgustin et al. 2013), and *Janthinobacterium agaricidamnosum* (Lincoln et al. 1999) as well as the recently announced species *Janthinobacterium violaceinigrum* sp. nov., *Janthinobacterium aquaticum* sp.

Significance

The species *Janthinobacterium lividum* is known for producing a variety of secondary metabolites. Those bioactive compounds are valuable for different biotechnological applications. Comparative genomics of *J. lividum* investigating the overall genomic structure and genome evolution are limited due to the lack of complete genome sequences. The here analyzed new isolates and their complete genomes give insight into their potential for bioactive compound discovery including violacein and xenoamicin. Moreover, we show that the chromosomes of *J. lividum* EIF1 and EIF2 have a conserved genome structure and that these two novel strains function as a blueprint for future genome comparisons throughout the *Janthinobacterium* genus, which deepens our understanding of this genera's evolution.

© The Author(s) 2020. Published by Oxford University Press on behalf of the Society for Molecular Biology and Evolution.

This is an Open Access article distributed under the terms of the Creative Commons Attribution Non-Commercial License (<http://creativecommons.org/licenses/by-nc/4.0/>), which permits non-commercial re-use, distribution, and reproduction in any medium, provided the original work is properly cited. For commercial re-use, please contact journals.permissions@oup.com

nov., and *Janthinobacterium rivuli* sp. nov. (Huibin et al. 2020). Members of *Janthinobacterium* are Gram-negative, motile, and rod-shaped (Baldani et al. 2014). They are strictly aerobic, chemoorganotrophic, and are proposed to grow at a temperature optimum of 25–30 °C (Baldani et al. 2014). In addition, psychrophilic isolates are known that are able to grow at 4 °C (Suman et al. 2015). *Janthinobacterium* strains inhabit different environments including soil (Asencio et al. 2014; Shoemaker et al. 2015; Wu et al. 2017), various aquatic habitats such as lakes (Suman et al. 2015), water sediments (McTaggart et al. 2015), and rainwater cisterns (Haack et al. 2016). Some *Janthinobacterium* isolates are also known as beneficial skin microsymbionts of amphibians (Brucker et al. 2008; Harris et al. 2009) and as pathogens of rainbow trouts (Oh et al. 2019). *Janthinobacterium* colonies have a purple-violet color produced by the pigment violacein. This colorful secondary metabolite (SM) is known to exhibit antimicrobial, antiviral, and antitumor properties (Andrighetti-Fröhner et al. 2003; Bromberg et al. 2010; Asencio et al. 2014) and thus bears great potential for biotechnological applications. In the current study, we assessed 1) the first complete genomes of two novel *J. lividum* isolates EIF1 and EIF2 and compared 2) the genetic localization of the violacein cluster within the genus *Janthinobacterium*. Additionally, we focused on 3) the potential for synthesis of bioactive SMs.

Materials and Methods

Isolation, Growth Conditions, and Genomic DNA Extraction

Janthinobacterium lividum EIF1 and EIF2 were obtained from environmental oligotrophic water surface and plant material including leaves and stem from opposite-leaved pondweed, *Groenlandia densa*. The samples were collected in Göttingen (Germany) on 11.09.2018 (51°33'58"N 9°56'22"E). Enrichment cultures were performed by using environmental water samples to inoculate peptone medium containing 0.001% (w/v) peptone (Carl Roth GmbH + Co. KG, Karlsruhe, Germany). Cultures were allowed to stand undisturbed for 3 weeks at 25 °C (Poindexter 2006). Both biofilm and water surface material were sampled and streaked on 0.05% peptone-containing agar medium supplemented with 1% vitamin solution No. 6 (Staley 1968). After colony formation, they were transferred to a new agar plate containing diluted peptone medium supplemented with CaCl₂ (PCa) (Poindexter 2006) and incubated for 4 days at 25 °C. For singularization of isolates, restreaking was performed at least four times. Individual single colonies were cultured in liquid PCa medium and genomic DNA was extracted with the MasterPure complete DNA and RNA purification kit as recommended by the manufacturer (Epicentre, Madison, WI). After the addition of 500 µl Tissue and Cell Lysis Solution, the resuspended cells were transferred into Lysing Matrix B tubes (MP

Biomedicals, Eschwege, Germany) and mechanically disrupted for 10 s at 6.5 m/s using FastPrep-24 (MP Biomedicals). The supernatant was cleared by centrifugation for 10 min at 11,000 × g, transferred into a 2.0-ml tube and 1 µl Proteinase K (20 mg/ml) (Epicentre) was added. The procedure was performed as recommended but the MPC Protein Precipitation Reagent was modified to 300 µl. The 16S rRNA genes of purified isolates were amplified with the primer pair 27F and 1492R (Fredriksson et al. 2013). Sanger sequencing of the polymerase chain reaction products was done by Seqlab (Göttingen, Germany).

Genome Sequencing, Assembly, and Annotation

Illumina paired-end sequencing libraries were prepared using the Nextera XT DNA Sample Preparation kit and sequenced by employing the MiSeq-system and reagent kit version 3 (2 × 300 bp) as recommended by the manufacturer (Illumina, San Diego, CA). For Nanopore sequencing, 1.5 µg DNA was used for library preparation employing the Ligation Sequencing kit 1D (SQK-LSK109) and the Native Barcode Expansion kit EXP-NBD103 (Barcode 3) for strain EIF1 and the Native Barcode Expansion kit EXP-NBD104 (Barcodes 7 and 12) for strain EIF2 as recommended by the manufacturer (Oxford Nanopore Technologies, Oxford, UK). Sequencing was performed for 72 h using the MinION device Mk1B and a SpotON Flow Cell R9.4.1 as recommended by the manufacturer (Oxford Nanopore Technologies) using MinKNOW software v19.05.0 for sequencing (strain EIF1 and first run of EIF2) and v19.06.8 for the second run of strain EIF2. For demultiplexing, Guppy versions v3.0.3 (strain EIF1), v3.1.5 (strain EIF2, first run), and v.3.2.1 (EIF2, second run) were used. Illumina raw reads were quality filtered with fastp v0.20.0 (Chen et al. 2018) using the following parameters: base correction by overlap, base phred score ≥ Q20, read clipping by quality score in front and tail with a sliding window size of 4, a mean quality of ≥ 20, and a required minimum length of 50 bp. Reads were additionally adapter trimmed by using cutadapt v2.5 (Martin 2011). For adapter trimming of Oxford Nanopore reads, Porechop (<https://github.com/rwwick/Porechop.git>; last accessed April 29, 2019) was used with default parameters. Quality filtering with fastp v0.20.0 (Chen et al. 2018) was performed by using following parameters: base phred score ≥ Q10, read clipping by quality score in front and tail with a sliding window size of 10, a mean quality of ≥ 10, and a required minimum length of 1,000 bp.

Janthinobacterium lividum EIF1 was de novo assembled using Unicycler v0.4.8 in normal mode (Wick et al. 2017) and quality checked with Bandage v0.8.1 (Wick et al. 2015).

For *J. lividum* EIF2, a de novo long-read-only assembly with Nanopore reads was performed using Unicycler v0.4.8 due to repetitive transposases in the genome and to avoid misassemblies of overrepresented repetitive regions by short-reads. To increase the quality of the Nanopore assembly, additional

polishing was performed with unicycler-polish (<https://github.com/rwick/Unicycler/blob/master/docs/unicycler-polish.md>; last accessed February 13, 2020) by mapping Illumina short-reads with bowtie2 v2.3.5.1 (Langmead and Salzberg 2012) against the Nanopore-based assembly and base correction by Pilon 1.23 (Walker et al. 2014). This routine corrects substitutions, indels as well as larger variants such as repetitive homo-stretches, deletions, and large deletions. The contiguity of the assembly was manually inspected and evaluated with Tablet v1.19.09.03 (Milne et al. 2013). Quality of the assembled genomes was assessed with CheckM v1.1.2 (Parks et al. 2015) and genome annotation was performed by using the Prokaryotic Genome Annotation Pipeline v4.11 (Tatusova et al. 2016) and subsequent manual curation of the genes encoding the violacein operon.

Phylogenetic Classification

The Genome Taxonomy Database Toolkit (GTDB-Tk) v1.0.1 (Chaumeil et al. 2019) was used to provide an initial taxonomic placement of the *J. lividum* isolates. Subsequently, an in-depth phylogenetic analysis was performed using ANIm method of pyani (<https://github.com/widowquinn/pyani> v0.2.9; last accessed March 05, 2020) (Arahal 2014) as described by Richter and Rosselló-Móra (2009). Based on the list of the type strain collection of the German Strain Collection of Microorganisms and Cell Cultures GmbH (DSMZ, Braunschweig, Germany), available type strain genomes were downloaded from the National Centre for Biotechnological Information (NCBI, accessed 05.03.2020) including *J. lividum* NCTC9796^T (PRJEB6403), *J. lividum* H-24^T (PRJNA309034), *J. svalbardensis* strain PAMC 27463^R (PRJNA407061), and *J. agaricidamnosum* DSM 9628^T (PRJEB4003). The type strain genome of the species *J. lividum* was sequenced twice (NCTC9796^T and H-24^T). Both were included in the analysis due to their incomplete sequencing status, difference in coverage, and used annotation pipelines.

Comparative Genomics

To investigate the metabolic potential of *J. lividum* EIF1 and EIF2, BlastKOALA v2.2 (Kanehisa et al. 2016) was used. Putative SM biosynthetic gene clusters and putative phage regions were identified with AntiSMASH v5.1.2 (Blin et al. 2019) and PHASTER (Arndt et al. 2016), respectively. Comparative analysis and visualization of the violacein operon was performed with Easyfig v2.2.3 (Sullivan et al. 2011). Whole-genome comparisons were performed by employing the BLAST Ring Image Generator v0.95 (Alikhan et al. 2011).

Results and Discussion

Genomic Features of *J. lividum* EIF1 and EIF2

We present the first complete genomes of two *J. lividum* strains EIF1 and EIF2, which originate from a surface water sample and a pondweed plant in Göttingen, respectively. The sequencing statistics are summarized in [supplementary table S1, Supplementary Material](#) online. The complete genomes were assembled from quality-filtered Oxford Nanopore reads (EIF1: 41,395 and EIF2: 237,547) with a mean length of 8,045 bp (EIF1) and 5,954 bp (EIF2) and Illumina reads with 3,271,600 (EIF1) and 2,562,634 (EIF2) reads in total. The de novo hybrid genome assembly of *J. lividum* EIF1 yielded a 6,373,589-bp circular chromosome, with a GC-content of 61.98% and a coverage of 181.3-fold. Short-read polished long-read Nanopore assembly of *J. lividum* EIF2 resulted in a circular chromosome (6,399,352 bp) and a circular plasmid (356,839 bp) with a coverage of 298.9-fold and 343.6-fold and a GC-content of 61.63% and 57.21%, respectively. In total, short-read polishing corrected 321 variants including substitutions, insertions, homo-stretches, deletions, and large deletions. Both assemblies were evaluated manually with Bandage v0.8.1 (Wick et al. 2015) and Tablet 1.19.09.03 (Milne et al. 2013). No CRISPR regions were detected in both genomes.

Phylogeny of *J. lividum* EIF1 and EIF2

The quality of the assemblies was evaluated with CheckM v1.1.2 (Parks et al. 2015) and revealed high purity with a completeness of 99.6% and a contamination rate of 2.38% (EIF1) and 1.58% (EIF2), respectively. The first taxonomic assignment of GTDB-Tk v1.0.1 (Chaumeil et al. 2019) based on fastANI values (97.66-EIF1 and 97.5-EIF2) demonstrated that both strains belong taxonomically to the species *J. lividum*. The available type and representative strains were used in the pyani analysis, which revealed that both *J. lividum* EIF1 and EIF2 build a cluster with the type strains *J. lividum* H-24^T and NCTC 9796^T (fig. 1A). In detail, *J. lividum* EIF1 and EIF2 cluster with 97.72% and 97.66% sequence identity, respectively, to the type strains *J. lividum* H-24^T and NCTC 9796^T. This is above the species boundary of ~94–95% and allows a reliable classification of both isolates EIF1 and EIF2 to the species *J. lividum*. The genomes of strains EIF1 and EIF2 share a sequence identity of 98.48%.

Metabolism and Production of Bioactive Compounds

Functional prediction of gene clusters was conducted with BlastKOALA. In total, 54.2% (EIF1) and 52.2% (EIF2) genes fall into 23 functional categories according to the Kyoto Encyclopedia of Genes and Genomes orthology. Among all categories, genes involved in signaling and processing (EIF1, 409 genes; EIF2, 431 genes), environmental processing (EIF1, 378 genes; EIF2, 391 genes), and genetic information

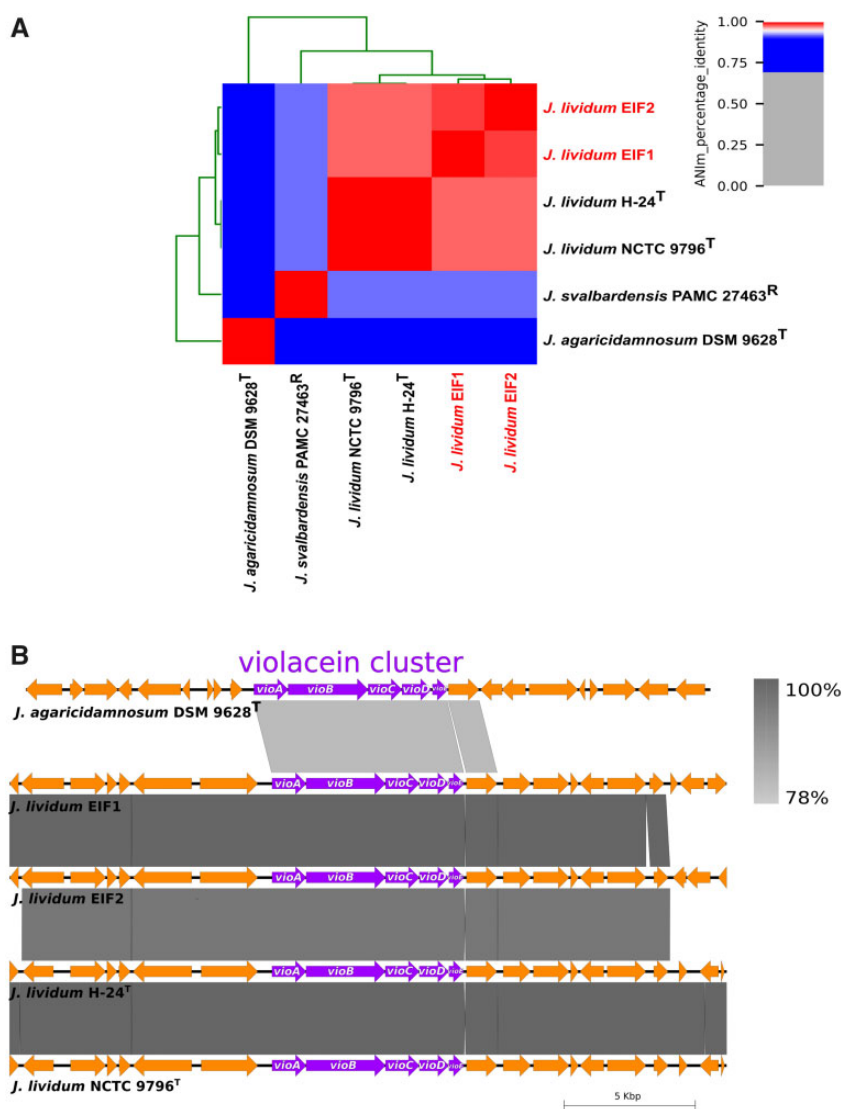


FIG. 1.—(A) Phylogenetic analysis of *Janthinobacterium lividum* EIF1 and EIF2 and (B) comparison of violacein operon of *Janthinobacterium*. (A) All available type strains (^T) and representative strains (^R) from the genus *Janthinobacterium* were considered. Calculations were done with pyani (<https://github.com/widdowquinn/pyani> v0.2.9; last accessed March 05, 2020) (Richter and Rosselló-Móra 2009; Arahal 2014) using the ANIm method with standard parameter. (B) The violacein operon is indicated in purple and surrounding genes in orange. Gray shading indicates regions of homology based on nucleotide level. Visualization was performed with Easyfig 2.2.3 (Sullivan et al. 2011).

processing (EIF1, 352 genes; EIF2, 361 genes) were most abundant. Additionally, several genes were affiliated to metabolic processing for substrate conversion including carbohydrate (EIF1, 292 genes; EIF2, 293 genes), nitrogen (19 genes), and sulfur (30 genes).

In total, 186 genes in EIF1 and 187 genes in EIF2 were associated with cell signaling including quorum sensing (52 genes), biofilm formation (EIF1, 77 genes; EIF2, 78 genes), and cell motility (57 genes). This indicates flexible genomes that enable the microorganism to sense and process diverse stimuli and substrates from the environment.

Members of the genus *Janthinobacterium* are a promising source for novel pharmaceutical compounds, as they bear the

potential to synthesize important SMs with exceptional antibacterial, antifungal, antiviral, and antiprotozoal properties (Brucker et al. 2008; Wang et al. 2012; Asencio et al. 2014; Suman et al. 2015; Durán et al. 2016). Both isolated strains showed a purple color during growth in liquid and solid media (supplementary fig. S1, Supplementary Material online), indicating the production of bioactive pigments. Genome analysis with AntiSMASH v5.1.2 (Blin et al. 2019) revealed that EIF1 comprises six and EIF2 seven putative SM gene clusters. In both genomes, genes typical for synthesis of terpene, bacteriocins, and violacein were detected.

The genomic comparison of the violacein operon (*vioABCDE* EIF1 3,947,675–3,970,695 bp and EIF2

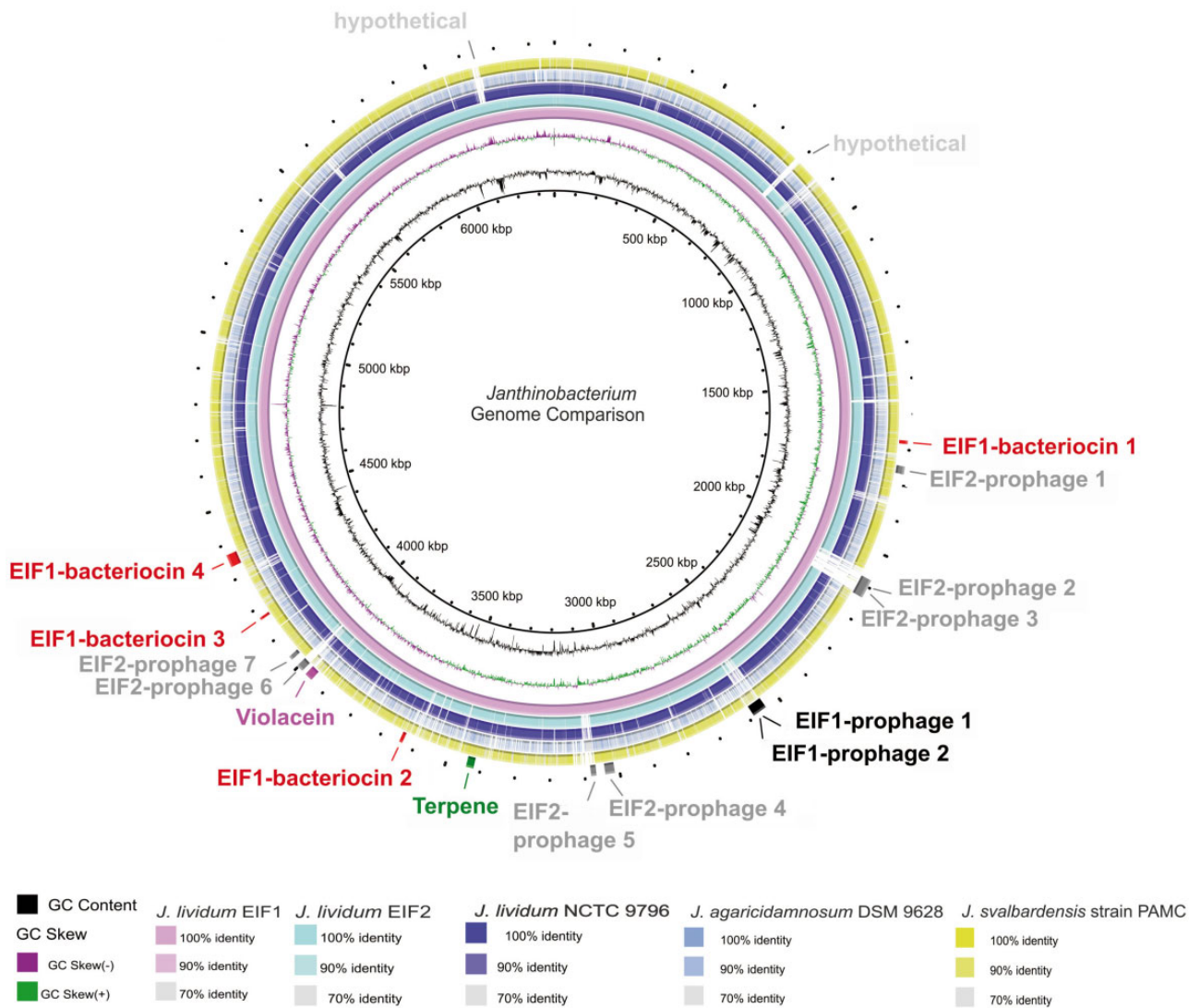


Fig. 2.—Comparison of two new complete genomes of *Janthinobacterium lividum* strains EIF1 and EIF2 and three draft genomes of *J. lividum* NCTC 9796^T, *Janthinobacterium agaricidamnorum* DSM 9628^T, and *Janthinobacterium svalbardensis* strain PAMC 27463^R. The figure was generated using BLAST Ring Image Generator (Ali Khan et al. 2011). As central reference, the *J. lividum* EIF1 chromosome is depicted (black ring with size, GC-content, and GC skew are indicated). BLAST matches between *J. lividum* EIF1 and other strains are shown as concentric colored rings on a sliding scale according to percentage identity (100%, 90%, or 70%). Regions of differences are labeled: bacteriocins (red), terpene (green), violacein (pink), prophages EIF1 (black), prophages EIF2 (gray), and regions of differences with hypothetical function (light gray).

3,934,551–3,957,571 bp) and surrounding genomic regions revealed a high conservation of the entire operon in the genomes of all different *J. lividum* strains and other *Janthinobacterium* species, that is, *J. agaricidamnorum* (fig. 1B). The genomic surrounding indicates conservation at intraspecies level only. In addition, the *J. lividum* EIF2 plasmid p356839 encodes a putative nonribosomal peptide synthetase cluster. This cluster showed an overall similarity to other known clusters synthesizing xenoamicin A/xenoamicin B by comprising eight core biosynthetic genes (G8765_29435–G8765_29465, G8765_29475), five additional biosynthetic genes (G8765_29470, G8765_29490, G8765_29500, G8765_29505, and G8765_29540), and three transport-

related genes (G8765_29520, G8765_29525, and G8765_29535). Xenoamicin A/B is known for its activity against *Plasmodium falciparum*, a unicellular protozoan parasite (Zhou et al. 2013). The comparison of the GC-content shows a difference of 4.42% between the chromosome and plasmid p356839 of strain EIF2 suggesting that the plasmid was obtained recently.

Comparative Genomics of *Janthinobacterium*

The two complete genomes of *J. lividum* (EIF1 and EIF2) presented here allow a reliable genomic structure simulation of incomplete available draft genomes of this species for the first

time. The overall genome comparison between *Janthinobacterium* genera revealed not only broad genome similarities but also species and strain specific differences (fig. 2) (Alikhan et al. 2011).

The chromosome organization of the species *J. lividum* follows a conserved structural genus blueprint, which is also detected in the species *J. agaricidamnorum* and *J. svalbardensis*. This highlights the high genomic conservation of the genus *Janthinobacterium*. To investigate regions of difference, the genomes were searched for putative prophage regions, which are known as drivers of genomic evolution (Casjens 2003; Brüßow et al. 2004; Canchaya et al. 2004). PHASTER analysis revealed two putative prophage regions (region 1: 2,543,591–2,585,344 bp; region 2: 2,565,749–2,585,385 bp) in *J. lividum* EIF1 (fig. 2). The regions comprise 41.7 and 19.6 kb and were classified as questionable and incomplete, respectively. However, both comprised phage attachment sites. In the genome of *J. lividum* EIF2, eight putative prophage regions were identified, of which seven reside within the chromosome (fig. 2) and one within the plasmid (315,441–324,647 bp, questionable). Two regions were classified as intact (region 1: 1,746,259–1,768,581 bp and region 3: 2,093,778–2,133,389 bp) and comprised the phage typical attachment sites AttL and AttR. These results support the hypothesis that bacterial strain diversification is mainly driven by phages interacting with the host chromosome (Canchaya et al. 2004) and extrachromosomal elements obtained by horizontal gene transfer (Giménez et al. 2019). Several SM clusters, such as the biosynthesis of bacteriocin, terpene, and violacein, were conserved among all investigated *J. lividum* isolates, indicating SM production as a common feature among this species.

In conclusion, we assembled two complete genomes derived from new isolates of the species *J. lividum* (EIF1 and EIF2) using Illumina and Nanopore technology. These are the first complete genomes described for this species and allowed in-depth genome analysis and comparisons. We have shown that both strains encode SM clusters, including the bioactive compounds violacein and xenoamicin A/B.

Supplementary Material

Supplementary data are available at *Genome Biology and Evolution* online.

Acknowledgments

We thank Anna Klassen and Melanie Heinemann for technical assistance. This research received no specific grant from any funding agency in the public, commercial, or not-for-profit sectors.

Literature Cited

- Alikhan N-F, Petty NK, Ben Zakour NL, Beatson SA. 2011. BLAST Ring Image Generator (BRIG): simple prokaryote genome comparisons. *BMC Genomics*. 12(1):402.
- Ambrozic Avgustin J, Bertok Zgur D, Kostanjsek R, Avgustin G. 2013. Isolation and characterization of a novel violacein-like pigment producing psychrotrophic bacterial species *Janthinobacterium svalbardensis* sp. nov. *Antonie Van Leeuwenhoek* 103:763–769.
- Andrighetti-Fröhner CR, Antonio RV, Creczynski-Pasa TB, Barardi CRM, Simões C. 2003. Cytotoxicity and potential antiviral evaluation of violacein produced by *Chromobacterium violaceum*. *Mem Inst Oswaldo Cruz* 98(6):843–848.
- Arahal DR. 2014. Whole-genome analyses: average nucleotide identity. In: Goodfellow M, Sutcliffe I, Chun J, editors. *Methods in microbiology: new approaches to prokaryotic systematics*. Vol. 41. Oxford: Elsevier Ltd/Academic Press. p. 103–122.
- Arndt D, et al. 2016. PHASTER: a better, faster version of the PHAST phage search tool. *Nucleic Acids Res.* 44(W1):W16–W21.
- Asencio G, et al. 2014. Antibacterial activity of the Antarctic bacterium *Janthinobacterium* sp. SMN 33.6 against multi-resistant Gram-negative bacteria. *Electron J Biotechnol.* 17(1):1–5.
- Baldani IJ, et al. 2014. The family *Oxalobacteraceae*. In: Rosenverg E, DeLong EF, Lory S, Stackebrandt E, Thompson F, editors. *The prokaryotes—alphaproteobacteria and betaproteobacteria*. Berlin/Heidelberg: Springer-Verlag. p. 919–974.
- Blin K, et al. 2019. antiSMASH 5.0: updates to the secondary metabolite genome mining pipeline. *Nucleic Acid Res.* 47:81–87.
- Bromberg N, et al. 2010. Growth inhibition and pro-apoptotic activity of violacein in Ehrlich ascites tumor. *Chem Biol Interact.* 186(1):43–52.
- Brucker RM, et al. 2008. Amphibian chemical defense: antifungal metabolites of the microsymbiont *Janthinobacterium lividum* on the salamander *Plethodon cinereus*. *J Chem Ecol.* 34(11):1422–1429.
- Brüßow H, Canchaya C, Hardt W-D. 2004. Phages and the evolution of bacterial pathogens: from genomic rearrangements to lysogenic conversion. *Microbiol Mol Biol Rev.* 68(3):560–602.
- Canchaya C, Fourmous G, Brüßow H. 2004. The impact of prophages on bacterial chromosomes. *Mol Microbiol.* 53(1):9–18.
- Casjens S. 2003. Prophages and bacterial genomics: what have we learned so far? *Mol Microbiol.* 49(2):277–300.
- Chaumeil P-A, Mussig AJ, Hugenholtz P, Parks DH. 2019. GTDB-Tk: a toolkit to classify genomes with the Genome Taxonomy Database. *Bioinformatics* 36:1925–1927.
- Chen S, Zhou Y, Chen Y, Gu J. 2018. fastp: an ultra-fast all-in-one FASTQ preprocessor. *Bioinformatics* 34(17):i884–i890.
- Durán N, et al. 2016. Advances in *Chromobacterium violaceum* and properties of violacein—its main secondary metabolite: a review. *Biotechnol Adv.* 34(5):1030–1045.
- Fredriksson NJ, Hermansson M, Wilén B-M. 2013. The choice of PCR primers has great impact on assessments of bacterial community diversity and dynamics in a wastewater treatment plant. *PLoS One* 8(10):e76431.
- Giménez M, Azziz G, Gill PR, Batista S. 2019. Horizontal gene transfer elements: plasmids in Antarctic microorganisms. In: Castro-Sowinski S, editor. *The ecological role of micro-organisms in the Antarctic environment*. Springer polar sciences. Cham (Switzerland): Springer. p. 85–107.
- Haack FS, et al. 2016. Molecular keys to the *Janthinobacterium* and *Duganella* spp. interaction with the plant pathogen *Fusarium graminearum*. *Front Microbiol.* 7:1668.
- Harris RN, et al. 2009. Skin microbes on frogs prevent morbidity and mortality caused by a lethal skin fungus. *ISME J.* 3(7):818–824.
- Huibin L, et al. 2020. *Janthinobacterium violaceinigrum* sp. nov., *Janthinobacterium aquaticum* sp. nov. and *Janthinobacterium rivuli*

- sp. nov., isolated from a subtropical stream in China. *Int J Syst Evol Microbiol.* 70(4):2719–2725.
- Kämpfer P, Falsen E, Busse H-J. 2008. Reclassification of *Pseudomonas mephitica* Claydon and Hammer 1939 as a later heterotypic synonym of *Janthinobacterium lividum* (Eisenberg 1891) De Ley et al. 1978. *Int J Syst Evol Microbiol.* 58(1):136–138.
- Kanehisa M, Sato Y, Morishima K. 2016. BlastKOALA and GhostKOALA: KEGG tools for functional characterization of genome and metagenome sequences. *J Mol Biol.* 428(4):726–731.
- Langmead B, Salzberg SL. 2012. Fast gapped-read alignment with Bowtie 2. *Nat Methods.* 9(4):357–360.
- Lincoln SP, Fermor TR, Tindall BJ. 1999. *Janthinobacterium agaricidamnorum* sp. nov., a soft rot pathogen of *Agaricus bisporus*. *Int J Syst Bacteriol.* 49(4):1577–1589.
- Martin M. 2011. Cutadapt removes adapter sequences from high-throughput sequencing reads. *EMBnet J.* 17(1):10.
- McTaggart TL, Shapiro N, Woyke T, Chistoserdova L. 2015. Draft genome of *Janthinobacterium* sp. RA13 isolated from Lake Washington sediment. *Genome Announc.* 3:13–14.
- Milne I, et al. 2013. Using Tablet for visual exploration of second-generation sequencing data. *Briefings Bioinf.* 14(2):193–202.
- Oh WT, et al. 2019. *Janthinobacterium lividum* as an emerging pathogenic bacterium affecting rainbow trout (*Oncorhynchus mykiss*) fisheries in Korea. *Pathogens* 8(3):146.
- Parks DH, Imelfort M, Skennerton CT, Hugenholtz P, Tyson GW. 2015. CheckM: assessing the quality of microbial genomes recovered from isolates, single cells, and metagenomes. *Genome Res.* 25(7):1043–1055.
- Poindexter JS. 2006. Dimorphic Prosthecate Bacteria: The Genera *Caulobacter*, *Asticcacaulis*, *Hyphomicrobium*, *Pedomicrobium*, *Hyphomonas* and *Thiodendron*. In: Dworkin M, Falkow S, Rosenberg E, Schleifer KH, Stackebrandt E, editors. *The Prokaryotes*. New York: Springer. p. 72–90.
- Richter M, Rosselló-Móra R. 2009. Shifting the genomic gold standard for the prokaryotic species definition. *Proc Natl Acad Sci U S A.* 106(45):19126–19131.
- Shoemaker WR, Muscarella ME, Lennon JT. 2015. Genome sequence of the soil bacterium *Janthinobacterium* sp. KBS0711. *Genome Announc.* 3:10–11.
- Staley JT. 1968. *Prosthecomicrobium* and *Ancalomicrobiutm*: new prosthecate freshwater bacteria. *J Bacteriol.* 95(5):1921–1942.
- Sullivan MJ, Petty NK, Beatson SA. 2011. Easyfig: a genome comparison visualizer. *Bioinformatics* 27(7):1009–1010.
- Suman R, Sharma P, Gupta S, Sourirajan A, Dev K. 2015. A novel psychrophilic *Janthinobacterium lividum* MMPP4 isolated from Manimahesh Lake of Chamba District of Himachal Pradesh, India. *J Biochem Technol.* 6:846–851.
- Tatusova T, et al. 2016. NCBI prokaryotic genome annotation pipeline. *Nucleic Acids Res.* 44(14):6614–6624.
- Walker BJ, et al. 2014. Pilon: an integrated tool for comprehensive microbial variant detection and genome assembly improvement. *PLoS One* 9(11):e112963.
- Wang H, et al. 2012. Biosynthesis and characterization of violacein, deoxyviolacein and oxyviolacein in heterologous host, and their antimicrobial activities. *Biochem Eng J.* 67:148–155.
- Wick RR, Judd LM, Gorrie CL, Holt KE. 2017. Unicycler: resolving bacterial genome assemblies from short and long sequencing reads. *PLoS Comput Biol.* 13:1–22.
- Wick RR, Schultz MB, Zobel J, Holt KE. 2015. Bandage: interactive visualization of de novo genome assemblies. *Bioinformatics* 31(20):3350–3352.
- Wu X, et al. 2017. Draft genome sequences of two isolated from pristine groundwater collected from the Oak Ridge Field Research Center. *Genome Announc.* 5:e00582.
- Zhou Q, et al. 2013. Structure and biosynthesis of xenoamcins from entomopathogenic *Xenorhabdus*. *Chem Eur J.* 19:16772–16779.

Associate editor: Howard Ochman

4. Complete genome sequence of *Stenotrophomonas indicatrix* DAIF1

Ines Friedrich¹, Jacqueline Hollensteiner¹, Janna Scherf¹, Judith Weyergraf¹, Anna Klassen¹, Anja Poehlein¹, Robert Hertel² and Rolf Daniel¹

Microbiology Resource Announcements (11 February 2021), **10**: e01484-20
<https://doi.org/10.1128/MRA.01484-20>

Affiliations

¹Genomic and Applied Microbiology & Göttingen Genomics Laboratory, Institute of Microbiology and Genetics, Georg-August-University of Göttingen, Grisebachstraße 8, 37077 Göttingen, Germany

²FG Synthetic Microbiology, Institute of Biotechnology, BTU Cottbus-Senftenberg, Senftenberg, Germany

Author contributions:

Conceptualization: **IF**, JH, RH, RD

Experiments: **IF**, AK

Data analysis: **IF**, JH, JS, JW, AP, RH

Writing: **IF**, JH, JS, JW, AK, AP, RH, RD



Complete Genome Sequence of *Stenotrophomonas indicatrix* DAIF1

Ines Friedrich,^a Jacqueline Hollensteiner,^a Janna Scherf,^a Judith Weyergraf,^a Anna Klassen,^a  Anja Poehlein,^a Robert Hertel,^b  Rolf Daniel^a

^aGenomic and Applied Microbiology and Göttingen Genomics Laboratory, Institute of Microbiology and Genetics, University of Göttingen, Göttingen, Germany

^bFG Synthetic Microbiology, Institute of Biotechnology, BTU Cottbus-Senftenberg, Senftenberg, Germany

ABSTRACT We present the complete genome of *Stenotrophomonas indicatrix* DAIF1, which was isolated from an oligotrophic pond in a water protection area. Whole-genome alignments indicated that strain DAIF1 belongs to the species *Stenotrophomonas indicatrix*. The whole genome (4,639,375 bp) harbors 4,108 protein-encoding genes, including 3,029 genes with assigned functions.

Stenotrophomonas indicatrix DAIF1 was isolated from an oligotrophic pond water sample from Germany (51°33'58"N, 9°56'22"E) as described previously (1). The genome of environmentally derived strain DAIF1 is of interest for comparative genome analysis with clinical isolates. For genomic DNA preparation, the strain was cultured in PCa medium (peptone medium supplemented with 0.015% CaCl₂) at 30°C (2). DNA was purified with the MasterPure complete DNA and RNA purification kit as recommended by the manufacturer (Epicentre, Madison, WI, USA). The isolated DNA was used to generate Illumina sequencing libraries using the Nextera XT DNA sample preparation kit and was sequenced on a MiSeq instrument with reagent kit v3 (2 × 300 bp, 600 cycles) as recommended by the manufacturer (Illumina, San Diego, USA). For sequencing with the MinION system, the 1D genomic DNA sequencing protocol in combination with the ligation sequencing 1D kit (SQK-LSK109) and the native barcode expansion kit (EXP-NBD103; barcode 11) were used as recommended by the manufacturer (Oxford Nanopore Technologies, Oxford, UK). Input DNA without size selection was end repaired with NEBNext FFPE repair mix (New England Biolabs, Ipswich, MA, USA). Nanopore sequencing was performed by using the SpotON flow cell Mk I (R9.4.1) for 72 h with MinKNOW software v18.12.6. Guppy v3.4.1 was employed in fast mode for demultiplexing and base calling. Default parameters were used for all software unless otherwise specified. Nanopore and Illumina reads were quality processed with fastp v0.19.5 (3), resulting in 35,352 Nanopore reads with sizes ranging from 10 to 50 kbp (N_{50} , 14.5 kbp) and 2,256,826 high-quality Illumina paired-end reads. A Nanopore long-read assembly with the racon v1.3.1 assembler as part of the Unicycler pipeline v0.4.7 (4) resulted in a single circular chromosome with a final coverage of 214-fold. Sequence polishing was performed using the Illumina reads and the unicycler_polish.py script (4); this resulted in a final genome of 4,639,375 bp with a GC content of 66.36%. Prokka v1.13.3 (5) was used for automatic annotation, which resulted in 4,108 protein-encoding genes, of which 3,029 were assigned functions. Furthermore, 76 tRNA genes, 1 transfer-messenger RNA gene, and 13 rRNA genes were identified.

In order to provide a first phylogenetic classification, a BLAST search against the NCBI nonredundant nucleotide database using the 16S rRNA gene sequence of DAIF1 was performed (6). The most similar 16S rRNA gene was from *Stenotrophomonas* sp. strain MYb57 (GenBank accession number [KU902436.1](https://www.ncbi.nlm.nih.gov/nuclseq/KU902436.1)), with an identity of 100%. To further classify DAIF1, its genome was compared with all available genomes of

Citation Friedrich I, Hollensteiner J, Scherf J, Weyergraf J, Klassen A, Poehlein A, Hertel R, Daniel R. 2021. Complete genome sequence of *Stenotrophomonas indicatrix* DAIF1. Microbiol Resour Announc 10:e01484-20. <https://doi.org/10.1128/MRA.01484-20>.

Editor J. Cameron Thrash, University of Southern California

Copyright © 2021 Friedrich et al. This is an open-access article distributed under the terms of the [Creative Commons Attribution 4.0 International license](https://creativecommons.org/licenses/by/4.0/).

Address correspondence to Rolf Daniel, rdaniel@gwdg.de.

Received 27 December 2020

Accepted 15 January 2021

Published 11 February 2021

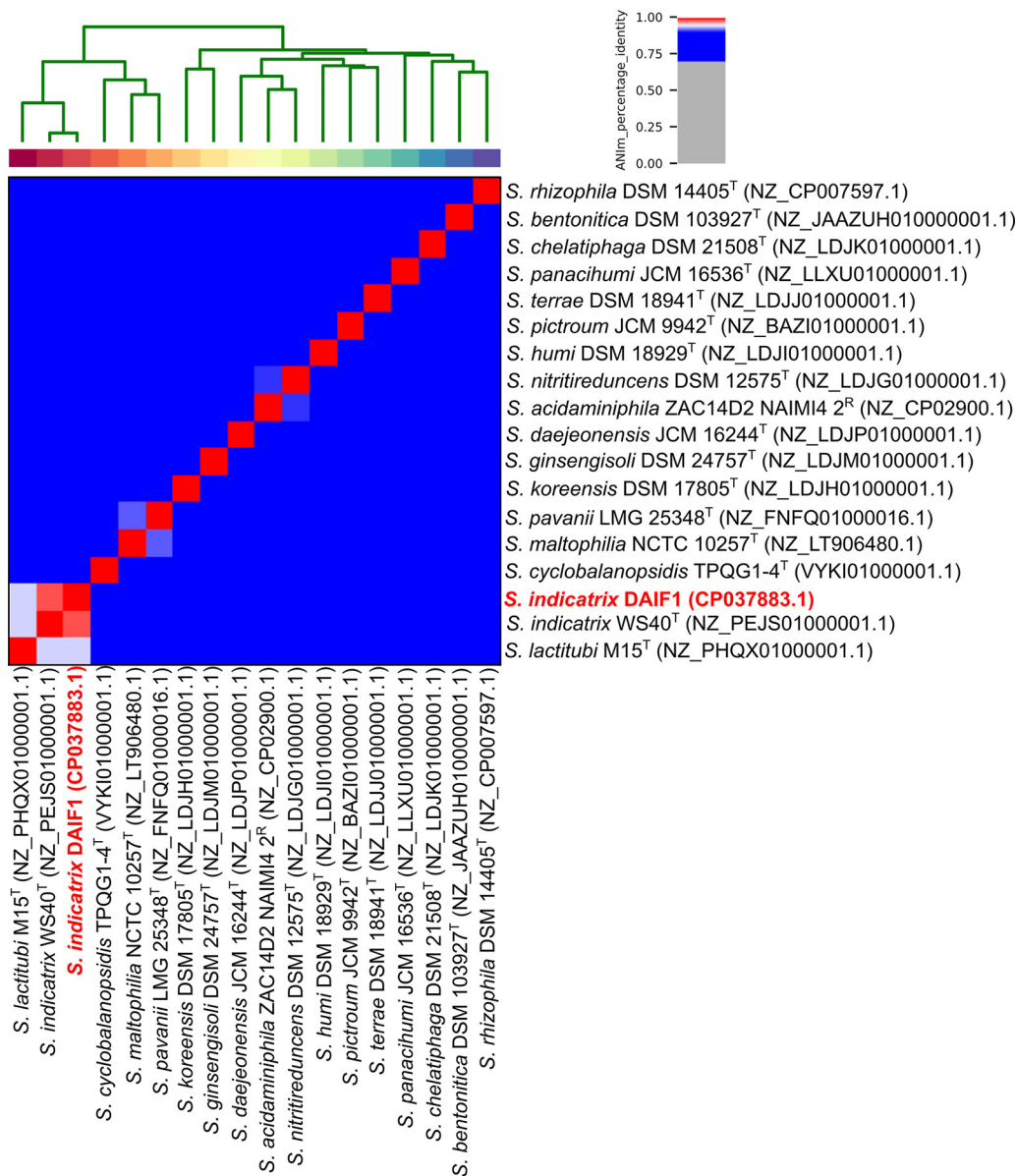


FIG 1 ANI analysis of the *Stenotrophomonas indicatrix* DAIF1 genome (red). All available genomes of type strains (superscript T) and representative strains (superscript R) from the genus *Stenotrophomonas* were taken into account. Calculations were performed with the Python pyANI package (9) using the ANIm (ANI calculated by using a MUMmer3 implementation) method with standard parameters. Analysis revealed a genome sequence identity of 98.29% for DAIF1 in comparison with the *S. indicatrix* WS40^T genome. GenBank accession numbers are provided in parentheses.

Stenotrophomonas type strains (Fig. 1) by using average_nucleotide_identity.py v0.2.10 (<https://github.com/widdowquinn/pyani>) with the option ANIm and MUMmer3 (7). Average nucleotide identity (ANI) analysis (8) showed that DAIF1 clustered with *S. indicatrix* WS40^T (GenBank accession number NZ_PEJS00000001.1). The recorded identity was 98.39% (Fig. 1). This is higher than the species boundary of approximately 94% (9) and allows assignment of DAIF1 as a new strain within the *S. indicatrix* species. Furthermore, the closed genome sequence of *S. indicatrix* DAIF1 is beneficial for comparative genomics with clinical isolates.

Data availability. The annotated genome sequence of *Stenotrophomonas* sp. DAIF1 and the 16S rRNA gene sequence were submitted to GenBank under the accession numbers CP037883 and MW078496, respectively. Raw reads were deposited in

the NCBI Sequence Read Archive (SRA) under the accession numbers [SRX6039405](#) (Nanopore reads) and [SRX6039404](#) (Illumina reads).

ACKNOWLEDGMENTS

We thank Sarah Teresa Schübler and Melanie Heinemann for technical assistance.

We acknowledge support by the Open Access Publication Funds of the University of Göttingen. The funders had no role in the study design, data collection and interpretation, or the decision to submit the work for publication.

REFERENCES

1. Friedrich I, Hollensteiner J, Schneider D, Poehlein A, Hertel R, Daniel R. 2020. First complete genome sequences of *Janthinobacterium lividum* EIF1 and EIF2 and their comparative genome analysis. *Genome Biol Evol* 12:1782–1788. <https://doi.org/10.1093/gbe/evaa148>.
2. Staley JT. 1968. *Prosthecomicrobium* and *Ancalomicrobium*: new prosthecate freshwater bacteria. *J Bacteriol* 95:1921–1942. <https://doi.org/10.1128/JB.95.5.1921-1942.1968>.
3. Chen S, Zhou Y, Chen Y, Gu J. 2018. fastp: an ultra-fast all-in-one FASTQ preprocessor. *Bioinformatics* 34:i884–i890. <https://doi.org/10.1093/bioinformatics/bty560>.
4. Wick RR, Judd LM, Gorrie CL, Holt KE. 2017. Unicycler: resolving bacterial genome assemblies from short and long sequencing reads. *PLoS Comput Biol* 13:e1005595. <https://doi.org/10.1371/journal.pcbi.1005595>.
5. Seemann T. 2014. Prokka: rapid prokaryotic genome annotation. *Bioinformatics* 30:2068–2069. <https://doi.org/10.1093/bioinformatics/btu153>.
6. Altschul SF, Gish W, Miller W, Myers EW, Lipman DJ. 1990. Basic local alignment search tool. *J Mol Biol* 215:403–410. [https://doi.org/10.1016/S0022-2836\(05\)80360-2](https://doi.org/10.1016/S0022-2836(05)80360-2).
7. Kurtz S, Phillippy A, Delcher AL, Smoot M, Shumway M, Antonescu C, Salzberg SL. 2004. Versatile and open software for comparing large genomes. *Genome Biol* 5:R12. <https://doi.org/10.1186/gb-2004-5-2-r12>.
8. Richter M, Rosselló-Móra R. 2009. Shifting the genomic gold standard for the prokaryotic species definition. *Proc Natl Acad Sci U S A* 106:19126–19131. <https://doi.org/10.1073/pnas.0906412106>.
9. Arahal DR. 2014. Whole-genome analyses: average nucleotide identity. *Methods Microbiol* 41:103–122. <https://doi.org/10.1016/bs.mim.2014.07.002>.

5. Complete genome sequence of *Kinneretia* sp. strain DAIF2, isolated from a freshwater pond

Jacqueline Hollensteiner¹, **Ines Friedrich**¹, Lucas Hollenstein¹, Jan-Philipp Lamping¹, Kalina Wolf¹, Heiko Liesegang¹, Anja Poehlein¹, Robert Hertel² and Rolf Daniel¹

Microbiology Resource Announcements (25 February 2021), **10**: e00003-21
<https://doi.org/10.1128/MRA.000003-21>

Affiliations

¹Genomic and Applied Microbiology & Göttingen Genomics Laboratory, Institute of Microbiology and Genetics, Georg-August-University of Göttingen, Grisebachstraße 8, 37077 Göttingen, Germany

²FG Synthetic Microbiology, Institute of Biotechnology, BTU Cottbus-Senftenberg, Senftenberg, Germany

Author contributions:

Conceptualization: JH, **IF**, RH, RD

Experiments: **IF**

Data analysis: JH, **IF**, LH, JPL, KW, HL, AP, RH

Writing: JH, **IF**, LH, JPL, KW, HL, AP, RH, RD



Complete Genome Sequence of *Kinneretia* sp. Strain DAIF2, Isolated from a Freshwater Pond

Jacqueline Hollensteiner,^a Ines Friedrich,^a Lucas Hollstein,^a Jan-Philipp Lamping,^a Kalina Wolf,^a Heiko Liesegang,^a
 Anja Poehlein,^a Robert Hertel,^b  Rolf Daniel^a

^aGenomic and Applied Microbiology and Göttingen Genomics Laboratory, Institute of Microbiology and Genetics, Georg-August University of Göttingen, Göttingen, Germany

^bFG Synthetic Microbiology, Institute of Biotechnology, BTU Cottbus-Senftenberg, Senftenberg, Germany

ABSTRACT *Kinneretia* sp. strain DAIF2 was isolated from a eutrophic freshwater pond. The genome consists of a single chromosome (6,010,585 bp) with a GC content of 69.3%. The whole-genome-based phylogeny of DAIF2 revealed a closest relation to the genus *Kinneretia*.

The Gram-negative *Kinneretia* sp. strain DAIF2 was isolated from a eutrophic pond in Göttingen, Germany. The sample (51°33'29"N, 9°56'41"E) was collected on 24 September 2018. The strain was enriched and isolated as described previously (1). DAIF2 was chosen for sequencing, since it was most similar at the 16S rRNA gene level to the genus *Kinneretia*, which was until now only represented by the type strain, *Kinneretia asaccharophila* DSM 25082 (2). For DNA isolation, DAIF2 was cultivated in PCa medium (peptone medium supplemented with 0.015% CaCl₂ [3]) at 25°C. DNA was extracted using the MasterPure complete DNA and RNA purification kit (Epicentre, Madison, WI, USA) as described previously (1). Illumina sequencing libraries were constructed using the Nextera XT DNA sample preparation kit (Illumina, San Diego, CA, USA) and sequenced using a MiSeq instrument and reagent kit v3 (600 cycles), as recommended by the manufacturer (Illumina). For Nanopore sequencing, a separate batch of 1.5 μg high-molecular-weight DNA was used for library preparation by employing the ligation sequencing kit 1D (SQK-LSK109) and the native barcode expansion kit (EXP-NBD114; barcode 19) as described by the manufacturer (Oxford Nanopore Technologies, Oxford, UK). The MinION device Mk1B, the SpotON flow cell R9.4.1, and MinKNOW software v19.06.8 were used for sequencing (72 h) as recommended by the manufacturer (Oxford Nanopore Technologies). For demultiplexing and base calling, Guppy v3.0.7 (Oxford Nanopore Technologies) was applied. Default parameters were used for all software unless otherwise specified. Sequencing resulted in 3,208,102 300-bp Illumina reads and 5,612,523 Nanopore reads with a mean length of 1,631 bp. The Illumina reads were quality filtered using Trimmomatic v0.36 (4), and paired reads were joined with FLASH (5). The Nanopore reads were adapter and quality trimmed with a length cutoff of 10 kb using fastp v0.20.0 (6), resulting in 75,898 Nanopore reads with an *N*₅₀ value of 31,759 bp. Together with the Illumina reads, a *de novo* hybrid assembly was performed using Unicycler v0.4.8 (7) in normal mode. The assembly revealed a single circular chromosome (6,010,585 bp) with a GC content of 69.28%. Coverages calculated with Qualimap v2.2.1 (8) using Bowtie 2 v2.3.5 (9) and minimap2 v2.17-r941 (10) were 127-fold (Illumina) and 204-fold (Nanopore). The Prokaryotic Genome Annotation Pipeline (PGAP) v4.11 (11) was used for automatic DAIF2 genome annotation. Annotation revealed 5,538 putative genes, 5,398 of which were protein coding. Moreover, 64 tRNA genes, 15 rRNA genes, 1 transfer-messenger (tmRNA) gene, and 3 noncoding RNA (ncRNA) genes were identified.

Citation Hollensteiner J, Friedrich I, Hollstein L, Lamping J-P, Wolf K, Liesegang H, Poehlein A, Hertel R, Daniel R. 2021. Complete genome sequence of *Kinneretia* sp. strain DAIF2, isolated from a freshwater pond. Microbiol Resour Announc 10:e00003-21. <https://doi.org/10.1128/MRA.00003-21>.

Editor Julia A. Maresca, University of Delaware

Copyright © 2021 Hollensteiner et al. This is an open-access article distributed under the terms of the [Creative Commons Attribution 4.0 International license](https://creativecommons.org/licenses/by/4.0/).

Address correspondence to Rolf Daniel, rdaniel@gwdg.de.

Received 4 January 2021

Accepted 5 February 2021

Published 25 February 2021

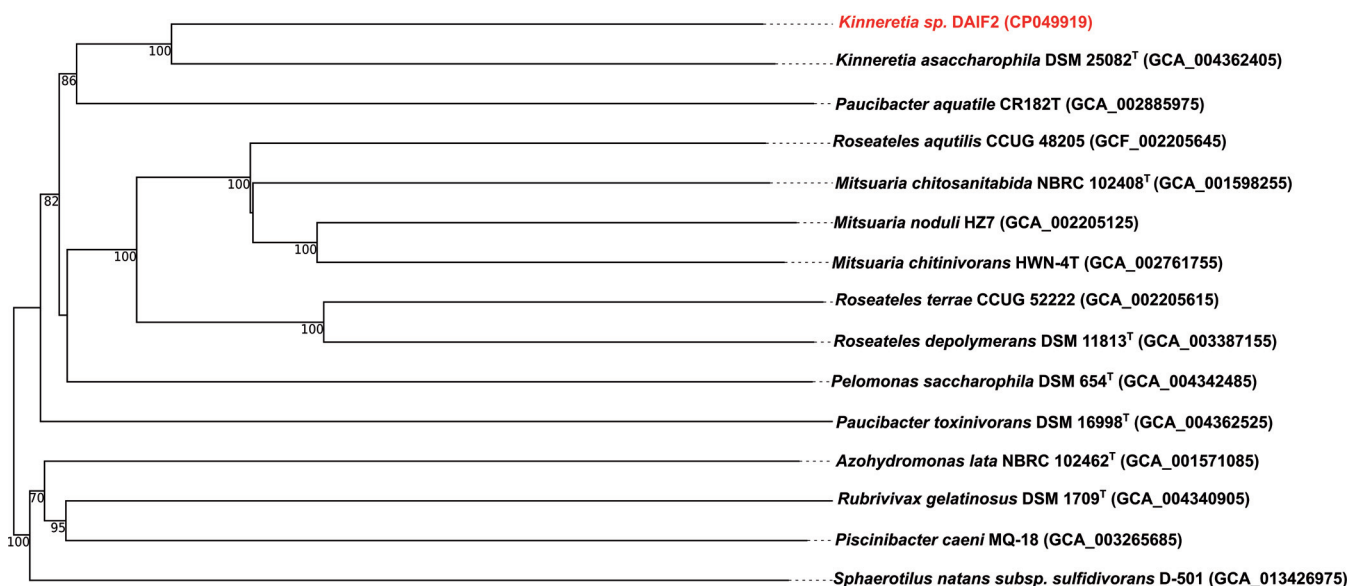


FIG 1 Phylogenetic classification of *Kinneretia* sp. strain DAIF2. The 14 closest related type strain genomes were used for phylogenetic analysis as described by TYGS (12). The tree was inferred with FastME 2.1.6.1 (13) using Genome BLAST Distance Phylogeny (GBDP) distances calculated from genome sequences. The branch lengths are scaled in terms of GBDP distance formula d5. The numbers above the branches are GBDP pseudobootstrap support values of >60% from 100 replications, with an average branch support of 85.8%. The tree was midpoint rooted (14).

Whole-genome-based phylogeny of the DAIF2 genome was performed with the Type (Strain) Genome Server (TYGS [12], accessed 12 November 2020). In general, close relationships of DAIF2 to the genera *Kinneretia*, *Paucibacter*, *Mitsuarina*, and *Roseateles*, which belong to the family *Comamonadaceae*, were detected (Fig. 1). The closest relative was the type strain *Kinneretia asaccharophila* DSM 25082 (GenBank accession number [NZ_SNXE0000000.1](https://doi.org/10.1093/gbe/evaa148)) of the genus *Kinneretia*, which was announced in 2010 as a new genus in the *Rubrivivax* branch (2), with a calculated digital DNA-DNA hybridization (dDDH) of 34.5%. This result indicates that strain DAIF2 may be a new species (Fig. 1).

Data availability. This complete genome sequence is available at DDBJ/ENA/GenBank under the accession number [CP049919.1](https://doi.org/10.1093/gbe/evaa148). The raw reads were deposited in the NCBI sequence read archive (SRA) under the accession numbers [SRX8059303](https://doi.org/10.1093/gbe/evaa148) (Illumina) and [SRX8059304](https://doi.org/10.1093/gbe/evaa148) (Nanopore).

ACKNOWLEDGMENTS

We thank Sarah Teresa Schübler for technical assistance.

We also acknowledge support by the Open Access Publication Funds of the University of Göttingen.

REFERENCES

- Friedrich I, Hollensteiner J, Schneider D, Poehlein A, Hertel D, Daniel R. 2020. First complete genome sequences of *Janthinobacterium lividum* EIF1 and EIF2 and their comparative genome analysis. *Genome Biol Evol* 12:1782–1788. <https://doi.org/10.1093/gbe/evaa148>.
- Gomila M, Pinhassi J, Falsen E, Moore ERB, Lalucat J. 2010. *Kinneretia asaccharophila* gen. nov., sp. nov., isolated from a freshwater lake, a member of the *Rubrivivax* branch of the family *Comamonadaceae*. *Int J Syst Evol Microbiol* 60:809–814. <https://doi.org/10.1099/ijs.0.011478-0>.
- Staley JT. 1968. *Prosthecomicrobium* and *Ancalomicrobium*: new prosthecate freshwater bacteria. *J Bacteriol* 95:1921–1942. <https://doi.org/10.1128/JB.95.5.1921-1942.1968>.
- Bolger AM, Lohse M, Usadel B. 2014. Trimmomatic: a flexible trimmer for Illumina sequence data. *Bioinformatics* 30:2114–2120. <https://doi.org/10.1093/bioinformatics/btu170>.
- Magoč T, Salzberg SL. 2011. FLASH: fast length adjustment of short reads to improve genome assemblies. *Bioinformatics* 27:2957–2963. <https://doi.org/10.1093/bioinformatics/btr507>.
- Chen S, Zhou Y, Chen Y, Gu J. 2018. fastp: an ultra-fast all-in-one FASTQ preprocessor. *Bioinformatics* 34:i884–i890. <https://doi.org/10.1093/bioinformatics/bty560>.
- Wick RR, Judd LM, Gorrie CL, Holt KE. 2017. Unicycler: resolving bacterial genome assemblies from short and long sequencing reads. *PLoS Comput Biol* 13:e1005595. <https://doi.org/10.1371/journal.pcbi.1005595>.
- Okonechnikov K, Conesa A, García-Alcalde F. 2016. Qualimap 2: advanced multi-sample quality control for high-throughput sequencing data. *Bioinformatics* 32:292–294. <https://doi.org/10.1093/bioinformatics/btv566>.
- Langmead B, Salzberg SL. 2012. Fast gapped-read alignment with Bowtie 2. *Nat Methods* 9:357–360. <https://doi.org/10.1038/nmeth.1923>.
- Li H. 2018. minimap2: pairwise alignment for nucleotide sequences.

- Bioinformatics 34:3094–3100. <https://doi.org/10.1093/bioinformatics/bty191>.
11. Tatusova T, DiCuccio M, Badretdin A, Chetvernin V, Nawrocki EP, Zaslavsky L, Lomsadze A, Pruitt KD, Borodovsky M, Ostell J. 2016. NCBI Prokaryotic Genome Annotation Pipeline. *Nucleic Acids Res* 44:6614–6624. <https://doi.org/10.1093/nar/gkw569>.
 12. Meier-Kolthoff JP, Göker M. 2019. TYGS is an automated high-throughput platform for state-of-the-art genome-based taxonomy. *Nat Commun* 10:2182. <https://doi.org/10.1038/s41467-019-10210-3>.
 13. Lefort V, Desper R, Gascuel O. 2015. FastME 2.0: a comprehensive, accurate, and fast distance-based phylogeny inference program. *Mol Biol Evol* 32:2798–2800. <https://doi.org/10.1093/molbev/msv150>.
 14. Farris JS. 1972. Estimating phylogenetic trees from distance matrices. *Am Nat* 106:645–667. <https://doi.org/10.1086/282802>.

6. Isolation of a host-confined phage metagenome allows the detection of phages both capable of plaque formation

Ines Friedrich¹, Robert Hertel^{1,2}

Methods in Molecular Biology (January 2023), **2555**:205–212
https://doi.org/10.1007/978-1-0716-2795-2_14

Affiliations

¹Genomic and Applied Microbiology & Göttingen Genomics Laboratory, Institute of Microbiology and Genetics, Georg-August-University of Göttingen, Grisebachstraße 8, 37077 Göttingen, Germany

²FG Synthetic Microbiology, Institute of Biotechnology, BTU Cottbus-Senftenberg, Senftenberg, Germany

Author contributions:

Conceptualization: **IF**, RH

Experiments: **IF**

Data analysis: **IF**, RH

Writing: **IF**, RH

Abstract

Bacteriophages, also called phages, are viruses of bacteria. They are the most common and diverse biological entities on this planet. For metagenomic investigation, their diversity is also their biggest obstacle. The direct metagenomic sequence of environmental phage communities often leads to short genomic fragments limiting the investigation to a few individual aspects of phage biology and diversity.

The presented protocol for generating a host-associated metagenome reduces the phage diversity to a concise and accessible size. Metagenome sequencing often leads to complete genomes, and the availability of a suitable host system ensures further experimental investigation.

Introduction

Bacteriophages, also called phages, are viruses of bacteria. They are the most common and diverse biological entities on this planet (1, 2). The traditional way of phage isolation is via a plaque assay. A viral suspension is applied to an agar-embedded host bacterial. Infected cells are locally consumed, resulting in clear cell-free areas known as phage plaques (3). The genomic era allows direct sequencing of the viral sphere and thus direct investigation of phage genome sequences.

Both approaches, individual isolation or metagenomic, have their specific weaknesses. The classical approach mainly allows the isolation of highly virulent phages. These phage types rely on rapid replication, rapid consumption of their host cells and the generation of large numbers of progeny. Phage types with deviant survival strategies, extended life cycles and small burst sizes, or which do not focus on immediate and absolute consumption of the host, are often overlooked. The sequence assembly of a direct metagenomic sequencing approach often results in very short contigs limiting the investigation to individual aspects of phage biology and diversity. Even with high sequence depth, complete viral genomes cannot be obtained (4).

The protocol presented here allows combining both systems' advantages and detecting both plaque-forming and non-forming phages in the new mesophilic species *Brevundimonas pondensis* LVF1^T (5). A defined host for enrichment creates a concise and experimentally accessible viral metagenome, which in turn allows a specific and more dept study of its phages.

For example, it is possible to directly address the different phage groups by specific isolation and sequencing of dsDNA, ssDNA, dsRNA and ssRNA genomic material (Figure 1).



Figure 1. Diverse and rich distribution of phage plaques after the infection of *B. pondensis* with sewage water.

Materials

Bacterial host strain

- *Brevundimonas pondensis* LVF1^T (5).

Media and working solutions

- PYE: 0.2% peptone, 0.1% yeast extract, 0.02% MgSO₄ x 7 H₂O.
- PYE agar/agarose: 0.2% peptone, 0.1% yeast extract, 0.02% MgSO₄ x 7 H₂O, 1.5% agar/0.4% agarose.
- 30% (w/v) PEG 8000 (Polyethylene Glycol 8000) with 1.5 M NaCl.
- 0.5 M EDTA (Ethylenediaminetetraacetic acid), pH 8.0.

- 100% Isopropanol.

Consumables

- Polypropylene copolymer (PPCO) centrifuge bottles with sealing closure (Thermo Fisher Scientific, Waltham, MA, USA).
- 15- and 50-mL sterile conical centrifuge tubes.
- 0.45 µm syringe compatible sterile filter (Sarstedt AG & Co. KG, Nümbrecht, Germany).
- 10- to 50-mL syringes.
- Sterile toothpicks.
- Petri dishes of 9-cm diameter.
- Non-specific salt-active endonuclease (SERVA, Heidelberg, Germany).
- MasterPure™ Complete DNA and RNA Purification kit (Lucigen, Middleton, WI, USA).
- S1 nuclease (Thermo Fisher Scientific).
- Ambion™ RNase III (Thermo Fisher Scientific).
- dsDNase (Thermo Fisher Scientific).
- Random Hexamer Primer (Thermo Fisher Scientific).
- Klenow Fragment (Thermo Fisher Scientific)
- 3 M Sodium acetate, pH 5.2.
- dNTPs.

Methods

Preparation of the host *B. pondensis* LVF1^T

1. Start an overnight culture of *B. pondensis* in 4.5 mL PYE medium in glass tubes at 30 °C and vigorous shaking. A fresh and dense culture of a host bacterium is required for bacteriophage enrichment (*see Note 1*).

Preparation of sewage water for bacteriophage enrichment

1. Request water of primary treatment from sewage plant (*see Note 2*).
2. The water sample of about 100 mL should be centrifuged at 6,000 x g for 15 min (*see Note 3*).
3. Filter the supernatant through a 0.45 µm non-pyrogenic, sterile PES-membrane (Sarstedt AG & Co. KG).
4. Add PEG 8000 to a final concentration of 10% (w/v) and NaCl to the final concentration of 0.5 M to the filtered sample, mix gently, and incubate the mixture overnight at 4 °C for phage particle precipitation (*see Note 4*).
5. After PEG-precipitation, centrifuge the viral suspension at 10,000 x g for 1 h at 4 °C in 50 mL conical tube (*see Note 5*).
6. After centrifugation, discard the supernatant and resuspend the phage pellet in 2.5 mL PYE for phages associated with *B. pondensis* LVF1^T.

Enrichment of host-specific bacteriophages via a plaque assay

1. Prepare fresh nutrient agar plates (PYE) in Petri dishes of 9-cm diameter and with about 25 mL of agar medium. Ensure no free water is present on the agar or at the edge of the plate.
2. Use a soft-agar overlay containing 0.4% (w/v) agarose for the second layer.
3. Mix 1 mL of the filtered and concentrated sewage water with 100 µL overnight cultures of host bacteria (OD₆₀₀ needs to be set to 0.1) (*see Note 6*).
4. Incubate the mixture for 10 min at room temperature.
5. Add 2.5 mL of prewarmed (50 °C) soft agar to the suspension, briefly vortex, and evenly distribute the cells on a 30 °C prewarmed Petri dish with the base agar.
6. After the overlay agar solidified, incubate the plate upside-down overnight at 30 °C (*see Note 7*).
7. A perfect result reveals a diverse and rich distribution of phage plaques with different plaque morphologies, sizes, and the presence or absence of halos (Figure 1) (*see Note 8*).
8. If individual viral isolates are desired, they can be picked with sterile toothpicks by gently penetrating the viral plaque in the soft agar overlay. Transfer the collected

virions into 500- μ L sterile medium in a 1.5-mL reaction tube by placing the toothpicks for 5 min into the medium (*see Note 9*).

9. Harvest the enriched viral pool from the plate by floating it with 4 mL PYE medium, incubating for about 30 min and transferring the supernatant into 15-mL conical centrifuge tubes (*see Note 10*).
10. Centrifuge the supernatant holding the phages for 10 min at 6,000 \times g and 4 °C.
11. Sterile filter the supernatant with a 0.45- μ m non-pyrogenic, sterile PES-membrane (Sarstedt AG & Co. KG) to remove insoluble matter and last host cells.
12. Add 1 μ L of non-specific salt-active endonuclease (~25 units) to the suspension obtained from one plate and mix everything thoroughly (*see Note 11*).
13. Add 10% PEG (w/v), 0.5 M NaCl and 1 mM MgSO₄ (*see Note 12*) final concentration (*see Note 13*).
14. Vortex the mixture and precipitate the phages overnight at 4 °C.
15. Pellet the precipitated phages with 10,000 \times g for 1 h at 4 °C and resuspend the phage pool in 2.0 mL PYE medium.

Total Nucleic Acids Purification

To extract total nucleic acids, we use the MasterPure™ Complete DNA and RNA Purification kit (Lucigen). The following protocol is modified for extracting nucleic acids from bacteriophages.

1. Dilute 5 μ L of Proteinase K (20 mg/mL) into 300 μ L of 2X T and C Lysis Solution for each sample.
2. Transfer 300 μ L of the fluid sample to a 2-mL reaction tube, add 300 μ L of 2X T and C Lysis Solution containing the Proteinase K and mix thoroughly.
3. Incubate at 65 °C for 15 minutes; vortex every 5 min.
4. Place the samples on ice for 3–5 minutes and proceed with total nucleic acid precipitation.
5. Add 300 μ L of MPC Protein Precipitation Reagent to 600 μ L of lysed sample and vortex vigorously for 10 s.

6. Pellet the precipitated proteins by centrifugation at 4 °C for 10 minutes at $\geq 10,000 \times g$. If the resultant pellet is clear, small, or loose, add an additional 25 μL of MPC Protein Precipitation Reagent, mix, and pellet again.
7. Transfer the supernatant to a clean microcentrifuge tube and discard the pellet.
8. Add 1000 μL of isopropanol to the recovered supernatant. Invert the tube 30-40 times.
9. Pellet the total nucleic acids by centrifugation at 4 °C for 10 minutes with 10,000 $\times g$.
10. Carefully pour off the isopropanol without dislodging the pellet.
11. Rinse twice with 70% (v/v) ethanol, careful not to dislodge the pellet. Centrifuge briefly and remove all the residual ethanol with a pipet.
12. Resuspend the total nucleic acids in 35 μL nuclease-free water.

Preparation of viral dsDNA, ssDNA, dsRNA and ssRNA

The simplest way to analyze the extracted metagenome is to sequence it. Separating the obtained nucleic acid into dsDNA, ssDNA, dsRNA and ssRNA can increase the information gain. The working scheme in Figure 2 shows how such an endeavor could be realized. The extracted dsRNA and ssRNA, as well as dsDNA, can then be sequenced with standard protocols in an NGS sequencing center. The ssDNA must first be turned into dsDNA in order to be conveniently sequenced using standard protocols. In the following, we provide a working instruction to realize the mentioned task.

Workflow scheme

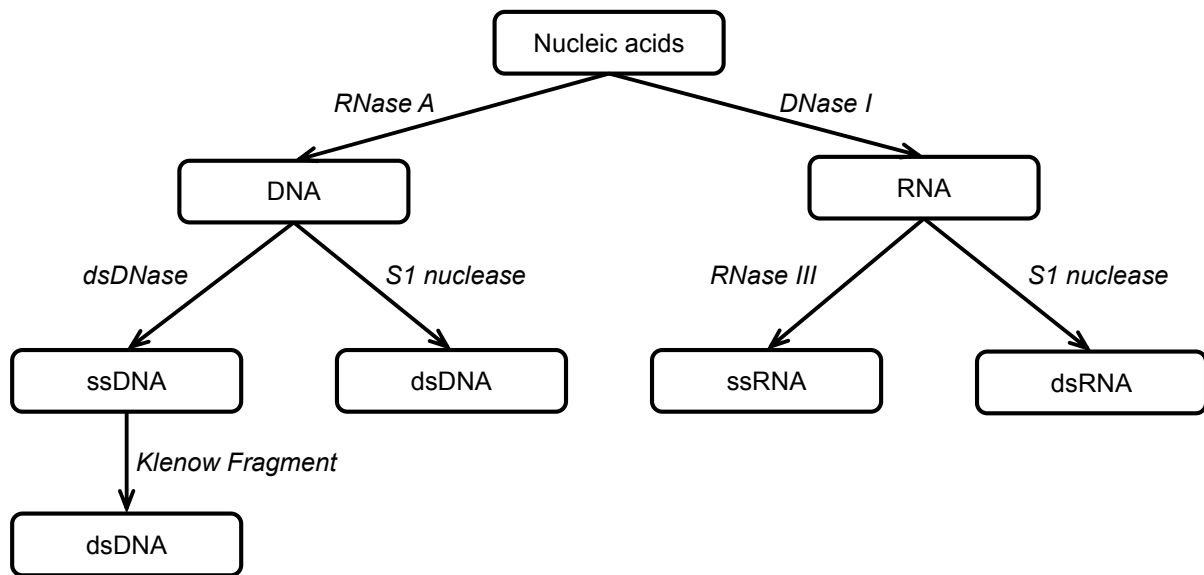


Figure 2. Nucleic acids separation workflow overview.

Preparation of dsDNA, dsRNA and ssRNA virome

1. Apply RNaseA (DNase free) to the total prepared total nucleic acids to obtain pure viral genomic DNA, or DNaseI (RNase free) to obtain pure viral genomic RNA.
2. Apply the S1 nuclease (Thermo Fisher Scientific) to total DNA preparation to exclude ssDNA and obtain pure dsDNA. Proceed likewise with RNA.
3. Apply Ambion™ RNase III to total RNA preparation to eliminate dsRNA and obtain pure ssRNA.

Transcription of viral ssDNA to dsDNA for NGS sequencing

1. Use the previously prepared viral ssDNA as starting materials to set up a 50- μ L reaction containing 2 μ g ssDNA, 0.1 mM Random Hexamer Primer, 10 units Klenow Fragment, 0.5 mM dNTPs, 1X Klenow Fragment Buffer (all reagents from Thermo Fisher Scientific, Waltham, MA, USA).
2. Incubate the reaction for 2 h at 37 °C.
3. Stop the reaction by adding 1 μ L of 0.5 M EDTA (pH 8.0).

4. For precipitation of DNA, add 5 μL of 3 M sodium acetate (pH 5.2; Thermo Fisher Scientific) and 50 μL cold isopropanol ($-20\text{ }^{\circ}\text{C}$), and mix gently.
5. Incubate the sample for 1 h at $-20\text{ }^{\circ}\text{C}$.
6. Pellet the DNA for 10 min at $10,000 \times g$ and $4\text{ }^{\circ}\text{C}$.
7. Wash the pellet twice with ice-cold 70% (v/v) ethanol.
8. Pellet after every washing step, as previously mentioned.
9. Dry the DNA for 2 min at $50\text{ }^{\circ}\text{C}$ in an open 2-mL tube. Resuspend the pellet in 20 μL sterile and pure water for at least 30 min at $4\text{ }^{\circ}\text{C}$.
10. Compare resulting dsDNA with the ssDNA used as starting material via TAE agarose gel electrophoresis.

PCR-based screening for phages incapable of plaque formation

By subtracting individual plaque-forming viral isolates from the metagenome, genomes of strains that are incapable of plaque formation can be identified.

1. Create specific primers from individual genomes that you bioinformatically extract from the viral metagenomes.
2. Perform a standard PCR reaction using these primers and 1 μL of viral suspension from previously picked plaques. Follow the manufacturer's instructions of the DNA Polymerase for the PCR reaction without further modification.
3. Verify the presence of a PCR product via TAE agarose gel electrophoresis. A primer pair that cannot be associated with an isolate implies that the genome observed in the metagenome belongs to a phage that cannot form plaques. A plaque-forming isolate not observed in the metagenome indicates a virus with modified bases in its genome. These may reduce sequence efficiency and lead to loss of genome sequence in the metagenome.

Notes

1. In general, this procedure can be performed with all mesophilic bacteria whose optimal growth and media compositions are known.
2. Preferably, use samples from your local sewage plant. We took samples from the sewage plant in Göttingen, Germany. Also, make sure that your host strains are present

in the sewage samples (e.g., through 16S amplicon sequencing). *Brevundimonas pondensis* LVF1^T is mostly present in the primary treatment step.

3. If more phages are needed, you can start with a larger starting amount and use PPCO centrifuge bottles with sealing closure (Thermo Fisher Scientific) as vessels for this. In our case, we centrifuged 1 L of the primary treatment step with these bottles.
4. The precipitation time can be extended up to three days if the viral sample is not sewage, contains unlikely aggressive detergents and a low concentration of the desired phage particles.
5. This step concentrates the free phages in the solution and extracts the viral particles from the aggressive wastewater in which they rapidly degenerate. This step is unnecessary if the density of the desired phages in the wastewater is high, and the sample is directly used.
6. Since one often does not know the phage density of a sample in advance, it is advisable to use a series with different phage amounts directly. If there are too few phages in the sample, hardly any plaques are visible. If there are too many phages in the sample, the plate will appear empty after incubation. Neither of these are ideal conditions. The use of an uninfected control plate as a reference point is advantageous.
7. During the incubation of the floated plate, phages diffuse into the liquid medium where most of the host remain demobilized in the overlay. However, if soft agar fragments are transferred along with the viral suspension, they will be removed by centrifugation during the next working step.
8. Plaques should not overlap each other, as this would imply competition for host cells, which may lead to impairment of the metagenomic diversity achieved. One must also consider local infections that do not manifest a visible plaque. Such infections still release virus particles in their environment that can be harvested for further studies.
9. Viral suspensions of individual isolates can be stored at 4 °C for several months.
For whole-genome sequencing, the picked isolates must be further singularized via stepwise dilution to produce plaques without any neighboring infection events within 3 cm in diameter.
10. This step allows bacterial debris to be pelleted and separated from the virions.

11. A nuclease is necessary to digest free DNA and RNA unprotected by a viral capsid and thus mainly of host origin. This host material strongly impacts later sequencing and therefore has to be removed. Alternatively, RNases or DNases can also be used.
12. The used nuclease is a metal-dependent nuclease and uses Mg^{2+} to facilitate phosphodiester bond breakage. Magnesium must only be supplied if no Mg^{2+} ions are present in the used medium.
13. Usually, we remove the free nucleic acids parallel with phage precipitation. However, we observed this procedure is not reliably applicable with all media. Thus, removal of nucleic acids prior precipitation can be appropriate.

Acknowledgements

We thank the Department of Genomic and Applied Microbiology and the Göttingen Genome Laboratory for an excellent working environment and constructive teamwork.

References

1. Hendrix RW (2009) Jumbo bacteriophages, In: Van Etten, J.L. (ed.) Lesser known large dsDNA viruses, pp. 229–240 Springer Berlin Heidelberg, Berlin, Heidelberg
2. Wu Q and Liu W-T (2009) Determination of virus abundance, diversity and distribution in a municipal wastewater treatment plant. *Water Res* 43:1101–1109
3. Calendar R, Ed, (1988) *The Bacteriophages*, Plenum Press, New York
4. Kieft K and Anantharaman K (2022) Virus genomics: what is being overlooked? *Curr Opin Virol* 53:101200
5. Friedrich I, Klassen A, Neubauer H, et al (2021) Living in a puddle of mud: Isolation and characterization of two novel *Caulobacteraceae* strains *Brevundimonas pondensis* sp. nov. and *Brevundimonas goettingensis* sp. nov. *Appl Microbiol* 1:38–59

7. *Brevundimonas* and *Serratia* as host systems for assessing associated environmental viromes and phage diversity by complementary approaches

Ines Friedrich¹, Hannes Neubauer¹, Alisa Kuritsyn¹, Bernhard Bodenberger¹, Faina Tskhay¹, Sara Hartmann¹, Anja Poehlein¹, Mechthild Böemeke,¹ Michael Hoppert², Dominik Schneider¹, Robert Hertel^{1,3} and Rolf Daniel¹

Accepted in Frontiers in Microbiology on 23 February 2023
<https://doi.org/10.1007/978-1-0716-2795-2>

Affiliations

¹Genomic and Applied Microbiology & Göttingen Genomics Laboratory, Institute of Microbiology and Genetics, Georg-August-University of Göttingen, Grisebachstraße 8, 37077 Göttingen, Germany

²General Microbiology, Institute of Microbiology and Genetics, Georg-August-University of Göttingen, Grisebachstraße 8, 37077 Göttingen, Germany

³FG Synthetic Microbiology, Institute of Biotechnology, BTU Cottbus-Senftenberg, Senftenberg, Germany.

Author contributions:

Conceptualization: **IF**, RH, RD

Experiments: **IF**, HN, AK, BB, FT, SH, MB

Data analysis: **IF**, RH, AP, DS, RD

Writing: **IF**, HN, AK, BB, FT, SH, AP, MH, DS, RH, RD

Abstract

The novel phage host systems *Brevundimonas pondensis* LVF1 and *Serratia marcescens* LVF3 were used to investigate biases introduced in the recovered phage diversity using the classic overlay plaque assay for isolation. The dsDNA, ssDNA, dsRNA, and ssRNA were isolated from phage plaques, and sequencing revealed new phage strains.

Of the 25 distinctive dsDNA phage isolates, 14 were associated with *Brevundimonas* and 11 with *Serratia*. Further TEM analysis revealed that six are of the *Myo*-, 18 of the *Sipho*- and one of the *Podo*-morphotype, while *Brevundimonas*-associated phages are all of the *Sipho*-morphotype. The associated viromes revealed that phage diversity is higher in summer than in winter and dsDNA phages are the dominant group. Isolation of vB_SmaP-Kaonashi was possible after investigating the viromes, demonstrating the great potential of accompanying metagenomic virome sequencing. The ssDNA virome analysis showed that the *B. pondensis* LVF1 system is associated with *Microviridae* and *Inoviridae*, even though no isolates could be obtained. The results mentioned above regarding the dsDNA virome and isolates demonstrate that the classical isolation technique is not exhausted, leading to the isolation of dsDNA phages that are unknown. New or additional approaches like the employed virome analysis are needed to expand our knowledge on phage diversity.

Introduction

Bacteriophages or phages are bacterial viruses that infect and replicate in bacterial cells and belong to the most diverse entities on the planet (Casas and Rohwer, 2007; Dion et al., 2020). With an estimated number of 10^{31} virions on earth, phages outnumber bacterial cells in various environments by approximately ten-fold (Dion et al., 2020). The highest phage densities were observed in wastewater treatment plants (WWTP).

As intracellular parasites, phages rely on their host metabolism for replication. The host range is phage-strain specific and may include single or multiple bacterial species (Garmaeva et al., 2019). They either reduce the population through direct replication (lytic route) (Carding et al., 2017) or enter a long-term relationship with their host by integrating into the host genome as a prophage (lysogenic route) (Principi et al., 2019). Prophages provide additional genetic information and can supply the host with extra properties resulting in a competitive advantage.

Today bacteriophages are classified based on their genomic sequence and organization (Dion et al., 2020). The resulting groups usually correlate with viral morphology. Some have a head-tail morphology (*Caudoviricetes*), others are filamentous (*Inoviridae*), pleomorphic (*Plasmaviridae*), or polyhedral (*Microviridae*, *Corticoviridae*, *Tectiviridae*, *Cystoviridae*, and *Leviviricetes*). In addition to the viral capsid, internal or external lipid membranes may also exist. Unlike other phages, pleomorphic phages do not have capsids and form a proteinaceous lipid vesicle. The phage genetic material comprises RNA or DNA, varying from single- to double-stranded and from linear to circular while no circular RNA phages have been reported so far (Dion et al., 2020).

Most of the characterized phages isolated to date are tailed and use dsDNA as genomic material (Dion et al., 2020; Zreløvs et al., 2020). Furthermore, some groups are particularly prominent regarding the virus type and the genome size (Zreløvs et al., 2020).

To explore virus types and genome sizes, we used *Brevundimonas pondensis* LVF1 (Friedrich et al., 2021b) and *Serratia marcescens* LVF3 (Friedrich et al., 2021a) as host systems. *B. pondensis* is an oligotrophic bacterium and belongs to the family *Caulobacteraceae*. This strain has a single flagellum, is Gram negative, aerobic, and grows best at 30 °C. *Serratia marcescens* LVF3 belongs to the family *Yersiniaceae*. It is Gram-negative, possesses a flagellum, and is a copiotrophic organism. The optimal growth temperature is also 30 °C. Both host systems are excellent for studying viral diversity, as both have yielded a variety of different plaques by plaque assay in preliminary experiments. We isolated individual phages and investigated the viral community associated with the two hosts by viral metagenome analysis.

Thereby, we assessed not just dsDNA material but also ssDNA, dsRNA, and ssRNA viromes. This was done using specific nucleases receiving the purified form of viromes mentioned above. We used sewage samples from a WWTP from two seasons (winter and summer) as source material. Isolates were characterized by morphology, genome sequence, and alignment to the virome sequencing data to explore the hidden potential of discovering new phages (Figure 1).

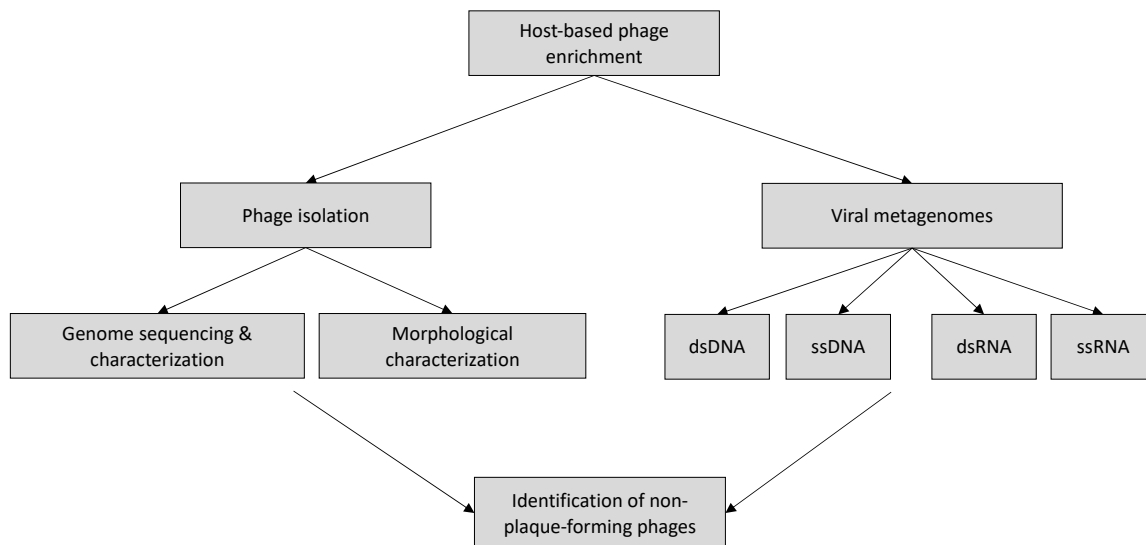


Figure 1. Overview of the experimental setup.

Materials and methods

Phage isolation and host-based phage enrichment

1 L primary treatment sewage from the municipal WWTP in Göttingen, Germany, collected in January 2019, July 2019, and January 2020, served as environmental phage sources. Samples were centrifuged at $6,000 \times g$ for 15 min. The supernatant containing phages was sterile-filtered, employing a $0.45 \mu\text{m}$ non-pyrogenic PES-membrane (Sarstedt AG & Co. KG, Nümbrecht, Germany). by adding polyethylene glycol (PEG) in a final concentration of 10% (w/v) and 0.5 M NaCl. After incubation at 4°C for 16 h, phages were harvested by centrifugation at $10,020 \times g$ and 4°C for 1 h. The supernatant was discarded, and phage pellets were resuspended in 25 mL PYE (0.2% peptone, 0.1% yeast extract, 0.02% $\text{MgSO}_4 \times 7 \text{H}_2\text{O}$) for phages associated with *B. pondensis* LVF1^T, and in TSB-10 (1.7% peptone from casein, 0.3% peptone from soybean, 0.25% K_2HPO_4 , 1% NaCl, 0.25% glucose monohydrate) for phages associated with *S. marcescens* LVF3^R (Friedrich et al., 2021b).

Phages were isolated via agar overlay plaque assay as described elsewhere (Kropinski et al., 2009) using host-specific culture media for the base agar (1.5% agarose) and overlay (0.4% agarose). Infected overlay plates were incubated overnight at 30°C . Morphologically distinct plaques representing individual phage isolates were picked with a sterile toothpick, and each was transferred to a $500 \mu\text{L}$ sterile culture medium. Further phage strain purification was performed via three subsequent reinfections, resulting in pure cultures.

To harvest the whole host-associated viral diversity, the initial overlay was washed with 4 mL respective medium, also allowing the harvest of phages that might not be able to form plaques under the given conditions. The phage suspensions were processed as described above. In addition, Salt Active Nuclease (SERVA, Heidelberg, Germany) was added to the phage suspensions (20 U/mL) prior to precipitation to digest non-particle-protected host-associated nucleic acids.

Preparation of total and specific nucleic acids

All kits and enzymes were used as recommended by the manufacturer if not otherwise stated. The MasterPure™ Complete DNA and RNA Purification kit (Lucigen, Middleton, WI, USA) were used with modifications to extract total viral nucleic acids. Due to the high protein content, we increased the amount of Proteinase K (20 mg/mL) to 5 µL in 300 µL of 2X T and C Lysis Solution, which was applied to 300 µL of phage suspension. We obtained pure viral genomic DNA by applying RNase A (DNase free) to the total nucleic acid preparation and DNase I (RNase free) for pure viral RNA.

To receive ssDNA, dsDNA was removed via dsDNA-specific dsDNase (Thermo Fisher Scientific, Waltham, MA, USA). Then, viral ssDNA was *in vitro* transformed to dsDNA using Klenow fragment (Thermo Fisher Scientific, Waltham, MA, USA) and random hexamer primers (Thermo Fisher Scientific, Waltham, MA, USA).

S1 nuclease (Thermo Fisher Scientific, Waltham, Ma, USA) was applied to the total nucleic acids to remove single-stranded molecules for dsDNA and dsRNA purification. RNase III (Thermo Fisher Scientific, Waltham, MA, USA) was used to remove dsRNA for ssRNA purification.

Phage genome and virome sequencing and sequence read processing

RNA samples were reverse transcribed to dsDNA *in vitro* and sequenced like dsDNA samples with an Illumina MiSeq-system (2 x 300 bp) as described previously (Kohm et al., 2022).

Potential host reads were removed by mapping to the host genome employing bowtie2 (Langmead and Salzberg, 2012, 2). Unmapped pairs were quality-processed employing Trimmomatic v0.39 (Bolger et al., 2014) and paired reads joined with FLASH v1.2.11 (Magoč and Salzberg, 2011). The quality-processed reads served as input for the Unicycler v0.4.9 assembly pipeline in normal mode (Wick et al., 2017), which included Spades v3.13.0

(Bankevich et al., 2012), makeblastdb v2.11.0+ and tblastn v2.11.0+ (BLAST® Command Line Applications User Manual [Internet], 2019), bowtie2 v2.4.4 (Langmead and Salzberg, 2012), SAMtools v1.12 (Li et al., 2009), java v.11.0.13 (Arnold et al., 2005), and Pilon v1.23 (Walker et al., 2014). Assembly was quality-assessed using QualiMap v2.2.2 (Okonechnikov et al., 2016). Genomes of individual phage isolates were annotated with VIBRANT (Kieft et al., 2020) and InterProScan v5.55-88.0 (Zdobnov and Apweiler, 2001), and data were submitted to GenBank (Benson et al., 2017).

Raw reads from the ssDNA, dsRNA and ssRNA virome were mapped to the assembled genome using bowtie2 v2.4.4 (Langmead and Salzberg, 2012) to remove putative dsDNA contamination. Unmapped reads were used for virome assembly with the Unicycler v0.4.9 assembly pipeline in normal mode (Wick et al., 2017). The resulting contigs were searched against BLAST nt database v2.12.0+ (accessed on 14 July 2022) (Altschul et al., 1990; Altschul, 1997; Camacho et al., 2009) to identify further contamination. Contigs derived from the ssDNA, dsRNA and ssRNA virome with significant similarities to prokaryotic sequences were considered contaminations and excluded from the analysis. Such contamination was only observed in samples from the summer season and only in the ssDNA virome of *B. pondensis* LVF1 and from both seasons in the RNA viromes of *S. marcescens* LVF3. The remaining contigs (larger than 1,000 bp) were mapped on all publicly available (Supplement Table S1) and our isolated phage genomes using pyani ANIb method (Pritchard et al., 2016). Contigs which showed a match with at least 70% nucleotide-to-nucleotide sequence identity to known phages were not further analyzed. The same method was applied to investigate matches of dsDNA phage contigs with ssDNA or ssRNA contigs. Contigs which showed a match in the ssDNA/ssRNA virome were not further investigated. Further, contigs which did not reach a coverage over 30 (output of QualiMap v2.2.2), were removed. All dsDNA and resulting ssDNA, dsRNA and ssRNA contigs were annotated with VIBRANT (Kieft et al., 2020) and InterProScan v5.55-88.0 (Zdobnov and Apweiler, 2001). Viromes, which could not be annotated via VIBRANT, were annotated with Phage Commander including RAST v2.0 (Aziz et al., 2008), MetaGene (Noguchi et al., 2006), GeneMark v2.5 (Borodovsky and McIninch, 1993), GeneMark.hmm v3.25 (Besemer et al., 2001), GeneMark with Heuristics v3.25 (Zhu et al., 2010), GeneMarkS v4.28 (Besemer et al., 2001), GeneMark S2 (Lomsadze et al., 2018), Glimmer v3.02 (Delcher et al., 2007), and Prodigal v.2.6.3 (Hyatt et al., 2020), as well

ARAGORN v1.2.41.c for identification of phage tRNAs (Laslett and Canback, 2004). Data of phage isolates and raw read sequences were submitted to GenBank (Benson et al., 2017).

Taxonomic classification of *Brevundimonas*- and *Serratia*-associated phages

Taxonomic classification was performed using pyani v0.2.11 (Pritchard et al., 2016) with the ANIm option. Average nucleotide identity (ANI) values $\geq 95\%$, presented in white to red, indicate isolates of the same species. ANI values between $\leq 95\%$ to 70% , presented in white to blue, indicate strains of the same genus (Parks et al., 2019).

Bacteriophages associated with the family *Caulobacteraceae* (for our *Brevundimonas*-associated phages) and genus *Serratia* were downloaded from NCBI Virus (Brister et al., 2015) (accessed December 01, 2021). These included *Brevundimonas*- and *Caulobacter*-associated phages and *Serratia*-associated phages (Supplement Table S1).

Morphology of phage isolates

Phage morphology was assessed by transmission electron microscopy (TEM). Data were imaged using the Digital Micrograph software (Gatan GmbH, Munich, Germany). The phage isolates were amplified and then, a negative staining technique was performed. For this purpose, a thin carbon film, evaporated by glow discharge onto freshly cleaved mica, was partly floated off on a drop of phage suspension. The mica was washed briefly with demineralized water and transferred to a thin copper-coated grid (PLANO GmbH, Marburg, Germany) and dried using a filter paper without touching the grid's surface. The grid was stained using 50 μL of 2% uranyl acetate droplet with the carbon film facing downwards for 1 s. The grid was dried carefully and ready for the TEM imaging.

Electron microscopy was performed with a Jeol 1011 transmission electron microscope (Jeol Ltd, Eching, Germany) equipped with a Gatan Orius SC1000 CCD camera (Gatan, Munich, Germany).

Nomenclature of bacteriophage isolates

Isolates were named based on the informal guide by Adriaenssens and Brister (Adriaenssens and Brister, 2017). Accordingly, vB stands for virus of bacteria, Bpo and Sma for the host organism (*B. pondensis* and *S. marcescens*, respectively), M for the myovirus and S for siphovirus and P for podovirus, followed by an individual naming which does not follow any

rules. Consequently, the full names of the viruses compose to e.g., vB_SmaM-Otaku abbreviated Otaku.

Results

Phage isolation and characterization

Brevundimonas pondensis LVF1 and *Serratia marcescens* LVF3 served as hosts for plaque assay-based phage isolation (Supplementary Figure S1), which was performed with sewage samples obtained in winter 2019, summer 2020 and winter 2020. 25 (2019) and 50 (2020) individual plaques associated with *B. pondensis* LVF1 and 25 (2019) and 50 (2020) plaques associated with *S. marcescens* LVF3 were picked. Redundancies were eliminated by determining specific genomic restriction patterns of all isolates. This analysis also revealed that all genomes of isolates were comprised of dsDNA. Subsequently, 25 unique phages were obtained, 14 associated with *B. pondensis* LVF1 and 11 with *S. marcescens* LVF3 (Table 1).

Transmission electron microscopy revealed head-tail morphology for all isolates, including 6 myoviruses, 18 siphoviruses and 1 podovirus with various individual structural features (Figure 2). The isolated *Brevundimonas*-associated phages were all siphoviruses whereas *Serratia* phages revealed three morphotypes (myovirus, siphovirus, and podovirus). Capsid diameter ranged from 45–381 nm and tail length from 98–400 nm (Table 1). Siphoviruses revealed two different types of elongated capsids. The elongation of the shorter type did not exceed twice the diameter of the head, whereas the longer head types frequently exceed three times the head diameter (Figure 2 J-Y and Table 1).

Table 1. Morphological properties of all bacteriophage isolates associated with *B. pondensis*, *S. marcescens*. Picture ID refers to Figure 2. Tail lengths were measured from the bottom of the neck to the base plate. Bacteriophages were named according to the recommendation by (Adriaenssens and Brister, 2017).

Picture ID	Host	Family	Name	Season	Phage size [nm]				
					Capsid width	Capsid length	Tail length	Total length	
A	<i>B. pondensis</i> LVF1	Siphoviridae	vB_BpoS-Papperlapapp	Jul 2019	53	363	400	763	
B	<i>B. pondensis</i> LVF1	Siphoviridae	vB_BpoS-Kabachok	Jan 2019	53	377	398	775	
C	<i>B. pondensis</i> LVF1	Siphoviridae	vB_BpoS-Domovoi	Jan 2019	55	381	381	762	
D	<i>B. pondensis</i> LVF1	Siphoviridae	vB_BpoS-Marchewka	Jan 2019	42	267	257	524	
E	<i>B. pondensis</i> LVF1	Siphoviridae	vB_BpoS-Bambus	Jan 2019	56	368	392	760	
F	<i>B. pondensis</i> LVF1	Siphoviridae	vB_BpoS-Gurke	Jul 2019	75	306	241	547	
G	<i>B. pondensis</i> LVF1	Siphoviridae	vB_BpoS-Kikimora	Jan 2019	92	278	317	595	
H	<i>B. pondensis</i> LVF1	Siphoviridae	vB_BpoS-Poludnitsa	Jul 2019	57	63	220	283	
I	<i>B. pondensis</i> LVF1	Siphoviridae	vB_BpoS-Leszy	Jan 2019	-	98	257	355	
J	<i>B. pondensis</i> LVF1	Siphoviridae	vB_BpoS-StAshley	Jan 2019	-	45	254	299	
K	<i>B. pondensis</i> LVF1	Siphoviridae	vB_BpoS-Malnes	Jan 2019	-	61	183	244	
L	<i>B. pondensis</i> LVF1	Siphoviridae	vB_BpoS-Strzyga	Jul 2019	-	60	155	215	
M	<i>B. pondensis</i> LVF1	Siphoviridae	vB_BpoS-Polewnik	Jul 2019	-	58	149	208	
N	<i>B. pondensis</i> LVF1	Siphoviridae	vB_BpoS-Babayka	Jul 2019	-	65	163	228	
O	<i>S. marcescens</i> LVF3	Myoviridae	vB_SmaM-Totoro	Jul 2019	-	111	200	311	
P	<i>S. marcescens</i> LVF3	Myoviridae	vB_SmaM-Kodama	Jul 2019	-	119	198	317	
Q	<i>S. marcescens</i> LVF3	Myoviridae	vB_SmaM-Sureiya	Jul 2019	-	128	202	330	
R	<i>S. marcescens</i> LVF3	Myoviridae	vB_SmaM-Yubaba	Jul 2019	-	113	211	324	
S	<i>S. marcescens</i> LVF3	Siphoviridae	vB_SmaS-ChuuTotoro	Jan 2020	-	81	164	245	

T	<i>S. marcescens</i> LVF3	<i>Myoviridae</i>	vB_SmaM-Kashira	Jan 2020	-	121	202	323
U	<i>S. marcescens</i> LVF3	<i>Siphoviridae</i>	vB_SmaS-Kamaji	Jan 2020	-	78	185	263
V	<i>S. marcescens</i> LVF3	<i>Siphoviridae</i>	vB_SmaS-ChibiTotoro	Jan 2020	-	54	125	179
W	<i>S. marcescens</i> LVF3	<i>Siphoviridae</i>	vB_SmaS-Susuwatari	Jul 2019	-	61	130	191
X	<i>S. marcescens</i> LVF3	<i>Podoviridae</i>	vB_SmaP-Kaonashi*	Jul 2019	-	55	158	213
Y	<i>S. marcescens</i> LVF3	<i>Myoviridae</i>	vB_SmaM-Otaku	Jul 2019	-	46	98	144

* Isolation was performed after virome analysis of the dsDNA virome.

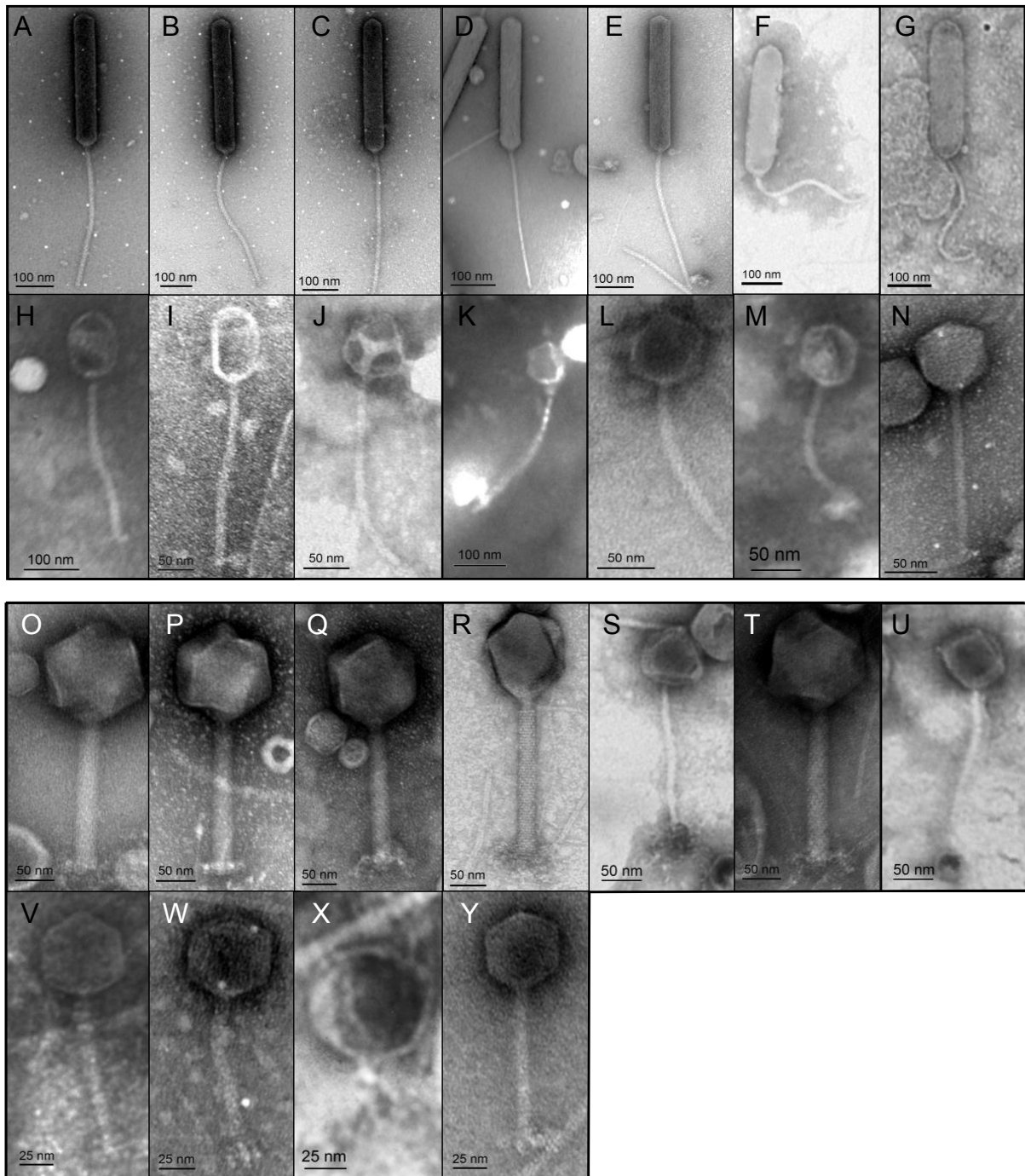


Figure 2. Transmission electron micrographs of all 25 isolates. Bacteriophage preparations were negatively stained with 2% (w/v) aqueous uranyl acetate. Samples were examined in a Jeol transmission electron microscope. Table 1 presents the respective physical properties of the shown virions.

Genome sequencing and characterization

Genomic DNA of each isolate was sequenced and assembled to complete high-quality genomes (Table 2). The genome size of *B. pondensis*-associated phages ranged from 42.3 to 356.9 kb, with a G + C content of 49.9% to 65.9% (host G + C content 67.0%). For *Serratia marcescens* LVF3-associated phages, genome size ranged from 39.9 to 278.8 kb with a G+C

content of 41.0% to 58.6% (host G + C content 59.3%). Phage genome sizes here range from lambda-like phages to jumbo (here *Serratia*-associated) or even giant (here *Brevundimonas*-associated) phages.

Annotation of the genomes revealed the presence of phage-specific protein-encoding genes and the presence of tRNA genes frequently. It must be noted that *Brevundimonas*-associated bacteriophages ≥ 300 kb contained with ≥ 24 an exceptionally high number of tRNA genes. Similar results were obtained for *Serratia* phages with a genome size of 112 to 148 kb (Table 2).

Table 2. Genome analyses of all phage isolates associated with *B. pondensis*, *B. goettingensis* and *S. marcescens*. Picture ID is corresponding to the isolates depicted in Figure 2 and Table 1. Coverage of phages was determined through QualiMap v2.2.2 (Okonechnikov et al., 2016), CDS and hypothetical proteins were determined employing VIBRANT v1.2.1 annotation (Kieft et al., 2020) and manual curation of gene function prediction using InterProScan v5.55-88.0 (Zdobnov and Apweiler, 2001) and Protein BLAST (Altschul et al., 1990). ARAGORN v1.2.41.c (Laslett and Canback, 2004) was used for the detection of tRNAs and tmRNAs (none could be detected).

Picture ID	Name	Genome size [bp]	Coverage	G + C % content	CDS	Hypothetical proteins	tRNAs	NCBI accession number
A	vB_BpoS-Papperlapapp	356,874	123.8-fold	65.54	564	475	24	ON529860
B	vB_BpoS-Kabachok	356,285	443.0-fold	65.53	566	486	24	ON529852
C	vB_BpoS-Domovoi	352,705	448.7-fold	65.54	561	473	25	ON529855
D	vB_BpoS-Marchewka	348,421	521.4-fold	65.87	558	473	24	ON529851
E	vB_BpoS-Bambus	348,100	330.6-fold	65.80	550	473	24	ON529853
F	vB_BpoS-Gurke	321,510	98.5-fold	63.08	499	431	29	ON529850
G	vB_BpoS-Kikimora	312,615	175.6-fold	62.85	495	418	29	ON529857
H	vB_BpoS-Poludnitsa	85,956	661.7-fold	61.80	111	88	0	ON529862
I	vB_BpoS-Leszy	85,646	367.0-fold	62.02	113	92	0	ON529856
J	vB_BpoS-StAshley	69,922	66.1-fold	50.07	106	82	0	ON529865
K	vB_BpoS-Maines	68,997	82.4-fold	49.90	99	75	1	ON529866
L	vB_BpoS-Strzyga	62,088	66.0-fold	59.30	82	60	0	ON529867
M	vB_BpoS-Polewnik	61,859	118.0-fold	59.07	81	59	0	ON529863
N	vB_BpoS-Babayka	42,321	913.2-fold	61.15	53	30	0	ON529868
O	vB_SmaM-Totoro	278,767	314.5-fold	46.27	346	272	1	ON287372
P	vB_SmaM-Kodama	275,052	347.9-fold	46.77	322	255	2	ON287376
Q	vB_SmaM-Sureiya	256,354	316.0-fold	41.04	267	205	4	ON287370
R	vB_SmaM-Yubaba	255,663	66.0-fold	41.05	266	207	4	ON287375
S	vB_SmaS-ChuuTotoro	147,447	47.19-fold	49.19	278	233	19	ON287369

T	vB_SmaM-Kashira	144,511	51.9-fold	50.90	266	221	20	ON287374
U	vB_SmaS-Kamaji	112,334	323.4-fold	44.69	153	100	21	ON287373
V	vB_SmaS-ChibiTotoro	44,971	342.1-fold	57.18	63	37	0	ON287368
W	vB_SmaS-Susuwatari	44,728	246.5-fold	58.62	63	38	0	ON287371
X	vB_SmaP-Kaonashi*	41,649	365.2-fold	53.92	50	20	0	ON287377
Y	vB_SmaM-Otaku	39,857	1,990.0-fold	57.41	62	44	0	ON087563

* Isolation was performed after virome analysis of the dsDNA virome.

Phylogenetic classification of the isolates

We downloaded all publicly available phage genomes associated with the bacterial host genera and used them for a BLASTn-based average nucleotide identity (ANI) analysis. Results revealed five genera which contain two or more species and eight orphan species for phages associated with *Caulobacteracea* (Figure 3A). Only three of our isolates were of the same species (vB_BpoS-Domovoi, vB_BpoS-Papperlapapp and vB_BpoS-Kabachok). All others were new species or even representatives of new genera (Figure 3A). *Serratia*-associated were affiliated to 13 genera which contain two or more species and eight orphan species. Except vB_SmaM-Kodama, all isolates represented new species, of which at most two were associated with the same genus (Figure 3B).

These results showed that even with applying the classical isolation technique resulting in isolation of dsDNA phages only, we were able to isolate unknown species and genera. Thus, the plaque technique is certainly not exhausted in its potential and can still lead to new discoveries.

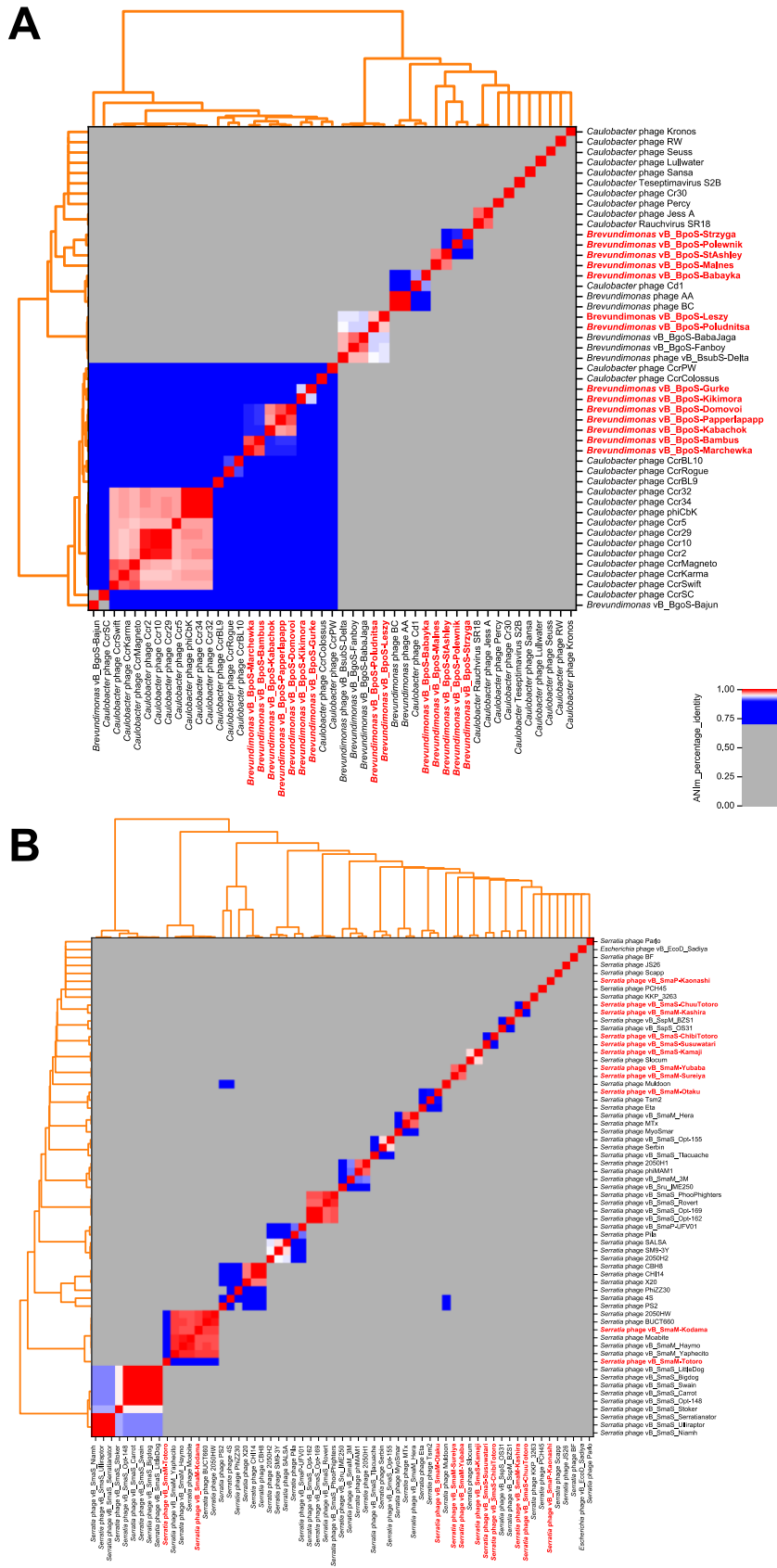


Figure 3. Genome-based phylogenetic analysis of *Caulobacteraceae*-associated (A) and *Serratia*-associated (B) bacteriophages. All genomes from NCBI Virus (Brister et al., 2015) and our own isolates (marked in bold red) were examined. Calculations were done with pyani (Pritchard et al., 2016) using ANIm method with default parameters.

Host-associated viromes

The plates from which we picked plaques and obtained the isolates also served as a starting point to generate host-associated viromes. The plates were washed with medium to collect all present phages, including those unable to form visible plaques and likely being overseen during preceding isolation. Viral derived nucleic acids were used to isolate dsDNA, ssDNA, dsRNA, and ssRNA specifically. The amounts recovered were highest for dsDNA (250–400 ng) followed by ssDNA (230–360 ng), ssRNA (60–200 ng) and dsRNA (20–40 ng). The amount of ssRNA compared to the amount of dsDNA seemed relatively high, which might indicate contamination with host RNA.

A total of 16 host-associated metaviromes were studied, consisting of dsDNA, ssDNA, dsRNA and ssRNA metaviromes from two seasons and two host systems. It is noticeable that the number of reads and resulting base pairs in the DNA virome were much larger than in the RNA virome of both host systems used (Table 3). Because the amount of dsRNA from both host systems was already low in both seasons, only a small number of reads could be passed down after sequencing, and therefore the dsRNA viromes were not considered further in the analysis. Although the *Brevundimonas*-associated ssRNA virome had a relatively high amount of ssRNA and many reads, the assembly and median contig size (N50) were low. Since no information can be derived from this, the analysis was not considered further. The amount of dsDNA and ssDNA was high and showed the highest chance of obtaining information (Table 3). The assembled dsDNA virome of *B. pondensis* LVF1 comprises 13 (winter season) and 334 (summer season) contigs. The winter and summer season ssDNA viromes contained 16 and 134 contigs, respectively. The *Brevundimonas*-associated dsRNA virome led to the assembly of only two contigs in the winter sample. Similarly, the *B. pondensis* LVF1-associated ssRNA virome also yielded only two contigs in winter and none in summer. These harbored ribosomal RNA of the host and were, therefore, contaminations.

The dsDNA metavirome associated with *S. marcescens* LVF3 led to 329 contigs for the summer season and only 26 for the winter season. The ssDNA viromes of both seasons exhibited a total of one circular contig with the same size of 39,857 bp, implying one phage associated with *Serratia* (dsDNA phage vB_SmaM-Otaku). The *S. marcescens* LVF3-associated dsRNA and ssRNA viromes led to no contigs for both seasons.

In summary, the data (Table 3) indicated that phage diversity is influenced by seasonal changes. Our results suggested that the phage diversity was higher in summer than in winter and that dsDNA phages were the dominant group associated to the hosts in the environment.

Virome entities not covered by phage isolates

To investigate which proportion of the viromes matched our isolates (Table 3), we compared the contigs from the host-associated viromes to genomes of the viral isolates at sequence level. For the winter season of the LVF1-associated dsDNA virome, all contigs matched our isolates, meaning the isolation was holistic, and we did not miss any individual phage. In contrast, 322 of 334 contigs of the summer season revealed similarity to our phages, and remaining 12 contigs were unique. Six of these contigs were determined as phage-associated using VIBRANT analysis (Kieft et al., 2020). The other six contigs were sample-specific (sequences only present in the sample without being phage-associated). Contigs not associated with our isolates indicated a diversity of close-related phages.

Investigation of the potential protein-encoding genes predicted from the unique contigs revealed similarities to DNA primases, phage terminases (large subunit), minor tail proteins, tail tip proteins, tail assembly proteins and putative baseplate hub proteins, DNA ligases and DNA polymerases (Supplementary Data File S1). Thus, these contigs were also phage-derived. For the summer season of the *S. marcescens* LVF3-associated dsDNA virome, 183 of the 329 non-circular contigs were not associated with our isolates. One hundred eighty of these contigs were phage-associated, and one of circular contigs implied a complete phage genome. The remaining two contigs were sample-specific. Noteworthy, some of the phage-associated contigs revealed sequence similarity to known phages associated with *Cronobacter*, *Erwinia*, *Escherichia*, *Salmonella*, and *Pseudomonas* (Supplementary Data File S2), implying a broad host range. In contrast, 13 of 26 contigs of the winter season revealed similarity to our phages, and 13 remained unique. We observed protein-encoding genes similar to tail tube proteins, putative virion structural proteins, DNA primases, ATP-dependent helicase, viral DNA polymerases, putative tail sheath protein and DNA ligase. The 13 unique contigs of the winter virome encoded putative virion structural proteins, DNA polymerase, major capsid protein, helicase, and putative tail sheath protein (Supplementary Data File S1).

To analyze the isolated viral fraction, we investigated the proportion of the sequences associated with our isolates (Figure 4).

Phage isolates associated with *B. pondensis* LVF1 comprised 67.4% of the dsDNA reads of the summer season and 96.1% of the winter season, whereas dsDNA reads of *S. marcescens* LVF3 comprised 76.4 and 94.0% of the summer and winter season, respectively. Both results revealed the main fraction of the dsDNA virome was successfully addressed by the overlay plaque assay. To analyze the presence of known but not isolated phages, we also mapped the reads on the genomes of related phages obtained from GenBank (accessed on 20 Jan 2022; Supplementary Tables S2–S5). The phage diversity seemed to be highest for *B. pondensis* LVF1 and *S. marcescens* LVF3 during the summer season. The dominant phage for LVF1 was vB_BpoS-Domovoi (24.6%), while during the winter season, this phage is barely detectable (1.0%). In contrast, vB_BpoS-Bambus was in summer almost absent (2.1%), while in winter dominant (62.9%). Phage diversity in the summer season of the *S. marcescens* virome was also high. The three dominant phages in the summer season were vB_SmaM-Otaku (18.9%), vB_SmaM-Sureiya (16.6%) and vB_SmaM-Yubaba (18.6%). In the winter season, vB_SmaM-Otaku (81.6%) was the prominent phage isolate, followed by vB_SmaM-Kashira (8.7%). The dsDNA viromes associated with LVF3 contained known *Serratia* phages, which were not isolated. These comprised 2050HW (2%), BUCT660 (2%), Moabite (1.6%), vB_SmaM_Hyamo (1.6%), vB_SmaM_Yaphecito (2.2%) and Tsm2 (2.0%).

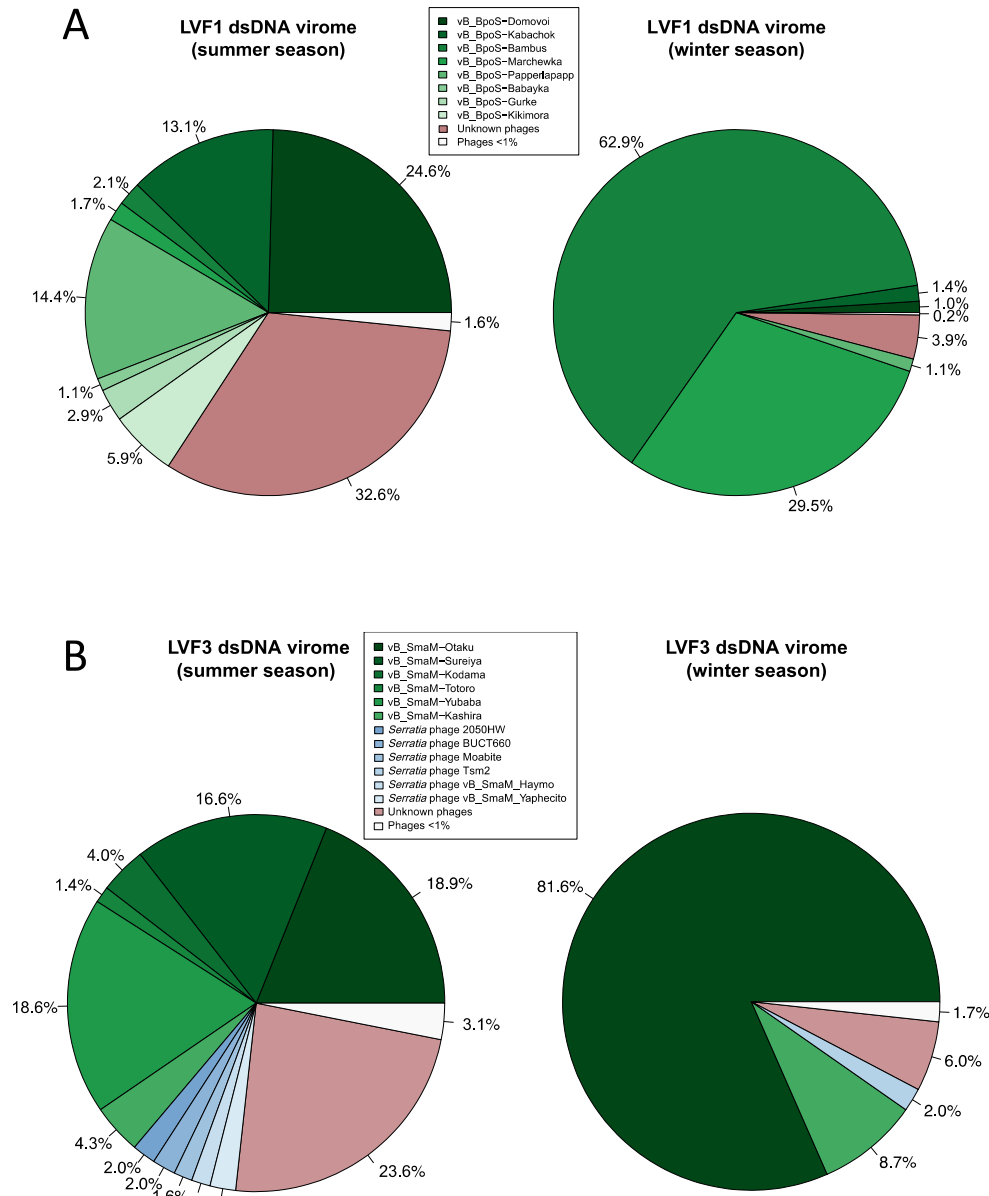


Figure 4. Mapping of viromes against all bacteriophage genomes available from NCBI as well our phage genomes from the isolates. (A) Pie chart of *B. pondensis* LVF1-associated dsDNA virome showing mapping against bacteriophage genomes associated with the family *Caulobacteraceae*. (B) Pie chart of *S. marcescens* LVF3-associated dsDNA virome depicting mapping against bacteriophage genomes associated with the genus *Serratia*. Number of mapped reads in relation to overall alignment is in percent. Visualized using RStudio (RStudio Team, 2020).

We conclude from the dsDNA virome results that we can efficiently isolate dsDNA phages using the plaque overlay method. However, depending on the sample, a considerable diversity remains unavailable, but we isolated the majority of the dominant phages.

A phage from the dsDNA virome

Virome contigs not belonging to the isolates could be assembled into a circular unit. Thus, it likely represents a complete phage genome, which provides a chance to isolate the respective phage from the remaining sample. In this way, phage vB_SmaP-Kaonashi (41,649 bp) (Figure 2) was identified through a specific PCR screening applied on various subsequently generated plaques and successfully isolated (Tables 1, 2). This example highlights the great potential of accompanying host-associated metavirome analysis.

A broad host dsDNA phage isolate

One of the frequent circular contigs associated with both host systems – *B. pondensis* and *S. marcescens* was phage vB_SmaM-Otaku (39,857 bp). We observed its presence in the *B. pondensis* LVF1 dsDNA virome of the summer season. We were able to isolate and characterize the phage genomically and morphologically. Through several reinfections via Overlay Plaque Assay of *S. marcescens* with vB_SmaM-Otaku, we received a pure phage isolate. A PCR screening confirmed its presence in the *B. pondensis*-associated metaviral sample as well. An infection of *B. pondensis* with the purified vB_SmaM-Otaku confirmed the ability of a broad-host infection as we could confirm its presence by revealing unequivocal plaques on an overlay assay (data not shown) and through PCR screening. Therefore, we concluded that vB_SmaM-Otaku is not a contamination, it is a phage with a broad host range.

ssDNA and RNA-associated viromes

Since we have not been able to isolate phages other than dsDNA, viromes based on a distinct nucleic acid are of particular interest. For the 17 ssDNA *B. pondensis* LVF1 virome-associated contigs from the winter season, all contigs did align to known dsDNA phages vB_BpoS-MaInes and vB_BpoS-StAshley. For the summer season, 115 of 134 contigs showed sequence similarity to known dsDNA phages.

Of the remaining 18 unique contigs, 14 were predicted as phage-associated. Some revealed sequence similarity to *Acinetobacter*- (contig 1) and *Bacillus*-associated (contigs 58 and 71) phages, but also to a *Siphoviridae* sp. isolate ctfaf4 (contig 74) and unknown bacteriophage sp. isolate ctu5M1 (contig 106). Some of the phage-associated contigs had no Blastn hits, although VIBRANT predicted some of them to be phage-associated (contigs 119, 162, and 289) containing genes coding for typical phage proteins such as portal protein, tail sheath protein,

DNA ligase and terminase. Seven of the unique contigs (contig 148, 167, 494, 634, 638, 700 and 707) were sample-specific. Also, the prediction of functional protein domains of the annotated genes resulted in the closest hit with e.g., 30% sequence identity with a DNA gyrase subunit B from *Bacillus* phage SP-15. The highest amino acid sequence identity (50%) of a protein sequence derived from the contig was to a hypothetical protein from vB_BpoS-Kikimora.

Noteworthy, we could identify high sequence similarity of contig 666 to *Microviridae* sp. isolate ctwNz7 (Figure 5A) and of contigs 178 and 225 to *Inoviridae* sp. isolate ctJk8/ctDT74 (Figure 5B,C). These two phage families use ssDNA as genomic material. Predicted proteins derived from the ssDNA contigs (*Inoviridae* and *Microviridae* hits) were similar to coat proteins, attachment proteins, RstB proteins and replication initiation proteins.

Thus, although our virome ssDNA preparation was imperfect and contained dsDNA fragments, we were able to detect the presence of ssDNA phages

Unfortunately, we could not confirm any RNA-associated contigs either from the dsRNA or the ssRNA sequence data independently from the season. Due to the low amount of dsRNA and the small number of reads that could be passed down after sequencing, these findings suggest no presence or a reduced presence of dsRNA phages that could not be replicated under the given circumstances. That also applies to the ssRNA virome. Besides the *Brevundimonas*-associated ssRNA virome from the summer season, which revealed the presence of host RNA, the remaining ssRNA viromes showed a low ssRNA amount.

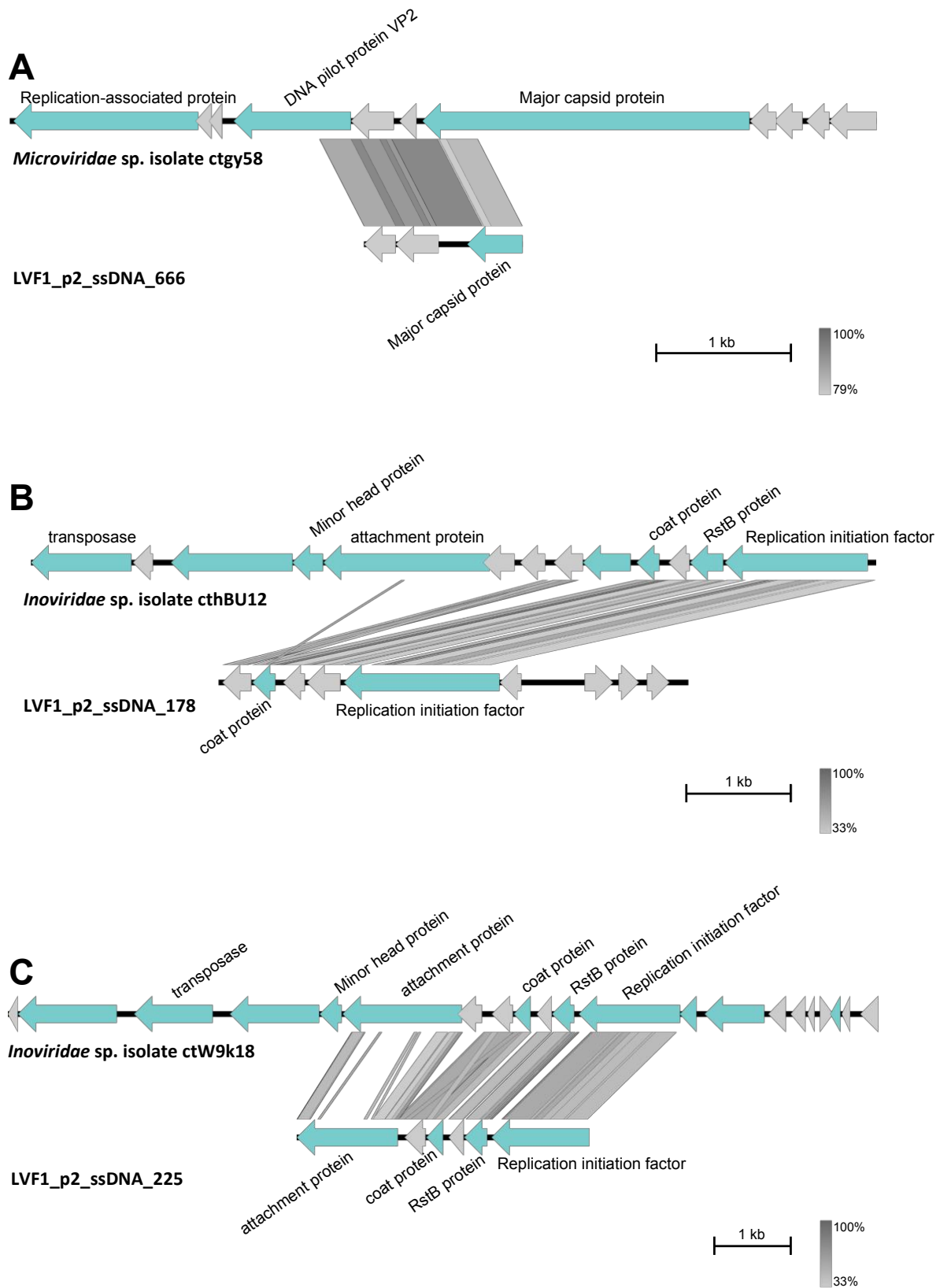


Figure 5. Comparison of the contigs with best Blastn matches. Arrow indicates gene direction. Phage specific gene products are shown in light blue with corresponding labeling, hypothetical proteins in light grey. Comparison of (A) contig 666 with *Microviridae* sp. isolate ctgy58, (B) contig 178 with *Inoviridae* sp. isolate cthBU12 and (C) contig 225 with *Inoviridae* sp. isolate ctW9k18. Plot was created with Easyfig (Sullivan et al., 2011).

Table 3. dsDNA, dsRNA, ssDNA and ssRNA viromes. LVF1_p1 stands for the virome associated with *Brevundimonas pondensis* LVF1 from January 2019, while LVF1_p2 is from July 2019. LVF3_p1 stands for the virome associated with *Serratia marcescens* LVF3 from July 2019, while LVF3_p2 is from January 2020. An overview of number of reads after host removal, number of bases [bp], the average length of sequences, number of contigs (consensus region of DNA after Unicycler assembly and further decontamination), unique and circular contigs (all contigs which do not map with isolates and might be circular), unique and circular associated with our host systems (contigs which show sequence-similarity with other *Brevundimonas*-, *Caulobacter*- and *Serratia*-associated phages and are unique), unique and non-circular associated with our host systems contigs (same as before but with non-circular contigs), and sample-specific contigs (closest Blastp and VIBRANT results reveal non-phage associated contigs) are listed.

Virome	Number of reads after host removal	Number of bases [bp]	Average length of sequences (N50)	Number of contigs	Unique contigs	Unique and circular contigs	Unique and circular contigs phage-associated	Unique and non-circular contigs phage-associated	Sample-specific contigs
LVF1_p1_dsDNA	2,258,351	355,765	238,301	13	0	0	0	0	0
LVF1_p1_ssDNA	833,717	165,362	29,017	16	0	0	0	0	0
LVF1_p1_dsRNA	679	2,600	1,423	2	0	0	0	0	0
LVF1_p1_ssRNA	3,201,470	3,273	2,194	2	0	0	0	0	0
LVF1_p2_dsDNA	1,780,267	1,743,018	8,002	334	12	0	0	6	6
LVF1_p2_ssDNA	733,624	2,823,776	5,508	134	18	0	0	14	4
LVF1_p2_dsRNA	175,323	0	0	0	0	0	0	0	0
LVF1_p2_ssRNA	2,181,863	7,235	2,789	0	0	0	0	0	0
LVF3_p1_dsDNA	2,916,604	2,047,018	10,104	329	183	1	1	180	2
LVF3_p1_ssDNA	2,372,672	39,857	5,508	1	0	0	0	0	0
LVF3_p1_dsRNA	50,454	7,800	2,324	0	0	0	0	0	0
LVF3_p1_ssRNA	40,012	7,436	2,310	0	0	0	0	0	0
LVF3_p2_dsDNA	2,913,723	273,795	39,857	26	13	0	0	13	0
LVF3_p2_ssDNA	2,391,113	39,857	39,857	1	0	0	0	0	0
LVF3_p2_dsRNA	30,299	7,235	1,460	0	0	0	0	0	0
LVF3_p2_ssRNA	34,970	9,759	2,036	0	0	0	0	0	0

Discussion

Host system selection

The bacterial strains *Brevundimonas* and *Serratua* were associated with diverse DNA and RNA viruses. Fukuda et al. successfully isolated dsDNA giant phage (Cp34) associated with *Caulobacter crescentus* (Fukuda et al., 1976). In addition, RNA phages were isolated by the group around the same time (Miyakawa et al., 1976). The ssDNA phage X174 (Sanger et al., 1977), dsDNA phage T7 (Demerec and Fano, 1945) and ssRNA phage MS2 (Davis et al., 1961) are associated with the genus *Escherichia*. Given the taxonomic proximity of *Serratia* to *Escherichia* and *Brevundimonas* to *Caulobacter*, we anticipated high viral diversity associated with *B. pondensis* LVF1 and *S. marcescens* LVF3. The preference for our host over established host systems was to ensure that, even when phage diversity was low, the isolated phages would likely be unique and contribute to viral diversity exploitation.

From our 25 isolates, five of the *Caulobacteraceae*-associated phages and seven of the *Serratia*-associated phages belong to new genera, underlining that there is still much to discover even with classical methods by employing new prokaryotic host systems. These comprised *Brevundimonas*-associated phages vB_BpoS-Strzyga, vB_BpoS-Polewnik, vB_BpoS-StAshley, vB_BpoS-MaInes, and vB_BpoS-Babayka. All five belonged to the same genus. In the case of vB_SmaP-Kaonashi, vB_SmaS-ChuuTotoro, vB_SmaM-Kashira, vB_SmaS-ChibiTotoro, vB_SmaS-Susuwatari, vB_SmaM-Yubaba, and vB_SmaM-Sureiya were distributed over four new phage genera. In comparison, no new viral genus of *Escherichia* phages has been described for decades to our knowledge. We were particularly surprised by the high number of jumbo and giant phages among the new isolates. Although jumbo phages like 2012-1 (Thomas et al., 2008) and CcrColossus (Gill et al., 2012) for the host systems *Pseudomonas* and *Caulobacter* as well as giant phages PA5oct and pEa_SNUABM_44 (Drulis-Kawa et al., 2014; Kim et al., 2020) for *Pseudomonas* and *Erwinia* host systems have already been described, these phages have rarely been observed, especially in model host systems despite various attempts (Schilling et al., 2018a, 2018b; Nordmann et al., 2019; Furrer et al., 2020). For example, only two species of jumbo phages were known to be associated with the model organism *Bacillus subtilis*, including the group of PBS1-like phages represented by the isolates PBS1 (Eiserling, 1967) and AR9 (Lavysh et al., 2016), and SP10. The latter has never been reisolated for more than half a century.

The reasons for the success in employing our host systems for the isolation of large phages are unknown. Nevertheless, it is evident that the slow-growing *B. pondensis* LVF1 (Friedrich et al., 2021b) led to the isolation of jumbo and giant phages rather than the faster-growing *S. marcescens* LVF3 (Friedrich et al., 2021a). The growth characteristics of LVF3 were very similar to that of the *Escherichia coli* model, and the isolated phage vB_SmaS-ChibiTotoro and vB_SmaS-Susuwatari also strongly resemble the known *Escherichia* phage Lambda morphologically and genomically (King et al., 2012c). Thus, we assume that host systems with slower growth rate give the larger phages more time to reproduce with their prolonged vegetative period and lead to a visible plaque on agar plates. We are unaware that phage isolation was tried on minimal media with established model host systems. Bacteria growth is at a much lower rate on minimal media, which prolongs the vegetative phases. Thus, it would be interesting to explore such conditions for the isolation of jumbo and giant phages of model host systems such as *E. coli*, *B. subtilis* and our *S. marcescens*.

We demonstrated that the overlay assay was able to grasp most of the viral dsDNA diversity. We could isolate most of the bacteriophages associated with both host strains, as confirmed by the host-associated metavirome data. Nevertheless, differences between the host systems were encountered and a seasonal impact was indicated. Further, we showed that *S. marcescens*-associated virome contained many phage-associated contigs, which are not part of the known phages infecting the *Yersiniaceae* family. These were *Erwinia*-, *Salmonella*- or *Cronobacter*-associated phages. They might not efficiently infect *S. marcescens*, but *S. marcescens*-associated phages show a broad host spectrum, i.e. the *Serratia* phage vB_SmaM-Otaku, which is able to infect *B. pondensis* (lysis was observed). Accordingly, *Serratia* phages are often able to infect related genera (Prinsloo and Coetzee, 1964; Prinsloo, 1966; Evans et al., 2010).

Viromes reveal a plethora of undetected host-associated phages

The dsDNA virome analysis showed that isolation with a classical plaque assay is very efficient and allows the recovery of the main present viral diversity. However, the complementary isolation of phages not initially detected demonstrated the value of accompanying host-associated metavirome analysis. For example, phage vB_SmaP-Kaonashi could only be isolated after identification in the corresponding virome dataset. Noteworthy, an important outcome of virome analysis was the identification of an isolate with a broad host

range. The alignment of reads against a foreign host system led to the identification of vB_SmaM-Otaku, which experimentally proved to infect both *B. pondensis* LVF1 and *S. marcescens* LVF3 successfully.

The low concentration of ssDNA and the with dsDNA contaminated ssDNA virome sequences imply that only very few ssDNA phages were present in our samples; thereby explaining the lack of isolates. However, this would be too simplistic. Note that classical isolation methods fundamentally discriminate against this group of phages. *Inoviridae* infections are not lethal and do not necessarily lead to a visible plaque, which is necessary to identify and isolate a phage. In addition, we were able to detect *Microviridae*-like phages using TEM of the host-associated virome sample from the summer season (data not shown). These were round and non-tailed with an icosahedral symmetry and a diameter of roughly 30 nm. Further, we were also able to detect filamentous structures (*Inoviridae*-like) in the metaviral sample. Nevertheless, ssDNA virome analysis has demonstrated that at least the *B. pondensis* LVF1 system is associated with *Microviridae* and *Inoviridae*. Thus, new or specifically optimized experimental approaches will be required to access these phages.

The situation is similar with RNA phages, and we have not succeeded in obtaining RNA phage isolates or virome-derived RNA phage sequences with both host systems. The nucleic acid amount of the dsRNA and ssRNA virome was low, except for the *B. pondensis* ssRNA virome from summer season. Further analysis confirmed contamination with ribosomal host RNA. An optimization of the methodology would be needed by getting rid of the host RNA and DNA. In addition, compared to DNA phages, RNA phages are much smaller regarding their genomic size (ssRNA phages 3,5–4,3 kb (King et al., 2012b) and dsRNA phages 12.7–15.0 kb (King et al., 2012a)). Therefore, we would suspect a higher DNA to RNA base ratio. Further, virome samples typically represent low-abundance viruses better than intracellular viral genomes such as non-replicating proviruses and virocells (Howard-Varona et al., 2020).

Again, we conclude that there is a need for novel approaches to access this realm of viral diversity rather than RNA phages being not associated with our hosts. Nevertheless, in a different study with *B. goettingensis*, we were able to discover the genome of an ssRNA phage of the *Leviviridae* family with the same nucleic acid isolation procedure (Friedrich et al., unpublished results).

Conclusion

We showed that the classical phage isolation methodology still bears great potential to detect organismic and genetic phage diversity as we were able to isolate 14 *Brevundimonas*- and 11 *Serratia*-associated phages. While the morphological and genomic diversity of *Serratia*-associated phages appears to be greater than that of *Brevundimonas*, the *Brevundimonas*-associated virome revealed other phage genome types, e.g., ssDNA phages. Nevertheless, the classical method has its limitations such as only the isolation of particle-protected phages. The range of host-associated phages can be expanded by complementation with sequencing-based metavirome analysis approaches, but the limitations cannot be entirely solved by employing these strategies.

Data Availability Statement

The genomes of the bacteriophages can be accessed at GenBank under the following accession numbers. Papperlapapp (ON529860), Kabachok (ON529852), Domovoi (ON529855), Marchewka (ON529851), Bambus (ON529853), Gurke (ON529850), Kikimora (ON529857), Poludnitsa (ON529862), Leszy (ON529856), StAshley (ON529865), MaInes (ON529866), Strzyga (ON529867), Polewnik (ON529863), Babayka (ON529868), Totoro (ON287372), Kodama (ON287376), Sureiya (ON287370), Yubaba (ON287375), ChuuTotoro (ON287369), Kashira (ON287374), Kamaji (ON287373), ChibiTotoro (ON287368), Susuwatari (ON287371), Kaonashi (ON287377), Otaku (ON087563).

The Sequence Read Archive (SRA) accessions of the viromes can be found under the BioProject accession number PRJNA837383 at NCBI (SRA accession numbers SRR19221870–SRR19221885). In addition, the 32 zipped FASTQ files are included in the BioProject.

Acknowledgements

We thank Melanie Heinemann for technical assistance.

References

- Adriaenssens, E., and Brister, J. R. (2017). How to name and classify your phage: An informal guide. *Viruses* 9, 70. doi: 10.3390/v9040070.
- Altschul, S. (1997). Gapped BLAST and PSI-BLAST: A new generation of protein database search programs. *Nucleic Acids Research* 25, 3389–3402. doi: 10.1093/nar/25.17.3389.

- Altschul, S. F., Gish, W., Miller, W., Myers, E. W., and Lipman, D. J. (1990). Basic local alignment search tool. *J. Mol. Biol.* 215, 403–10. doi: 10.1016/S0022-2836(05)80360-2.
- Arnold, K., Gosling, J., and Holmes, D. (2005). *The Java programming language*. 4th ed. Lebanon, Indiana, USA: Addison-Wesley Professional.
- Aziz, R. K., Bartels, D., Best, A. A., DeJongh, M., Disz, T., Edwards, R. A., et al. (2008). The RAST Server: Rapid Annotations using Subsystems Technology. *BMC Genom.* 9, 75. doi: 10.1186/1471-2164-9-75.
- Bankevich, A., Nurk, S., Antipov, D., Gurevich, A. A., Dvorkin, M., Kulikov, A. S., et al. (2012). SPAdes: A new genome assembly algorithm and its applications to single-cell sequencing. *J Comput Biol* 19, 455–477. doi: 10.1089/cmb.2012.0021.
- Benson, D. A., Cavanaugh, M., Clark, K., Karsch-Mizrachi, I., Lipman, D. J., Ostell, J., et al. (2017). GenBank. *Nucleic Acids Res.* 45, D37–D42. doi: 10.1093/nar/gkw1070.
- Besemer, J., Lomsadze, A., and Borodovsky, M. (2001). GeneMarkS: A self-training method for prediction of gene starts in microbial genomes. Implications for finding sequence motifs in regulatory regions. *Nucleic Acids Res* 29, 2607–2618. doi: 10.1093/nar/29.12.2607.
- BLAST® Command Line Applications User Manual [Internet] (2019). Available at: <https://www.ncbi.nlm.nih.gov/books/NBK279690/> [Accessed November 20, 2020].
- Bolger, A. M., Lohse, M., and Usadel, B. (2014). Trimmomatic: A flexible trimmer for Illumina sequence data. *Bioinformatics* 30, 2114–2120. doi: 10.1093/bioinformatics/btu170.
- Borodovsky, M., and McIninch, J. (1993). GENMARK: Parallel gene recognition for both DNA strands. *Comput. Chem.* 17, 123–133. doi: 10.1016/0097-8485(93)85004-V.
- Brister, J. R., Ako-Adjei, D., Bao, Y., and Blinkova, O. (2015). NCBI viral genomes resource. *Nucleic Acids Res.* 43, D571–D577. doi: 10.1093/nar/gku1207.
- Camacho, C., Coulouris, G., Avagyan, V., Ma, N., Papadopoulos, J., Bealer, K., et al. (2009). BLAST+: architecture and applications. *BMC Bioinform* 10, 421. doi: 10.1186/1471-2105-10-421.
- Carding, S. R., Davis, N., and Hoyles, L. (2017). Review article: the human intestinal virome in health and disease. *Aliment Pharmacol Ther* 46, 800–815. doi: 10.1111/apt.14280.
- Casas, V., and Rohwer, F. (2007). “Phage Metagenomics,” in *Methods in Enzymology* (Elsevier), 259–268. doi: 10.1016/S0076-6879(06)21020-6.
- Davis, J. E., Sinsheimer, R. L., and Strauss, J. H. (1961). Bacteriophage MS2-another RNA phage. *Amer Assoc Advancement Science* 134, 1427.
- Delcher, A. L., Bratke, K. A., Powers, E. C., and Salzberg, S. L. (2007). Identifying bacterial genes and endosymbiont DNA with Glimmer. *Bioinformatics* 23, 673–679. doi: 10.1093/bioinformatics/btm009.
- Demerec, M., and Fano, U. (1945). Bacteriophage-resistant mutants in *Escherichia coli*. *Genetics* 30, 119–136. doi: 10.1093/genetics/30.2.119.
- Dion, M. B., Oechslin, F., and Moineau, S. (2020). Phage diversity, genomics and phylogeny. *Nat Rev Microbiol* 18, 125–138. doi: 10.1038/s41579-019-0311-5.
- Drulis-Kawa, Z., Olszak, T., Danis, K., Majkowska-Skrobek, G., and Ackermann, H.-W. (2014). A giant *Pseudomonas* phage from Poland. *Arch Virol* 159, 567–572. doi: 10.1007/s00705-013-1844-y.
- Eiserling, F. A. (1967). The structure of *Bacillus subtilis* bacteriophage PBS 1. *J. Ultrastruct. Res.* 17, 342–347. doi: 10.1016/S0022-5320(67)80053-4.

- Evans, T. J., Crow, M. A., Williamson, N. R., Orme, W., Thomson, N. R., Komitopoulou, E., et al. (2010). Characterization of a broad-host-range flagellum-dependent phage that mediates high-efficiency generalized transduction in, and between, *Serratia* and *Pantoea*. *Microbiology* 156, 240–247. doi: 10.1099/mic.0.032797-0.
- Friedrich, I., Bodenberger, B., Neubauer, H., Hertel, R., and Daniel, R. (2021a). Down in the pond: Isolation and characterization of a new *Serratia marcescens* strain (LVF3) from the surface water near frog's lettuce (*Groenlandia densa*). *PLOS ONE* 16, e0259673. doi: 10.1371/journal.pone.0259673.
- Friedrich, I., Klassen, A., Neubauer, H., Schneider, D., Hertel, R., and Daniel, R. (2021b). Living in a puddle of mud: Isolation and characterization of two novel *Caulobacteraceae* strains *Brevundimonas pondensis* sp. nov. and *Brevundimonas goettingensis* sp. nov. *Appl Microbiol* 1, 38–59. doi: 10.3390/applmicrobiol1010005.
- Fukuda, A., Miyakawa, K., Iba, H., and Okada, Y. (1976). A flagellotropic bacteriophage and flagella formation in *Caulobacter*. *Virology* 71, 583–592. doi: 10.1016/0042-6822(76)90383-4.
- Furrer, A. D., Bömeke, M., Hoppert, M., and Hertel, R. (2020). Phage vB_BveM-Goe7 represents a new genus in the subfamily *Bastillevirinae*. *Arch Virol* 165, 959–962. doi: 10.1007/s00705-020-04546-1.
- Garmaeva, S., Sinha, T., Kurilshikov, A., Fu, J., Wijmenga, C., and Zhernakova, A. (2019). Studying the gut virome in the metagenomic era: challenges and perspectives. *BMC Biol* 17, 84. doi: 10.1186/s12915-019-0704-y.
- Gill, J. J., Berry, J. D., Russell, W. K., Lessor, L., Escobar-Garcia, D. A., Hernandez, D., et al. (2012). The *Caulobacter crescentus* phage phiCbK: genomics of a canonical phage. *BMC Genom.* 13, 542. doi: 10.1186/1471-2164-13-542.
- Howard-Varona, C., Lindback, M. M., Bastien, G. E., Solonenko, N., Zayed, A. A., Jang, H., et al. (2020). Phage-specific metabolic reprogramming of virocells. *ISME J* 14, 881–895. doi: 10.1038/s41396-019-0580-z.
- Hyatt, D., Chen, G.-L., LoCascio, P. F., Land, M. L., Larimer, F. W., and Hauser, L. J. (2020). Prodigal: prokaryotic gene recognition and translation initiation site identification. *BMC Bioinform.* 11, 119. doi: 10.1186/1471-2105-11-119.
- Kieft, K., Zhou, Z., and Anantharaman, K. (2020). VIBRANT: Automated recovery, annotation and curation of microbial viruses, and evaluation of viral community function from genomic sequences. *Microbiome* 8, 90. doi: 10.1186/s40168-020-00867-0.
- Kim, S., Lee, S., Giri, S., Kim, H., Kim, S., Kwon, J., et al. (2020). Characterization of novel *Erwinia amylovora* jumbo bacteriophages from *Eneladusvirus* genus. *Viruses* 12, 1373. doi: 10.3390/v12121373.
- King, A. M. Q., Adams, M. J., Carstens, E. B., and Lefkowitz, E. J. eds. (2012a). "Family - *Cystoviridae*," in *Virus Taxonomy* (San Diego, CA, USA: Elsevier), 515–518. doi: 10.1016/B978-0-12-384684-6.00047-1.
- King, A. M. Q., Adams, M. J., Carstens, E. B., and Lefkowitz, E. J. eds. (2012b). "Family - *Leviviridae*," in *Virus Taxonomy* (San Diego, CA, USA: Elsevier), 1035–1043. doi: 10.1016/B978-0-12-384684-6.00089-6.
- King, A. M. Q., Adams, M. J., Carstens, E. B., and Lefkowitz, E. J. eds. (2012c). "Family - *Siphoviridae*," in *Virus Taxonomy* (San Diego, CA, USA: Elsevier), 86–98. doi: 10.1016/B978-0-12-384684-6.00004-5.
- Kohm, K., Floccari, V. A., Lutz, V. T., Nordmann, B., Mittelstädt, C., Poehlein, A., et al. (2022). The *Bacillus* phage SPβ and its relatives: A temperate phage model system reveals new strains, species, prophage integration loci, conserved proteins and lysogeny management components. *Environ. Microbiol.* 24, 2098–2118. doi: 10.1111/1462-2920.15964.
- Kropinski, A. M., Mazzocco, A., Waddell, T. E., Lingohr, E., and Johnson, R. P. (2009). Enumeration of bacteriophages by double agar overlay plaque assay. *Methods Mol Biol* 501, 69–76. doi: 10.1007/978-1-60327-164-6_7.

- Langmead, B., and Salzberg, S. L. (2012). Fast gapped-read alignment with Bowtie 2. *Nat Methods* 9, 357–359. doi: 10.1038/nmeth.1923.
- Laslett, D., and Canback, B. (2004). ARAGORN, a program to detect tRNA genes and tmRNA genes in nucleotide sequences. *Nucleic Acids Res* 32, 11–16. doi: 10.1093/nar/gkh152.
- Lavysch, D., Sokolova, M., Minakhin, L., Yakunina, M., Artamonova, T., Kozyavkin, S., et al. (2016). The genome of AR9, a giant transducing *Bacillus* phage encoding two multisubunit RNA polymerases. *Virology* 495, 185–196. doi: 10.1016/j.virol.2016.04.030.
- Lazeroff, M., Ryder, G., Harris, S. L., and Tsourkas, P. K. (2021). Phage commander, an application for rapid gene identification in bacteriophage genomes using multiple programs. *Phage* 2, 204–213. doi: 10.1089/phage.2020.0044.
- Li, H., Handsaker, B., Wysoker, A., Fennell, T., Ruan, J., Homer, N., et al. (2009). The sequence alignment/map format and SAMtools. *Bioinformatics* 25, 2078–2079. doi: 10.1093/bioinformatics/btp352.
- Lomsadze, A., Gemayel, K., Tang, S., and Borodovsky, M. (2018). Modeling leaderless transcription and atypical genes results in more accurate gene prediction in prokaryotes. *Genome Res.* 28, 1079–1089. doi: 10.1101/gr.230615.117.
- Magoč, T., and Salzberg, S. L. (2011). FLASH: Fast length adjustment of short reads to improve genome assemblies. *Bioinformatics* 27, 2957–2963. doi: 10.1093/bioinformatics/btr507.
- Miyakawa, K., Fukuda, A., Okada, Y., Furuse, K., and Watanabe, I. (1976). Isolation and characterization of RNA phages for *Caulobacter crescentus*. *Virology* 73, 461–467. doi: 10.1016/0042-6822(76)90407-4.
- Noguchi, H., Park, J., and Takagi, T. (2006). MetaGene: Prokaryotic gene finding from environmental genome shotgun sequences. *Nucleic Acids Res.* 34, 5623–5630. doi: 10.1093/nar/gkl723.
- Nordmann, B., Schilling, T., Hoppert, M., and Hertel, R. (2019). Complete genome sequence of the virus isolate vB_BthM-Goe5 infecting *Bacillus thuringiensis*. *Arch Virol* 164, 1485–1488. doi: 10.1007/s00705-019-04187-z.
- Okonechnikov, K., Conesa, A., and García-Alcalde, F. (2016). Qualimap 2: Advanced multi-sample quality control for high-throughput sequencing data. *Bioinformatics* 32, 292–294. doi: 10.1093/bioinformatics/btv566.
- Parks, D. H., Chuvochina, M., Chaumeil, P. A., Rinke, C., Mussig, A. J., and Hugenholtz, P. (2019). Selection of representative genomes for 24,706 bacterial and archaeal species clusters provide a complete genome-based taxonomy. *bioRxiv*. doi: 10.1101/771964.
- Principi, N., Silvestri, E., and Esposito, S. (2019). Advantages and limitations of bacteriophages for the treatment of bacterial infections. *Front Pharmacol* 10, 513. doi: 10.3389/fphar.2019.00513.
- Prinsloo, H. E. (1966). Bacteriocins and phages produced by *Serratia marcescens*. *J Gen Microbiol* 45, 205–212. doi: 10.1099/00221287-45-2-205.
- Prinsloo, H. E., and Coetzee, J. N. (1964). Host-range of temperate *Serratia marcescens* bacteriophages. *Nature* 203, 211. doi: 10.1038/203211a0.
- Pritchard, L., Glover, R. H., Humphris, S., Elphinstone, J. G., and Toth, I. K. (2016). Genomics and taxonomy in diagnostics for food security: Soft-rotting enterobacterial plant pathogens. *Anal Methods* 8, 12–24. doi: 10.1039/c5Ay02550h.
- RStudio Team (2020). RStudio: Integrated development for R. Available at: <http://www.rstudio.com/>.
- Sanger, F., Air, G. M., Barrell, B. G., Brown, N. L., Coulson, A. R., Fiddes, J. C., et al. (1977). Nucleotide sequence of bacteriophage ϕ X174 DNA. *Nature* 265, 687–695. doi: 10.1038/265687a0.

-
- Schilling, T., Hoppert, M., Daniel, R., and Hertel, R. (2018a). Complete genome sequence of vB_BveP-Goe6, a virus infecting *Bacillus velezensis* FZB42. *Genome Announc* 6, e00008-18. doi: 10.1128/genomeA.00008-18.
- Schilling, T., Hoppert, M., and Hertel, R. (2018b). Genomic analysis of the recent viral isolate vB_BthP-Goe4 reveals increased diversity of ϕ 29-like phages. *Viruses* 10, 624. doi: 10.3390/v10110624.
- Sullivan, M. J., Petty, N. K., and Beatson, S. A. (2011). Easyfig: A genome comparison visualizer. *Bioinformatics* 27, 1009–1010. doi: 10.1093/bioinformatics/btr039.
- Thomas, J. A., Rolando, M. R., Carroll, C. A., Shen, P. S., Belnap, D. M., Weintraub, S. T., et al. (2008). Characterization of *Pseudomonas chlororaphis* myovirus 201 ϕ 2-1 via genomic sequencing, mass spectrometry, and electron microscopy. *Virology* 376, 330–338. doi: 10.1016/j.virol.2008.04.004.
- Walker, B. J., Abeel, T., Shea, T., Priest, M., Abouelliel, A., Sakthikumar, S., et al. (2014). Pilon: An integrated tool for comprehensive microbial variant detection and genome assembly improvement. *PLoS ONE* 9, e112963. doi: 10.1371/journal.pone.0112963.
- Wick, R. R., Judd, L. M., Gorrie, C. L., and Holt, K. E. (2017). Unicycler: Resolving bacterial genome assemblies from short and long sequencing reads. *PLoS Comput Biol* 13, 1–22. doi: 10.1371/journal.pcbi.1005595.
- Zdobnov, E. M., and Apweiler, R. (2001). InterProScan - An integration platform for the signature-recognition methods in InterPro. *Bioinformatics* 17, 847–848. doi: 10.1093/bioinformatics/17.9.847.
- Zhang, Z., Schwartz, S., Wagner, L., and Miller, W. (2000). A greedy algorithm for aligning DNA sequences. *J Comput Biol* 7, 203–214. doi: 10.1089/10665270050081478.
- Zhu, W., Lomsadze, A., and Borodovsky, M. (2010). *Ab initio* gene identification in metagenomic sequences. *Nucleic Acids Res.* 38, e132–e132. doi: 10.1093/nar/gkq275.
- Zrelavs, N., Dislers, A., and Kazaks, A. (2020). Motley Crew: Overview of the currently available phage diversity. *Front Microbiol* 11, 1–6. doi: 10.3389/fmicb.2020.579452.

Supplement

Supplement Data File S1. Gene annotation of phage-associated contigs. Annotation was performed using VIBRANT (Kieft et al., 2020) and Phage Commander (Lazeroff et al., 2021).

The data file can be found on the enclosed CD and .zip folder:

Supplement\Chapter_3.7\Supplement_Data_File_S1.fasta

Supplement Data File S2. DNA sequence alignment of unique contigs. Alignment was done using blastn v2.12.0+ (accessed on 17 June 2022) (Zhang et al., 2000).

The data file can be found on the enclosed CD and .zip folder:

Supplement\Chapter_3.7\Supplement_Data_File_S2.fasta

Supplement Table S1. Overview of all *Caulobacteraceae*- and *Serratia*-associated bacteriophages from the NCBI Virus database with corresponding accession numbers.

Supplement Table S2. Result of raw read mapping of all *Caulobacteraceae*-associated bacteriophages from the NCBI Virus database and own isolates for the virome of the winter season.

Supplement Table S3. Result of raw read mapping of all *Caulobacteraceae*-associated bacteriophages from the NCBI Virus database and own isolates for the virome of the summer season.

Supplement Table S4. Result of raw read mapping of all *Serratia*-associated bacteriophages from the NCBI Virus database and own isolates for the virome of the winter season.

Supplement Table S5. Result of raw read mapping of all *Serratia*-associated bacteriophages from the NCBI Virus database and own isolates for the virome of the summer season.

The tables can be found on the enclosed CD:

Supplement\Chapter_3.7\Supplement_Tables_S1-S5.xlsx

Supplement Figure S1. *B. pondensis* LVF1 and *S. marcescens* LVF3 challenged with sewage phage suspension. Different plaque morphologies can be observed.

The figure can be found on the enclosed CD and .zip folder:

Supplement\Chapter_3.7\Supplement_Figure_S1.pdf

8. Isolation and characterization of a *Janthinobacterium lividum*-associated bacteriophage and analysis of its prophage

Ines Friedrich¹, Alisa Kuritsyn¹, Hannes Neubauer¹, Robert Hertel^{1,2} and Rolf Daniel¹

*Re-submitted to FEMS Microbiology Letters on 23 September 2022
(currently under revision)*

Affiliations

¹Genomic and Applied Microbiology & Göttingen Genomics Laboratory, Institute of Microbiology and Genetics, Georg-August-University of Göttingen, Grisebachstraße 8, 37077 Göttingen, Germany

²FG Synthetic Microbiology, Institute of Biotechnology, BTU Cottbus-Senftenberg, Senftenberg, Germany

Author contributions:

Experiments: **IF**, **AK**

Visualization: **AK**, **HN**, **IF**

Revision: **RD**

Conceptualization: **IF**, **RH**, **RD**

Writing: **IF**, **RH**

Writing – review & editing: **IF**, **AK**, **NH**, **RH**, **RD**

Abstract

Janthinobacterium lividum is a species of the family *Oxalobacteraceae*, for which hardly any information on its phages is available. In the present study, we bioinformatically analyzed the *J. lividum* EIF1 prophage and experimentally confirmed its ability to form phage particles and precisely pack its viral genome. The prophage genome (41,739 bp) harbors 17 bp long attL/R sites. We could verify the integration into a serine tRNA gene. Apart from the prophage analysis, we successfully established an overlay plaque assay to isolate phages with *J. lividum* as host species and isolated and sequenced the first genome of a *J. lividum* phage named vB_JliM-Donnerlittchen. The phage is of the *Myo* morphotype with an icosahedral head (61 nm), an elongated tube, a sheath at the tube's lower part, and tail spikes (tail length is 96 nm). Its genome is 58,220 bp, containing one tRNA and 74 protein-encoding genes. The infection of *J. lividum* EIF1 with vB_JliM-Donnerlittchen triggers the release of an unknown signaling molecule, which stimulates uninfected cells to produce violacein, an antiviral substance of economic and medical relevance.

Introduction

Bacteriophages or phages are bacterial viruses that infect and replicate in bacterial cells. They are among the most diverse organisms on our planet (Casas and Rohwer 2007; Dion, Oechslin and Moineau 2020). The highest phage densities have been observed in wastewater treatment plants (WWTPs), which are 10–1000 times higher than in any other aquatic habitat (Wu and Liu 2009).

Phages depend on the metabolism of their host for replication. The host range is phage strain specific and can include single or multiple bacterial strains (Garmaeva *et al.* 2019). They can reduce the host population through direct lytic replication (lytic path) (Carding, Davis and Hoyles 2017) or integrate their genome in the host chromosome and thrive as prophage (lysogenic path) (Principi, Silvestri and Esposito 2019). As prophages, they provide additional genetic information to their hosts and can endow the host with additional features providing competitive advantages (Kohm and Hertel 2021).

This study addresses the prophages and phages associated with *Janthinobacterium lividum* EIF1, which was isolated from surface water near frog's lettuce (*Groenlandia densa*) (Friedrich *et al.* 2020, 2021b). The genus *Janthinobacterium* belongs to the family *Oxalobacteraceae*, which is part of the β -subclass Proteobacteria and includes 13 genera (Baldani *et al.* 2014). *Janthinobacterium* contains the species *J. agaricidamnorum* (Lincoln, Fermor and Tindall 1999), *J. aquaticum* (Lu *et al.* 2020), *J. lividum* (De Ley, Segers and Gillis 1978), *J. psychrotolerans* (Gong *et al.* 2017), *J. rivuli* (Lu *et al.* 2020), *J. svalbardensis* (Ambrožič Avguštin *et al.* 2013), *J. tructae* (Jung *et al.* 2021), and *J. violaceinigrum* (Lu *et al.* 2020).

Janthinobacterium members are motile, rod-shaped, and Gram-negative. They are strictly aerobic, chemoorganotrophic, and have a temperature optimum of 25–30 °C (Baldani *et al.* 2014). Members of this genus are present in soils, lakes, rainwater cisterns, or water sediments (Asencio *et al.* 2014; McTaggart *et al.* 2015; Shoemaker, Muscarella and Lennon 2015; Haack *et al.* 2016; Wu *et al.* 2017). A distinctive feature is the ability to produce a violet-purple color caused by the pigment violacein. This secondary metabolite has antimicrobial, antiviral, and antitumor properties (Andrighetti-Fröhner *et al.* 2003; Bromberg *et al.* 2010; Asencio *et al.* 2014), giving its producer organisms industrial value (Li *et al.* 2016). However, as some strains of this genus are the causing agent of agriculture-relevant mushroom (*Agaricus biosporus*) infections (Lincoln, Fermor and Tindall 1999) or pathogens of rainbow trout (*Oncorhynchus mykiss*) (Oh *et al.* 2019), biological control mechanisms, like *Janthinobacterium*-associated bacteriophages, are of interest.

To our knowledge, only one lytic *Janthinobacterium*-associated bacteriophage (MYSP06) infecting the purple pigment-producing strain *Janthinobacterium* sp. MYB06 has been isolated but not sequenced yet (Li *et al.* 2016). Thus, we investigated the environmental viral diversity associated with the *Janthinobacterium* genus and sequenced isolates.

Materials and methods

Phage isolation and prophage preparation

1 L primary treatment sewage from the municipal WWTP in Göttingen (Germany) was used as an environmental phage source. The samples were centrifuged at 6,000 × *g* for 15 min. The

supernatant with the phages was sterile-filtered, employing a 0.45 µm PES-membrane (Sarstedt AG & Co. KG, Nümbrecht, Germany). by adding polyethylene glycol in a final concentration of 10% (w/v) and 0.5 M NaCl. After incubation at 4 °C for 16 h phages were harvested by centrifugation at 10,020 x g and 4 °C for 1 h. The resulting phage pellet was solved in 25 mL PCa (0.2% peptone, 0.02% MgSO₄ x 7 H₂O, 0.015% CaCl₂ x 2 H₂O) (Friedrich *et al.* 2020). Phages were isolated via agar overlay plaque assay as described elsewhere (Kropinski *et al.* 2009) using host-specific culture media for the base agar (1.5% agarose) and overlay (0.4% agarose). Infected overlay plates were incubated overnight at 30 °C. Morphologically distinct plaques representing individual phage isolates were picked with a sterile toothpick, and each was transferred to a 500 µL sterile PCa medium. Further phage strain purification was realized three times reinfection.

For prophage preparation, an overnight culture of *J. lividum* EIF1 was set up in a 100 mL Erlenmeyer flask using 25 mL of PCa medium. The incubation and further purification and isolation steps were done as described previously (Friedrich *et al.* 2021a).

Preparation of total and specific nucleic acids

All kits and enzymes were used as recommended by the manufacturer if not otherwise stated. The MasterPure™ Complete DNA and RNA Purification kit (Lucigen, Middleton, WI, USA) were used with modifications to extract total viral nucleic acids. Due to the high protein content, we increased the amount of Proteinase K (20 mg/mL) to 5 µL in 300 µL of 2X T and C Lysis Solution, which was applied to 300 µL of phage suspension. We obtained pure viral genomic DNA by applying RNase A (DNase-free) to the prepared total nucleic acids.

Bacteriophage and prophage genome sequencing

As described previously, DNA samples were sequenced with an Illumina MiSeq-system (2 x 300 bp) (Kohm *et al.* 2022). The phage genome was annotated with VIBRANT (Kieft, Zhou and Anantharaman 2020) and InterProScan v5.55-88.0 (Zdobnov and Apweiler 2001), and data were submitted to GenBank (Benson *et al.* 2017). After Illumina MiSeq raw paired-ends were merged, adapter- and quality-trimmed, sequences were mapped against the host genome

using bowtie2 v2.4.4 (Langmead and Salzberg 2012). SAM table was converted to TDS format (input for Transcriptome Viewer (TraV)) (Dietrich, Wiegand and Liesegang 2014). Integration sites of the prophage (*attL* and *attR* sites) by comparing experimentally indicated *att* regions (1 kb to each side from the indicated coordinate), against the remaining genome sequence.

Phylogenetic classification of vB_JliS-Donnerlittchen

A phylogenetic analysis was performed with VIRIDIC v1 (Moraru, Varsani and Kropinski 2020). All available phage genomes, associated with Burkholderiales were downloaded from NCBI Virus (Brister *et al.* 2015) (downloaded on 2 Jul 2022).

Morphology

The phage morphology of the isolate was observed by transmission electron microscopy (TEM). Data were visualized using the software program digital Micrograph (Gatan GmbH, Munich, Germany). The phage isolate was amplified, and a negative staining technique was performed. Cell suspension (5 μ L) was mixed with the same amount of diluted 1% phosphotungstic acid (3% stock, pH 7.0) and was transferred to a vaporized carbon mica for 1 min. Subsequently, the mica was briefly washed in demineralized water and transferred to a thin copper-coated grid (PLANO GmbH, Marburg, Germany). The coated grids were dried at room temperature and were examined by Jeol 1011 TEM (Georgia Electron Microscopy, Freising, Germany).

Naming of the bacteriophage isolate

The isolate naming followed Adriaenssens and Brister's informal guide (Adriaenssens and Brister 2017). Accordingly, vB stands for virus of bacteria, Jli for the host organism *J. lividum*, and M for the virus family *Myo* morphotype, followed by individual naming that does not follow any pattern. Therefore, the full name of the virus is composed of vB_JliM-Donnerlittchen, abbreviated Donnerlittchen.

Determination of purple pigmentation

J. lividum EIF1 was used for the determination of purple pigmentation. For this purpose, 100 µL of EIF1 was infected with 1,000 µL of a phage suspension containing 2.86×10^5 PFU/mL, and a plaque assay was performed as described with dilutions ranging from 10^{-1} until 10^{-6} . Incubation was performed for 24 h at 30 °C. All measurements were performed in biological replicates for each phage sample.

After incubation, plates were scanned using the same settings (measurement 2193 x 2267, width 2193-pixel, length 2267-pixel, horizontal and vertical resolution 600 dpi, 48-Bit, reflective, dark background) employing an Epson scanner model Perfection 4990 Photo. Hexadecimal values were obtained using Gimp v2.10.14. Hexadecimal values were converted to decimal values using the hexadecimal-to-decimal converter Rapid Tables (<https://www.rapidtables.com/convert/number/het-to-decimal.html>; accessed 20 April 2022). Five different points (always the same spots) were used to determine the average decimal value of all biological replicates from the same phage dilution. The collected data were illustrated with R studio version 2022.02.1 (RStudio Team RStudio, 2020) using the ggplot2 package (Wickham 2009).

Results and discussion

The host and its prophage

In an initial investigation, we sequenced and characterized the strains *J. lividum* EIF1 and EIF2 and addressed their potential prophages (Friedrich *et al.* 2020).

J. lividum EIF1 harbored two predicted prophage regions in its chromosome and EIF2 seven (Table 1). The lower prophage content made EIF1 a promising phage isolation host, as prophages can confer resistance to related and unrelated phage strains (Kohm and Hertel 2021). However, the two putative EIF1 prophage regions (region 1: 2,543,591–2,585,344 bp = 41.7; region 2: 2,565,749–2,585,385 bp = 19.6 kb) were bioinformatically classified as questionable and incomplete. To clarify this prediction, we performed a ProphageSeq (Hertel *et al.* 2015) by sequencing phage particle-packed dsDNA. We tracked the sequence origin by mapping sequence reads on the bacterial genomes (Figure 1). The reads were distributed evenly with consistent coverage between base 2,543,607 and 2,585,345 bp. The same reads

were used for direct genome assembly, resulting in one circular contig of 41,739 bp representing the genome of one phage.

Table 1. Overview of all PHASTER-predicted prophages of strain EIF1 and EIF2.

Strain	Prophage region	Coordinate [bp]	Size [bp]
EIF1 chromosome	1	2,543,591–2,585,344	41,753
	2	2,565,749–2,585,385	19,636
EIF2 chromosome	1	1,746,259–1,768,581	22,323
	2	2,079,134–2,112,833	33,700
	3	2,093,778–2,133,374	39,597
	4	3,013,907–3,041,617	27,711
	5	3,066,783–3,082,324	15,542
	6	3,983,515–4,003,718	20,204
	7	4,025,659–4,037,342	11,684
EIF2 plasmid	1	315,441–324,647	9,206

Aligning the phage genome with the chromosome of EIF1 enabled us to precisely locate the corresponding prophage between 2,543,591 and 2,585,345 bp and identify the prophage attachment sites *attL* and *attR* as almost perfect direct repeats of 17 bp (CACCGTCTCCGCCAGTg/a) with only one base deviation at position 17. In addition, a serine tRNA was identified as the integration locus of the prophage.

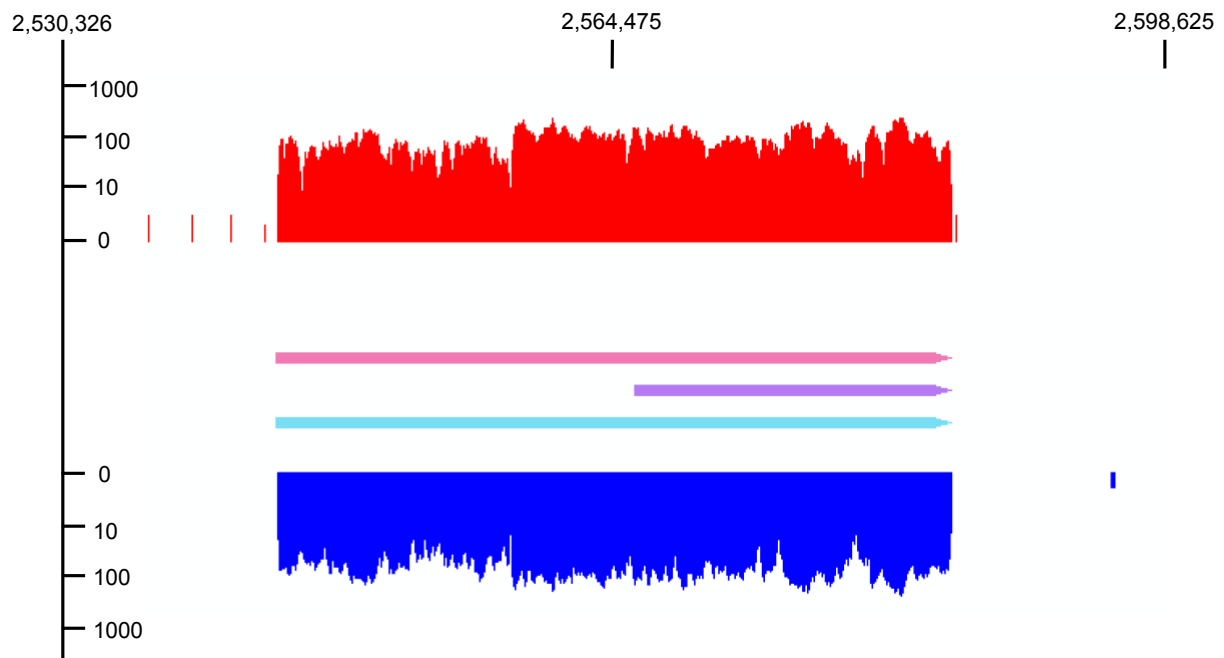


Figure 1. Read coverage profile of EIF1 sequenced prophages, mapped onto the corresponding host genome. The pinkish and purplish arrow depicts the prophages predicted with PHASTER (Arndt et al. 2016). In cyan blue is the experimentally verified prophage region. The image displays the read coverage of the EIF1 genome between base 2,530,326 to 2,598,625 (68,299 bp).

In conclusion, we experimentally confirmed one prophage region in *J. lividum* EIF1, which can still produce phage particles with a precisely packed viral genome. Unfortunately, we cannot comment on the extent to which this prophage is still infectious or can complete an entire replication cycle. Furthermore, no suitable host strain was available.

Isolation of a *J. lividum* phage

We successfully generated plaque assays using sewage as a phage source and *J. lividum* EIF1 as a host on a chemically defined diluted peptone medium supplemented with CaCl₂ (PCa medium) (Figure 2). Complex media like tryptic soy agar (TSA) proved less suitable and led to not defined plaques and inhomogeneous overlays (Figure 2). We suspect the host bacterium itself to be the reason for that. The glucose in the TSA medium may impact the *N*-acyl homoserine lactone formation, which is involved in quorum sensing regulators and biofilm formation (Pantarella et al. 2006). Thus, using the glucose-containing medium results in flocculation of *J. lividum* EIF1, as observed in liquid medium (data not shown), and might also explain the observations with the overlay. We conclude that a glucose-free minimal medium is best for phage isolation in combination with the overlay plaque assay technique.

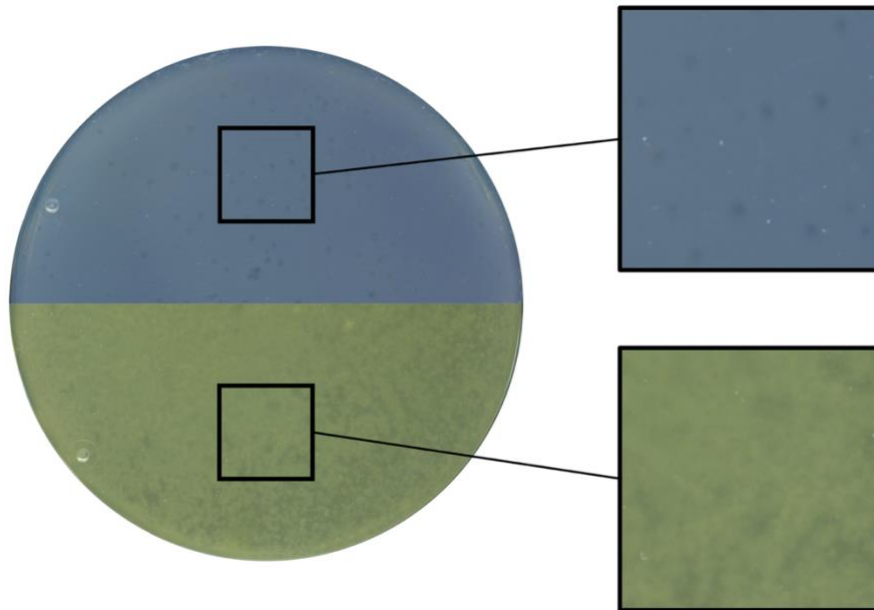


Figure 2. Infection of bacterial strain EIF1. The upper scan of the plate (blueish) shows a PCa agar plate with plaques after infection (zoomed in plaque region) of the bacterial strain EIF1 with sewage water from the primary treatment step and incubation overnight at 30 °C. The same procedure was performed for the TSA agar plate (lower greenish plate). The bacterial lawn looks flocculent (zoomed-in the region), and no singular plaques can be observed.

J. lividum EIF1 proved to be a suitable host. Plaques from the PCa plates were picked, and redundancies were eliminated by determining specific genomic restriction patterns of all isolates. This analysis revealed, via a unique restriction pattern, that only one phage strain was present. Further attempts to isolate ssDNA or RNA phages were unsuccessful (data not shown).

Phage characterization

Transmission electron microscopy revealed head-tail morphology (Figure 3). The phage consists of a head, collar, elongated tube with a pseudo-sheath at the lower part of the tube, and tail spikes. The capsid diameter was 61 nm. The tail was semi-inflexible and had an additional structure at the lower tail end. The tail length was 96 nm. The total length of the isolate was 157 nm.

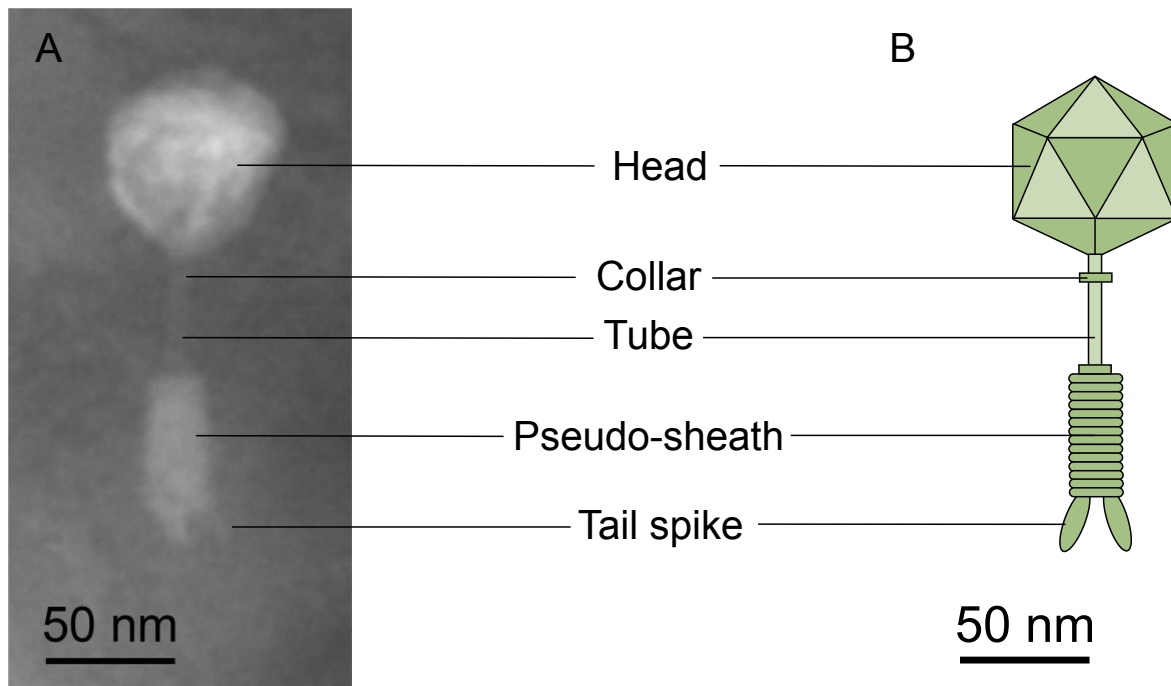


Figure 3. TEM micrograph of vB_JliM-Donnerlittchen. (A) Close-up of a representative particle indicating morphological structures. (B) Schematic illustration of A to better illustrate the observed morphological structures.

As outlined above, we sequenced the viral DNA from four different plaques to verify that only one viral strain was present. The assembled genomes proved identical, with a size of 58,220 bp and a G + C content of 67.75% (host G + C content of 61.98%). The phage genome contains one tRNA and 74 putative protein-encoding genes, of which 49 showed no similarities to known proteins and were annotated as hypothetical proteins. However, we could also identify genes similar to typical phage-related genes, like genes encoding phage tail tube-like protein, a tape measure protein, a tip attachment protein, a helicase, a DNA polymerase, and a terminase (Figure 4). The only other known *Janthinobacterium*-associated bacteriophage MYSP06 was not sequenced, but its genome size was determined by analyzing restriction digestion patterns to range from 65–70 kb (Li *et al.* 2016). Thus, both isolates show considerable differences concerning genome size and are probably unrelated. Also, the morphotype of bacteriophage MYSP06 is *Sihpo* with a long tail and an icosahedral head. At the same time, our isolate also has an icosahedral head with a short tail containing tail spikes and a pseudo-sheath.

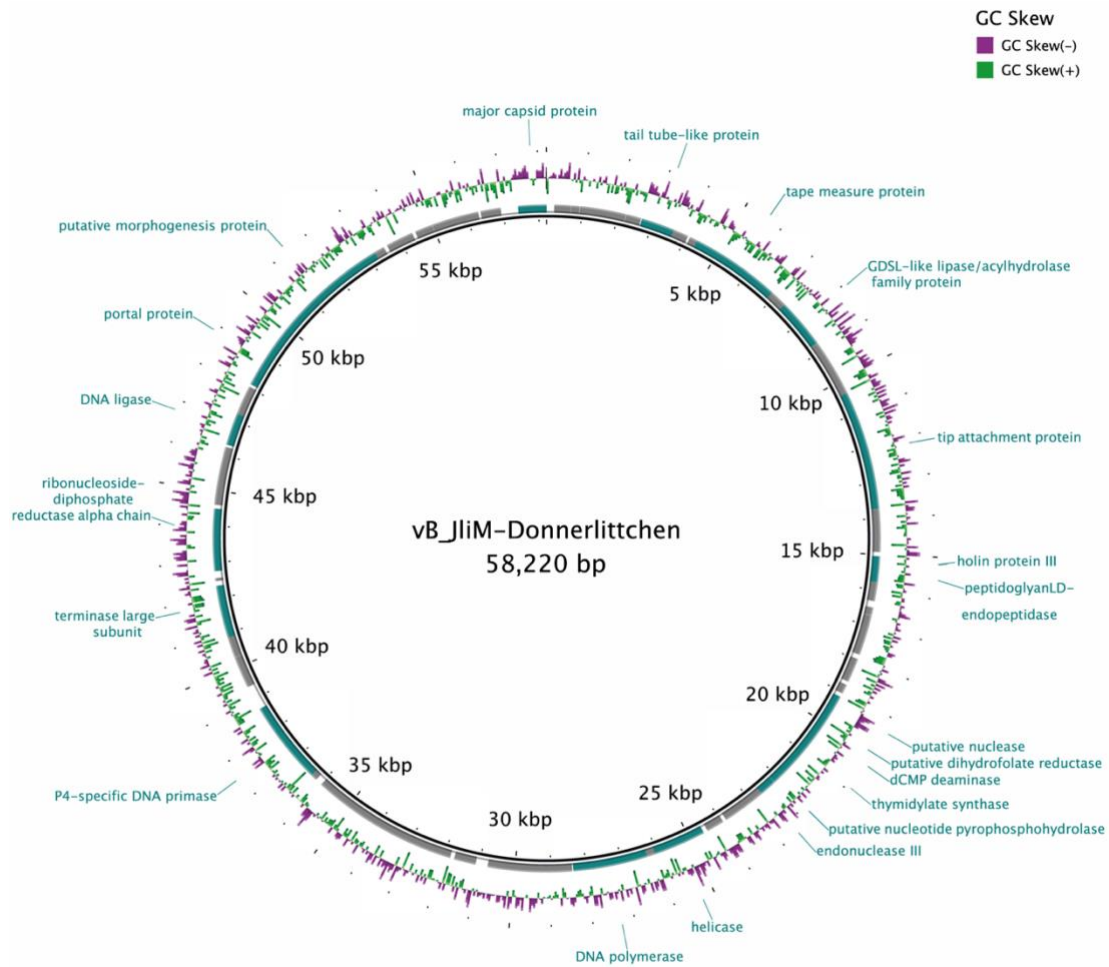


Figure 4. Schematic map of the circular genome of *Janthinobacterium* phage vB_JliM-Donnerlittchen. The inner ring shows the genome location, GC Skew - (purple) and + (green). Identified open reading frames are depicted in teal. Visualization using BRIG (Alikhan et al. 2011).

Based on the morphological and genomic investigations, we named our phage vB_JliM-Donnerlittchen (vB = virus of bacteria, Jli = *J. lividum*, M = *Myoviridae* morphotype, Donnerlittchen = specific phage name). As vB_JliM-Donnerlittchen is the first sequenced *J. lividum* phage, we compared its genome to other phages associated with the Burkholderiales. Results revealed a novel phage infecting member of the order Burkholderiales (Supplement Table S1). Although vB_JliM-Donnerlittchen genomically seemed part of the *Siphoviridae* family, its morphology reveals a *Myo* morphotype. As a *Sipho* morphotype, it should only consist of a tube and tail spikes, while the *Myo* morphotype additionally consists of a sheath. Our bacteriophage shows a sheath positioned on the tube's lower end. Additional attempts to

infect the sister species *J. lividum* EIF2 with vB_JliM-Donnerlittchen showed no plaque formation. This result underlined our initial assumption that prophages could confer resistance to related and unrelated phages (Kohm and Hertel 2021).

Impact of violacein on phage infection

During phage reinfection via plaque overlay assay, we observed that our PCa plates frequently became purple, and we studied if this observation is connected to phage presence. Therefore, we serially diluted our initial phage lysate up to 10^{-6} and used these dilutions for reinfection experiments. The results showed plates with a gradient in violet coloration, with the strongest at the lowest dilution and the weakest at the highest (Figure 5). Regarding the phages, we detected, that contrary to expectations, plaque counts were higher at higher dilutions (Figure 5). In more detail, we observed an uncountable number of plaques in the 10^{-6} dilutions and significantly fewer and countable ones in the lower dilutions, like 98 for 10^{-5} and 7 for 10^{-4} . No plaques in the dilutions below.

At the moment, we can only speculate on the reason for this result. Since we used only a sterile-filtered lysate for reinfection, it likely contained unknown components released by the lysed bacteria responsible for the violet staining and reduction of phage infectivity. We can exclude that the substance in the lysate is directly responsible for the decline of the viral phages, as the initial lysates were prepared, diluted, and used at different times. However, the coloration and plaque results were consistent in the replicates. Therefore, we can rule out that the substance triggered a possible receptor conformation change, as reported with phage T5, to prevent the adsorption of the phage to the host and thereby prevent infection (Breyton *et al.* 2013). The activation of an intracellular defense can also be excluded. In both cases, no plaques would have been observed. However, the assumed substance is responsible for violacein formation, which could be responsible for plaque reduction. Previous studies have confirmed violacein to inactivate human herpes simplex virus type 1 and polio (Andrighetti-Fröhner *et al.* 2003).

We hypothesize that an initial interaction of the phage with its host triggers the host to release a signal molecule, which stimulates uninfected cells to produce the protective violacein. Since we processed the initial lysate only by sterile filtration, we transferred and

diluted the phages and the signal molecule for subsequent experiments. In the lower phage dilutions, the high signal molecule concentration triggered a strong violacein production in the few non-infected cells. That, in turn, either prevented the production of viral particles or immediately inactivated the released virions.

In the higher dilutions, we could still observe plaques. Here, violacein production was insufficient for total protection. However, as some initial infections could produce enough progeny and lead to a few subsequent infections. As soon as only two subsequent infections followed, the second release in the immediate vicinity increased the phage concentration to such an extent that the present violacein concentration was no longer sufficient to prevent plaque formation.

In conclusion, the results indicated a putative new phage defense mechanism, which includes post-infection signaling to induce protective violacein production in uninduced cells. However, the nature of this defense cascade and the signaling molecule remain to be clarified by future studies.

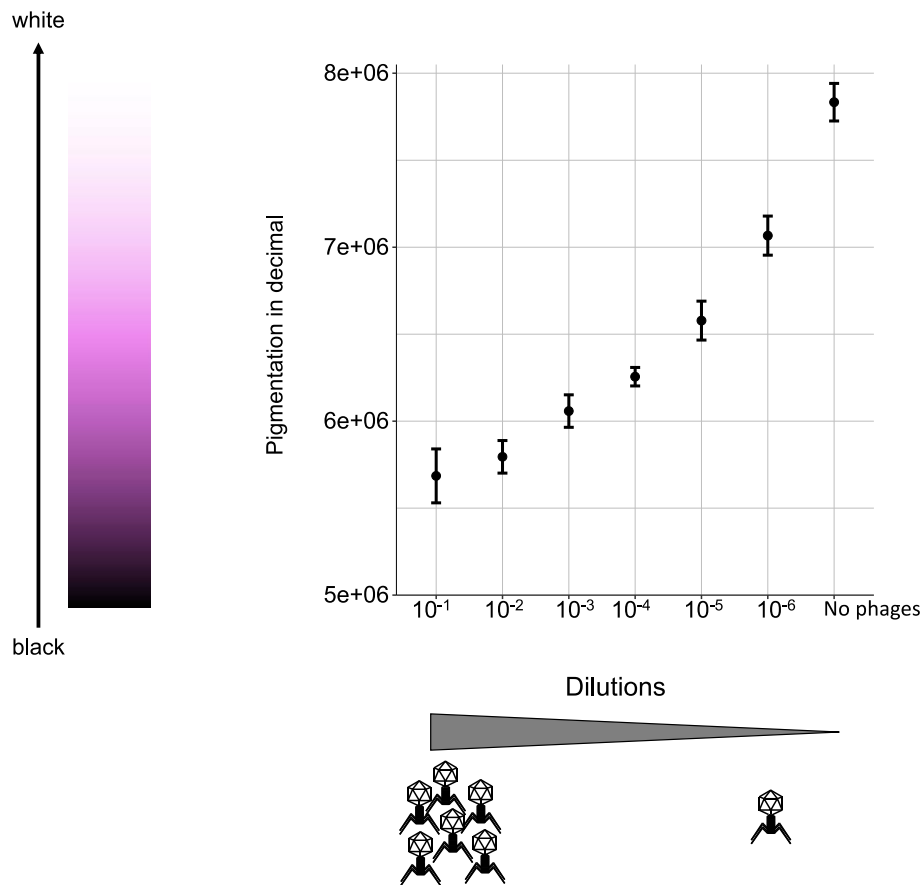


Figure 5. Correlation between plaque number (PFU/mL) and pigmentation (decimal values). The X-axis shows the plaque count (PFU/mL), and the Y-axis shows decimal values of color. Decimal values can only be between 0 (black) and 16,777,215 (white). That means that the higher the value, the “whiter” a plate is.

Data Availability Statement

The phage genome of vB_JliM-Donnerlittchen has been deposited at GenBank under the accession number ON529854. The whole-genomes *J. lividum* strain EIF1 and EIF2 projects have been deposited at DDBJ/ENA/GenBank (Friedrich et al., 2020). The genome of *J. lividum* EIF1 is accessible under accession number CP048832. The genome of *J. lividum* EIF2 is accessible under accession numbers CP049828 (EIF2 chromosome) and the plasmid under CP049829 (EIF2 plasmid p356839).

Acknowledgements

We thank Dr. Anja Poehlein for sequencing and Mechthild Bömeke for technical assistance, Dr. Michael Hoppert for support with TEM-imaging, and Dr. Jacqueline Hollensteiner for the helpful suggestions regarding the characterization of phage vB_JliM-Donnerlittchen.

References

- Adriaenssens E, Brister JR. How to name and classify your phage: An informal guide. *Viruses* 2017;**9**:70.
- Alikhan N-F, Petty NK, Ben Zakour NL *et al.* BLAST Ring Image Generator (BRIG): Simple prokaryote genome comparisons. *BMC Genom* 2011;**12**:402.
- Ambrožič Avguštin J, Žgur Bertok D, Kostanjšek R *et al.* Isolation and characterization of a novel violacein-like pigment producing psychrotrophic bacterial species *Janthinobacterium svalbardensis* sp. nov. *Antonie Leeuwenhoek* 2013;**103**:763–9.
- Andrighetti-Fröhner C, Antonio R, Creczynski-Pasa T *et al.* Cytotoxicity and potential antiviral evaluation of violacein produced by *Chromobacterium violaceum*. *Mem Inst Oswaldo Cruz* 2003;**98**:843–8.
- Arndt D, Grant JR, Marcu A *et al.* PHASTER: a better, faster version of the PHAST phage search tool. *Nucleic Acids Res* 2016;**44**:W16–21.
- Asencio G, Lavin P, Alegría K *et al.* Antibacterial activity of the Antarctic bacterium *Janthinobacterium* sp. SMN 33.6 against multi-resistant Gram-negative bacteria. *Electron J Biotechnol* 2014;**17**:1–5.
- Baldani JL, Rouws L, Cruz LM *et al.* The family *Oxalobacteraceae*. In: Rosenberg E, DeLong EF, Lory S, *et al.* (eds.). *The Prokaryotes*. Berlin, Heidelberg: Springer Berlin Heidelberg, 2014, 919–74.
- Benson DA, Cavanaugh M, Clark K *et al.* GenBank. *Nucleic Acids Res* 2017;**45**:D37–42.
- Breyton C, Flayhan A, Gabel F *et al.* Assessing the conformational changes of pb5, the receptor-binding protein of phage T5, upon binding to its *Escherichia coli* receptor PhuA. *Int J Biol Chem* 2013;**288**:30763–72.
- Brister JR, Ako-Adjei D, Bao Y *et al.* NCBI viral genomes resource. *Nucleic Acids Res* 2015;**43**:D571–7.
- Bromberg N, Dreyfuss JL, Regatieri CV *et al.* Growth inhibition and pro-apoptotic activity of violacein in Ehrlich ascites tumor. *Chem-Biol Interact* 2010;**186**:43–52.
- Carding SR, Davis N, Hoyles L. Review article: the human intestinal virome in health and disease. *Aliment Pharmacol Ther* 2017;**46**:800–15.
- Casas V, Rohwer F. Phage Metagenomics. *Methods in Enzymology*. Vol 421. Elsevier, 2007, 259–68.
- De Ley J, Segers P, Gillis M. Intra- and intergeneric similarities of *Chromobacterium* and *Janthinobacterium* ribosomal ribonucleic acid cistrons. *Int J Syst Evol Microbiol* 1978;**28**:154–68.
- Dietrich S, Wiegand S, Liesegang H. TraV: a genome context sensitive transcriptome browser. *PLOS ONE* 2014;**9**, DOI: 10.1371/journal.pone.0093677.
- Dion MB, Oechslin F, Moineau S. Phage diversity, genomics and phylogeny. *Nat Rev Microbiol* 2020;**18**:125–38.
- Friedrich I, Bodenberger B, Neubauer H *et al.* Down in the pond: Isolation and characterization of a new *Serratia marcescens* strain (LVF3) from the surface water near frog's lettuce (*Groenlandia densa*). Kuo C-H (ed.). *PLOS ONE*

2021a;**16**:e0259673.

Friedrich I, Hollensteiner J, Schneider D *et al.* First complete genome sequences of *Janthinobacterium lividum* EIF1 and EIF2 and their comparative genome analysis. *Genome Biol Evol* 2020;**12**:1782–8.

Friedrich I, Klassen A, Neubauer H *et al.* Living in a puddle of mud: Isolation and characterization of two novel *Caulobacteraceae* strains *Brevundimonas pondensis* sp. nov. and *Brevundimonas goettingensis* sp. nov. *Appl Microbiol* 2021b;**1**:38–59.

Garmaeva S, Sinha T, Kurilshikov A *et al.* Studying the gut virome in the metagenomic era: challenges and perspectives. *BMC Biol* 2019;**17**:84.

Gong X, Skrivergaard S, Korsgaard BS *et al.* High quality draft genome sequence of *Janthinobacterium psychrotolerans* sp. nov., isolated from a frozen freshwater pond. *Stand in Genomic Sci* 2017;**12**:8.

Haack FS, Poehlein A, Kröger C *et al.* Molecular keys to the *Janthinobacterium* and *Duganella* spp. interaction with the plant pathogen *Fusarium graminearum*. *Front Microbiol* 2016;**7**, DOI: 10.3389/fmicb.2016.01668.

Hertel R, Rodríguez DP, Hollensteiner J *et al.* Genome-based identification of active prophage regions by next generation sequencing in *Bacillus licheniformis* DSM13. *PLOS ONE* 2015;**10**:1–18.

Jung WJ, Kim SW, Giri SS *et al.* *Janthinobacterium tructae* sp. nov., isolated from kidney of rainbow trout (*Oncorhynchus mykiss*). *Pathogens* 2021;**10**:229.

Kieft K, Zhou Z, Anantharaman K. VIBRANT: Automated recovery, annotation and curation of microbial viruses, and evaluation of viral community function from genomic sequences. *Microbiome* 2020;**8**:90.

Kohm K, Floccari VA, Lutz VT *et al.* The *Bacillus* phage SP β and its relatives: A temperate phage model system reveals new strains, species, prophage integration loci, conserved proteins and lysogeny management components. *Environ Microbiol* 2022;**24**:2098–118.

Kohm K, Hertel R. The life cycle of SP β and related phages. *Arch Virol* 2021;**166**:2119–30.

Kropinski AM, Mazzocco A, Waddell TE *et al.* Enumeration of bacteriophages by double agar overlay plaque assay. *Methods Mol Biol* 2009;**501**:69–76.

Langmead B, Salzberg SL. Fast gapped-read alignment with Bowtie 2. *Nat Methods* 2012;**9**:357–9.

Li M, Wang J, Zhang Q *et al.* Isolation and characterization of the lytic cold-active bacteriophage MYSPO6 from the Mingyong Glacier in China. *Curr Microbiol* 2016;**72**:120–7.

Lincoln SP, Fermor TR, Tindall BJ. *Janthinobacterium agaricidamnorum* sp. nov., a soft rot pathogen of *Agaricus bisporus*. *Int J Syst Evol Microbiol* 1999;**49**:1577–89.

Lu H, Deng T, Cai Z *et al.* *Janthinobacterium violaceinigrum* sp. nov., *Janthinobacterium aquaticum* sp. nov. and *Janthinobacterium rivuli* sp. nov., isolated from a subtropical stream in China. *Int J Syst Evol Microbiol* 2020;**70**:2719–25.

McTaggart TL, Shapiro N, Woyke T *et al.* Draft genome of *Janthinobacterium* sp. RA13 isolated from Lake Washington sediment. *Genome Announc* 2015;**3**:e01588-14.

Moraru C, Varsani A, Kropinski AM. VIRIDIC—A novel tool to calculate the intergenomic similarities of prokaryote-infecting viruses. *Viruses* 2020;**12**:1268.

Oh WT, Giri SS, Yun S *et al.* *Janthinobacterium lividum* as An emerging pathogenic bacterium affecting rainbow trout (*Oncorhynchus mykiss*) fisheries in Korea. *Pathogens* 2019;**8**:146.

Pantanella F, Berlutti F, Passariello C *et al.* Violacein and biofilm production in *Janthinobacterium lividum*. *J Appl Microbiol* 2006;**102**:992–9.

Principi N, Silvestri E, Esposito S. Advantages and limitations of bacteriophages for the treatment of bacterial

infections. *Front Pharmacol* 2019;**10**:513.

Shoemaker WR, Muscarella ME, Lennon JT. Genome sequence of the soil bacterium *Janthinobacterium* sp. KBS0711. *Genome Announc* 2015;**3**:e00689-15.

Wickham H. *Ggplot2 – Elegant Graphics for Data Analysis*. New York, NY: Springer New York, 2009:3.

Wu Q, Liu W-T. Determination of virus abundance, diversity and distribution in a municipal wastewater treatment plant. *Water Res* 2009;**43**:1101–9.

Wu X, Deutschbauer AM, Kazakov AE *et al.* Draft genome sequences of two *Janthinobacterium lividum* strains, isolated from pristine groundwater collected from the Oak Ridge Field Research Center. *Genome Announc* 2017;**5**:e00582-17.

Zdobnov EM, Apweiler R. InterProScan - An integration platform for the signature-recognition methods in InterPro. *Bioinformatics* 2001;**17**:847–8.

Supplementary Material

Supplementary Table S1. Phylogenetic analysis of all available Burkholderiales-associated phages. Analysis was performed with VIRIDIC v1 (Moraru, Varsani and Kropinski 2020).

The table can be found on the enclosed CD and .zip folder:

Supplement\Chapter_3.8\Supplementary_Table_S1.xlsx

9. *Luteibacter flocculans* sp. nov., isolated from a eutrophic pond and introduction of *Luteibacter* phage vB_LflM-Pluto

Ines Friedrich¹, Alisa Kuritsyn¹, Robert Hertel^{1,2} and Rolf Daniel¹

Microorganisms (24 January 2023), 11(2):307
<https://doi.org/10.3390/microorganisms11020307>

Affiliations

¹Genomic and Applied Microbiology & Göttingen Genomics Laboratory, Institute of Microbiology and Genetics, Georg-August-University of Göttingen, Grisebachstraße 8, 37077 Göttingen, Germany

²FG Synthetic Microbiology, Institute of Biotechnology, BTU Cottbus-Senftenberg, Senftenberg, Germany

Author contributions:

Conceptualization: IF, RH, RD

Data curation: IF

Formal analysis: IF, RH, RD

Funding acquisition: RD

Investigation: IF, AK

Project administration: RD

Supervision: RD

Validation: IF, RH, RD

Visualization: IF, AK

Writing – original draft: IF

Writing – review & editing: IF, AK, RH, RD

Abstract

Luteibacter is a genus of the *Rhodanobacteraceae* family. The present study describes a novel species within the genus *Luteibacter* (EIF3^T). The strain was analyzed genomically, morphologically, and physiologically. Average nucleotide identity analysis revealed that it is a new species of *Luteibacter*. *In silico* analysis indicated two putative prophages (one incomplete, one intact). EIF3^T cells form an elliptical morphotype with an average length of 2.0 µm and width of 0.7 µm and multiple flagella at one end. The bacterial strain is an aerobic Gram-negative with optimal growth at 30 °C. EIF3^T is resistant towards erythromycin, tetracycline and vancomycin. We propose the name *Luteibacter flocculans* sp. nov. with EIF3^T (=DSM 112537^T = LMG 32416^T) as type strain. Further, we describe the first known *Luteibacter*-associated bacteriophage called vB_LflM-Pluto.

Introduction

The genus *Luteibacter* is part of the family *Rhodanobacteraceae*, which belongs to the γ -subclass of the Proteobacteria. The family contains 17 genera, *Aerosticca*, *Ahniella*, *Aquimonas*, *Chiayivirga*, *Denitratimonas*, *Dokdonella*, *Dyella*, *Frateuria*, *Fulvimonas*, *Luteibacter*, *Oleigrimonas*, *Pinirhizobacter*, *Pseudofulvimonas*, *Rehabacterium*, *Rhodanobacter*, *Rudaea*, and *Tahibacter*, of which two are not validly published (*Denitratimonas* and *Pinirhizobacter*) (1). The genus *Luteibacter* was established by Johansen et al. (2) based on the species *Luteibacter rhizovicinus* DSM 16549^T. It currently comprises five species of which three are validly published: *L. rhizovicinus* DSM 16549^T (2), *L. yeojuensis* DSM 17673^T (3,4), *L. anthropi* CCUG 25036^T (4), *L. jiangsuensis* (5), and *L. pinisoli* (6). Members of the *Luteibacter* genus were isolated from various environments such as rhizospheric soil (2,6), greenhouse soil (3), and human blood (4). They are described as motile, aerobic Gram-negatives with a rod-like shape and yellow-coloring. Further, they are catalase- and oxidase-positive and urease-negative.

To date, *Luteibacter*- or even *Rhodanobacteraceae*-associated phages are unknown. Phages or bacteriophages are viruses that infect bacteria. While temperate phages can incorporate into the bacterial genome, lytic phages begin multiplying directly after infection. The temperate phages replicate their incorporated genome alongside the host genome, leading to a prophage

and a lysogenic bacterium. Through the addition of its genetic material, a prophage can provide new abilities, defending the host from infection by related and unrelated viruses (23).

In a previous study, we were able to isolate an environmental *Luteibacter* sp. nov. strain from a eutrophic pond located in Göttingen, Germany. The *Luteibacter* strain was isolated as a prospective model strain to investigate the local viral diversity associated with it. Despite the fact that 16S rRNA gene analysis validated its species assignment, no additional characterization was performed (31).

Here, we describe a novel environmental *Luteibacter* isolate, which was characterized morphologically, physiologically and genomically. In addition, we investigated the potential of the host strain to access the environmental diversity of *Luteibacter*-associated phages.

Material and methods

Luteibacter flocculans EIF3 strain isolation, DNA extraction, and 16S rRNA gene sequencing

Luteibacter flocculans EIF3^T (Figure S1) was isolated from the surface water of a eutrophic pond located at the North Campus of the Georg-August University in Göttingen, Germany (51° 33' 29" N 9° 56' 41" E 173 m, collected on 24 September 2018) (31). This study was conducted at a public pond in Göttingen that required no specific permissions; 25 mL LB (1% peptone from casein, 0.5% yeast extract, 0.5% NaCl) was used as a culture medium. DNA was extracted and the 16S rRNA gene sequenced as described by Friedrich et al., 2021 (31).

Sequencing, assembly, and annotation of bacterial and phage genome

Friedrich et al. 2021 describe the genome sequencing, assembly and annotation procedures. Briefly, Illumina paired-end sequencing libraries were generated using the Nextera XT DNA Sample Preparation kit. For sequencing, the MiSeq System and Reagent Kit version 3 (2 x 300 bp) were used according to the manufacturer's instructions (Illumina, San Diego, CA, USA) (31). For Nanopore sequencing, the Ligation Sequencing Kit (SQK-LSK109) and the Native Barcode Expansion Kit EXP-NBD114 (Oxford Nanopore Technologies, Oxford, UK) were utilized (31). The same kit was used to prepare total and specific nucleic acids from the

bacteriophage. To remove proteins, 5 μ L of Proteinase K (20 mg/mL) were added to 300 μ L of 2X T and C Lysis. This solution was applied to 300 μ L of phage suspension. The pure viral genomic DNA was extracted from total nucleic acids using RNase A (DNase free).

CRISPRCasFinder (9) was used to identify potential CRISPR areas. Assembled bacterial genomes were quality-checked with CheckM v1.1.2 (10). Genome annotation was performed using the Prokaryotic Genome Annotation Pipeline v4.13 (PGAP) (11).

Raw bacteriophage reads were quality-processed using Trimmomatic v0.39 (12) and paired-end reads were merged using FLASH v1.2.11 (13). The quality-processed reads served as input for the Unicycler v0.4.9 assembly pipeline in normal mode (14), which consisted of Spades v3.13.0 (15), makeblastdb v2.11.0+ and tblastn v2.11.0+ (16), bowtie2-build v2.4.4 and bowtie2 v2.4.4 (17), SAMtools v1.12 (18), java v.11.0.13 (19), and Pilon v1.23 (20). The quality of assembly was evaluated using QualiMap v2.2.2 (21). Annotations were performed using VIBRANT (22) and InterProScan v5.55-88.0 (23).

The whole-genome sequence of *Luteibacter flocculans* EIF3^T has been submitted to GenBank under the accession number CP063231. The BioSample (SAMN16456042) is part of the BioProject with the accession number PRJNA669578. The raw reads have been submitted to the NCBI SRA database with the accession numbers SRR12951264 (Oxford Nanopore) and SRR12951265 (Illumina), as well as BioProject PRJNA669578. The strain was deposited at the DSMZ (Deutsche Sammlung von Mikroorganismen und Zellkulturen, Braunschweig, Germany) with the collection number DSM 112537 and at the BCCM/LMG (Belgian Coordinated Collections of Microorganisms) with the collection number LMG 32416. The whole-genome sequence of *Luteibacter*-associated bacteriophage vB_LflM-Pluto is available under the accession number ON529861 at GenBank.

***Luteibacter flocculans* sp. nov. EIF3^T phylogenetic classification**

The Genome Taxonomy Database Toolkit (GTDB-Tk) v1.0.2 (24) as well as whole-genome-based phylogeny with Type (Strain) Genome Server (TYGS (25), accessed on 10 July 2022) were used to provide an initial taxonomic classification of the *Luteibacter flocculans* isolate,. The ANIm method, which is provided in pyani v0.2.10 (26), was used with a species boundary of 95% ANI for in-depth phylogenetic analysis (24). Based on the DSMZ and the NCBI, the

genome of the isolate was compared to all available type strain and reference genomes (accessed on 10 July 2022) comprising *Frateuria flava* (GCF_017837635), *F. defendens* (GCF_001182895), *Dyella solisilvae* (GCA_003351225), *D. kyungheensis* (GCF_016905005), *Luteibacter pinisoli* (GCF_006385595), *L. jiangsuensis* (GCA_011742555), *L. yeojuensis* (GCA_011742875), *L. anthropi* (GCA_011759365), *D. terrae* (GCA_004322705), *Fulvimonas soli* (GCA_003148905), *D. thiooxydans* (GCA_001641285), as well as *L. rhizovicinus* (GCA_001010405).

Genomic comparison

BlastKOALA v2.2 (27) was used to study the metabolic capacities of *Luteibacter flocculans* (Figure S2). AntiSMASH v6.0.0 (28) was employed to identify putative secondary metabolite biosynthetic gene clusters. PHASTER (29) was utilized to identify putative phage regions. Resfams v1.2.2 (30) was applied to examine presence of antibiotic resistance genes.

Cell morphology and Gram staining techniques

Microscopy (Primo Star, Zeiss, Carl Zeiss Microscopy, Jena, Germany) was used to examine the morphology of single colonies after 72 hours of growth on LB solid medium (Fluka, Munich, Germany). Hucker's crystal violet, an iodine and safranin solution and 1-propanol were used for Gram staining (31). Microscopic images and stains were processed and analyzed using the software ZEISS Labscope (Carl Zeiss).

Bacterial and phage isolate transmission electron microscopy

The morphology of *Luteibacter flocculans* and *Luteibacter* phage vB_LflM-Pluto was studied using transmission electron microscopy (TEM). The digital Micrograph software (Gatan GmbH, Munich, Germany) was used for imaging. *Luteibacter flocculans* was cultivated overnight in liquid LB medium at 30 °C. A negative staining was then conducted using 5 µL cell or phage suspension. The suspension was mixed with an equal quantity of diluted 0.5% (for bacterial isolate) or 1% (for viral isolate) phosphotungstic acid (3% stock, pH 7). The mixture was transferred to a vaporized carbon mica for one minute. Before placing the mica

on a thin copper-coated grid (PLANO GmbH, Marburg, Germany), it was gently cleaned with demineralized water. The coated grids were allowed to dry at room temperature and examined with a Jeol 1011 TEM (Georgia Electron Microscopy, Freising, Germany).

Determination of salt tolerance and optimal temperature

EIF3^T was incubated at 30 °C in 4 mL LB medium adjusted with 0 and 5 g/L NaCl and 10 to 60 g/L NaCl in increments of 10 g to determine salt tolerance. The optical density of the cell suspensions was measured at 600 nm (OD₆₀₀) using the Ultraspec 3300 pro photometer (Amersham Pharmacia Biotec Europe GmbH, Munich, Germany). At the start of the experiment, the OD₆₀₀ of the cell suspensions was set to 0.1 (32), followed by a 12-hour incubation period at 30 °C and 180 rpm in an Infors HT shaker (Orbitron, Einsbach, Germany). To determine growth, the OD₆₀₀ was measured after 12 h of incubation (32). Every measurement was carried out in biological replicates. The temperature optimum was determined by culturing the isolate in 4 mL LB-0 medium under shaking (180 rpm) at 10, 20, 30, 37, 40 and 50 °C. The cultures' starting OD₆₀₀ was set to 0.1. After 12 h, the optical cell density of EIF3^T was determined. R studio version 4.0.0 (33) and the ggplot2 package v3.3.6 (34) were used to visualize the data.

Growth kinetics determination

The cell growth quantifier (CGQuant 8.1; Aquila Biolabs GmbH, Baesweiler, Germany) was used to evaluate growth kinetics in liquid cultures under shaking (180 rpm) for 47 h at 30 °C. 250 mL shake flasks were filled with 25 mL of EIF3^T culture in LB-0 medium (final OD₆₀₀ of 0.1) and placed for measurement on the CGQuant sensor plate. Experiments were carried out using three biological replicates. The CGQuant uses a dynamic method of backscattered light measurement, allowing real-time monitoring of growth in liquid culture (35). All data were plotted with R studio version 4.0.0 (33) and the ggplot2 package v3.3.6 (36).

Antibiotic resistances and metabolic activity

For assessment of metabolic activity, API ZYM and API 20 NE tests (BioMérieux, Nuertingen, Germany) were used. Both tests were carried out according to the manufacturer's instructions. Catalase activity was measured with 3% H₂O₂ (37). Antibiotic resistances with discs and strips (Oxoid, Thermo Fisher Scientific) were determined using a soft-agar (0.4% (w/v) agarose in LB medium) overlay technique. Discs and strips contained ampicillin (25 µg), kanamycin (30 µg), oxytetracycline (30 µg), rifampicin (2 µg), streptomycin (10 µg), vancomycin (30 µg), tetracycline (0.015–256 µg), and erythromycin (0.015–256 µg). 2.5 mL of soft agar with a final OD₆₀₀ of 0.1 was utilized. Discs or strips containing an antibiotic substance were then added on top of the soft agar. Antibiotic resistances were determined after overnight incubation at 30 °C.

Examination of plaques

The approach described by Willms and Hertel, 2016 (38) and Willms et al., 2017 (38,39) was used for phage enrichment. Sewage samples were collected in February 2022. In order to identify plaque morphologies such clear or turbid, plaque size, and halo presence, plaque assays generally require the ability of the host to grow in bacterial lawns (40). Phages were isolated via agar overlay plaque assay as described elsewhere (40) using host-specific culture media for the base agar (1.5% (w/v) agar) and overlay (0.4% (w/v) agarose). Infected overlay plates were incubated overnight at 30 °C. Individual phages appeared as morphologically distinct plaques, which were picked with a sterile toothpick and transferred into 500 µL sterile LB-0 medium. Reinfection was repeated three times to purify the phage strain.

Naming of the bacteriophage isolates

The bacteriophage was named according to Adriaenssens and Brister's informal guide (41). As a result, vB stands for virus of bacteria, Lfl for the host organism *L. flocculans*, M for the virus family Myo-morphotype, and Pluto is an individual name. As a result, the complete names of the virus is vB_LflM-Pluto, abbreviated Pluto in the following.

Results and Discussion

Morphological characterization

EIF3^T colonies were spherical and yellow with an average diameter of 1.93 mm on solid LB medium. The ability of *Luteibacter flocculans* sp. nov. to flocculate was apparent during growth in liquid LB or TSB media (S1 Fig). Gram staining of EIF3^T resulted in red/pink cells indicating a Gram-negative bacterial species. Cells were straight rods with rounded ends and ranged from 5.3 to 5.8 μm in size (Figure 1). The isolate matched typical morphological features of the family *Rhodanobacteraceae*, such as motility via polar flagella, a cell size ranging from 1 to 4.5 μm and rod-shaped cells with rounded ends (42).

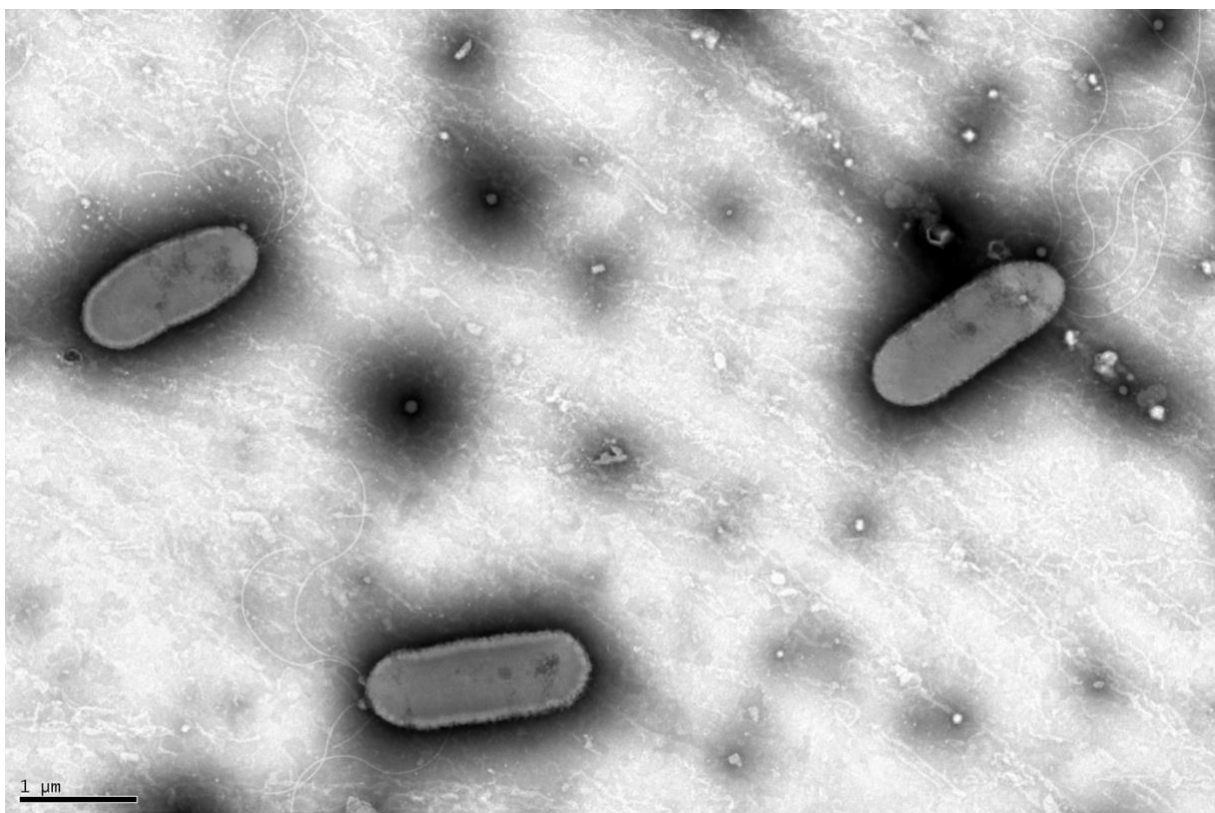


Figure 1. Transmission electron micrograph of EIF3^T. The micrograph depicts the rod-shaped, flagellated morphotype of the *Luteibacter* EIF3 isolate. The image was taken using TEM after 24 h of cell growth at 30 °C in LB medium followed by negative staining..

Physiological characterization

EIF3^T grew in LB medium with up to 4% (w/v) NaCl, with optimal growth achieved in the absence of added NaCl (Figure 2A). The strain is a mesophilic organism since it can grow at temperatures between 20 and 40 °C. The largest cell densities were observed at 30 °C with an

OD₆₀₀ of 3.403 (which is a ratio of 34.033) (Figure 2B). This observation is consistent with results derived from closely related strains (2).

We determined the bacterial growth of EIF3^T at the optimal temperature and salt concentration. The lag phase lasted for approximately 3.5 hours. It was followed by a 10 h log-phase and a transient phase with diminished growth. After approximately 21 hours of incubation, the highest cell densities were recorded. The doubling of our isolate was 221 minutes and the growth rate μ was 0.19 hour⁻¹.

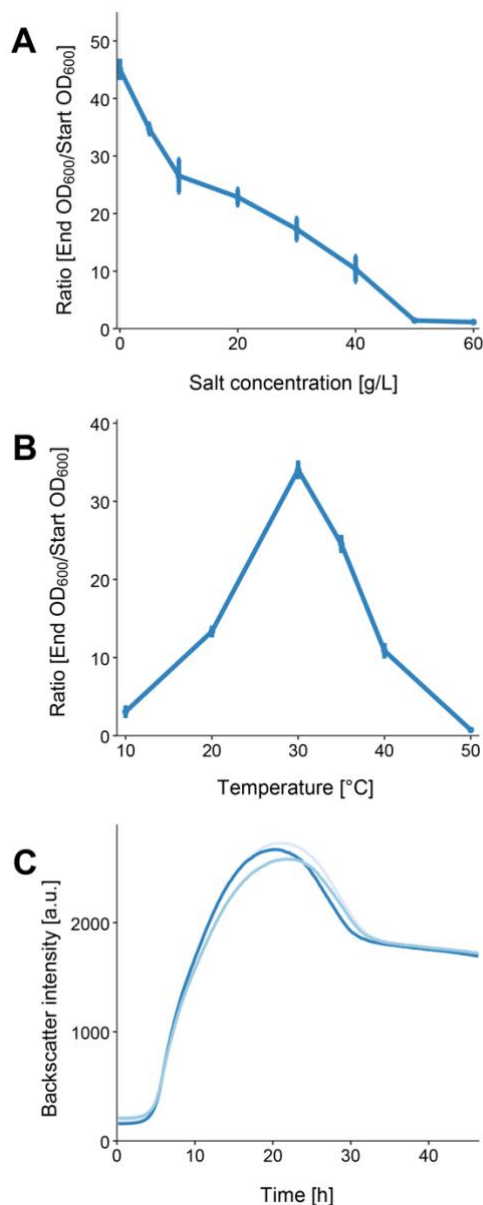


Fig 2. *L. flocculans* sp. nov. growth characteristics. (A) Growth of EIF3^T in 4 mL LB medium after 12 h of incubation at 180 rpm and 30 °C with different salt concentrations. (B) EIF3^T growth at various temperatures in LB-0 medium after 12 h of incubation at 180 rpm. (C) Growth characterization of EIF3^T in 25 mL LB-0 medium at the optimal temperature (30 °C). Triplicate measurements were conducted. Standard deviations in (A, B) are indicated by the error bars. In (C) various shades of blue represent each biological replicate.

Using the API ZYM and the API 20 NE assays, the metabolic capabilities of EIF^T were examined. Twenty distinct enzyme activities were identified for the novel *Luteibacter* isolate using API ZYM. In six cases, no enzyme activity was detected. Activities of alkaline phosphatase, esterase, esterase lipase, leucine arylamidase, valine arylamidase, cysteine arylamidase, acid phosphatase, naphthol-AS-BI-phosphohydrolase, β -galactosidase, α -glucosidase, β -glucosidase, and N-acetyl- β -glucosaminidase were recorded. Corresponding genes were identified in the genome (Table S1). In addition, *Luteibacter flocculans* shared features with closely related bacteria such as *L. rhizovicinus*, *L. yeojuensis* and *L. jiangsuensis* (2,3,5).

EIF3^T was oxidase- and catalase-positive, which is characteristic of certain *Rhodanobacteraceae* family members (42). Table 1 provides an overview of the enzymatic activities of the strain and closely related bacteria from TYGS (25). According to the antibiogram, EIF3^T was resistant to erythromycin (up to 4 μ g/disc), tetracycline (up to 1 μ g/disc), and vancomycin (30 μ g/disc). Resfams *in silico* analysis (30) identified genes encoding an ABC transporter for erythromycin or vancomycin (PRJNAA669578|IM816_002307) and a tetracycline inactivation enzyme (IM816_003460; Table S2). The *in silico* analysis of EIF3^T confirmed the measured antibiotic resistance (Table 1).

Further, it suggested, that EIF3^T can generate secondary metabolites such as arylpolyene xanthomonadin (Table S3). Xanthomonadin is a yellow membrane-bound pigment, which is insoluble in water. Rajagopal et al. discovered that xanthomonadin may protect *Xanthomonas oryzae* against photodamage (43). Moreover, this discovery is consistent with the characteristics of the family *Rhodanobacteraceae* (42).

Fatty acid analysis confirmed typical *Luteibacter* characteristics for our isolate and related strains. The most abundant fatty acids are branched fatty acids iso-C_{15:0} with 18.3%, iso-C_{17:1} ω 9c with 29.4%, and iso-C_{17:0} with 18.2% (Table 2). These corresponded to the main branched fatty acids of the *Luteibacter* described by Johansen et al. (2).

Table 1: Phenotypic differences between strains EIF3^T and phylogenetically related species *L. yeojuensis* DSM 17673^T, *L. jiangsuensis* CGMCC 1.10133^T, *L. anthropi* CCUG 25036^T, and *L. rhizovicinus* DSM 16549^T. Taxa: 1, strain *L. flocculans* EIF3^T; 2, strain *L. yeojuensis* DSM 17673^T (3), 3, strain *L. jiangsuensis* CGMCC 1.10133^T (data from (5,44)); 4, strain *L. anthropi* CCUG 25036^T (data from (4) and BacDive (45) accessed on 31 July 2022); 5, strain *L. rhizovicinus* DSM 16549^T (data from (2) and BacDive (45) accessed on 31 July 2022); +, Positive; -, negative; n/a, data not available.

Characteristics	<i>L. flocculans</i> EIF3 ^T	<i>L. yeojuensis</i> DSM 17673 ^T	<i>L. jiangsuensis</i> CGMCC 1.10133 ^T	<i>L. anthropi</i> CCUG 25036 ^T	<i>L. rhizovicinus</i> DSM 16549 ^T
Source of isolation	Eutrophic pond	Rhizosphere soil	Soil	Human blood	Rhizosphere soil
Motility	+	+	-	+	+
Temperature (°C)					
Range	10–45	5–37	4–42	15–37	5–30
Optimum	30	28	25–30	28	17.5
NaCl (g/L)					
Range	0–40	0–50	0–40	n/a	0–30
Optimum	0	n/a	n/a	n/a	15
Enzymatic activity					
Alkaline phosphatase	+	+	+	n/a	+
Esterase	+	+	n/a	n/a	-
Esterase lipase	+	+	n/a	+	-
Lipase	+	-	+	n/a	-
Leucine arylamidase	+	+	n/a	n/a	+
Valine arylamidase	+	+	n/a	n/a	+
Cysteine arylamidase	+	+	n/a	n/a	-
Trypsin	-	-	n/a	n/a	-
α-Chymotrypsin	-	-	n/a	n/a	-
Acid phosphatase	+	+	n/a		+
Naphthol-AS-BI-phosphohydrolase	+	+	+	n/a	+
α-Galactosidase	-	+	n/a	n/a	+
β-Galactosidase	+	+	+	+	+
β-Glucuronidase	-	-	n/a	n/a	-
α-Glucosidase	+	+	+	n/a	+
β-Glucosidase	+	+	n/a	n/a	+
N-Acetyl-β-glucosaminidase	+	+	+	n/a	-
α-Mannosidase	-	-	n/a	n/a	-
α-Fucosidase	-	-	n/a	n/a	-
Utilization of					
Potassium nitrate	-	-	+	n/a	-
L-Tryptophane	-	-	n/a	n/a	-
D-Glucose (fermentation)	-	-	n/a	-	-
L-Arginine	-	-	+	n/a	-
Urea	-	-	-	n/a	-

Esculin/ferric citrate	+	+	+	n/a	+
Gelatin	-	+	+	-	+
4-Nitrophenyl- β -D-galactopyranoside	-	-	n/a	n/a	-
D-Glucose (assimilation)	+	+	-	+	+
L-Arabinose	-	-	+	n/a	-
D-Mannose	+	+	+	+	+
D-Mannitol	-	-	-	+	-
N-Acetyl-D-glucosamine	+	+	n/a	+	+
D-Maltose	-	+	+	n/a	-
Potassium gluconate	-	-	n/a	+	-
Capric acid	-	-	n/a	n/a	-
Adipic acid	-	-	n/a	n/a	-
Malic acid	+	-	-	+	-
Trisodium citrate	-	-	n/a	n/a	-
Phenylacetic acid	-	-	n/a	n/a	-
Catalase	+	+	+	-	+
Oxidase	+	+	+	+	+
Resistance to					
Ampicillin	-	n/a	n/a	n/a	n/a
Erythromycin	+	n/a	n/a	n/a	n/a
Kanamycin	-	n/a	n/a	n/a	n/a
Oxytetracycline	-	n/a	n/a	n/a	n/a
Rifampicin	-	n/a	n/a	n/a	n/a
Tetracycline	+	n/a	n/a	n/a	n/a
Streptomycin	-	n/a	n/a	n/a	n/a
Vancomycin	+	n/a	n/a	n/a	n/a
G + C %	64.8	63.0	63.6	65.3	63.0

In bold: Sorted by categories.

Table 2: Composition of cellular fatty acids (%) in strain EIF3^T and phylogenetically related species *L. yeojuensis* DSM 17673^T, *L. jiangsuensis* CGMCC 1.10133^T, *L. anthropi* CCUG 25036^T, and *L. rhizovicinus* DSM 16549^T. Taxa: 1, strain *L. flocculans* EIF3^T; 2, strain *L. yeojuensis* DSM 17673^T (3,4), 3, strain *L. jiangsuensis* CGMCC 1.10133^T (data from (5)); 4, strain *L. anthropi* CCUG 25036^T (data from (4)); 5, strain *L. rhizovicinus* DSM 16549^T (data from (4)); -, not detected/not reported.

Fatty acid	<i>L. flocculans</i> EIF3 ^T	<i>L. yeojuensis</i> DSM 17673 ^T	<i>L. jiangsuensis</i> CGMCC 1.10133 ^T	<i>L. anthropi</i> CCUG 25036 ^T	<i>L. rhizovicinus</i> DSM 16549 ^T
Unknown 11.799	-	2.3	-	0.8	2.2
iso-C _{11:0}	4.3	3.8	4.7	3.6	4.0
iso-C _{11:0} 3-OH	4.1	4.2	1.6	2.9	3.9
iso-C _{13:0}	0.2	-	-	0.4	0.5
iso-C _{12:0} 3-OH	0.1	1.0	-	-	-
iso-C _{14:0}	0.2	1.1	-	-	-
C _{14:0}	0.1	-	-	0.5	0.4

iso-C _{13:0} 3-OH	3.2	2.4	2.6	1.2	2.7
iso-C _{15:0}	18.3	14.5	24.0	21.7	17.0
anteiso-C _{15:0}	8.0	6.9	9.7	2.4	4.0
iso-C _{16:0}	2.8	21.3	2.2	0.5	0.8
Summed feature 3*	5.8	5.2	4.1	6.5	9.2
C _{16:0}	2.1	1.8	4.2	5.6	6.5
iso-C _{17:1 ω9c}	29.4	26.5	20.3	23.8	24.4
iso-C _{17:0}	18.2	14.9	20.2	27.0	22.4
anteiso-C _{17:0}	1.3	1.6	1.2	0.9	0.6
C _{18:0}	0.1	–	0.8	0.5	–
iso-C _{17:0} 3-OH	0.7	0.8	–	–	0.5

* Summed feature 3 contains C_{16:1 ω7c} and/or iso-C_{15:0} 2-OH

Genome characterization

The closed genome of EIF3^T comprised one circular chromosome (4,299,254 bp) with a GC content of 64.82%. It encoded 3,672 putative proteins, 59 rRNAs and 49 tRNAs. No CRISPR regions and plasmids were identified (Table 3).

Table 3. Genome statistics of the EIF3^T chromosome.

Features	Chromosome
Genome size (bp)	4,299,254
GC content (%)	64.82
Coverage	280.1-fold
CDS	3,672
rRNA genes	59
tRNA genes	49
ncRNA	4
CRISPR	0
Prophage(s)	2

GTDB-Tk pipeline was used for the genome-based taxonomic classification of strain EIF3^T (Data S1 File) (24). It demonstrated an average nucleotide identity (ANI) of approximately 96% to the most closely related species, *Luteibacter* sp. UNCMF366Tsu5.1 (ANI value of 96.48). The digital DNA-DNA hybridization value (dDDH) via Type Strain Genome Server (TYGS) is

39.9% in comparison to *L. jiangsuensis*. As the new species criterion for dDDH is less than 70% (46), this suggested that our strain is a potential new species (Figure S2; Table S4). Figure 3 shows an ANI-analysis of 12 most closely related type strain genomes in the TYGS database (25) (data in Table S5). No clustering with any other described *Luteibacter* strain was recorded. EIF3^T shares 85.52% ANI with *L. yeojuensis* DSM 17673^T, 85.41% with *L. jiangsuensis* CGMCC 1.10133^T, 84.73% with *L. anthropi* CCUG 25036^T and 84.60% with *L. rhizovicinus* DSM 16549^T.

Luteibacter flocculans sp. nov. EIF3^T was therefore considered as a novel type strain within the *Luteibacter* genus.

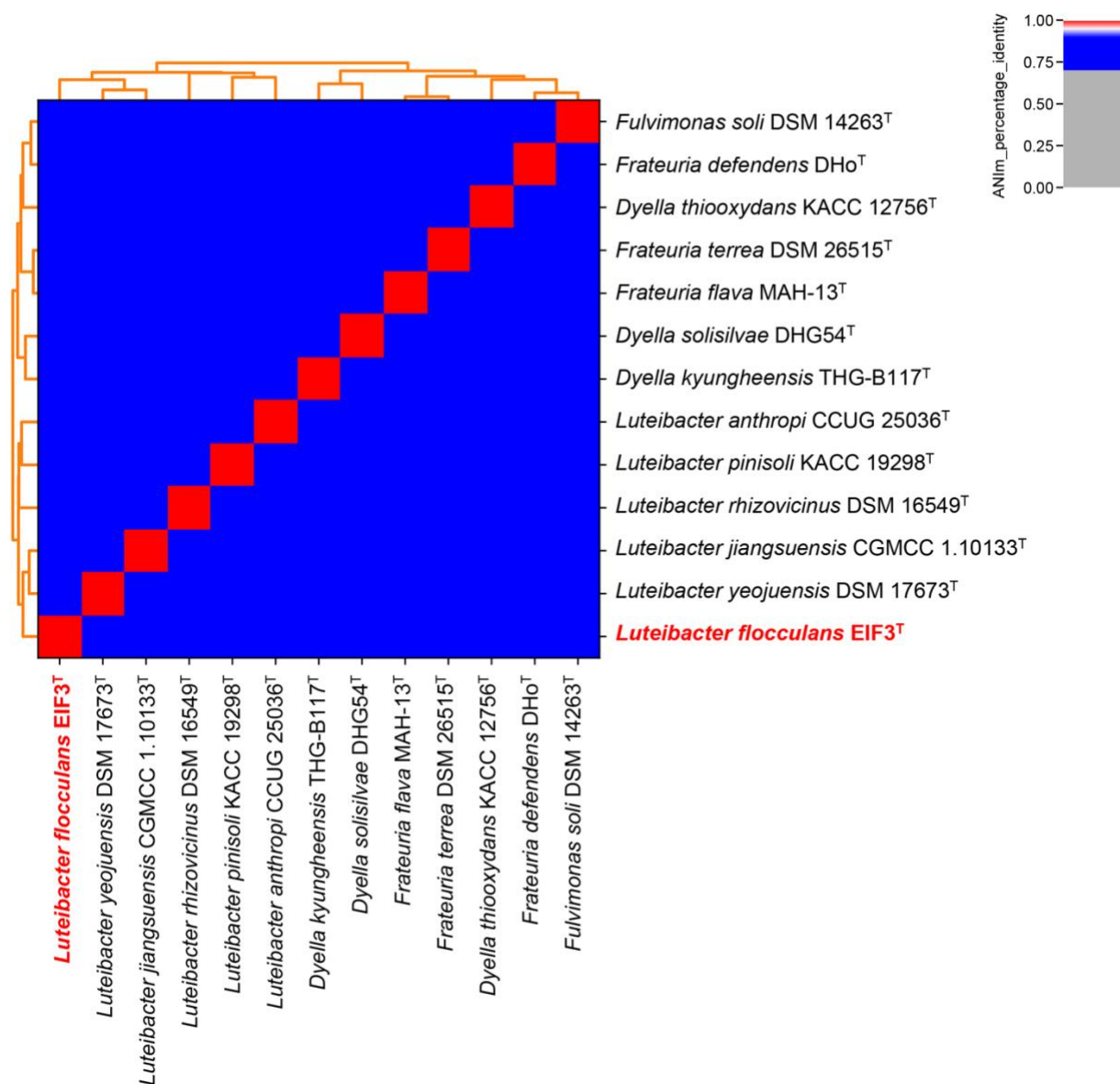


Fig 3. Genome-based classification of *Luteibacter flocculans* EIF3^T. All genome sequences from available type strains (T) listed in the TYGS database (25) were examined. Pyani (26,47) was used to calculate relatedness employing the ANIm technique and default settings. EIF3^T is highlighted in bold red letters.

Prophage Analysis

EIF3^T represented a prospective host system for the investigation of the environmental diversity of phages. Thus, the capabilities to host prophages was of particular interest in this study. Initial analysis of prophage regions with PHASTER (29) revealed two putative prophage regions (region 1, 1,300,438–1,322,193; region 2, 1,306,588–1,352,491). The regions were 21.7 and 45.9 kb in size. It was estimated that region 1 was incomplete and region 2 intact. In addition, region 1 was part of region 2 (Table S6). Since prophages can provide phage-resistance of the host, the genome of a potential for phage isolation must have a low number of prophages or none at all (7), which is applicable for EIF3^T.

Phage isolation and characterization

Luteibacter flocculans has proven to be an organism with minimal requirements for cultivation and proliferation. This provided a solid foundation for its prospective use in molecular biology. To evaluate its viability as a host strain for environmental phage isolations, EIF3^T was infected with a viral suspension obtained from raw sewage. To determine cell infection, an overlay plaque test was performed. To avoid redundancies during phage isolation, picked plaques were assessed by identifying the unique genetic restriction patterns of each phage isolate. This approach led to the isolation of a novel *Luteibacter*-associated phage.

Transmission electron microscopy shows a *Myo*-morphotype head-tail morphology (Figure 4). The phage consisted of an icosahedral head, contractile tail and tail spikes. The diameter of the capsid was 75 nm and the length of the tail 110 nm, resulting in a total length of 185 nm. We sequenced the viral DNA and assembled the genome with a high coverage of 690.1-fold. The assembled viral genome exhibited a size of 67,528 bp and a G + C content of 57.7% (host G + C content 64.8%). A total of 99 CDS of which 79 encode hypothetical proteins were detected. We detected genes similar to phage-related genes. These included genes such as encoding baseplate protein J, spike protein, major capsid protein, terminase large subunit and DNA polymerase.

Resulting from the morphological and genomic investigations, our phage was named vB_LflM-Pluto (vB = virus of bacter, Lfl = *L. flocculans*, M = *Myoviridae* morphotype, Pluto =

specific phage name). Our results represented the first description of a phage from the bacterial *Rhodanobacteraceae* family. In addition, we showed that *Luteibacter flocculans* sp. nov. is a suitable host strain for phage isolation.



Fig 4. *Luteibacter*-associated bacteriophage vB_LfIM-Pluto.

Conclusion

The results demonstrated the suitability of the novel *Luteibacter* species *L. flocculans* for the isolation of environmental phages. The isolation and characterization of a novel *Luteibacter*-associated phage vB_LfIM-Pluto, the first documented *Luteibacter*-associated phage, further supported this.

Description of *Luteibacter flocculans* sp. nov.

Luteibacter flocculans (floc.cu'ilans N.L. part. adj. *flocculans*, flocculating, pertaining to the organism's ability to flocculate in liquid cultures). *L. flocculans* cells were Gram-negative rod-shaped, 2.0 μm long and 0.7 μm wide. They did not form spores and were motile by means of lophotrichous bacteria. After 72 h of growth on LB medium, colonies were 1.93 mm in diameter and showed yellow pigmentation. Cells grow at 10–45 $^{\circ}\text{C}$ (optimum 30 $^{\circ}\text{C}$) and at 0–4% NaCl (optimum without addition of NaCl). The strain was catalase and oxidase positive. Cell growth occurred on R2A agar, TSA and LB agar. The strain was susceptible to erythromycin, tetracycline, and vancomycin, but not to ampicillin, kanamycin,

oxytetracycline, rifampicin and streptomycin. It utilized esculin/ferric citrate, D-glucose (assimilation), D-mannose, N-acetyl-D-glucosamine and malic acid employing the API 20NE test system. Alkaline phosphatase, esterase, esterase lipase, lipase, leucine arylamidase, valine arylamidase, cysteine arylamidase, acid phosphatase, naphthol-AS-BI-phosphohydrolase, β -galactosidase, α -glucosidase, β -glucosidase, and N-acetyl- β -glucosaminidase were detected with API ZYM test system. In Tables 1 and 2, additional phenotypic characteristics are depicted.

The type strain EIF3^T (=DSM 112537^T = LMG 32416^T), was isolated from a eutrophic pond located on the North Campus of the Georg-August University in Göttingen, Germany. The major fatty acids were C_{15:0 iso}, C_{17:0 iso}, and summed feature 9 (C_{17:1 iso} ω9c). The genome of the type strain showed a DNA G + C content of 64.8 mol%.

Acknowledgments

We thank Anja Poehlein for sequencing, Mechthild Bömeke for technical assistance, Dominik Schneider for his help with bioinformatics and Michael Hoppert for support with TEM-imaging. We thank Avril von Hoyningen-Huene for her meticulous proofreading of the manuscript.

References

1. Parte AC, Carbasse JS, Meier-Kolthoff JP, Reimer LC, Göker M. List of prokaryotic names with standing in nomenclature (LPSN) moves to the DSMZ. *Int J Syst Evol Microbiol.* 2020;70(11):5607–12.
2. Johansen JE, Binnerup SJ, Kroer N, Mølbak L. *Luteibacter rhizovicinus* gen. nov., sp. nov., a yellow-pigmented gammaproteobacterium isolated from the rhizosphere of barley (*Hordeum vulgare* L.). *Int J Syst Evol Microbiol.* 2005;55(6):2285–91.
3. Kim BY, Weon HY, Lee KH, Seok SJ, Kwon SW, Go SJ, et al. *Dyella yejuensis* sp. nov., isolated from greenhouse soil in Korea. *Int J Syst Evol Microbiol.* 2006;56(9):2079–82.
4. Kämpfer P, Lodders N, Falsen E. *Luteibacter anthropi* sp. nov., isolated from human blood, and reclassification of *Dyella yejuensis* Kim et al. 2006 as *Luteibacter yejuensis* comb. nov. *Int J Syst Evol Microbiol.* 2009;59(11):2884–7.
5. Wang L, Wang GL, Li SP, Jiang JD. *Luteibacter jiangsuensis* sp. nov.: a methamidophos-degrading bacterium isolated from a methamidophos-manufacturing factory. *Curr Microbiol.* 2011;62(1):289–95.
6. Akter S, Huq MdA. *Luteibacter pinisoli* sp. nov., a casein degrading bacterium isolated from rhizospheric soil of *Pinus koraiensis*. *Arch Microbiol.* 2018;200(7):1017–23.

7. Kohm K, Hertel R. The life cycle of SP β and related phages. *Arch Virol*. 2021;166(8):2119–30.
8. Friedrich I, Klassen A, Neubauer H, Schneider D, Hertel R, Daniel R. Living in a puddle of mud: Isolation and characterization of two novel *Caulobacteraceae* strains *Brevundimonas pondensis* sp. nov. and *Brevundimonas goettingensis* sp. nov. *Appl Microbiol*. 2021;1(1):38–59.
9. Couvin D, Bernheim A, Toffano-Nioche C, Touchon M, Michalik J, Néron B, et al. CRISPRCasFinder, an update of CRISPRFinder, includes a portable version, enhanced performance and integrates search for Cas proteins. *Nucleic Acids Res*. 2018;46(W1):W246–51.
10. Parks DH, Imelfort M, Skennerton CT, Hugenholtz P, Tyson GW. CheckM: assessing the quality of microbial genomes recovered from isolates, single cells, and metagenomes. *Genome Res*. 2015;25(7):1043–55.
11. Tatusova T, DiCuccio M, Badretdin A, Chetvernin V, Nawrocki EP, Zaslavsky L, et al. NCBI prokaryotic genome annotation pipeline. *Nucleic Acids Res*. 2016;44(14):6614–24.
12. Bolger AM, Lohse M, Usadel B. Trimmomatic: A flexible trimmer for Illumina sequence data. *Bioinformatics*. 2014;30(15):2114–20.
13. Magoč T, Salzberg SL. FLASH: Fast length adjustment of short reads to improve genome assemblies. *Bioinformatics*. 2011;27(21):2957–63.
14. Wick RR, Judd LM, Gorrie CL, Holt KE. Unicycler: Resolving bacterial genome assemblies from short and long sequencing reads. *PLoS Comput Biol*. 2017;13(6):1–22.
15. Bankevich A, Nurk S, Antipov D, Gurevich AA, Dvorkin M, Kulikov AS, et al. SPAdes: A new genome assembly algorithm and its applications to single-cell sequencing. *J Comput Biol*. 2012;19(5):455–77.
16. Camacho C, Coulouris G, Avagyan V, Ma N, Papadopoulos J, Bealer K, et al. BLAST+: architecture and applications. *BMC Bioinform*. 2009;10(1):421.
17. Langmead B, Salzberg SL. Fast gapped-read alignment with Bowtie 2. *Nat Methods*. 2012;9(4):357–9.
18. Li H, Handsaker B, Wysoker A, Fennell T, Ruan J, Homer N, et al. The sequence alignment/map format and SAMtools. *Bioinformatics*. 2009;25(16):2078–9.
19. Arnold K, Gosling J, Holmes D. The Java programming language. 4th ed. Lebanon, Indiana, USA: Addison-Wesley Professional; 2005.
20. Walker BJ, Abeel T, Shea T, Priest M, Abouelliel A, Sakthikumar S, et al. Pilon: An integrated tool for comprehensive microbial variant detection and genome assembly improvement. *PLoS ONE*. 2014;9(11):e112963.
21. Okonechnikov K, Conesa A, García-Alcalde F. Qualimap 2: Advanced multi-sample quality control for high-throughput sequencing data. *Bioinformatics*. 2016;32(2):292–4.
22. Kieft K, Zhou Z, Anantharaman K. VIBRANT: Automated recovery, annotation and curation of microbial viruses, and evaluation of viral community function from genomic sequences. *Microbiome*. 2020;8(1):90.
23. Zdobnov EM, Apweiler R. InterProScan - An integration platform for the signature-recognition methods in InterPro. *Bioinformatics*. 2001;17(9):847–8.
24. Chaumeil PA, Mussig AJ, Hugenholtz P, Parks DH. GTDB-Tk: a toolkit to classify genomes with the Genome Taxonomy Database. *Bioinformatics*. 2019;36(6):1925–7.
25. Meier-Kolthoff JP, Göker M. TYGS is an automated high-throughput platform for state-of-the-art genome-based taxonomy. *Nat Commun*. 2019;10(1):2182.
26. Pritchard L, Glover RH, Humphris S, Elphinstone JG, Toth IK. Genomics and taxonomy in diagnostics for food security: Soft-rotting enterobacterial plant pathogens. *Anal Methods*. 2016;8(1):12–24.

27. Kanehisa M, Sato Y, Morishima K. BlastKOALA and GhostKOALA: KEGG tools for functional characterization of genome and metagenome sequences. *J Mol Biol.* 2016;428(4):726–31.
28. Blin K, Shaw S, Kloosterman AM, Charlop-Powers Z, van Wezel GP, Medema MH, et al. antiSMASH 6.0: improving cluster detection and comparison capabilities. *Nucleic Acids Res.* 2021;49(W1):W29–35.
29. Arndt D, Grant JR, Marcu A, Sajed T, Pon A, Liang Y, et al. PHASTER: a better, faster version of the PHAST phage search tool. *Nucleic Acids Res.* 2016;44(Web Server issue):W16–21.
30. Gibson MK, Forsberg KJ, Dantas G. Improved annotation of antibiotic resistance determinants reveals microbial resistomes cluster by ecology. *ISME J.* 2015;9(1):207–16.
31. Claus D. A standardized Gram staining procedure. *World J Microbiol Biotechnol.* 1992;8(4):451–2.
32. Abraham WR, Strompl C, Meyer H, Lindholm S, Moore ERB, Christ R, et al. Phylogeny and polyphasic taxonomy of *Caulobacter* species. Proposal of *Maricaulis* gen. nov. with *Maricaulis maris* (Poindexter) comb. nov. as the type species, and emended description of the genera *Brevundimonas* and *Caulobacter*. *Int J Syst Evol Microbiol.* 1999;49(3):1053–73.
33. R Core Team. R: a language and environment for statistical computing [Internet]. R Foundation for Statistical Computing, Vienna, Austria; 2020. Available from: <https://www.r-project.org/>
34. Wickham H. ggplot2 – elegant graphics for data analysis. Vol. 77, *Journal of Statistical Software*. New York, NY: Springer New York; 2009. 1 p.
35. Bruder S, Reifenrath M, Thomik T, Boles E, Herzog K. Parallelized online biomass monitoring in shake flasks enables efficient strain and carbon source dependent growth characterization of *Saccharomyces cerevisiae*. *Microb Cell Fact.* 2016;1–14.
36. Wickham H. *Journal of Statistical Software.* 2017;77:3–5.
37. Clarke PH, Cowan ST. Biochemical methods for bacteriology. *J Gen Microbiol.* 1952;6(1–2):187–97.
38. Willms IM, Hertel R. Phage vB_BsuP-Goe1: the smallest identified lytic phage of *Bacillus subtilis*. *FEMS Microbiol Lett.* 2016;363(19):fnw208.
39. Willms I, Hoppert M, Hertel R. Characterization of *Bacillus subtilis* viruses vB_BsuM-Goe2 and vB_BsuM-Goe3. *Viruses.* 2017;9(6):146.
40. Kropinski AM, Mazzocco A, Waddell TE, Lingohr E, Johnson RP. Enumeration of bacteriophages by double agar overlay plaque assay. *Methods Mol Biol.* 2009;501:69–76.
41. Adriaenssens E, Brister JR. How to name and classify your phage: An informal guide. *Viruses.* 2017;9(4):70.
42. Naushad S, Adeolu M, Wong S, Sohail M, Schellhorn HE, Gupta RS. A phylogenomic and molecular marker based taxonomic framework for the order Xanthomonadales: proposal to transfer the families *Algiphilaceae* and *Solimonadaceae* to the order Nevskiales ord. nov. and to create a new family within the order Xanthomonadales, the family *Rhodanobacteraceae* fam. nov., containing the genus *Rhodanobacter* and its closest relatives. *Antonie Leeuwenhoek.* 2015;107(2):467–85.
43. Rajagopal L, Sundari CS, Balasubramanian D, Sonti RV. The bacterial pigment xanthomonadin offers protection against photodamage. *FEBS Lett.* 1997;415(2):125–8.
44. Zhao F, Guo X qi, Wang P, He L yan, Huang Z, Sheng X fang. *Dyella jiangningensis* sp. nov., a γ -proteobacterium isolated from the surface of potassium-bearing rock. *Int J Syst Evol Microbiol.* 2013;63(Pt_9):3154–7.
45. Reimer LC, Vetcininova A, Carbasse JS, Söhngen C, Gleim D, Ebeling C, et al. BacDive in 2019: bacterial phenotypic data for high-throughput biodiversity analysis. *Nucleic Acids Res.* 2019;47(Database issue):D631–6.

-
46. Chun J, Oren A, Ventosa A, Christensen H, Arahal DR, da Costa MS, et al. Proposed minimal standards for the use of genome data for the taxonomy of prokaryotes. *Int J Syst Evol Microbiol.* 2018;68(1):461–6.
47. Richter M, Rosselló-Móra R. Shifting the genomic gold standard for the prokaryotic species definition. *PNAS.* 2009;106(45):19126–31.

Supporting Information

Data File S1. GTDB-Tk of *Luteibacter flocculans* sp. nov. isolate.

The data can be found on the enclosed CD and .zip folder:

Supplement\Chapter_3.9\S1_Data_File.tsv

Table S1. KEGG Mapper Reconstruction Result of *Luteibacter flocculans* EIF3^T chromosome.

Table S2. Resfams prediction of *Luteibacter flocculans* EIF3^T.

Table S3. List of putative biosynthetic gene clusters in *Luteibacter flocculans* EIF3^T.

Table S4. Pairwise comparisons of EIF3 against type strain genomes from TYGS (Meier-Kolthoff and Göker, 2019).

Table S5. Phylogenetic analysis for *Luteibacter flocculans* EIF3^T.

Table S6. PHASTER analysis of *Luteibacter flocculans* EIF3^T.

The tables can be found on the enclosed CD and .zip folder:

Supplement\Chapter_3.9\Tables_S1-S6.xlsx



Figure S1. Flocculation of EIF3^T in LB medium.

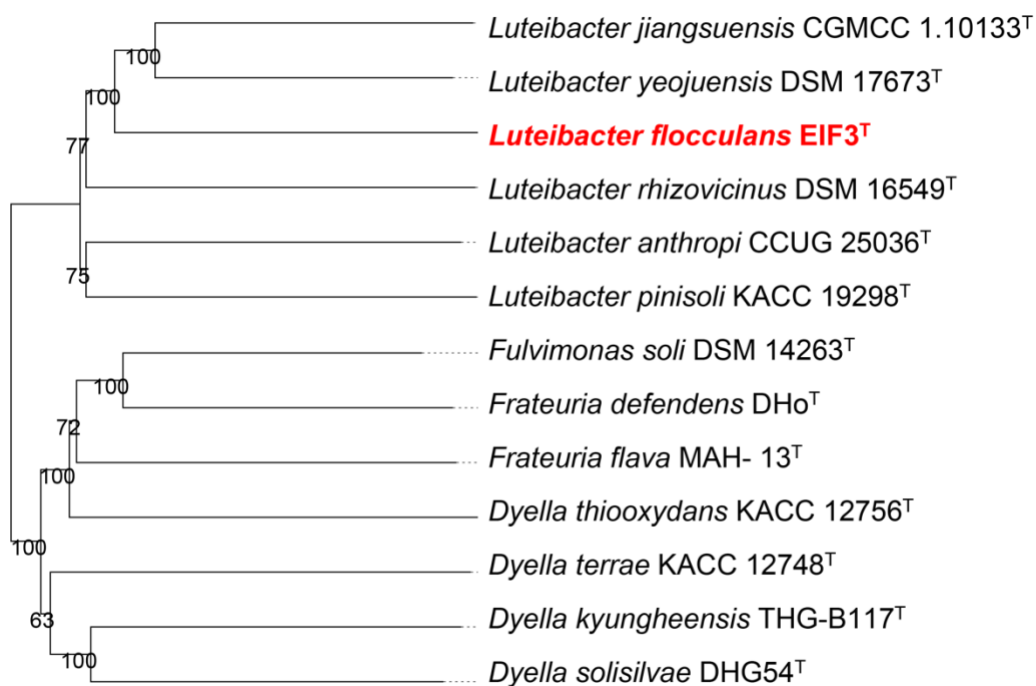


Figure S2. Phylogenetic classification of *Luteibacter flocculans* EIF3^T. The 12 closest related type strain genomes were used for phylogenetic analysis as described by TYGS (Meier-Kolthoff and Göker, 2019). The tree was inferred with FASTME 2.1.6.1 (Lefort et al., 2015) using Genome Blast Distance Phylogeny (GBDP) distances calculated from genome sequences. The branch lengths are scaled in terms of GBDP distance formula d5. The numbers above the branches are GBDP pseudo-bootstrap support values of >60% from 100 replications, with an average branch support of 85.1%. The tree was rooted at the midpoint (Farris, 1972). Meier-Kolthoff JP, Göker M. TYGS is an automated high-throughput platform for state-of-the-art genome-based taxonomy. Nat Commun. 2019;10(1):2182.

Lefort V, Desper R, Gascuel O. FastME 2.0: a comprehensive, accurate, and fast distance-based phylogeny inference program. Mol Biol Evol. 2015;32(10):2798–800.

Farris JS. Estimating phylogenetic trees from distance matrices. Am Nat. 1972;106(951):645–68.

General Discussion

Due to the employed strategy's impact on assessing phages, it is essential to apply various techniques to uncover viral diversity. Different approaches have been developed to characterize the variety of phages within biological communities. These include, culture and microscopy, genomics of an isolated single virus and metagenomics. The combination of culturing procedures and transmission electron microscopy observations enabled the discovery of phages that would otherwise be missed due to sequencing biases. Single-virus genomics allows the sequencing of individual virions, which helps to assess phage populations with a high level of microdiversity that typically blocks genome assembly in metagenomic workflows. The rapid discovery of an astounding number of phages in different environmental settings, ranging from the human digestive tract to the depths of the ocean, has been assisted by technological advances in viral metagenomics. While it has been shown that these developments have expanded our understanding of the genomic variety of phages, it has also demonstrated that we have just begun the process of discovering novel viruses. One may conclude from searching sequence databases of viral genomes, that dsDNA bacteriophages comprise the majority of the viral world. Therefore, the purpose of this thesis was to establish whether this is true or just a systematic artifact of how we often approach the viral world. This was investigated by using host systems which might be associated with various RNA and DNA viruses. These bacterial host systems were isolated and characterized regarding their morphological, physiological, and genomic features.

1. Isolation of bacterial host systems and their characterization

In Chapter 3.1, enrichment of water samples showed that in the oligotrophic samples mostly members of the order Burkholderiales, Enterobacterales, and Pseudomonadales were present.

The eutrophic samples showed a more diverse distribution of bacterial orders. Copiotrophic and oligotrophic bacteria may coexist in freshwater ponds due to changes in nutrient availability and the presence of microniches. The pond selected for sampling was located in the Northern part of Weende, Göttingen, Germany and has a permanent water flow-through from a water extraction plant. Similar results were obtained in marine environments (Rodrigues and de Carvalho, 2022). In this work, a total of 37 new bacterial strains were isolated successfully, of which ten belong to Burkholderiales, three to Enterobacteriales, and three to Pseudomonadales. The remaining 24 isolates are distributed over the orders Flavobacteriales, Aeromonadales, Xanthomonadales, Pseudonocardiales, Lysobacterales, Sphingobacteriales, Caulobacterales, Micrococcales, and Sphingomonadales.

In this thesis, eight bacterial strains from oligotrophic or eutrophic environments were successfully isolated, sequenced, assembled and their whole genome sequences were analyzed (Chapter 3.1–3.5, 3.8, and 3.9). The suitability of the strains as viral host systems was investigated. A total of four bacterial isolates were characterized additionally regarding their morphology and physiology (*Brevundimonas pondensis*, *B. goettingensis*, *Serratia marcescens*, *Janthinobacterium lividum* and *Luteibacter flocculans*). An overview of the important characteristics is shown in Table 1. All, except *J. lividum* EIF2, proved to be suitable host systems due to their small number of prophages. Prophages provide additional genetic information and can supply the host with extra properties such as bacterial fitness through the transfer of beneficial genes (e.g., antibiotic-resistance genes) or protection from superinfecting phages resulting in a competitive advantage.

Table 1. Characteristics of bacterial isolates for the investigation of viral communities. PW: oligotrophic pond water, PUW: puddle water, WSP: surface water near frog's lettuce, PM: frog's lettuce, WSA: surface water near pond algae, POW: surface water of eutrophic pond; n/a: not available.

Strain	Origin	Chromosome size [bp]	Plasmid size [bp]	Prophages in chromosome	Prophages in plasmid	Motile
<i>Brevundimonas pondensis</i> LVF1	PW	3,550,773	-	2	-	yes
<i>Brevundimonas goettingensis</i> LVF2	PUW	3,984,955	-	1	-	yes
<i>Janthinobacterium lividum</i> EIF1	WSP	6,737,589	-	2	-	yes
<i>Janthinobacterium lividum</i> EIF2	PM	6,399,352	356,839	8	1	yes
<i>Kimmeretia</i> sp. DAIF2	WSA	6,010,585	-	1	-	n/a
<i>Luteibacter flocculans</i> EIF3	POW	4,299,254	-	2	-	yes
<i>Serratia marcescens</i> LVF3	WSP	5,440,698	87,710	2	-	yes
<i>Stenotrophomonas indicatrix</i> DAIF1	PM	4,639,375	-	3	-	n/a

For the investigation of viral isolates and their viral communities, the most suitable putative host strains were *Brevundimonas pondensis* EIF1, *Brevundimonas goettingensis* EIF2 and *Serratia marcescens*. These species are closely related with *Caulobacter* and *Escherichia*, respectively. Both named species are associated with DNA and diverse RNA viruses. For *Caulobacter crescentus* dsDNA giant phage ϕ Cp34 has been isolated (Fukuda et al., 1976), as well RNA phages (Miyakawa et al., 1976). The genus *Escherichia* is associated with ssDNA phage ϕ X174 (Sanger et al., 1977), dsDNA phage T7 (Demerec and Fano, 1945) and ssRNA phage MS2 (Davis et al., 1961).

In chapter 3.1, even though, a member of the *Caulobacter* genus could not be isolated, two other interesting isolates were recovered – the two bacterial isolates *Brevundimonas pondensis* LVF1 and *Brevundimonas goettingensis* LVF2. Both were considered as putative host organisms as several species of the genus *Caulobacter* were grouped into the genus *Brevundimonas* during reclassification (Abraham et al., 1999). Whole-genome sequencing showed them to be new type species which have been deposited at the DSMZ (Deutsche Sammlung von Mikroorganismen und Zellkulturen), CCUG (Culture Collection University of Gothenburg), and BCCM (Belgian Co-ordinated Collections of Micro-organisms). Besides the differences in the genomes, both species also exhibit phenotypic and morphological differences. LVF1 colonies are grayish-white, while LVF2 colonies are yellow. Genes coding for carotenoids were found in the genome of LVF2 (yellowish colony). Some *Brevundimonas* species are capable of synthesizing carotenoids (Abraham et al., 2014), which are likely the source of the pigmentation. Carotenoids are secondary metabolites that play crucial roles in the adaptation of heterotrophic bacteria. In addition to protecting cells from UV radiation and oxidative damage (Krinsky, 1978; Miller et al., 1996), carotenoids are also involved in mechanisms controlling membrane fluidity (Jagannadham et al., 2000; Subczynski et al., 1992) as they are located in the cell membrane as lipophilic compounds (Seel et al., 2020). Growth at low temperatures and the management of nutrient transport depend on the fluidity and structure of the cell membrane. Seel et al. found that at low temperatures in *Staphylococcus xylosus* there is an increase in membrane order accompanied by an increase in membrane fluidity, as well as a broadening of the phase transition (Seel et al., 2020). In *Brevundimonas goettingensis*, the production of carotenoids could also be observed during growth at an extreme temperature, such as 4 °C (Friedrich et al., 2021c). In the genome of LVF1 (white

colony), no putative genes to produce carotenoids were identified, which may be the reason for its inability to grow at low temperatures (Friedrich et al., 2021c). *B. goettingensis* LVF2 revealed both prosthecate and non-prosthecate vibrio-shaped cell types, while *B. pondensis* LVF1 exclusively showed motile cells with polar flagella.

From the remaining 35 isolates, the copiotrophic bacterial isolate *Serratia marcescens* LVF3 (chapter 3.2) was chosen as the second host system, as it is part of the same order (Enterobacterales) as *Escherichia*. In addition, Falkow et al. showed that a phage isolated from sewage was able to infect *Serratia marcescens* and *Escherichia coli* (Falkow et al., 1961). This indicated the potential of *Serratia marcescens* as host for infection by phages with a broad host range. The *S. marcescens* LVF3 isolate displays typical morphological characteristics of the genus *Serratia*. These are motile by means of polar flagella, their cell size ranges from 0.9–2.0 µm and are rod-shaped cells with rounded ends (Grimont and Grimont, 1978). Further, *S. marcescens* LVF3 showed growth up to 10% (w/v) NaCl in TSB medium, which was also observed for related strains (Grimont and Grimont, 1978). To conclude, *B. pondensis* LVF1 and *S. marcescens* LVF3 were chosen as they are closely related to either *Caulobacter* or *Escherichia*, in which a huge number of DNA and RNA phages could potentially be isolated and sequenced.

The strains *Janthinobacterium lividum* EIF1 and EIF2 (Chapter 3.3) are able to produce the purple pigment violacein which has antitumor, antiviral, antifungal and antimicrobial properties (Andrighetti-Fröhner et al., 2003; Asencio et al., 2014; Bromberg et al., 2010). In Chapter 3.8, we discovered phage-based induction of violacein synthesis by *J. lividum* EIF1. Violacein is a medically relevant antibacterial agent. It appears that phage vB_JliS-Donnerlittchen induces its host to release a signaling molecule that stimulates uninfected cells to produce violacein. A previous study demonstrate that violacein inhibits the replication of human herpes simplex virus type 1 and polio (Andrighetti-Fröhner et al., 2003). The study by Lee et al. found that violacein-embedded membranes inactivate viruses within 4 h (influenza and coronavirus) and bacteria within 2 h (Lee et al., 2022). This makes the discovery of violacein's antiviral activity even more important. *Janthinobacterium* phage vB_JliS-Donnerlittchen is the first sequenced *Janthinobacterium*-associated bacteriophage. In the study of Li et al., one *Janthinobacterium*-associated bacteriophage was isolated but not sequenced. It

proved to be of a *Sipho* morphotype with a probable genome size between 65 and 70 kb (Li et al., 2016), and shows no relation to isolate vB_JliS-Donnerlittchen. Further phage genomes are unknown for the *Oxalobacteraceae* family. The order Burkholderiales harbors 341 associated bacteriophages (mostly dsDNA, but also some ssDNA phages) in the NCBI Virus database (Brister et al., 2015) (accessed on 30 August 2022). None of these belong to the same genus as *Janthinobacterium*-associated phage vB_JliS-Donnerlittchen.

Another interesting novel host strain is *Luteibacter flocculans* EIF3 (chapter 3.9) which differs from other *Luteibacter* strains (Akter and Huq, 2018; Johansen et al., 2005; Kämpfer et al., 2009) in that it has multiple flagella at one end (lophotrichous), which might be an explanation for its ability to flocculate in liquid medium. In a previous study of *Bacillus*, *Pseudomonas*, *Vibrio*, and *Escherichia* on biofilm formation showed, that flagella were regulated on the short term to either inhibit rotation or modulate the basal flagellar inversion. Whereas over the long term, flagellar gene transcription was inhibited and flagella were not produced and result in non-motile bacteria (Guttenplan and Kearns, 2013). Further, isolate *L. flocculans* produces the yellow pigment xanthomonadin, which is water insoluble. This result is in good agreement with characteristics of *Rhodanobacteraceae* family members (Naushad et al., 2015). In a study by Rajagopal et al., the authors discovered that xanthomonadin may protect *Xanthomonas oryzae* against photodamage (Rajagopal et al., 1997). For the genus *Luteibacter* and the whole order Lysobacterales, no bacteriophage has been isolated or sequenced. The isolated *Luteibacter* phage vB_LflM-Pluto is the first sequenced, described, morphologically and genomically characterized phage of this order. TEM imaging of the bacteriophage indicated a myovirus morphotype like T4 phage (Yap et al., 2016). This was further confirmed through genome analysis, showing that it harbors genes coding for baseplate or spike proteins. The genus *Kinneretia* is part of the family *Comamonadaceae* which shows high abundances in freshwater habitats and is therefore ubiquitous (Moon et al., 2018). Only a small number of 17 phages are associated with the family *Comamonadaceae* of which all are dsDNA phages (Brister et al., 2015). Further studies on isolate *Kinneretia* sp. DAIF2 (Chapter 3.5) and other strains could help to investigate the viral diversity associated with this bacterial isolate. In Chapter 3.4, *Stenotrophomonas indicatrix* DAIF1 proved to be a promising host strain for comparative genomics using clinical isolates (Friedrich et al., 2021b) but also for phage enrichment (Table 1). Phages associated with the genus *Stenotrophomonas* are also of great interest, as the human

pathogen *S. maltophilia* is known as a multidrug resistance opportunistic pathogen (Brooke, 2012). Since *Stenotrophomonas indicatrix* is not pathogenic, viral diversity associated with *Stenotrophomonas* can be studied without risking exposure to the pathogenic bacterium *S. maltophilia*. Immunocompromised patients should especially be concerned about the rising frequency of nosocomial and community-acquired *S. maltophilia* infections, as this bacterial pathogen is associated with a high fatality-to-case ratio. Currently, 81 phage genomes (either consisting of dsDNA or ssDNA) are available in the NCBI Virus database (Brister et al., 2015).

2. Ways to analyze phage-host interaction

Here, the classical plaque assay and NGS-based methods were used in a complementary approach to isolate new phages (Chapter 3.6). The isolation of 25 novel phages was possible, 14 of which are *Brevundimonas pondensis*- and 11 are *Serratia marcescens*-associated bacteriophages. Chapter 3.7 showed that the overlay assay is capable of capturing the majority of viral dsDNA diversity. Most bacteriophages associated with both host strains were isolated, as confirmed by the virome data. However, differences in the host system and a seasonal effect were observed. In addition, the study demonstrated that the *S. marcescens*-associated virome contained numerous phage-associated contigs that did not belong to known *Yersiniaceae*-infecting phages. These were phages associated with *Erwinia*, *Salmonella*, or *Cronobacter*. Phages associated with *Serratia* are often able to infect other genera (Evans et al., 2010; Prinsloo, 1966; Prinsloo and Coetzee, 1964).

The dsDNA virome of both isolates – *Serratia marcescens* LVF3 and *Brevundimonas pondensis* LVF1 – showed that the classical plaque assay is very efficient, however ssDNA, ssRNA and dsRNA bacteriophages could not be isolated using this approach. The isolation of phages not initially detected by the classical approach of plaque-picking demonstrated the value of performing a concomitant host-associated virome analysis. For example, the phage vB_SmaP-Kaonashi could only be isolated after identification in the corresponding virome dataset. Since only dsDNA phages could be isolated, gel filtration chromatography was used in a preliminary experiment. This is a common biochemical method for the analysis and

purification of proteins within a mixture. Since bacteriophages consist of a capsid composed of protein-compromising subunits, the aim was to investigate whether gel filtration chromatography could be used to separate bacteriophages according to their molecular weight and thus be able to potentially isolate them. For the phage isolates from *Brevundimonas* phages vB_BpoS-Domovoi and vB_BpoS-Babayka, separation by gel filtration chromatography was generally possible and plaque assays showed that they retained the ability to infect. However, the experiment also highlighted the disadvantage that some phages may have lost their tails and were therefore present as “contaminants”, although they were no longer infectious (determined through PCR analysis). One of the next steps would be to optimize this method for later separation of virome samples according to size, in order to isolate potentially smaller phages (RNA or ssDNA phages). In comparison, the method of Vandenneuvel et al., successfully used anion-exchange chromatography to purify one phage (Vandenneuvel et al., 2018) depending on the affinity of the phage to an immobilized ligand. In contrast, gel filtration chromatography-based separation depends on the differences in molecular weight or size of the sample.

Further, in another study, the virome and viral diversity of *Brevundimonas goettingensis* LVF2 was investigated (unpublished data). Interestingly, the bacteriophages associated with these bacterial strains differ considerably, although *B. pondensis* and *B. goettingensis* belong to the same genus. Whereas the majority of the virome associated with *B. pondensis* (from both seasons) are giant phages (genome size over 300,000 bp), the *B. goettingensis*-associated virome contains phages with a much smaller genome size of approximately 85 kb (Supplement Table S1). This could be due to the different life cycles of the two host strains. It appears that the giant phages are dependent on the swarmer cell stage of *B. pondensis*, as they require more time to replicate compared to “usual” phages. This can be investigated in future studies by infecting *B. goettingensis* with phages associated with *B. pondensis*. In a study by Johnson et al., the same trend was observed with *Caulobacter*-associated phages infecting only swarmer cells (Johnson et al., 1977).

The ssDNA virome sequence analysis of *Brevundimonas pondensis* suggested that only a small number of ssDNA phages were present in the samples, which would explain the absence of isolates. Infection of this group of phages is reduced by the use of traditional

isolation methods. *Inoviridae* infections are not fatal and do not always result in a visible plaque, which is required for the identification and isolation of a phage. *Microviridae*-like phages in the metaviral sample of the summer could be detected using transmission electron microscopy (Figure 8A, Chapter 3.7). The phages were spherical and lacked tails, possessed an icosahedral symmetry, and measured around 30 nm in diameter. A preliminary experiment could also detect filamentous *Inoviridae*-like phage structures in a metaviral sample (Figure 8B, Chapter 3.7). In summary, the combination of morphological analysis and ssDNA virome research demonstrated that the *B. pondensis* LVF1 host system might be infected with *Microviridae* and *Inoviridae* phages.

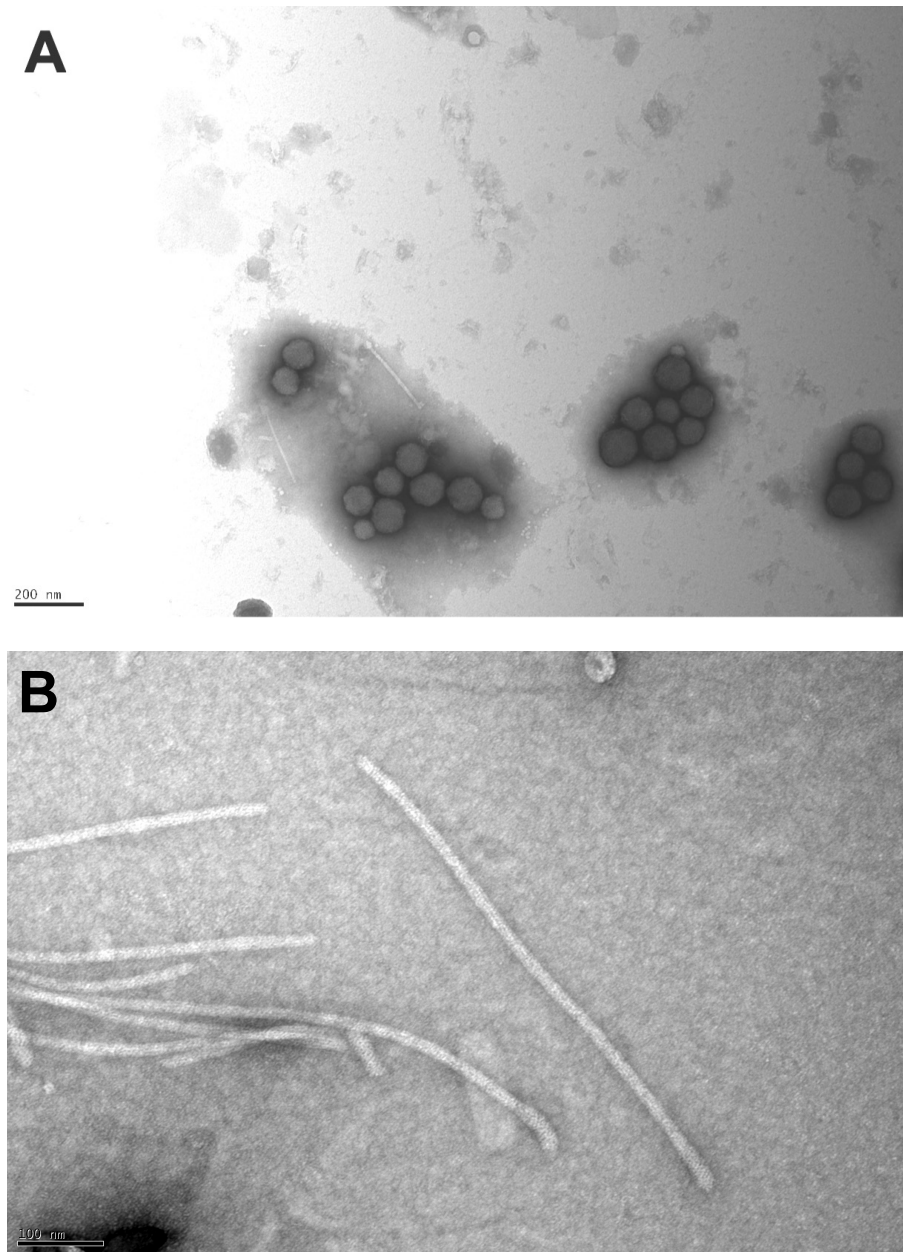


Figure 8. TEM images of potential (A) *Microviridae* and (B) *Inoviridae* phages associated with *Brevundimonas pondensis* LVF1.

In the study with *B. goettingensis* as host an RNA contig displayed a significant degree of similarity with phiCb5 (Supplement File S1), a ssRNA phage of *Caulobacter crescentus*, which is a member of the *Leviviridae* family (Plevka et al., 2009). Following annotation of this contig, a gene encoding RNA-dependent RNA-polymerase was identified (Supplement File S2; Figure 9, Chapter 3.7). Bendis and Shapiro discovered that bacteriophage phiCb5 infects exclusively the swarmer cell type of the dimorphic stalked bacterium (Bendis and Shapiro, 1970). Here, the question arises if the temperate stadium of a swarmer cell somehow promotes

infections with RNA phages. In future, the putative phage showing high similarity to phiCb5 should be isolated and investigated in detail. Also, it should be tested whether the sister strain of *B. goettingensis* – *B. pondensis* – can be infected by the same RNA phage similar to phiCb5.

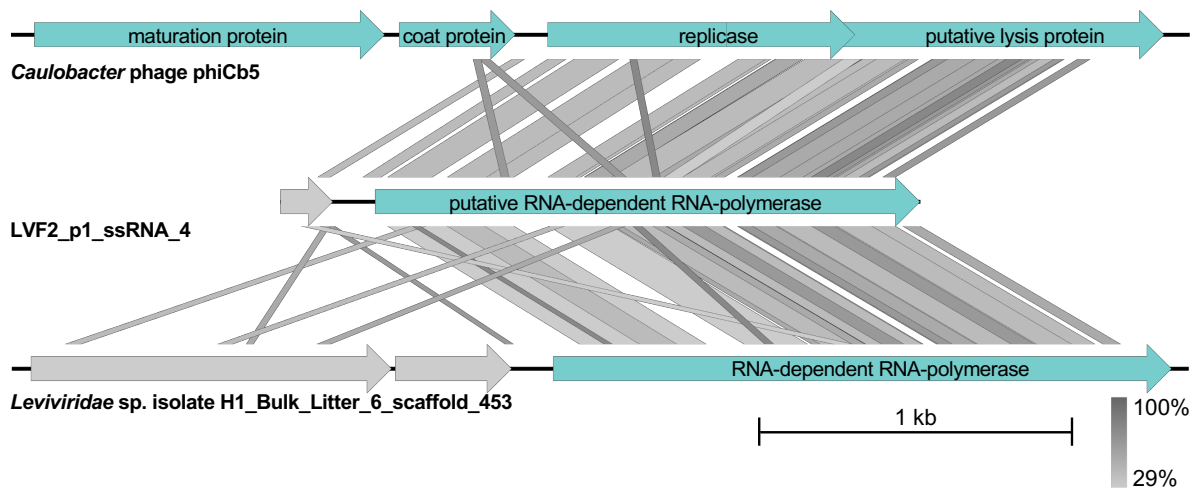


Figure 9. Comparing the contigs with best Blastn matches. Arrow indicates gene direction. Phage specific gene products are shown in light blue with corresponding labeling and hypothetical proteins in light grey. Comparison of contig 4 with *Caulobacter* phage phiCb5 and *Leviviridae* sp. isolate H1_Bulk_Litter_6_scaffold_453. Plot was done using Easyfig (Sullivan et al., 2011)

To access predicted bacteriophages in the future, new or specialized experimental methods will be required. Here, a combination of two methods could be used. The virome after phage enrichment via plaque assay could be further separated via gel filtration chromatography regarding the phage sizes present in the virome. With gel filtration chromatography, smaller phages e.g., ssDNA and RNA phages could therefore be isolated and would give more insights into phages associated with their bacterial host systems. Further, the study of the virome associated with *Brevundimonas goettingensis* and *Brevundimonas pondensis* indicates that viral diversity differs from species to species even within close relatives of a genus. This should further be considered. The environmental niche of the bacterial hosts must also be chosen carefully. In a study by Wu et al., bacterial populations were effectively eliminated by the phages under eutrophic conditions, while the rate of lysis slowed down under oligotrophic conditions (Wu, Hanqing et al., 2022). This

phenomenon could be an answer to why the phage diversity of *Brevundimonas* seems to be much higher than that of *Serratia*.

The results of this thesis showed that the viral sphere is still dark matter. Classical methods using overlay plaque assay still bear a high potential for the investigation of novel phages (especially dsDNA phages). Nevertheless, the study provided an excellent starting point for isolation of new phages by combining NGS-based approaches with phage isolation using plaque overlay assays. With this approach, vB_SmaP-Kaonashi, a virus that uses both host systems for replication was identified (Chapter 3.7). This thesis showed that by combining metagenomics, single-virus genomics, and microscopy, the viral diversity can further be uncovered. These results further indicate that dsDNA phages are the most abundant type of phages. Nonetheless, the results of ssDNA and ssRNA viromes provide insights into the diversity of potential phages, which are usually overlooked. Here, further isolation needs to be done following optimization of the method. By not only using the overlay plaque assay method, liquid cell cultures with and without shaking can lead to recovery of a different phage diversity. Another possibility is the use of gel filtration chromatography after phage centrifugation and filtration to obtain phages with a smaller molecular weight. These could include small ssDNA phages like *Microviridae* and ssRNA phages like *Leviviridae*. In addition, the phage isolate vB_JliS-Donnerlittchen has yielded interesting results as it stimulates violacein production in *J. lividum* EIF1. The purple pigment violacein can be further investigated by isolating it and determining its effect on phage infection during exposure to different *Janthinobacterium* species.

General References

Abraham, W.-R., Estrela, A.B., Nikitin, D.I., Smit, J., Vancanneyt, M., 2010. *Brevundimonas halotolerans* sp. nov., *Brevundimonas poindexteræ* sp. nov. and *Brevundimonas staleyi* sp. nov., prosthecate bacteria from aquatic habitats. *Int J Syst Evol Microbiol* 60, 1837–1843. <https://doi.org/10.1099/ijs.0.016832-0>

Abraham, W.-R., Rohde, M., Bennasar, A., 2014. The family *Caulobacteraceae*, in: Rosenberg, E., DeLong, E.F., Lory, S., Stackebrandt, E., Thompson, F. (Eds.), *The Prokaryotes*. Springer Berlin Heidelberg, Berlin, Heidelberg, pp. 179–205. https://doi.org/10.1007/978-3-642-30197-1_259

Abraham, W.-R., Strompl, C., Meyer, H., Lindholst, S., Moore, E.R.B., Christ, R., Vancanneyt, M., Tindall, B.J., Bennasar, A., Smit, J., Tesar, M., 1999. Phylogeny and polyphasic taxonomy of *Caulobacter* species. Proposal of *Maricaulis* gen. nov. with *Maricaulis maris* (Poindexter) comb. nov. as the type species, and emended description of the genera *Brevundimonas* and *Caulobacter*. *Int J Syst Evol Microbiol* 49, 1053–1073. <https://doi.org/10.1099/00207713-49-3-1053>

Abreo, E., Altier, N., 2019. Pangenome of *Serratia marcescens* strains from nosocomial and environmental origins reveals different populations and the links between them. *Sci Rep* 9, 1–8. <https://doi.org/10.1038/s41598-018-37118-0>

Adeolu, M., Alnajar, S., Naushad, S., S. Gupta, R., 2016. Genome-based phylogeny and taxonomy of the ‘Enterobacteriales’: proposal for Enterobacterales ord. nov. divided into the families *Enterobacteriaceae*, *Erwiniaceae* fam. nov., *Pectobacteriaceae* fam. nov., *Yersiniaceae* fam. nov., *Hafniaceae* fam. nov., *Morganellaceae* fam. nov., and *Budviciaceae* fam. nov. *Int J Syst Evol Microbiol* 66, 5575–5599. <https://doi.org/10.1099/ijsem.0.001485>

Ajithkumar, B., Ajithkumar, V.P., Iriye, R., Doi, Y., Sakai, T., 2003. Spore-forming *Serratia marcescens* subsp. *sakuensis* subsp. nov., isolated from a domestic wastewater treatment tank. *Int J Syst Evol Microbiol* 53, 253–258. <https://doi.org/10.1099/ijs.0.02158-0>

Akter, S., Huq, Md.A., 2018. *Luteibacter pinisoli* sp. nov., a casein degrading bacterium isolated from rhizospheric soil of *Pinus koraiensis*. *Arch Microbiol* 200, 1017–1023. <https://doi.org/10.1007/s00203-018-1515-1>

Ambrožič Avguštin, J., Žgur Bertok, D., Kostanjšek, R., Avguštin, G., 2013. Isolation and characterization of a novel violacein-like pigment producing psychrotrophic bacterial species *Janthinobacterium svalbardensis* sp. nov. *Antonie Leeuwenhoek* 103, 763–769. <https://doi.org/10.1007/s10482-012-9858-0>

Andrighetti-Fröhner, C., Antonio, R., Creczynski-Pasa, T., Barardi, C., Simões, C., 2003. Cytotoxicity and potential antiviral evaluation of violacein produced by *Chromobacterium violaceum*. *Mem Inst Oswaldo Cruz* 98, 843–848. <https://doi.org/10.1590/S0074-02762003000600023>

- Asencio, G., Lavin, P., Alegría, K., Domínguez, M., Bello, H., González-Rocha, G., González-Aravena, M., 2014. Antibacterial activity of the Antarctic bacterium *Janthinobacterium* sp. SMN 33.6 against multi-resistant Gram-negative bacteria. *Electron J Biotechnol* 17, 1–5. <https://doi.org/10.1016/j.ejbt.2013.12.001>
- Baldani, J.I., Rouws, L., Cruz, L.M., Olivares, F.L., Schmid, M., Hartmann, A., 2014. The family *Oxalobacteraceae*, in: Rosenberg, E., DeLong, E.F., Lory, S., Stackebrandt, E., Thompson, F. (Eds.), *The Prokaryotes*. Springer Berlin Heidelberg, Berlin, Heidelberg, pp. 919–974. https://doi.org/10.1007/978-3-642-30197-1_291
- Beilstein, F., Dreiseikelmann, B., 2006. Bacteriophages of freshwater *Brevundimonas vesicularis* isolates. *Res Microbiol* 157, 213–219. <https://doi.org/10.1016/j.resmic.2005.07.005>
- Bendis, I., Shapiro, L., 1970. Properties of *Caulobacter* ribonucleic acid bacteriophage ϕ Cb5. *J Virol* 6, 847–854. <https://doi.org/10.1128/jvi.6.6.847-854.1970>
- Bennett, J.W., Bentley, R., 2000. Seeing red: the story of prodigiosin. *Adv Appl Microbiol* 47, 1–32. [https://doi.org/10.1016/s0065-2164\(00\)47000-0](https://doi.org/10.1016/s0065-2164(00)47000-0)
- Bhetwal, A., Maharjan, A., Shakya, S., Satyal, D., Ghimire, S., Khanal, P.R., Parajuli, N.P., 2017. Isolation of potential phages against multidrug-resistant bacterial isolates: promising agents in the rivers of Kathmandu, Nepal. *Biomed Res Int* 1–10. <https://doi.org/10.1155/2017/3723254>
- Brister, J.R., Ako-Adjei, D., Bao, Y., Blinkova, O., 2015. NCBI viral genomes resource. *Nucleic Acids Res.* 43, D571–D577. <https://doi.org/10.1093/nar/gku1207>
- Bromberg, N., Dreyfuss, J.L., Regatieri, C.V., Palladino, M.V., Durán, N., Nader, H.B., Haun, M., Justo, G.Z., 2010. Growth inhibition and pro-apoptotic activity of violacein in Ehrlich ascites tumor. *Chem-Biol Interact* 186, 43–52. <https://doi.org/10.1016/j.cbi.2010.04.016>
- Brooke, J.S., 2012. *Stenotrophomonas maltophilia*: an emerging global opportunistic pathogen. *Clin Microbiol Rev* 25, 2–41. <https://doi.org/10.1128/CMR.00019-11>
- Carding, S.R., Davis, N., Hoyles, L., 2017. Review article: the human intestinal virome in health and disease. *Aliment Pharmacol Ther* 46, 800–815. <https://doi.org/10.1111/apt.14280>
- Carter, M.E., Chengappa, M.M., 1990. Enterobacteria, in: *Diagnostic Procedure in Veterinary Bacteriology and Mycology*. Elsevier, pp. 107–128. <https://doi.org/10.1016/B978-0-12-161775-2.50014-1>
- Casas, V., Rohwer, F., 2007. Phage Metagenomics, in: *Methods in Enzymology*. Elsevier, pp. 259–268. [https://doi.org/10.1016/S0076-6879\(06\)21020-6](https://doi.org/10.1016/S0076-6879(06)21020-6)
- Choi, J.H., Kim, M.S., Roh, S.W., Bae, J.W., 2010. *Brevundimonas basaltis* sp. nov., isolated from black sand. *Int J Syst Evol Microbiol* 60, 1488–1492. <https://doi.org/10.1099/ijs.0.013557-0>
- Davis, J.E., Sinsheimer, R.L., Strauss, J.H., 1961. Bacteriophage MS2-another RNA phage. *Amer Assoc Advancement Science* 134, 1427.
- De Ley, J., Segers, P., Gillis, M., 1978. Intra- and intergeneric similarities of *Chromobacterium* and *Janthinobacterium* ribosomal ribonucleic acid cistrons. *Int J Syst Evol Microbiol* 28, 154–168. <https://doi.org/10.1099/00207713-28-2-154>
- Demerec, M., Fano, U., 1945. Bacteriophage-resistant mutants in *Escherichia coli*. *Genetics* 30, 119–136. <https://doi.org/10.1093/genetics/30.2.119>
- Devi, K.A., Pandey, P., Sharma, G.D., 2016. Plant growth-promoting endophyte *Serratia marcescens* AL2-16 enhances the growth of *Achyranthes aspera* L., a medicinal plant. *Hayati* 23, 173–180. <https://doi.org/10.1016/j.hjb.2016.12.006>

- D'Hérelle, F., 1917. Sur un microbe invisible antagoniste des bacilles dysentériques. C R Acad Sci 165, 373–375.
- Dion, M.B., Oechslin, F., Moineau, S., 2020. Phage diversity, genomics and phylogeny. Nat Rev Microbiol 18, 125–138. <https://doi.org/10.1038/s41579-019-0311-5>
- Estrela, A.B., Abraham, W.R., 2010. *Brevundimonas vancouverensis* sp. nov., isolated from blood of a patient with endocarditis. Int J Syst Evol Microbiol 60, 2129–2134. <https://doi.org/10.1099/ijs.0.015651-0>
- Evans, T.J., Crow, M.A., Williamson, N.R., Orme, W., Thomson, N.R., Komitopoulou, E., Salmond, G.P.C., 2010. Characterization of a broad-host-range flagellum-dependent phage that mediates high-efficiency generalized transduction in, and between, *Serratia* and *Pantoea*. Microbiology 156, 240–247. <https://doi.org/10.1099/mic.0.032797-0>
- Falkow, S., Marmur, J., Carey, W.F., Spilman, W.M., Baron, L.S., 1961. Episomic transfer between *Salmonella typhosa* and *Serratia marcescens*. Genetics 46, 703–706. <https://doi.org/10.1093/genetics/46.7.703>
- Frederick, G.L., Lloyd, B.J., 1995. Evaluation of bacteriophage as a tracer and a model for virus removal in waste stabilization ponds. Water Sci. Technol. 31, 291–302. [https://doi.org/10.1016/0273-1223\(95\)00517-Q](https://doi.org/10.1016/0273-1223(95)00517-Q)
- Friedrich, I., Bodenberger, B., Neubauer, H., Hertel, R., Daniel, R., 2021a. Down in the pond: Isolation and characterization of a new *Serratia marcescens* strain (LVF3) from the surface water near frog's lettuce (*Groenlandia densa*). PLOS ONE 16, e0259673. <https://doi.org/10.1371/journal.pone.0259673>
- Friedrich, I., Hollensteiner, J., Scherf, J., Weyergraf, J., Klassen, A., Poehlein, A., Hertel, R., Daniel, R., 2021b. Complete genome sequence of *Stenotrophomonas indicatrix* DAIF1. Microbiol Resour Announc 10, 15–17. <https://doi.org/10.1128/MRA.01484-20>
- Friedrich, I., Klassen, A., Neubauer, H., Schneider, D., Hertel, R., Daniel, R., 2021c. Living in a puddle of mud: Isolation and characterization of two novel *Caulobacteraceae* strains *Brevundimonas pondensis* sp. nov. and *Brevundimonas goettingensis* sp. nov. Appl Microbiol 1, 38–59. <https://doi.org/10.3390/applmicrobiol1010005>
- Fukuda, A., Miyakawa, K., Iba, H., Okada, Y., 1976. A flagellotropic bacteriophage and flagella formation in *Caulobacter*. Virology 71, 583–592. [https://doi.org/10.1016/0042-6822\(76\)90383-4](https://doi.org/10.1016/0042-6822(76)90383-4)
- Garmaeva, S., Sinha, T., Kurilshikov, A., Fu, J., Wijmenga, C., Zhernakova, A., 2019. Studying the gut virome in the metagenomic era: challenges and perspectives. BMC Biol 17, 84. <https://doi.org/10.1186/s12915-019-0704-y>
- Gillis, A., Rodríguez, M., Santana, M.A., 2013. *Serratia marcescens* associated with bell pepper (*Capsicum annuum* L.) soft-rot disease under greenhouse conditions. Eur J Plant Pathol 138, 1–8. <https://doi.org/10.1007/s10658-013-0300-x>
- Gomila, M., Pinhassi, J., Falsen, E., Moore, E.R.B., Lalucat, J., 2010. *Kinneretia asaccharophila* gen. nov., sp. nov., isolated from a freshwater lake, a member of the Rubrivivax branch of the family Comamonadaceae. Int J Syst Evol Microbiol 60, 809–814. <https://doi.org/10.1099/ijs.0.011478-0>
- Gong, X., Skrivergaard, S., Korsgaard, B.S., Schreiber, L., Marshall, I.P.G., Finster, K., Schramm, A., 2017. High quality draft genome sequence of *Janthinobacterium psychrotolerans* sp. nov., isolated from a frozen freshwater pond. Stand in Genomic Sci 12, 8. <https://doi.org/10.1186/s40793-017-0230-x>
- Gorbatyuk, B., Marczynski, G.T., 2005. Regulated degradation of chromosome replication proteins DnaA and CtrA in *Caulobacter crescentus*. Mol Microbiol 55, 1233–1245. <https://doi.org/10.1111/j.1365-2958.2004.04459.x>
- Grimont, P.A.D., Grimont, F., 1978. The genus *Serratia*. Annu Rev Microbiol 32, 221–248. <https://doi.org/10.1146/annurev.mi.32.100178.001253>

- Guttenplan, S.B., Kearns, D.B., 2013. Regulation of flagellar motility during biofilm formation. *FEMS Microbiol Rev* 37, 849–871. <https://doi.org/10.1111/1574-6976.12018>
- Haack, F.S., Poehlein, A., Kröger, C., Voigt, C.A., Piepenbring, M., Bode, H.B., Daniel, R., Schäfer, W., Streit, W.R., 2016. Molecular keys to the *Janthinobacterium* and *Duganella* spp. interaction with the plant pathogen *Fusarium graminearum*. *Front Microbiol* 7. <https://doi.org/10.3389/fmicb.2016.01668>
- Henrici, A.T., Johnson, D.E., 1935. Studies of freshwater bacteria: II. Stalked bacteria, a new order of Schizomycetes. *J Bacteriol* 30, 61–93. <https://doi.org/10.1128/JB.30.1.61-93.1935>
- Jagannadham, M.V., Chattopadhyay, M.K., Subbalakshmi, C., Vairamani, M., Narayanan, K., Mohan Rao, C., Shivaji, S., 2000. Carotenoids of an Antarctic psychrotolerant bacterium, *Sphingobacterium antarcticus*, and a mesophilic bacterium, *Sphingobacterium multivorum*. *Arch Microbiol* 173, 418–424. <https://doi.org/10.1007/s002030000163>
- Jin, L., Lee, H.-G., Kim, H.-S., Ahn, C.-Y., Oh, H.-M., 2014. *Caulobacter daechungensis* sp. nov., a stalked bacterium isolated from a eutrophic reservoir. *Int J Syst Evol Microbiol* 63, 2559–2564. <https://doi.org/10.1099/ijs.0.048884-0>
- Johansen, J.E., Binnerup, S.J., Kroer, N., Mølbak, L., 2005. *Luteibacter rhizovicinus* gen. nov., sp. nov., a yellow-pigmented gammaproteobacterium isolated from the rhizosphere of barley (*Hordeum vulgare* L.). *Int J Syst Evol Microbiol* 55, 2285–2291. <https://doi.org/10.1099/ijs.0.63497-0>
- Johnson, R.C., Wood, N.B., Ely, B., 1977. Isolation and characterization of bacteriophages for *Caulobacter crescentus*. *J Gen Virol* 37, 323–335. <https://doi.org/10.1099/0022-1317-37-2-323>
- Jung, W.J., Kim, S.W., Giri, S.S., Kim, H.J., Kim, S.G., Kang, J.W., Kwon, J., Lee, S.B., Oh, W.T., Jun, J.W., Park, S.C., 2021. *Janthinobacterium tructae* sp. nov., isolated from kidney of rainbow trout (*Oncorhynchus mykiss*). *Pathogens* 10, 229. <https://doi.org/10.3390/pathogens10020229>
- Kämpfer, P., Lodders, N., Falsen, E., 2009. *Luteibacter anthropi* sp. nov., isolated from human blood, and reclassification of *Dyella yeojuensis* Kim et al. 2006 as *Luteibacter yeojuensis* comb. nov. *Int J Syst Evol Microbiol* 59, 2884–2887. <https://doi.org/10.1099/ijs.0.009100-0>
- Kazaks, A., Voronkova, T., Rumnieks, J., Dishlers, A., Tars, K., 2011. Genome structure of *Caulobacter* phage phiCb5. *J Virol* 85, 4628–4631. <https://doi.org/10.1128/JVI.02256-10>
- Khan, A.R., Park, G.S., Asaf, S., Hong, S.J., Jung, B.K., Shin, J.H., 2017. Complete genome analysis of *Serratia marcescens* RSC-14: a plant growth-promoting bacterium that alleviates cadmium stress in host plants. *PLOS ONE* 12, 1–17. <https://doi.org/10.1371/journal.pone.0171534>
- Khanna, A., Khanna, M., Aggarwal, A., 2013. *Serratia marcescens* – a rare opportunistic nosocomial pathogen and measures to limit its spread in hospitalized patients. *J Clin Diagn Res* 7, 243–246. <https://doi.org/10.7860/JCDR/2013/5010.2737>
- Kieft, K., Zhou, Z., Anantharaman, K., 2020. VIBRANT: Automated recovery, annotation and curation of microbial viruses, and evaluation of viral community function from genomic sequences. *Microbiome* 8, 90. <https://doi.org/10.1186/s40168-020-00867-0>
- Kim, B.-Y., Weon, H.-Y., Lee, K.-H., Seok, S.-J., Kwon, S.-W., Go, S.-J., Stackebrandt, E., 2006. *Dyella yeojuensis* sp. nov., isolated from greenhouse soil in Korea. *Int J Syst Evol Microbiol* 56, 2079–2082. <https://doi.org/10.1099/ijs.0.64175-0>
- Krinsky, N.I., 1978. Non-photosynthetic functions of carotenoids. *Phil Trans R Soc Lond B* 284, 581–590. <https://doi.org/10.1098/rstb.1978.0091>

- Lazeroff, M., Ryder, G., Harris, S.L., Tsourkas, P.K., 2021. Phage commander, an application for rapid gene identification in bacteriophage genomes using multiple programs. *Phage* 2, 204–213. <https://doi.org/10.1089/phage.2020.0044>
- Lee, J., Bae, J., Youn, D.-Y., Ahn, J., Hwang, W.-T., Bae, H., Bae, P.K., Kim, I.-D., 2022. Violacein-embedded nanofiber filters with antiviral and antibacterial activities. *Chem Eng J* 444, 136460. <https://doi.org/10.1016/j.cej.2022.136460>
- Li, M., Wang, J., Zhang, Q., Lin, L., Kuang, A., Materon, L.A., Ji, X., Wei, Y., 2016. Isolation and characterization of the lytic cold-active bacteriophage MYSP06 from the Mingyong Glacier in China. *Curr Microbiol* 72, 120–127. <https://doi.org/10.1007/s00284-015-0926-3>
- Lincoln, S.P., Fermor, T.R., Tindall, B.J., 1999. *Janthinobacterium agaricidamnosum* sp. nov., a soft rot pathogen of *Agaricus bisporus*. *Int J Syst Evol Microbiol* 49, 1577–1589. <https://doi.org/10.1099/00207713-49-4-1577>
- Lu, H., Deng, T., Cai, Z., Liu, F., Yang, X., Wang, Y., Xu, M., 2020. *Janthinobacterium violaceinigrum* sp. nov., *Janthinobacterium aquaticum* sp. nov. and *Janthinobacterium rivuli* sp. nov., isolated from a subtropical stream in China. *Int J Syst Evol Microbiol* 70, 2719–2725. <https://doi.org/10.1099/ijsem.0.004097>
- Mahlen, S.D., 2011. *Serratia* infections: from military experiments to current practice. *Clin Microbiol Rev* 24, 755–791. <https://doi.org/10.1128/CMR.00017-11>
- Maki, D.G., Hennekens, C.G., Phillips, C.W., Shaw, W.V., Bennett, J.V., 1973. Nosocomial urinary tract infection with *Serratia marcescens*: an epidemiologic study. *J Infect Dis* 128, 579–587. <https://doi.org/10.1093/infdis/128.5.579>
- Manfredi, R., Nanetti, A., Ferri, M., Chiodo, F., 2000. Clinical and microbiological survey of *Serratia marcescens* infection during HIV disease. *Eur J Clin Microbiol Infect Dis* 19, 248–253. <https://doi.org/10.1007/s100960050471>
- Matsushita, K., Uchiyama, J., Kato, S., Ujihara, T., Hoshihara, H., Sugihara, S., Muraoka, A., Wakiguchi, H., Matsuzaki, S., 2009. Morphological and genetic analysis of three bacteriophages of *Serratia marcescens* isolated from environmental water. *FEMS Microbiol Lett* 291, 201–208. <https://doi.org/10.1111/j.1574-6968.2008.01455.x>
- McTaggart, T.L., Shapiro, N., Woyke, T., Chistoserdova, L., 2015. Draft genome of *Janthinobacterium* sp. RA13 isolated from Lake Washington sediment. *Genome Announc* 3, e01588-14. <https://doi.org/10.1128/genomeA.01588-14>
- Miller, N.J., Sampson, J., Candeias, L.P., Bramley, P.M., Rice-Evans, C.A., 1996. Antioxidant activities of carotenes and xanthophylls. *FEBS Lett* 384, 240–242. [https://doi.org/10.1016/0014-5793\(96\)00323-7](https://doi.org/10.1016/0014-5793(96)00323-7)
- Miyakawa, K., Fukuda, A., Okada, Y., Furuse, K., Watanabe, I., 1976. Isolation and characterization of RNA phages for *Caulobacter crescentus*. *Virology* 73, 461–467. [https://doi.org/10.1016/0042-6822\(76\)90407-4](https://doi.org/10.1016/0042-6822(76)90407-4)
- Moon, K., Kang, I., Kim, S., Kim, S.-J., Cho, J.-C., 2018. Genomic and ecological study of two distinctive freshwater bacteriophages infecting a *Comamonadaceae* bacterium. *Sci Rep* 8, 7989. <https://doi.org/10.1038/s41598-018-26363-y>
- Naushad, S., Adeolu, M., Wong, S., Sohail, M., Schellhorn, H.E., Gupta, R.S., 2015. A phylogenomic and molecular marker based taxonomic framework for the order Xanthomonadales: proposal to transfer the families *Algiphilaceae* and *Solimonadaceae* to the order Nevskiales ord. nov. and to create a new family within the order Xanthomonadales, the family *Rhodanobacteraceae* fam. nov., containing the genus *Rhodanobacter* and its closest relatives. *Antonie Leeuwenhoek* 107, 467–485. <https://doi.org/10.1007/s10482-014-0344-8>
- Parte, A.C., Carbasse, J.S., Meier-Kolthoff, J.P., Reimer, L.C., Göker, M., 2020. List of prokaryotic names with standing in nomenclature (LPSN) moves to the DSMZ. *Int J Syst Evol Microbiol* 70, 5607–5612. <https://doi.org/10.1099/ijsem.0.004332>

- Plevka, P., Kazaks, A., Voronkova, T., Kotelovica, S., Dishlers, A., Liljas, L., Tars, K., 2009. The structure of bacteriophage phiCb5 reveals a role of the RNA genome and metal ions in particle stability and assembly. *J Mol Biol* 391, 635–647. <https://doi.org/10.1016/j.jmb.2009.06.047>
- Poindexter, J.S., 1964. Biological properties and classification of the *Caulobacter* group. *Bacteriol Rev* 28, 231–295. <https://doi.org/10.1128/mmbr.28.3.231-295.1964>
- Principi, N., Silvestri, E., Esposito, S., 2019. Advantages and limitations of bacteriophages for the treatment of bacterial infections. *Front Pharmacol* 10, 513. <https://doi.org/10.3389/fphar.2019.00513>
- Prinsloo, H.E., 1966. Bacteriocins and phages produced by *Serratia marcescens*. *J Gen Microbiol* 45, 205–212. <https://doi.org/10.1099/00221287-45-2-205>
- Prinsloo, H.E., Coetzee, J.N., 1964. Host-range of temperate *Serratia marcescens* bacteriophages. *Nature* 203, 211. <https://doi.org/10.1038/203211a0>
- Rajagopal, L., Sundari, C.S., Balasubramanian, D., Sonti, R.V., 1997. The bacterial pigment xanthomonadin offers protection against photodamage. *FEBS Lett* 415, 125–128. [https://doi.org/10.1016/S0014-5793\(97\)01109-5](https://doi.org/10.1016/S0014-5793(97)01109-5)
- Rascoe, J., Berg, M., Melcher, U., Mitchell, F.L., Bruton, B.D., Pair, S.D., Fletcher, J., 2003. Identification, phylogenetic analysis, and biological characterization of *Serratia marcescens* strains causing cucurbit yellow vine disease. *Phytopathology* 93, 1233–1239. <https://doi.org/10.1094/phyto.2003.93.10.1233>
- Ray, U., Dutta, S., Chakravarty, C., Sutradhar, A., 2015. A case of multiple cutaneous lesions due to *Serratia marcescens* in an immunocompromised patient. *JMM Case Rep* 2, 1–4. <https://doi.org/10.1099/jmmcr.0.000059>
- Reardon, S., 2014. Phage therapy gets revitalized. *Nature* 510, 15–16. <https://doi.org/10.1038/510015a>
- Rodrigues, C.J.C., de Carvalho, C.C.C.R., 2022. Cultivating marine bacteria under laboratory conditions: overcoming the “unculturable” dogma. *Front Bioeng Biotechnol* 10, 964589. <https://doi.org/10.3389/fbioe.2022.964589>
- Ryu, S.H., Park, M., Lee, J.R., Yun, P.-Y., Jeon, C.O., 2007. *Brevundimonas aveniformis* sp. nov., a stalked species isolated from activated sludge. *Int J Syst Evol Microbiol* 57, 1561–1565. <https://doi.org/10.1099/ijms.0.64737-0>
- Sanger, F., Air, G.M., Barrell, B.G., Brown, N.L., Coulson, A.R., Fiddes, J.C., Hutchison, C.A., Slocombe, P.M., Smith, M., 1977. Nucleotide sequence of bacteriophage φX174 DNA. *Nature* 265, 687–695. <https://doi.org/10.1038/265687a0>
- Schmidt, J.M., Stainer, R.Y., 1965. Isolation and characterization of bacteriophages active against stalked bacteria. *J Gen Microbiol* 39, 95–107. <https://doi.org/10.1099/00221287-39-1-95>
- Seel, W., Baust, D., Sons, D., Albers, M., Etzbach, L., Fuss, J., Lipski, A., 2020. Carotenoids are used as regulators for membrane fluidity by *Staphylococcus xylosus*. *Sci Rep* 10, 330. <https://doi.org/10.1038/s41598-019-57006-5>
- Segers, P., Vancanneyt, M., Pot, B., Torck, U., Hoste, B., Dewettinck, D., Falsen, E., Kersters, K., De Vos, P., 1994. Classification of *Pseudomonas diminuta* Leifson and Hugh 1954 and *Pseudomonas vesicularis* Büsing, Döll, and Freytag 1953 in *Brevundimonas* gen. nov. as *Brevundimonas diminuta* comb. nov. and *Brevundimonas vesicularis* comb. nov., respectively. *Int J Syst Evol Microbiol* 44, 499–510. <https://doi.org/10.1099/00207713-44-3-499>
- Shoemaker, W.R., Muscarella, M.E., Lennon, J.T., 2015. Genome sequence of the soil bacterium *Janthinobacterium* sp. KBS0711. *Genome Announc* 3, e00689-15. <https://doi.org/10.1128/genomeA.00689-15>
- Sikora, E.J., Bruton, B.D., Wayadande, A.C., Fletcher, J., 2012. First report of the cucurbit yellow vine disease caused by *Serratia marcescens* in watermelon and yellow squash in Alabama. *Plant Dis* 96, 761. <https://doi.org/10.1094/pdis-09-11-0739-pdn>

- Staley, J.T., 1968. Prosthecomicrobium and Ancalomicrobium: new prosthecate freshwater bacteria. *J Bacteriol* 95, 1921–1942. <https://doi.org/10.1128/JB.95.5.1921-1942.1968>
- Stove, J.L., Stanier, R.Y., 1962. Cellular differentiation in stalked bacteria. *Nature* 196, 1189–1192. <https://doi.org/10.1038/1961189a0>
- Subczynski, W.K., Markowska, E., Gruszecki, W.I., Siewiewsiuk, J., 1992. Effects of polar carotenoids on dimyristoylphosphatidylcholine membranes: a spin-label study. *Biochim Biophys Acta* 1105, 97–108. [https://doi.org/10.1016/0005-2736\(92\)90167-K](https://doi.org/10.1016/0005-2736(92)90167-K)
- Sullivan, M.J., Petty, N.K., Beatson, S.A., 2011. Easyfig: A genome comparison visualizer. *Bioinformatics* 27, 1009–1010. <https://doi.org/10.1093/bioinformatics/btr039>
- Tóth, E., Szuróczki, S., Kéki, Zs., Kosztik, J., Makk, J., Bóka, K., Spröer, C., Márialigeti, K., Schumann, P., 2017. *Brevundimonas balnearis* sp. nov., isolated from the well water of a thermal bath. *Int J Syst Evol Microbiol* 67, 1033–1038. <https://doi.org/10.1099/ijsem.0.001746>
- Tsubouchi, T., Koyama, S., Mori, K., Shimane, Y., Usui, K., Tokuda, M., Tame, A., Uematsu, K., Maruyama, T., Hatada, Y., 2014. *Brevundimonas denitrificans* sp. nov., a denitrifying bacterium isolated from deep subseafloor sediment. *Int J Syst Evol Microbiol* 64, 3709–3716. <https://doi.org/10.1099/ijms.0.067199-0>
- Vandenheuvel, D., Rombouts, S., Adriaenssens, E.M., 2018. Purification of bacteriophages using anion-exchange chromatography, in: Clokie, M.R.J., Kropinski, A.M., Lavigne, R. (Eds.), *Bacteriophages, Methods in Molecular Biology*. Springer New York, New York, NY, pp. 59–69. https://doi.org/10.1007/978-1-4939-7343-9_5
- Vu, H.T.T., Manangkil, O.E., Mori, N., Yoshida, S., Nakamura, C., 2010. Post-germination seedling vigor under submergence and submergence-induced SUB1A gene expression in indica and japonica rice (*Oryza sativa* L.). *Aust J Crop Sci* 4, 264–272. <https://doi.org/10.1099/ijms.0.043364-0>
- Wang, J., Zhang, J., Ding, K., Xin, Y., Pang, H., 2012. *Brevundimonas viscosa* sp. nov., isolated from saline soil. *Int J Syst Evol Microbiol* 62, 2475–2479. <https://doi.org/10.1099/ijms.0.035352-0>
- Wang, L., Wang, G.-L., Li, S.-P., Jiang, J.-D., 2011. *Luteibacter jiangsuensis* sp. nov.: a methamidophos-degrading bacterium isolated from a methamidophos-manufacturing factory. *Curr Microbiol* 62, 289–295. <https://doi.org/10.1007/s00284-010-9707-1>
- Wijewanta, E., Fernando, M., 1970. Infection in goats owing to *Serratia marcescens*. *Vet Rec* 87, 282–284. <https://doi.org/10.1136/vr.87.10.282>
- Wilhelm, R.C., 2018. Following the terrestrial tracks of *Caulobacter* - redefining the ecology of a reputed aquatic oligotroph. *ISME J* 12, 3025–3037. <https://doi.org/10.1038/s41396-018-0257-z>
- Wu, Hanqing, Wan, Sichen, Ruan, Chujin, Niu, Xinyao, Chen, Guowei, Liu, Ying, Zhu, Kun, Schulin, Rainer, Wang, Gang, 2022. Phage-bacterium interactions and nutrient availability can shape C and N retention in microbial biomass. *Eur J Soil Sci* 73. <https://doi.org/10.1111/ejss.13296>
- Wu, Q., Liu, W.-T., 2009. Determination of virus abundance, diversity and distribution in a municipal wastewater treatment plant. *Water Res* 43, 1101–1109. <https://doi.org/10.1016/j.watres.2008.11.039>
- Wu, X., Deutschbauer, A.M., Kazakov, A.E., Wetmore, K.M., Cwick, B.A., Walker, R.M., Novichkov, P.S., Arkin, A.P., Chakraborty, R., 2017. Draft genome sequences of two *Janthinobacterium lividum* strains, isolated from pristine groundwater collected from the Oak Ridge Field Research Center. *Genome Announc* 5, e00582-17. <https://doi.org/10.1128/genomeA.00582-17>

-
- Yap, M.L., Klose, Thomas, Arisaka, Fumio, Rossmann, Michael G., 2016. Role of bacteriophage T4 baseplate in regulating assembly and infection. *Proc Natl Acad Sci U S A* 113, 2654–2659. <https://doi.org/10.1073/pnas.1601654113>
- Yoon, J.H., Kang, S.J., Oh, H.W., Lee, J.S., Oh, T.K., 2006. *Brevundimonas kwangchunensis* sp. nov., isolated from an alkaline soil in Korea. *Int J Syst Evol Microbiol* 56, 613–617. <https://doi.org/10.1099/ijs.0.63784-0>
- Zhang, Z., Schwartz, S., Wagner, L., Miller, W., 2000. A greedy algorithm for aligning DNA sequences. *J Comput Biol* 7, 203–214. <https://doi.org/10.1089/10665270050081478>
- Zrelavs, N., Dislers, A., Kazaks, A., 2020. Motley Crew: Overview of the currently available phage diversity. *Front Microbiol* 11, 1–6. <https://doi.org/10.3389/fmicb.2020.579452>

Appendix

1. Supplement

S1 Data File. Gene annotation of phage-associated contig. Annotation was performed using VIBRANT (Kieft et al., 2020) and Phage Commander (Lazeroff et al., 2021).

*The data file can be found on the enclosed CD:
Supplement\Appendix\S1_Data_File.gbk*

S2 Data File. Sequence alignment of unique contig. Alignment was done using blastn v2.12.0+ (accessed on 17 June 2022) (Zhang et al., 2000).

*The data file can be found on the enclosed CD:
Supplement\Appendix\S2_Data_File.fasta*

S1 Table. Result of raw read mapping of all *Caulobacteraceae*-associated bacteriophages from the NCBI Virus database and own isolates for the virome of the winter season.

*The table can be found on the enclosed CD:
Supplement\Appendix\S1_Table.xlsx*

2. Publications

1. **Friedrich I**, Hertel R (2023) Isolation of a host-confined phage metagenome allows the detection of phages both capable and incapable of plaque formation. In *Methods in Molecular Biology* 2555:192-203. doi:10.1007/978-1-0716-2795-2_14.
2. Kohm K, Lutz VT, **Friedrich I**, Hertel R (2023) CRISPR-Cas9 shaped viral metagenomes associated with *Bacillus subtilis*. In *Methods in Molecular Biology* 2555:205-212. doi:10.1007/978-1-0716-2795-2_15.
3. **Friedrich I**, Hertel R (2022) Habe ich eine neue Spezies entdeckt? In *Biologie in unserer Zeit* 52(2):123-126. doi:10.11576/biuz-5433.
4. Hertel R, Schöne K, Mittelstädt C, Meißner J, Zschoche N, Collignon M, Kohler C, **Friedrich I**, Schneider D, Hoppert M, Kuhn R, Schwedt I, Scholz P, Poehlein A, Martienssen M, Ischebeck T, Daniel R, Commichau FM (2022) Characterization of glyphosate-resistant *Burkholderia anthina* and *Burkholderia cenocepacia* isolates from a commercial Roundup® solution. In *Environmental Microbiology Reports* 14(1):70-84. doi:10.1111/1758-2229.13022.
5. **Friedrich I**, Bodenberger B, Neubauer H, Hertel R, Daniel R (2021) Down in the pond: Isolation and characterization of a new *Serratia marcescens* strain (LVF3) from the surface water near frog's lettuce (*Groenlandia densa*). In *PLoS One* 16(11):e0259673. doi:10.1371/journal.pone.0259673.
6. **Friedrich I**, Klassen A, Neubauer H, Schneider D, Hertel R, Daniel R (2021) Living in a puddle of mud: isolation and characterization of two novel *Caulobacteraceae* strains *Brevundimonas pondensis* sp. nov. and *Brevundimonas goettingensis* sp. nov.. In *Applied Microbiology* 1:38-59. doi:10.3390/applmicrobiol1010005.
7. Hollensteiner J, **Friedrich I**, Hollstein L, Lamping J-P, Wolf K, Liesegang H, Poehlein A, Hertel R, Daniel R (2021) Complete genome sequence of *Kinneretia* sp. strain DAIF2, isolated from a freshwater pond. In *Microbiology Resource Announcements* 10(8):e00003-21. doi:10.1128/MRA.00003-21.
8. **Friedrich I**, Hollensteiner J, Scherf J, Weyergraf J, Klassen A, Poehlein A, Hertel R, Daniel R (2021) Complete genome sequence of *Stenotrophomonas indicatrix* DAIF1. In *Microbiology Resource Announcements* 10(6):e01484-20. doi:10.1128/MRA.01484-20.

-
9. Aloo BN, Mbega ER, Makumba BA, **Friedrich I**, Hertel R, Daniel R (2020) Whole-genome sequences of three plant growth-promoting rhizobacteria isolated from *Solanum tuberosum* L. rhizosphere in Tanzania. In *Microbiology Resource Announcements*, 9(20):e00371-20. doi:10.1128/MRA.00371-20.
 10. Egelkamp R, **Friedrich I**, Hertel R, Daniel R (2020) From sequence to function: a new workflow for nitrilase identification. In *Applied Microbiology and Biotechnology*, 104:4957–4970. doi:10.1007/s00253-020-10544-9.
 11. **Friedrich I**, Hollensteiner J, Schneider D, Poehlein A, Hertel R, Daniel R (2020) First complete genome sequences of *Janthinobacterium lividum* EIF1 and EIF2 and their comparative genome analysis. In *Genome Biology and Evolution*, 12(10):1782-1788. doi:10.1093/gbe/evaa148.
 12. Poehlein A, **Friedrich I**, Krüger L, Daniel R (2016) First insights into the genome of the moderately thermophilic bacterium *Clostridium tepidiprofundum* SG 508T. In *Genome Announcements*, 4(3):e00379-16. doi:10.1128/genomeA.00379-16.

3. Posters at conferences

1. **Friedrich I**, Klassen A, Bodenberger B, Tskhay F, Hartmann S, Schneider D, Hertel R, Daniel R (2021) Expanding viromes associated with *Brevundimonas* and *Serratia*. Microbiology Society, online. Poster.
2. **Friedrich I**, Egelkamp R, Hertel R, Daniel R (2017) Characterization of nitrilases isolated from enrichment cultures. *ProkaGENOMICS*, Göttingen, Germany. Poster.

Acknowledgements

Without the help of many people, this work would not have been possible. I am thankful for the last few years. There are too many people to list, but I want you to know that I appreciate everything you have done for me, no matter how small.

My first thank you goes to Prof. Dr. Rolf Daniel for the opportunity to accomplish one of the biggest goals in my life. Thank you for all the support and advice you have given me over the past eight years. I appreciate my time in the lab since my Bachelor's lab rotation in 2014.

Thank you to PD Dr. Michael Hoppert, who was not only the second examiner of this thesis but also gave me advice and support during the thesis committee meetings and took the time to introduce my group of students to the electron microscope. Thanks also to Prof. Dr. Stefanie Pöggeler for being a member of my thesis committee and for the great conversations during the GGNB Retreats.

I would also like to thank the remaining members of my examination board Prof. Dr. Kai Heimel, Prof. Dr. Gerhard Braus, and Prof. Dr. Jan de Vries, for agreeing to read in reading and evaluate this thesis and approaching the defense.

I am very grateful to Dr. Robert Hertel. Not only that, I was part of your famous "Slughorn Club," which was great. Thank you for your good advice, motivation, fruitful discussions, shared knowledge, support, and patience. Without you, I would not be where I am today. Thank you, Robert!

I had the pleasure of being mentored by two masters. Therefore, I would like to thank Dr. Dominik Schneider. Thank you for your motivation and tips and tricks regarding the virome. Thank you for your incredible support, help and the fun conversations while pushing the next finished Ph.D. student with the wagon to the Gänseliesel. Thank you, Dominik!

I would also like to thank the great post-doc team, the former (Dr. Bernd Wemheuer, Dr. Robert Hertel, Dr. Birgit Pfeiffer, Dr. Heiko Nacke) and the current (Dr. Dominik Schneider, Dr. Jacqueline Hollensteiner, Dr. Heiko Liesegang, Dr. Anja Poehlein). Thank you, Jacky and Birgit, for help and tips and our chat time. I would also like to thank Anja for her encouraging words and who spent a lot of time optimizing the phage and virome sequencing. For me, it was always a privilege being able to count on so many people with various skills, always willing to help and offer knowledge, experience, and advice.

Also, I would like to thank our technical assistance team (Mechthild Bömeke, Melanie Heinemann, and Christiane Wohlfeil). Thank you to Mechthild, from whom I have learned so much over the years and whose laboratory organization has made my life much easier. A special thanks also go to our scientific coordinator, Dr. Petra Ehrenreich, and Nicole Dörjer, who have been extremely helpful throughout the paperwork process. Finally, a big thank you goes to our IT guys, Mirco and Paul.

Special thanks go to my fellow doctoral students Miri, Tim, Alina, and Stefi, and those who already graduated: Avi, Tati, Dirk (Fanboy!), Inka, Richard, Genis, Randi, Amélie, Mingji, and Cynthia. I have enjoyed my time with you guys, as you have no idea. I will always keep in my happy memories our parties, jokes, dinners, trips, grills, chats, movies, discussions, laughs, or walks after lunch. This thesis was also done with the enormous contribution of several students who worked with me. Anna Klassen, Bernhard Bodenberger, Faina Tskhay, Sara Hartmann, Hannes Neubauer, and Alisa Kuritsyn. Thank you, guys.

A special thanks go to Kelly, who is the same kind of crazy as me. Thank you for our walks to the donkeys, trips to the playground, or being together in the hedgehog ambulance 🦔. Thank you for being one of my biggest supporters! Avi and Señorita Tati, thank you for your supportive walks, gifs, and all-around advice. Thank you to Noa for being an amazing friend. Thank you also goes to Ani for the chat time we could take during a tough lab day. Finally, a huge thank you goes to the USA to Brianna; thank you for all your support, and time being my friend, despite the long distance between us.

Thank you to my parents and my sisters for always supporting me. Without your support I would never be where I am today. Thank you for always believing in me. Я люблю вас!

Thank you to my little family of adventurers and supporters. Thank you for being who you are and for your unconditional love and immense support. Thank you for inspiring me. Kocham was i jestem z was dumna!

